Mechanical characterisation of masonry in existing structures by means of laboratory and in-situ experimental techniques

Albert Cabané Cañas

Barcelona, April 2023

Supervisors
Pere Roca i Fabregat
Luca Pelà

PhD DISSERTATION

Thesis by compendium of publications

Universitat Politècnica de Catalunya, BarcelonaTech
Departament d'Enginyeria Civil i Ambiental
Programa de Doctorat en Enginyeria de la Construcció

UNIVERSITAT POLITÈCNICA DE CATALUNYA BARCELONATECH

Mechanical characterisation of masonry in existing structures by means of laboratory and in-situ experimental techniques

-thesis by compendium of publications-

Albert Cabané Cañas

MECHANICAL CHARACTERISATION OF MASONRY IN EXISTING STRUCTURES BY MEANS OF LABORATORY AND IN-SITU EXPERIMENTAL TECHNIQUES

Doctoral Thesis submitted in fulfilment of the requirements for the
Degree of Doctor of Philosophy in Construction Engineering

by

ALBERT CABANÉ CAÑAS

Barcelona, Abril 2023

Thesis by compendium of publications

Universitat Politècnica de Catalunya, BacelonaTech
Escola Tècnica Superior d'Enginyers de Camins, Canals i Ports de Barcelona
Departament d'Enginyeria Civil i Ambiental
Programa de Doctorat en Enginyeria de la Construcció

Thesis Supervisors:

Pere Roca Fabregat – Universitat Politècnica de Catalunya, UPC-BacelonaTech

Luca Pelà – Universitat Politècnica de Catalunya, UPC-BacelonaTech

Board of Examiners:

Ignacio Lombillo Vozmediano – Universidad de Cantabria, UniCan

Còssima Cornadó Bardón – Universitat Politècnica de Catalunya, UPC-BacelonaTech

Sabino Nicola Tarque Ruiz – Universidad Politécnica de Madrid, UPM

To my family: Rebeca and Emma

Itaque primum de lateribus; qua de terra duci eos oporteat, dicam. Non enim de harenoso neque calculoso luto neque sabulonoso luto sunt ducendi, quod ex his generibus cum sint ducti, primum fiunt graves, deinde, cum ab imbribus in parietibus sparguntur, dilabuntur et dissolvuntur paleaque in his non cohaerescunt propter asperitatem. Faciendi autem sunt ex terra albida cretosa sive de rubrica aut etiam masculo sabulone; haec enim genera propter levitatem habent firmitatem et non sunt in opere ponderosa et faciliter aggerantur. Ducendi autem sunt per vernum tempus et autumnale, ut uno tempore siccescant. Qui enim per solstitium parantur, ideo vitiosi fiunt, quod, summum corium sol acriter cum praecoquit, efficit ut videatur aridum, interior autem sit non siccus; et cum postea siccescendo se contrahit, perrumpit ea quae erant arida. Ita rimosi facti efficiuntur imbecilli. Maxime autem utiliores erunt, si ante biennium fuerint ducti, namque non ante possunt penitus siccescere.

De Architectura, Opus in Libris Decem, Liber Secundus,

M. Vitruvii Pollionis (1st c.)

Architecture begins with putting two bricks together carefully.

Ludwig Mies van der Rohe (20th c.)

Acknowledgements

This thesis would have not been possible without the predoctoral financial support provided by the *Agencia Estatal de Investigación* (AEI) of the *Ministerio de Ciencia e Innovación* (MCIU) of the Spanish Government (BES-2016-078433), as well as that of the European Regional Development Fund (ERDF) through projects MULTIMAS (Multiscale techniques for the experimental and numerical analysis of the reliability of masonry structures, ref. num. BIA2015-63882-P) and SEVERUS (Multilevel evaluation of seismic vulnerability and risk mitigation of masonry building in resilient historical urban centres, ref. num. RTI2018-099589-B-I00).

I would like to express my deepest gratitude towards my supervisors Prof. Pere Roca I Fabregat and Prof. Luca Pelà for giving me this opportunity, for all their support and encouragement through all these years. I would also like to thank you for believing in my research and work, even in the darkest moments. Luca Pelà provided me with a great number of contacts within existing historical buildings in the city of Barcelona, which increased the value of the investigation.

The experimental programme was carried out at the Laboratory of Technology of Structure and Construction Materials (LATEM) at the Technical University of Catalonia (UPC-BarcelonaTech). I'm extremely grateful for the staff of LATEM, Jordi Martín and Sergio Rodríguez from the other side, Robert Michael McAloon for always having the right tool and the right recipe for making the mortar, Carlos Hurtado for always being willing to lend a cable or a software, Tomas García for his dedication to unravelling failures in development, as well as, helping with calibration of experimental tests; and I would like to extend my sincere thanks to Jordi Cabrerizo for his involvement in the development and materialization of the experimental test, participating in the development and creation of new apparatus and supports for testing specimens. I would like to express our gratitude to *Ceràmica La Coma S.A.* for their generous contribution to our research. Their provision of solid extruded bricks has made a significant difference which has enabled research to be carried out.

There were many fruitful collaborations and I was lucky to find support during my research which allowed to me to complete this work. Jorge Segura guided and advised me during my first years in the laboratory and in my first characterisation campaigns in existing buildings. Diego Aponte offered his infinite knowledge about the materials, we had many talks and ramblings about the experimental physical results obtained. Larisa Garcia-Ramonda always had the answer to any problem or bureaucratic request. Maria del Carmen Lloret and Ana Beatriz Pérez helped me reading and correcting the English texts. Also I wish to thank for their help, the colleagues of the Team Roca and friends: Savvas, Nirvan, Sara, Camila, Belén, Philip, Francesco and Emerson.

A huge thanks to my parents, Mati and Pedro for their unconditional support, for encouraging me to pursuit my dreams and for helping making it possible. Thanks to my brother Carlos and my sister Marina for their care and company.

And last but always first in my heart, thanks to my wife, Rebeca Gutiérrez, for her love, her patient, and for supporting me in the most difficult moments by being an amazing wife and an exceptional mother.

Barcelona, April 2023

Albert Cabané Cañas

Abstract

Masonry structures are among the most abundant construction typologies in the world, having been commonly built until the second half of the 20th century. The determination of the mechanical properties of these structures entails significant difficulties given the intrinsic complexity of masonry as a composite material. For this reason, the accurate evaluation of masonry buildings against vertical and horizontal actions requires the development and improvement of techniques for the characterisation of the mechanical properties of existing masonry and their components.

This thesis presents an extensive experimental program on the characterisation of solid fired clay bricks, including the case of both handmade bricks and mechanically extruded ones. The research has also comprised extensive campaigns on the mechanical characterisation of bricks and mortar in existing historic buildings in Barcelona (Spain), using minor destructive tests (MDT). The main objective of the in-situ experimental campaigns was the calibration and validation of the MDT techniques by comparison with results obtained through destructive tests (DT) applied in the laboratory.

The laboratory experimental campaigns involved the study and improvement of existing techniques and the development of new ones for the mechanical characterisation of masonry components. The research has focused on the measurement of mechanical parameters of solid clay bricks, such as the compressive strength and the modulus of elasticity. Currently, there is a lack of unanimity in the scientific literature and also among the standards on how to evaluate the compressive strength, which in any case requires of a large number of specimens and the use of various tools and techniques. Also, there are no reference standards on the determination of the modulus of elasticity and, therefore, new proposals on standardizable methodologies are needed. In spite of the challenges encountered in the experimental characterization of bricks, different methodod have been proposed in this research in order to allow their mechanical characterization. The proposed approaches and method have shown their suitability and practical applicability.

Finally, a test methodology is recommended for each of the parameters studied in the research, whose final objective is the correlation between the MDT values and the DT values.

Keywords: Masonry, MDT, Laboratory tests, Solid clay brick, Lime mortar, Compressive strength, Modulus of elasticity, Historical buldings.

Resumen

Las estructuras de obra de fábrica de ladrillo se hayan entre los tipos constructivos más abundantes a escala mundial, habiendo sido comúnmente construidas hasta la segunda mitad del siglo XX. La determinación de las propiedades mecánicas de estas estructuras conlleva dificultades significativas dada la intrínseca complejidad de la mampostería como material compuesto. Por este motivo, la evaluación estructural precisa de los edificios de obra de fábrica ante acciones verticales y horizontales requiere el desarrollo de técnicas para la caracterización de las propiedades mecánicas de la obra de fábrica y de sus componentes.

Esta tesis presenta un extenso programa experimental relativo a la caracterización de ladrillos macizos de arcilla cocida, incluyendo tanto el caso de ladrillos fabricados a mano como de ladrillos fabricados por extrusión. La tesis también ha comprendido extensas campañas relativas a la caracterización de ladrillos y mortero en edificios históricos existentes de la ciudad de Barcelona (España) mediante ensayos moderadamente destructivos (MDT). El objetivo principal de las campañas experimentales desarrolladas in-situ ha sido la comparación, validación y calibración de las técnicas MDT con resultados de los ensayos destructivos (DT) obtenidos en laboratorio.

Las campañas experimentales conllevaron el estudio y mejora de técnicas existentes y el desarrollo de nuevas técnicas para la caracterización mecánico-resistente de los materiales componentes de la obra de fábrica. La investigación se ha centrado en la medida de parámetros mecánicos de ladrillos macizos, tales como la resistencia a compresión y el módulo de elasticidad. El estado del conocimiento muestra falta de unanimidad entre las propuestas de la comunidad científica y entre las diferentes normativas vigentes en relación a cómo medir la resistencia a compresión, lo cual en cualquier caso requiere un gran número de probetas y la utilización de diversas herramientas y técnicas. El estado del conocimiento también muestra la inexistencia de estándares de referencia para la determinación del módulo de elasticidad, siendo necesaria la propuesta de una metodología estandarizable para esta finalidad.

A pesar de los retos hallados en la caracterización experimental de ladrillos, la presente investigación ha propuesto distintos métodos propuestos para su caracterización mecánica.

Palabras clave: Mampostería, MDT, Ensayos de laboratorio, Ladrillo macizo, Mortero de cal, Compresión, Modulo de elasticidad, Construcciones históricas.

Sommario

Le strutture in muratura costruite in mattoni sono tra le tipologie costruttive più numerose al mondo, essendo state comunemente costruitefino alla seconda metà del XX secolo. La determinazione delle proprietà meccaniche di queste strutture comporta notevoli difficoltà, data la complessità intrinseca della muratura come materiale composito. Per questo motivo, la valutazione precisa degli edifici in muratura nei confronti delle azioni verticali e orizzontali richiede lo sviluppo e il miglioramento delle tecniche per la caratterizzazione delle propietà meccaniche delle murature esistenti e dei loro componenti.

Questa tesi di dottorato presenta un ampio programma sperimentale relativo alla caratterizzazione di mattoni pieni in argilla cotta, sia realizzati a mano che realizzati per estrusione. La ricerca ha considerato anche ampie campagne sulla caratterizzazione meccanica di mattoni e malte di edifici storici esistenti nella città di Barcellona (Spagna), utilizzando prove moderatamente distruttive (MDT). L'obiettivo principale delle campagne sperimentali in situ è stato la calibrazione e la validazione delle tecniche MDT rispetto ai risultati delle prove distruttive (DT) ottenute in laboratorio.

Le campagne sperimentali di laboratorio hanno riguardato lo studio e il miglioramento delle tecniche esistenti e lo sviluppo di nuove per la caratterizzazione meccanico-resistente dei componenti dell'opera muraria. La ricerca si è concentrata sulla misura di parametri meccanici di mattoni pieni, quali la resistenza a compressione e il modulo di elasticità. Attualmente non vi è unanimità nella letteratura scientifica e nemmeno sulle norme su come valutare la resistenza a compressione, che comunque richiede un numero elevato di campioni e l'utilizzo di vari strumenti e tecniche. Inoltre, non esistono norme di riferimento sulla determinazione del modulo di elasticità e, pertanto, sono necessarie nuove proposte su metodologie standardizzabili. Nonostante le difficoltà incontrate nella caratterizzazione sperimentale dei mattoni, in questa ricerca sono stati proposti diversi metodi per eseguire la loro caracterizzazione meccanica. Gli approcci ed il metodo proposti hanno dimostrato la loro idoneità e applicabilità pratica.

Infine, si raccomanda una metodologia di prova per ciascuno dei parametri studiati nella ricerca, il cui obiettivo finale è la correlazione tra i valori MDT ei valori DT.

Parole chiavi: Muratura, MDT, Prove di laboratorio, Mattone pieno, Malta di calce, Compressione, Modulo di elasticità, Costruzioni storiche.

Contents

List of Figures

List of Tables

List of Symbols

Geometrical Properties Characters

Symbol	Name	Place
t	Thickness	
t_t	Thickness of the tile	[Paper I]
t_m	Thickness of the mortar	[Paper I]
w	Width	
w_t	Width of the tile	[Paper I]
w_m	Width of the mortar	[Paper I]
l	Length	
h	Height	
h_t	Height of the tile	[Paper I]
h_m	Height of the mortar	[Paper I]
A	Area	
λ	Slenderness as (h/w)	
L	Length of the helix tie (HPT)	[Paper VI]
D_e	Diameter of the helix tie (HPT)	[Paper VI]

Mechanical Properties Characters

Symbol	Name	Place
F_{ult}	Maximum compressive load testing mortar joints (UIC Leaflet 778-3R [1] DIN 1855-9:2019-04 [2])	[Paper VI]
$f_{c,k}$	Characteristic compressive strength of masonry (Eurocode 6, EN 1996-1-1:2011+A1:2013 [3])	
$f_{c,ACI}$	Characteristic compressive strength of masonry (ACI 530.1-05/ASCE 6-05/TMS 602-05 [4])	
f_b	Characteristic compressive strength of the brick	
f_c	Uniaxial compressive strength	
$f_{b,c}$	Biaxial compressive strength	
$f_{c,b}$	Compressive strength of the brick	
$f_{c,\mathrm{TILE}}$	Compressive strength of the tile	[Paper I]
$f_{c\,\mathrm{TILE,num}}$	Numerical compressive strength of the tile	[Paper I]
$f_{c,\mathrm{wh}}$	Compressive strength of the sample: Whole specimen	[Paper III]
$f_{c,\mathrm{ha}}$	Compressive strength of the sample: Half specimen	[Paper III]
$f_{c,100}$	Compressive strength of the sample: 100 × 100 × 40 mm³ specimen	[Paper II]
$f_{c,\mathrm{C40}}$	Compressive strength of the sample: 40 × 40 × 40 mm³ specimen	[Paper II]
$f_{c,\mathrm{TR}}$	Compressive strength of the sample with bearing surface treatment	[Paper III]
$f_{c,\mathrm{GR}}$	Compressive strength of the sample with grinded bearing surface	[Paper III]
$f_{c,40_{40}}$	Compressive strength of the sample: 40 × 40 × 40 mm³ specimen	[Paper IV]
$f_{c,(\mathrm{S})\_40_{80}}$	Compressive strength of the sample: stacked 40 × 40 × 80 mm³ specimen	[Paper IV]
$f_{c,(\mathrm{US})\_40_{80}}$	Compressive strength of the sample: unstacked 40 × 40 × 80 mm³ specimen	[Paper IV]

δ_{100}	Shape factor referring to a cubic specimen of 100 mm edge (Khalaf et al [5])	[Paper III]
f_t	Tensile strength	
$f_{t,b}$	Tensile strength of the brick	
E_b	Elastic modulus of the brick	
$E_{b,10\text{-}30}$	Elastic modulus of the brick obtained in the range of 10% f_c to 30% f_c	[Paper V]
ν	Poisson's ratio	
G f_c	Compressive fracture energy	[Paper I]
G f_t	Tensile fracture energy	[Paper I]
ρ_{nu}	Net dry density	
ρ_{gu}	Gross dry density	
W_s	Water absortion	
f_m	Compressive strength of the mortar	
f_{m_DPT}	Compressive strength of the mortar joint by DPT (DIN 1855-9:2019-04 [2] and UIC Leaflet 778-3R [1])	[Paper VI]
f_{m_EN}	Compressive strength of the mortar testing 40 × 40 × 40 mm^3 specimen (EN 1015-11:2020 [6])	[Paper VI]
$f_{flex,m}$	Bending strength of the mortar	
E_m	Elastic modulus of the mortar	
f_{gy}	Compressive strength of the gypsum	[Paper III]
$f_{flex,gy}$	Bending strength of the gypsum	[Paper III]
τ_H	Tangential stress produced during the Helix extraction	[Paper VI]

General Characters and Symbols

Symbol	Name	Place
κ	Parameter that control the shear response in the numerical study	[Paper I]
ρ	Parameter that the triaxial compression in the numerical study	[Paper I]
σ	Standard Deviation	
μ	Average / Mean	
ø	Diameter	
π	Pi	
©	Copyright	

Acronyms

Symbol	Name	Place
N.	Number of specimens	
CV	Coeficient of variation	
2D	Two-dimensions	
3D	Three-dimensions	
ASTM	American Society for Testing and Materials / ASTM International	
EN	European Standard developed by the European Committee for Standardization (CEN)	
DIN	Deutsches Institut für Normung e.V. / German Institute for Standardisation Registered Association	
CAN/CSA	Canadian Standards Association	
AS/NZS	Standards Australia (and New Zeland)	
ABNT	Associação Brasileira de Normas Técnicas	
ISO	International Organization for Standardization	
UIC	International Union of Railway	

MDF	Medium Density Fibreboard	[Paper III]
PTFE	Polytetrafluoroethylene (Teflon ©)	[Paper III]
NHL	Natural Hydraulic Lime mortar	[Paper VI]
CL	Calcium Lime mortar	[Paper VI]
NDT	Non-Destructive Test	[Paper VI]
MDT	Minor Destructive Test	[Paper VI]
DT	Destructive Technique	[Paper VI]
DPT	Double Punch Test	[Paper VI]
PPT	Pin Penetration Test	[Paper VI]
HPT	Helix screw Pull-out Test	[Paper VI]
LTK	Load Test Key	[Paper VI]
LTU	Load Test Unit	[Paper VI]

Chapter 1

Introduction

1.1. Background and Motivation

A large part of the built stock of many regions in the world consists of modern and historical masonry structures still in use. Many of such structures are considered as architectural heritage due to their cultural value and to their contribution to the identity of historical towns and urban centres. The protection, conservation and preservation of the architectural heritage of historical masonry buildings requires, among other needs, to evaluate and preserve their structural capacity, both at a global level and at the level of their individual components. When dealing with architectural heritage, not only the strength capacity has to be considered but also, given the building's cultural value, also the structure's authenticity has to be considered. According to the ICOMOS Venice letter (1964) "*The conservation of monuments is always facilitated by making use of them for some socially useful purpose. Such use is therefore desirable but it must not change the lay-out or decoration of the building. It is within these limits only that modifications demanded by a change of function should be envisaged and may be permitted.*".

The most common materials in historical masonry buildings are stone, solid clay bricks, adobe, and lime mortar. Solid fired clay brick masonry has been one of the most recurrent construction technologies for centuries. Generally, brick masonry has not deserved a research attention (including experimental research) comparable to that devoted to more modern structural materials such as concrete or steel.

To design masonry buildings, tradition and imitation were the only tools throughout history. From "*De Architectura*" by Vitruvius or "*De Re Aedificatoria*" by Leon Battista Alberti until the 19th century, architectural treatises only included suggestions on good building practice and rules of thumb based mainly on proportionality. During the 20th century, bricks masonry continued to be an important building material. Architects such as

Louis Sullivan, Frank Lloyd Wright, and Le Corbusier wrote extensively about the use of bricks in their buildings.

The determination of the mechanical properties of masonry structures faces significant challenges due to the intrinsic complexity of this composite material. The masonry compressive strength depends largely on that of the components, which include units and mortar. Specifically, the masonry compressive strength is highly dependent on the compressive strength of the components, and, in fact, it can be estimated using available empirical or analytical equations using the properties of the components as basic input data. The equation (1) is proposed by the Eurocode 6, EN 1996-1-1:2011+A1:2013 [3], where $f_{c,k}$ is the characteristic compressive strength of the masonry (in MPa), f_b and f_m is the compressive strength of the bricks and mortar respectively, and K is a constant. The equation (2) is proposed in the Commentary on Specification for Masonry Structures (ACI 530.1-05/ASCE 6-05/TMS 602-05) [4], where $f_{c,ACI}$ is the compressive strength of masonry (in psi), f_b is the compressive strength of bricks, and A and B are constant. Other equations such as those proposed by Hilsdorf, Khoo and Hendry, or Otto also used the properties of the components as basic input data. An analytical study of these equations is presented by Segura et al. [7].

$$f_{c,k} = K \cdot f_b^{0.7} \cdot f_m^{0.3} \quad (1)$$

$$f_{c,ACI} = A \cdot (400 + B \cdot f_b) \quad (2)$$

Regardless of the type and materials of the unit, the experimental compressive strength of the units depends on the specimen's dimensions and the confinement produced between the specimen and the press platens. Despite encouraging advancements, significant additional research is still needed for an accurate and efficient characterization of the mechanical properties of masonry components in existing buildings. Actually, the experimental assessment of the compressive strength on solid fired clay units has always been a subject of debate, and many standards describe different specimen shapes, sizes and bearing surfaces treatments, showing an existing lack of consensus about a common criteria and procedures. In addition, available international standards and studies usually propose characterisation procedures and methodologies which ignore parameters such as unit shape, the form, the material and the manufacturing process, which are parameters known to influence largely of the mechanical parameters and, specifically, on the brick compressive strength.

The structural verification of existing masonry buildings, aimed to their maintenance or refurbishment, requires a detailed analysis of the performance against both gravity loads and horizontal actions. The analysis of existing masonry buildings, however, faces significant difficulties due to the complexity of masonry as both construction technology and structural material. One of the main difficulties lies in the realistic characterization of the mechanical

properties and, more specifically, of the masonry compressive strength, which has often a critical influence on the structural performance of masonry members. In addition, the mechanical characterisation of solid fired clay bricks from samples extracted from existing buildings poses specific challenges due to the fact that sample extraction is severely restricted in architectural heritage buildings.

Outstanding examples of contemporary architecture have incorporated brick masonry as structural material. Eladio Dieste, a Uruguayan architect, is known for his innovative use of reinforced brick structures. He developed a system of brick construction that was both economical and efficient, using thin, curved bricks to create vaulted structures that were remarkably strong and stable, as in the Cristo Obrero Church in Atlántida, Uruguay. Rafael Moneo, a Spanish architect, is known for his sensitivity to the local context and his use of traditional materials in his buildings. Moneo has used brick extensively in his work, often using it to create subtle textures and patterns that reflect the surrounding environment, as in the Museum of Roman Art in Mérida, Spain.

Current masonry societies such as American Society for Testing and Materials (ASTM), the European Committee for Standardization (CEN), the Council of Standards Australia and New Zealand (AS/NZS), the Standard Council of Canada (CAN/CSA), or the International Union of Laboratories and Experts in Construction Materials, Systems and Structures (RILEM), have issued and adopted standards and recommendations dealing with testing procedures for masonry. Nevertheless, meaningful contradictions can be found among the along with, in many cases, absence of specifications for certain mechanical properties, proposed procedures in need to of more detailed and clear specifications. In specific, it can be seen that the value determined for the compressive strength of the masonry units can depend strongly on the standards being applied. In turn, there is no standard dealing with testing procedures for the determination of the elastic modulus or tensile strength of masonry clay units. These limitations suggest that there is a clear need for additional criteria and procedures for the mechanical characterization of solid fired clay units. These procedures should consider, in specific, the physical parameters that influence on the experimental tests and the resulting mechanical properties.

In the case of heritage masonry buildings, the premise of minimal material destruction highlights the importance of Minor Destructive Tests (MDT) and Non-Destructive Tests (NDT) as preferred approaches for the characterization of the material. However, these procedures require an accurate previous calibration validation.

The accomplishment of the above needs and aims is requires the development of accurate procedures for the mechanical characterisation of the masonry components. First, there is the necessity to develop and/or improve existing procedures for the measurement of the compressive strength of the solid fired clay bricks taking into account the parameter that influence on the strength, such as the specimen dimensions and the confinement produced between the specimen and the press platens. Second and third, there is the necessity to

develop a methodology for the measurement of the modulus of elasticity and the tensile strength on solid bricks. And fourth, there is also the need to calibrate minor destructive tests (MDT) allowing the characterisation in-situ of the mechanical properties of the masonry components in existing buildings. The pursuit of a methodology that can effectively be used for the characterisation of masonry components is an on-going challenge. Advances in characterization methods during the 20th century have significantly contributed to it. It is the motivation of this work to address these challenges, and investigate the physical conditionings that influence on the laboratory experimental test and on the representativity of in-situ MDT tests.

1.2. Scope and Objectives

The general objective of this research is to propose a body of methodologies for the characterisation of masonry components (units and mortars) using a combination of destructive tests (DT), applied in the laboratory on masonry samples, and minor destructive tests (MDT) applied in-situ over the structure being investigated. The proposal is based on a critical analysis of the limitations of the current procedure for the mechanical characterisation of masonry units. More specifically, the research focuses on historical masonry made of solid fired clay bricks and lime mortar.

The following specific objectives have been envisaged in order to attain the aforementioned general objectives:

- To investigate comprehensively the state-of-the-art on the mechanical characterisation of the existing masonry components, including both solid fired clay bricks and lime mortar joints. In particular, to carry out an exhaustive study of the state-of-the-art on destructive tests (DT) applicable in the mechanical characterization of masonry components executed in the laboratory and minor destructive tests (MDT) applicable in-situ over existing masonries.

- To improve the experimental knowledge on testing methodologies applied to mechanically characterise solid fired clay bricks based on destructive tests (DT) carried out in the laboratory. These techniques are investigated, in specific, for mechanically extruded bricks and handmade ones. This objective includes the following aims:
    - To develop and validate a novel methodology for the mechanical characterisation of thin bricks (with small thickness) as those used in the construction of timbrel vaults. In specific, to develop a technique for the measurement of the compressive strength.

- To validate the use of the non-standard 40 x 40 x 40 mm^3 specimen for the measurement of the compressive strength of brick extracted from existing masonry building. In specific, and through a detailed experimental comparison, to correlate the brick compressive strength measured with such specimen with that obtained with the standard 100 x 100 x 40 mm^3 specimen defined in the European standards.
- To characterize the brick material anisotropy by testing cubic specimens under compression along the three brick directions (length, width and thickness), and validate the observations through a statistical approach.
- To formulate a method for the estimation of an equivalent compressive strength in brick specimens that exhibit an hardening response without identifiable stress peaks. The method is based on the identification of singular points separating material transformed states in the experimental stress-displacement curves.
- To evaluate the influence of a series of parameters such as the cross-section aspect ratio, the bearing surface treatment, the stacking procedure, and the specimen slenderness on the compressive strength of solid fired clay brick.
- To compare the characteristic compressive strengths obtained through the use of different methods proposed by the main masonry standards, including: ASTM [8], CEN [9], CAN/CSA [10], and AS/NZS [11].
- To develop and validate a novel methodology for the experimental measurement on laboratory of the elastic modulus of brick specimens, and to derive an experimental ratio between the elastic modulus and the compressive strength.

- To improve and validate experimental testing methodologies to characterise solid fired clay bricks and mortar joints by using in-situ minor destructive tests (MDT) in existing masonry structures. The MDT should be calibrated by comparison with results obtained by means of destructive tests (DT) executed in laboratory. This objective includes the following aims:
  - To select tests set-ups to adequate for the in-situ application of the MDT on masonry components.
  - Calibrate and validate the experimental MDT measurements by comparison with results obtained with laboratory standardized DT.
  - Provide a feasible correlation between the results of both testing methodologies (DT and MDT) allowing the in-situ characterisation of mechanical properties of masonry components.

1.3. Methodology

The methodology applied to fulfil the aforementioned general and specific objectives has been based on the following tasks:

- First, a detailed literature review on experimental techniques for the measurement of mechanical properties, allowed to select the testing techniques and procedures to be analysed.

- Second, a sample of different types of solid fired clay bricks was carefully selected in order to gather a representative sample of the most common bricks used in masonry structures. The sample includes both mechanically extruded and handmade manufactured bricks.

- Third, a series of experimental campaigns were carried out on the brick samples selected. In specific, some aspects influencing on the experimental strength value were investigated. Four independent campaigns were performed, including: (1) the measurement of the compressive strength of tiles characterized by a limited thickness, (2) the characterisation of the material anisotropy, (3) the study of the influence of the cross section aspect ratio and the confinement produced by the bearing surface treatment on the compressive strength, and (4) the study of the influence of the stacking procedure and the specimen slenderness on the compressive strength. These experimental campaigns have resulted in Papers I, II, III, and IV, already published or into review and mentioned in the following section.

- Fourth, a novel procedure is proposed to determine the elastic modulus of solid clay bricks. Three main aspects were investigated: (1) how to provide an stable and reliable support to the transducer during the test, (2) the investigation of the influence of the specimen shape, i.e., slenderness and cross-sectional loading area, and (3) the testing procedure itself. The results of the elastic modulus allowed to: (1) characterize the material anisotropy, and (2) identify an experimental relationship between the compressive strength and the elastic modulus. The results are presented in Paper V mentioned in Chapter 2.

- And additional experimental programme was performed on existing buildings in Barcelona (Spain). The campaigns allowed the calibration and validation of the MDT used to characterize the mechanical properties of the existing masonry components. These campaigns are presented in Paper VI mentioned in Chapter 3.

- Each of the different experimental campaigns progressed according to the following phases:

  - Compile a specific state-of-the-art to detect the research needs,
  - Design the individual campaigns,
  - Perform the tests executed on specimens prepared in the laboratory,
  - Perform the MDT tests executed in-situ in existing masonry buildings.
  - Analyse and validate the experimental results,
  - Compare the experimental results with available databases and the scientific literature,
  - Draw conclusions.

- Once the experimental campaigns were performed and the papers were prepared, the latter were organised into this document. Papers dealing with the mechanical characterisation of the unit were included in Chapter 2, while the paper dealing with the application of MDT was included in Chapter 3.

- Finally, global conclusions were drawn with respect to the experimental program carried out, and future lines of works were proposed.

1.4. Outline of the thesis

This work is organised in four chapters. The first chapter introduces the motivation, the scope and the objectives and the methodology of the present thesis. The remaining three chapters are organised in the following way.

Chapter 2: Characterisation of Masonry Units

This chapter contains the mechanical characterisation of the masonry units, including the evaluation of the compressive strength and the elastic modulus. The characterisation is carried out testing mechanically extruded solid fired clay bricks and handmade ones. Handmade bricks include modern manufactured bricks and historic ones collected from existing building in Barcelona (Spain). The compressive strength analysis of the masonry unit is organised in subsections depending on the objectives of analysis: (1) the measurement of the compressive strength of tiles characterized by a limited thickness, (2) the characterisation of the material anisotropy, (3) the study of the influence of the cross section aspect ratio and the confinement produced by the bearing surface treatment on the compressive strength, and (4) the study of the influence of the stacking procedure and the specimen slenderness on the compressive strength. The chapter also includes the study of a methodology to test the elastic modulus of the bricks.

Chapter 3: Calibration of MDT

This chapter details two minor destructive tests (MDT) to characterise in-situ the masonry components, bricks and mortar joints. The MDT values has been compared with the destructive tests (DT) results carried out in the laboratory. The MDT include the pin penetration test (PPT) and the helix screw pull-out test (HPT). The analysis helps to calibrate the MDT offering the possibility of testing in-situ the masonry components avoiding the destruction of part of the masonry wall.

Chapter 4: Conclusions

The closing chapter of the thesis summarizes and recapitulates the conclusions drawn in the preceding chapters and highlight the main conclusions reached. Finally, it presents suggestions for future works.

1.5. Research Dissemination

This doctoral thesis is presented as a compendium of publications as allowed by the Universitat Politècnica de Catalunya. All the scientific publications are related to masonry characterisation and are published in journals that belong to the category Construction and Building Technology in Journal Citation Reports (JCR), classified within the first quartile (Q1) as required by the specific Doctoral School regulations. The research conducted in this manuscript has resulted in the following scientific publications at the moment of submission of the PhD thesis:

Articles in peer-reviewed published in an international journal that belongs to the category Construction & Building Technology in Journal Citation Reports (JCR), classified within the first quartile (Q1):

- **Paper I** - Cabané, A., Saloustros, S., Pelà, L., Roca, P. (2021) Experimental setup and numerical evaluation of the compression test on thin tiles for masonry timbrel vaults. *Construction and Building Materials*, Vol 313, p. 125294. *doi.org/10.1016/j.conbuildmat.2021.125294*

- **Paper II** - Cabané, A., Pelà, L., Roca, P. (2022) Anisotropy and compressive strength evaluation of solid fired clay bricks by testing small specimens. *Construction and Building Materials*, Vol 344, p. 128195. *doi.org/10.1016/j.conbuildmat.2022.128195*

- **Paper III -** Cabané, A., Pelà, L., Roca, P. (2023) Effect of cross section aspect ratio and bearing surfaces treatment on the compressive strength of solid fired clay brick specimens. *Construction and Building Materials*, Vol 383, p. 131397. *doi.org/10.1016/j.conbuildmat.2023.131397*

Articles under review for publication in a journal that belongs to the category Construction & Building Technology in Journal Citation Reports (JCR), classified within the first quartile (Q1):

- **Paper IV -** Cabané, A., Pelà, L., Roca, P. Influence of specimen slenderness and stacking on the experimental strength of solid fired clay bricks. *Under review. Journal of Building Engineering.*

- **Paper V -** Cabané, A., Pelà, L., Roca, P. Experimental evaluation of the elastic modulus of solid fired clay bricks and correlation with compressive strength. *Under review. Construction and Building Materials.*

- **Paper VI -** Cabané, A., Pelà, L., Roca, P. Laboratory and in-situ mechanical characterisation of masonry components by comparing destructive and minor destructive testing techniques. *Under review.*

Two more papers referring to the characterisation of the masonry containing my participation have not been incorporated in this document.

- Segura, J., Pelà, L., Roca, P., Cabané, A. (2019) Experimental analysis of the size effect on the compressive behaviour of cylindrical samples core-drilled from existing brick masonry. *Construction and Building Materials*, Vol 228, p. 116759. *doi.org/10.1016/j.conbuildmat.2019.116759*

- Makoond, N., Cabané, A., Pelà, L., Molins, C. (2020) Relationship between the static and dynamic elastic modulus of brick masonry constituents. *Construction and Building Materials*, Vol 259, p. 120386. *doi.org/10.1016/j.conbuildmat.2020.120386*

Additionally, articles and presentations in international conferences:

- Cabané, A., Pelà, L., Roca, P. (2021) Laboratory and in-situ characterisation of masonry materials in a large historical industrial building in Barcelona. *Proceeding of 12th International conference on Structural Analysis of Historical Constructions, Barcelona, Spain.* DOI: 10.23967/sahc.2021.144

- Cabané, A., Pelà, L., Roca, P. (2023) Measurement of solid brick compressive strength and anisotropy on non-standard small cubic specimen. *Accepted for presentation in 13th International conference on Structural Analysis of Historical Constructions, Kyoto, Japan.*

Chapter 2

Characterisation of Masonry Units

2.1. Introduction

Characterizing solid fired clay bricks mechanical properties presents difficulties related to their shape and testing procedures. Based on the literature reviewed, this research addresses some of the needs encountered to characterize the masonry units in relation with: the thickness of the brick samples, the material anisotropy, the cross-section aspect ratio between the length and width, the loading bearing surface treatment, the stacked procedure and the specimen slenderness.

Section 2.2 reproduces Paper I, devoted to the experimental setup and numerical evaluation of the compression test on thin tiles for masonry timbrel vaults. This paper presents an experimental campaign and a numerical validation of a novel testing setup for estimating the compressive strength of thin clay tiles used in timbrel vaults. The experimental campaign focuses on two different types corresponding to historical and modern handmade tiles.

Section 2.3 reproduces Paper II, devoted to the anisotropy and compressive strength evaluation of solid fired clay bricks by testing small specimens. This paper presents a study on the use of a non-standard $40 \times 40 \times 40$ mm^3 specimen for the experimental measurement of the compressive strength of solid fired clay bricks extracted from existing masonry buildings. The viability of such specimen has been assessed by comparison with experimental results obtained with the standard $100 \times 100 \times 40$ mm^3 specimen. Using the mentioned small cubic specimen, a detailed research on the compressive strength and the anisotropy of different solid clay brick types has been carried out by applying a statistical approach.

Section 2.4 reproduces Paper III, devoted to the effect of cross section aspect ratio and bearing surfaces treatment on the compressive strength of solid fired clay brick specimens. This study addresses the evaluation of the confinement effect in the experimental

determination of compressive strength in solid fired clay units. The research considers different standard specimens, such as whole or half brick, and 100 × 100 × 40 mm^3 specimen, and non-standard 40 × 40 × 40 mm^3 specimen, subjected to different standard bearing surface treatments, i.e., grinding, capping with cement mortar or gypsum plaster, placing with birch plywood or fibreboard. Additionally, two novel bearing surface treatments are proposed, i.e., covering with gypsum powder, and placing two oiled PTFE leaves.

Section 2.5 reproduces Paper IV, devoted to the influence of specimen slenderness and stacking on the experimental strength of solid fired clay bricks. This study addresses the evaluation of the slenderness effect in the experimental determination of compressive strength in solid fired clay units. The research considers different standard and non-standard specimens with 40, 50, 60, 70, 80, 90, and 100 mm width and 40, 80 and 120 mm height.

Section 2.6 reproduces Paper V, devoted to propose a novel procedure to determine the elastic modulus of solid clay bricks. Three main aspects were investigated: (1) how to provide a stable and reliable support to the transducer during the test, (2) the investigation of the influence of the specimen shape, i.e., slenderness and cross-sectional loading area, and (3) the testing procedure itself. The results of the elastic modulus allowed to: (1) characterize the material anisotropy, and (2) identify an experimental relationship between the compressive strength and the elastic modulus. One this procedure was calibrated and a methodology was recommended, a second research with Makoond et al. [12] was carried out to propose an empirical expression that can be used to estimate the static elastic modulus from the dynamic modulus of the tested bricks calibrating a Non-Destructive Tests (NDT).

2.2. Paper I – Experimental setup and numerical evaluation of the compression test on thin tiles for masonry timbrel vaults

A. Cabané, S. Saloustros, L. Pelà, P. Roca

Construction Building Materials 313 (2021) 125294

https://doi.org/10.1016/j.conbuildmat.2021.125294

Abstract. Compressive tests on clay tiles used in historical masonry timbrel vaults are hindered by the relatively small thickness of the specimens, resulting in buckling or confinement problems depending on the loading direction. This paper presents an experimental campaign and a numerical validation of a novel testing setup for estimating the compressive strength of thin clay tiles used in timbrel vaults. The experimental campaign focuses on two different types corresponding to historical and modern handmade tiles. Experimental and numerical results show that the proposed test setup can be used for the estimation of the compressive strength of thin clay tiles.

I.1. Introduction

Timbrel vaults or timbrel arches are masonry elements made with thin clay tiles (with approximate dimensions 300 × 150 × 15/20 mm[3]) and mortar (gypsum, lime or cement). The singularity of timbrel structures lies in their construction system. They are generally built with two or more layers of tiles placed with their bed tangent to the circumference of the vault or arch. The construction starts by fixing the first tiles to the walls at the sides of the vault using fast-setting mortar. Then, the first layer is developed through the gradual placement of tiles next to the previously placed ones. The use of fast-setting mortar makes possible a fast construction without scaffolding or supporting formwork. While the first layer is under construction, the following layer of tiles is built over the first one, using a mortar layer with a thickness of few millimetres between the two layers. Each successive layer is constructed adopting a head joint discontinuity with the previous one. This traditional construction technique is described in detail in works by Truñó [13], Moya [14] or Gulli [15]. The main characteristic of timbrel vaults and arches is their limited thickness, sometimes as small as 0.07 m, which is enabled by the use of the thin clay tiles. Another geometric characteristic is the high slenderness, intended as the ratio between the span and the thickness, reaching values even around one hundred [16]. This construction technique has been historically used to make vaults of a great variety of shapes and dimensions. The largest timbrel vault ever built is the dome over the crossing in St. John the Divine, New York, with a span of 33 m [17].

This construction system has been historically present in some littoral Mediterranean countries such as Spain ("bóveda tabicada" or "volta a la catalana"), France ("voûte plate" or "voûte à la Roussillon") and Italy ("volta in foglio"). The first architectural text that refers to the construction of the timbrel vaults, Arte y Uso de la Arquitectura [18], was written by Fray Lorenzo de San Nicolás in the 17th century and defines some stability rules relating the dimensions of the supporting wall to the length of the vault. In the middle of the 18th century, d'Espie [19] and Laugier [20] described the construction system of the timbrel vault making special mention to its lightness and its incombustibility. In all of them, until well into the 19th century, the proportion rule was the main form for the design of these vaulted structures [21]. During the following 18th and 19th centuries the development of the scientific theory of the vaulted structures begins based on an equilibrium analysis and using graphical methods for the definition of the line of thrust within the arch. In this context, at the end of the 19th century, Gaudí [22,23] used funicular models in his constructions, and in 1892 Guastavino Moreno [24] executed strength tests in tension, bending and shear of some specimens to understand the structural behaviour of the timbrel vaults, classified as "cohesive constructions" (Fig. 1a).

Fig. 1 Example of two buildings with timbrel vaults using thin clay tile. A) Guastavino standing on a timbrel arch with the timbrel vaults under construction [Photograph adapted from [25], distributed under a CC BY 2.0 license]. B) Weaving room in Can Batlló industry in Barcelona at the beginning of the 20th century [Photograph by [26], AGDB. Diputació de Barcelona ©]

The structural analysis of timbrel vaults between the end of the 19th century until today is characterized in general by two approaches. On the one hand, the assumption of a zero tensile strength of masonry motivated the use of equilibrium analysis, such as the membrane theory for domes developed by Rankine and popularized by Dunn [27]. In the middle of the 20th century, the equilibrium approach and the development of the fundamental theorems of plasticity were applied to masonry vaults in Heyman's limit analysis theories [28,29]. On the other hand, the application of Navier's elastic theory was applied to study the equilibrium of timbrel vaults based on the concepts of material strength and the principles of mechanics considering a homogeneous and isotropic material. Towards the end of the 20th century and until today, the Finite Element Analysis has been widely adopted as way to model vaulted structures [30]. The main challenge in this approach is the need for a detailed knowledge of the material properties, which for the case of existing timbrel vaults, is still a challenge due to the limited thickness of the utilized tiles and mortar joints.

The timbrel arches and vaults are present in traditional [31,32], industrial [33] (Fig. 1b) and vernacular [34] architecture. During the last century, Guastavino Expósito, the GATCPAC ("Grup d'Arquitectes i Tècnics Catalans per al Progrés de l'Arquitectura Contemporània", Group of Catalan Architects and Technicians for the progress of modern architecture), Le Corbusier [35], Moya [14,36], Dieste [37], and many others designed architectural structures based on this constructive system. Nowadays, the importance of the conservation and restoration of this type of masonry construction, considering not only its architectural value but also its structural authenticity [38], motivates the use of accurate analysis methods. Such tools are strongly necessary to estimate the strength capacity, their safety level against exceptional actions such as earthquakes, and the effect of possible changes in the use requiring a load increase. Furthermore, these structures have begun to play an important role in the 21st century architecture [39,40] thanks to the development of new computerized methods by Block et al. [41,42] allowing the design of innovative structures with great geometric versatility [43,44].

Modern structural analysis techniques for the design of new vaults or the structural assessment of existing ones, based either on FEM or other analytical approaches, require the knowledge of the materials' properties and in particular of the compressive strength of the vault's components. The compressive strength of the mortar from existing timbrel vaults can be obtained by the Double Penetration Test following the DIN 18555-9:2019-04 [2,45,46]. With regard to the compressive strength of the units, the European EN 772-1:2011+A1:2016 [9] or the American ASTM C67/C67M-21 [47] are the main related standards, but present some limitations as for their applicability to thin tiles. EN 772-1:2011+A1:2016 [9] considers testing the brick specimens flatwise with thicknesses over 40 mm for the determination of compressive strength. ASTM C67/C67M-21 [47] allows testing the bricks specimens flatwise, that is, with the load applied in the same direction of the depth of the unit, considering half

unit. The same standard also allows testing structural clay tile specimens in a position "such that the load is applied in the same direction as in service".

It becomes apparent that testing an entire thin tile unit flatwise or edgewise presents important drawbacks. Flatwise test configuration produces an overestimated strength due to the excessive confinement exerted by the loading platens to the small thickness specimen, while the edgewise test configuration may lead to an underestimated strength due to the geometrical effects provided by the excessive slenderness of the specimen [48]. Previous researches focused on tests on whole tiles applying the load perpendicular to the stretcher or header with a considerable specimen slenderness [49–53]. Testing a single tile perpendicular to the stretcher, the slenderness is around 7.5, and testing perpendicular to the header, the slenderness is around 15. This slenderness value is excessive for a compression test as the maximum capacity may be influenced by buckling of the specimens. To the authors' knowledge, no other recommendations are available in the literature.

This paper proposes a new methodology for testing thin clay tiles that overcomes the problems arising from their limited thickness, i.e., increased confinement or slenderness depending on the loading direction. For this purpose, a new test specimen assembled by two clay tiles is proposed. Considering the fact that tiles experience compression perpendicular to the stretcher and/or header direction within a timbrel vault, as well as the anisotropy of some types of clay units [54–56], the loading direction of the proposed specimen is perpendicular to the stretchers or headers of the tiles. The test on an assembled specimen instead of a single tile permits the reduction of the slenderness until values similar to those recommended by standards EN 772-1:2011+A1:2016 [9] (0.4 to 3.84) or by the available literature on clay units (2.0 to 2.5) [57] or concrete units (1.5 to 4) [58,59].

The validation of the proposed testing setup for the characterization of the compressive strength of thin tiles is carried out through an experimental and numerical study. An experimental campaign was carried out on existing tiles extracted from timbrel vaults of two 19th century industrial buildings in Barcelona (Spain), one of them with an extension built at the beginning of the 20th century, as well as on modern handmade bricks with known mechanical characteristics. The latter case study allowed the comparison of the experimental results obtained from the new developed specimens with those derived from the standardized specimens. This research pays special attention to the use of a new type of specimen and a test protocol for the strength characterisation of thin tiles with the following specific objectives: (1) Exploring the possibility of evaluating the mechanical behaviour of the tile under compression by means of laboratory tests; (2) analysing the consistency and reliability of the results obtained, as well as the acceptability of the experimental scattering; (3) determining size-effect correlations in the estimation of the compressive strength based on the comparison between experimental results and Finite Element simulations.

The paper is structured in five sections. After this introduction, Section I.2 presents the experimental campaign performed on thin-tile units, including the description of the

material, the specimen preparation, the test procedure and the experimental results. Section I.3 presents the Finite Element (FE) simulation of the compression tests on thin clay tiles. Section I.4 analyses the influence of the specimen geometry comparing the experimental and numerical simulation strength on modern handmade units. The paper ends with Section I.5 presenting some concluding remarks.

I.2. Experimental study

This section presents the experimental campaign on historical thin-tiles and modern handmade bricks for determining their compressive strength. Details are provided related with the description of the materials, the preparation of the proposed specimen and its geometry, the testing setup and the experimental results. As mentioned, the historical samples were collected from two 19th century industrial buildings in Barcelona and the early 20th century building extension. All experimental tests were carried out at the Laboratory of Technology of Structures and Materials of the Technical University of Catalonia (UPC-BarcelonaTech).

I.2.1. Materials

In this work, two types of solid clay units were studied (Fig. 2). The first type of units corresponds to modern handmade solid clay bricks identified with the acronym 'Mo'. The second type of units corresponds to historical thin-tiles collected from three different timbrel vaults of two industrial buildings in Barcelona (Spain) and are identified with the acronyms 'Hi/I'. Both types, 'Mo' and 'Hi/I', were traditionally manufactured in a brickyard by moulding. They were shaped in a wooden mould sprinkled with dry fine sand and, after extracted from the mould, the bricks were fired into a coal-fired kiln. The number of the tested historical thin-tiles ('Hi/I') was limited due to the restrictions imposed by the cultural value of the surveyed buildings, while the modern handmade ('Mo') gave the possibility to test a larger number of specimens.

Table 1 presents a description of the sampled materials in terms of origin, acronym, number of tested specimens and average dimensions measured according to EN 772-16:2011 [60]. With regard to the modern handmade units 'Mo', half of them were tested keeping their original thickness ('Mo$_1$'), while for the other half (Mo$_2$) their thickness was reduced to approximately 30 mm through polishing of the bed surfaces by a grinder fitted with a rotary diamond-impregnated disc.

Table 1 Sampled materials in terms of origin, acronym, number of specimens collected and average dimensions. Values in brackets correspond to the coefficients of variation.

Sampled materials			
Origin	Acronym	Number of tiles	Av. dimensions (mm) [Coefficient of variation %]
Modern Handmade	Mo_1	6	306 [1.4%] × 146 [1.5%] × 45.7 [2.7%]
	Mo_2	6	306 [1.4%] × 146 [1.5%] × 30.1 [5.9%]
1878 – Industrial building	Hi/I_1	7	294 [0.4%] × 145 [0.8%] × 20.8 [2.6%]
Early 20th c. – Industrial building	Hi/I_2	7	284 [7.1%] × 145 [1.0%] × 18.4 [2.8%]
1870/75 – Industrial building	Hi/I_3	6	299 [1.3%] × 146 [1.4%] × 20.0 [4.1%]

The modern handmade bricks ('Mo') have dimensions of 306 × 146 × 45.7 mm³, which allowed their mechanical characterization in the laboratory following the EN 772-1:2011+A1:2016 [9]. Cut specimens with size 100 × 100 × 40 mm³ were tested under compression and the result was corrected by considering the corresponding shape factor of 0.7 indicated by the standard to account for the confinement effect ($f_{c,b}$). The net and gross dry density (ρ_{nu} and ρ_{gu}) were obtained according to EN 772-13:2001 [61] and EN 772-3:1999 [62], and the water absorption (W_s) following EN 772-21:2011 [63]. The values of Young's Modulus (E_b) and Poisson's ratio (ν) were determined following the testing procedures proposed in Makoond et al. [12], while the tensile strength ($f_{t,b}$) was measured through uniaxial tensile tests [64]. Table 2 presents the mechanical characteristics of the modern handmade bricks ('Mo').

Table 2 Mechanical characteristics of the modern handmade brick ('Mo'). Values in brackets correspond to the coefficients of variation

	$f_{c,b}$ (MPa)	E_b (GPa)	ν (-)	$f_{t,b}$ (MPa)	ρ_{nu} (kg/m³)	ρ_{gu} (kg/m³)	W_s (%)
	EN 772-1	Makoond et al. [12]	Makoond et al. [12]	uniaxial test	EN 772-13	EN 772-13	EN 772-21
Modern Handmade	17.4 [8%]	5.55 [23%]	0.11 [51%]	1.4 [36%]	1631 [6%]	1761 [1%]	15.7 [7%]

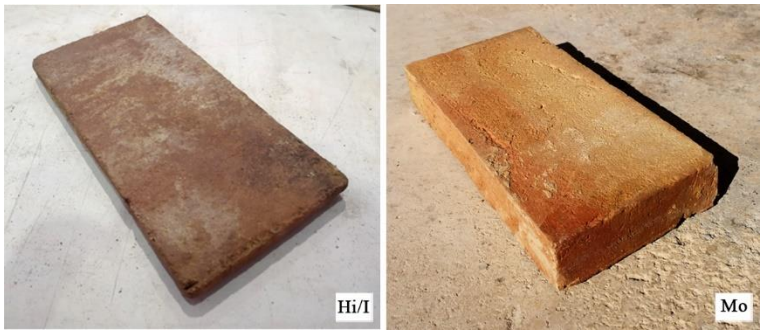

Fig. 2 Historical solid fired clay tile from industrial building ('Hi/I') (left) and modern handmade solid fired clay brick ('Mo') (right)

I.2.2. Preparation of specimens and testing procedure

The motivation behind the proposal of a new test setup for the derivation of the compressive strength from thin clay tiles lies on their slender geometry. In particular, the small thickness of the tiles used in timbrel vault construction (ranging between 15 mm and 20 mm) does not comply with the testing recommendations of EN 772-1:2011+A1:2016 [9] and ASTM C67/C67M-21 [47].

As an alternative to the testing of a single tile specimen, it is proposed here to test an assembled specimen consisting of two tile portions, bonded with a layer of cement mortar that is not in contact with the platens of the hydraulic press. The two specimens should be obtained from the same unit to reduce the variation in strength and stiffness between the two tiles. According to Table A.1. of standard EN 772-1:2011+A1:2016 [9], the height of the tested specimen can have any of the following values: 100 mm, 65 mm, 50 mm and 40 mm. Height values of 65 mm, 50 mm and 40 mm were discarded to reduce the effect of possible internal material imperfections that could increase the dispersion of the results. Fig. 3 presents the final geometry and composition of the proposed specimen, consisting of two portions of the same tile measuring 100 × 100 × t_t mm^3 each of them, bonded with an intermediate cement mortar joint with a thickness of 20 mm. The central cement mortar joint ensures an efficient coupling of the two tile portions, allowing the load transfer on both of them during the compressive test.

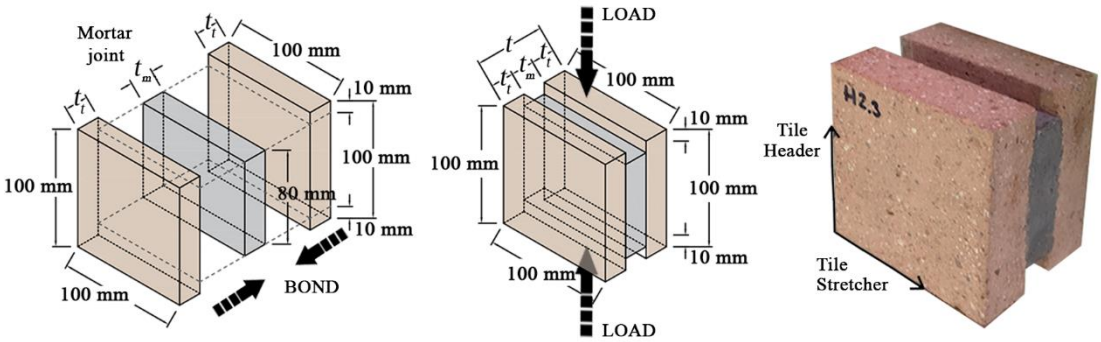

Fig. 3 Specimen proposed to obtain the compressive strength of the tile: specimen components (left), loading direction considered over the specimen (centre), and photography of Mo$_2$ specimen (right)

The extraction of the historical tiles from the vault was carefully carried out in situ with a chisel and a hammer, as shown in Fig. 4. First, was used a jackhammer to remove the pavement or the plaster and one tile was broken and removed with hammer and chisel. Then, a thin chisel was used to remove all the lime mortar joints around the tile to be extracted. Finally, a trapezoidal trowel was slowly inserted under the bed of the tile from the stretcher side and used as a lever. While levering the tile up, the trowel was lightly tapped with a nylon hammer, trying to avoid any crack appearance in the tiles. The tiles 'Hi/I$_3$' were extracted

from the intrados of the vault after the removal of the plaster, while the 'Hi/I_1' and 'Hi/I_2' samples were extracted from the extrados of the vaults after the removal of the pavement. All mortar remains on the surface of the extracted tiles were manually removed using a wire brush with metal bristles without damaging the ceramic unit. Finally, the tiles were packaged, labelled and transported to the laboratory.

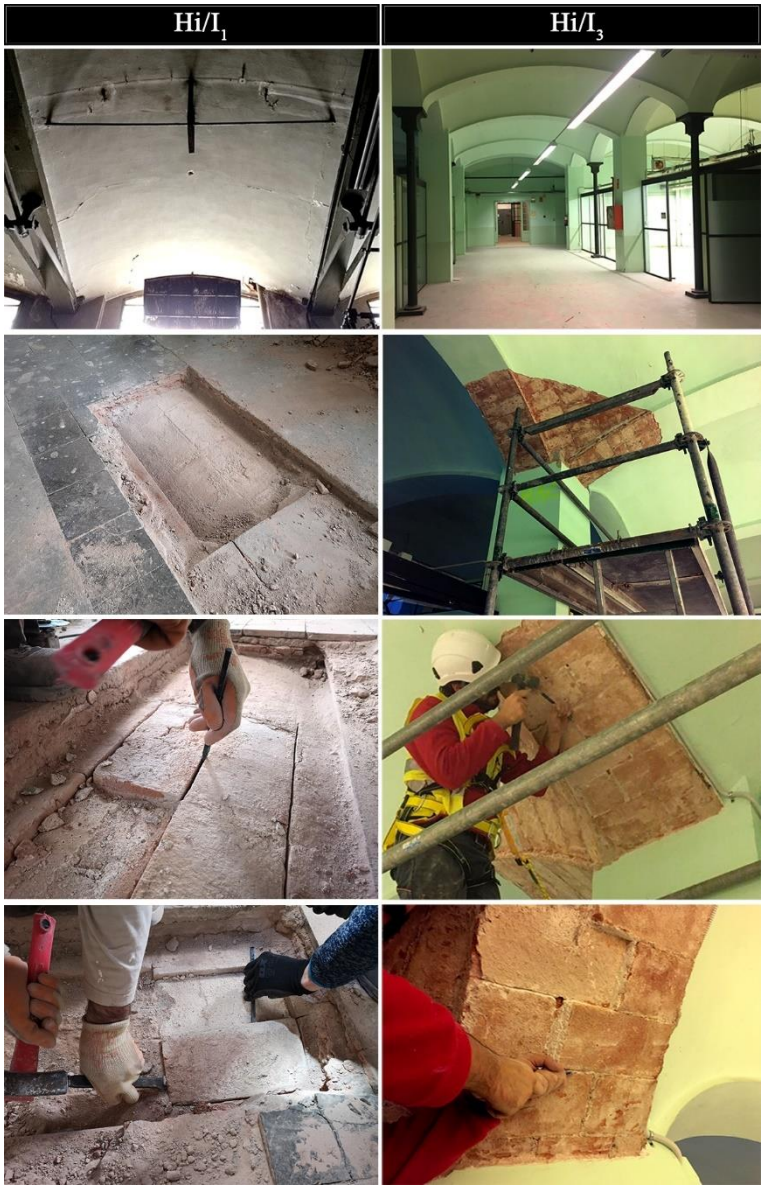

Fig. 4 The extraction process of the historical tiles from the existing vaults in two different buildings. The left column shows the extraction of 'Hi/I_1' samples from the extrados of the timbrel vault, and the right column shows the extraction of 'Hi/I_3' ones from the intrados of the timbrel vault

The proposed specimens were assembled in the laboratory according to the procedures specified in European Standards EN 772-1:2011+A1:2016 [9] for solid clay units and the EN 998-2:2018 [65] for cement mortar. Each tile was divided into two portions of 100 × 110 × t mm^3 (width × height × thickness) using a table saw equipped with a water jet (Fig. 5a). After

the tile portions were saturated with water, they were connected with a fast-setting cement mortar layer using a mould specially developed for this test (Fig. 5b). This cement mortar layer with dimensions 100 × 80 × 20 mm^3 (width × height × thickness) was centred at the middle height of the two tiles. It is noted that the mortar does not reach the upper and lower boundaries of the tiles and thus it is not in contact with the hydraulic press platens. As a result, the mortar does not carry the load during the test and acts only as a coupling device between the two tiles. The compressive strength (f_m) and the bending strength ($f_{flex,m}$) of the binding mortar were evaluated according to EN 1015-11:2020 [6], by using prisms with dimensions of 160 × 40 × 40 mm^3 that were casted with the same material employed by the mason during the construction of the assembled specimens. The evaluation of the Young's modulus (E_m) was carried out on mortar prismatic specimens of 160 × 40 × 40 mm^3 according to the testing procedures proposed in [12]. A summary of the results is presented in Table 3. After 24 hours of the mortar casting, the assembled specimen was removed from the mould and was left to dry in a laboratory environment for a minimum of 14 days at a temperature above 15ºC and a relative humidity below 65%. Lastly, the load surfaces of the assembled specimen were dry-polished by a 3-axis vertical milling machine fitted with a rotary diamond disc to reduce with high precision the height from 110 mm to 100 mm (Fig. 5c). This aimed to guarantee that the loading surfaces were smooth and on the same plane, avoiding any possible source of imperfection on the loading planes. Finally, 29 specimens were obtained, 12 of modern handmade brick (6 'Mo$_1$' and 6 'Mo$_2$') and 17 of historical tiles (5 'Hi/I$_1$', 7 'Hi/I$_2$' and 5 'Hi/I$_3$').

Table 3 Mechanical characteristics of the binding mortar. Values in brackets correspond to the coefficients of variation

	f_m (MPa) EN 1015-11	$f_{flex,m}$ (MPa) EN 1015-11	E_m (GPa) Makoond et al. [12]
Mortar	61.4 [28%]	7.6 [22%]	34.2 [31%]

The assembled specimens were tested making use of an Ibertest testing machine composed by a steel frame with a load cell of 200 kN (AUTOTEST 200/10 SW) and connected to a MD5 electronic module for data acquisition. The assembled specimens were centred on the steel plates with the grinded surfaces orthogonal to the direction of the loading, and tested under displacement control at a rate of 0.2 mm/min (Fig. 5d). The rate of 0.2 mm/min was calibrated empirically in order to guarantee, at least, a test duration of 60 s. The tests were stopped manually after registering part of the post-peak softening response.

Fig. 5 Manufacturing process of the proposed specimen. A) Tile portions with dimensions of 100 × 110 × t mm^3 obtained by cutting the tiles. B) Mould used to connect the two tiles together with a fast setting cement mortar. C) Dry polishing with a 3-axis vertical milling machine fitted with a rotary diamond disc of the assembled specimen. D) Assembled specimen tested in a hydraulic press

I.2.3. Experimental results

Table 4 presents the thickness and the slenderness of the tiles used in each tested specimen, the slenderness of the specimen and the average compressive strength ($f_{c\ TILE}$) with the coefficients of variations. Table 4 also reports the ratio between the standardized strength of the standard specimen ($f_{c,b}$) and the experimental compressive strength of the developed specimens 'Mo$_1$' and 'Mo$_2$' ($f_{c\ TILE}$). The slenderness of the assembled specimen is defined as the ratio between the height and the total width of the specimen, considering as the total width the distance between the external faces of the specimen (i.e., the thickness of the two tiles plus the thickness of the cement mortar joint). The compressive strength of the tested specimens ($f_{c\ TILE}$) was calculated by dividing the maximum compressive load by the cross-sectional area of both tiles, without considering the area of the mortar layer. The displacement during the test was measured with the transducer from the actuator.

The coefficients of variation for the assembled specimens range between 20%-34% and 11%-18% for historical and modern tiles, respectively. The higher variation in historical tiles is due to the larger inhomogeneity of the tiles as well as their non-industrialised manufacturing. However, the historical tiles 'Hi/I$_1$' and 'Hi/I$_2$', extracted from the same building, exhibited higher average strength than the modern ones due to the higher quality of the material. The assembled modern handmade specimens, 'Mo$_1$' and 'Mo$_2$', have close experimental compressive strengths despite the difference of 38% in the slenderness. The ratio between the standardized strength of the single tiles 'Mo$_1$' and 'Mo$_2$' and the compressive strength of the respective assembled specimens is 1.08 and 1.10 respectively. The geometrical influence of the specimens' configuration and the correlation with the standardized strength is presented in the Section I.4.

Fig. 6 shows the stress-displacement curves obtained during the uniaxial compressive load test of the assembled tile specimens. The stresses acting on the samples were computed as the ratio between the applied load and the area including the cross sections of both the tiles. The use of the displacement readings from the actuator result in an initial part with increasing stiffness in all stress-displacement curves. This behaviour is related with the adjustment of the platens to the faces of the tiles. After this, all curves present an approximately initial linear branch up to the maximum compressive strength. Just before the maximum load, the curves of the 'Mo_1'_1, 'Mo_1'_4, 'Mo_2'_1 and 'Mo_2'_3 specimens presented a slight stress drop with subsequent increase up to the strength value. This point usually corresponds to the failure of the interface between the mortar and tile. Once the maximum load was reached, a brittle softening response followed with decreasing stress under increasing strain. The 'Hi/I' specimens presented a more fragile post-peak response with a sudden stress drop.

The observed failure modes developed in two phases. First, thin vertical cracks parallel to the load direction appeared at the upper and lower parts of the tiles which were in contact with the platens [Fig. 7a]. Then, as the load continued to increase, these cracks spread further producing an arch-shaped crack that split the tile into two parts [Fig. 7b]. These cracks went through the total width of the tile causing the complete separation of the outer part [Fig. 7c]. As previously mentioned, some specimens presented a sudden vertical crack between the mortar joint and the tile, close to the maximum load capacity, which corresponded to a stress drop before the maximum capacity in their stress-strain relationship [Fig. 7d].

Table 4 Thickness and slenderness of the tiles and the assembled specimens, average compressive strength of the tested specimens ($f_{c\,TILE}$), ratio between the normalized strength of the standard specimen ($f_{c,b}$) and the compressive strength of the developed specimen $f_{c,b}/f_{c\,TILE}$. Values in brackets correspond to the Coefficients of Variation

Tested Specimens						
		t_t (mm)	Tile Slenderness	Specimen Slenderness	$f_{c\,TILE}$ (MPa)	$f_{c,b}/f_{c\,TILE}$
Mo_1	6	46.0 [3.2%]	2.18 [2.7%]	0.89 [2.4%]	16.1 [11%]	1.08
Mo_2	6	30.1 [5.9%]	3.32 [7.2%]	1.25 [5.9%]	15.8 [18%]	1.10
Hi/I_1	5	21.0 [2.4%]	4.88 [2.8%]	1.73 [2.7%]	22.8 [22%]	--
Hi/I_2	7	18.3 [3.1%]	5.53 [3.6%]	1.90 [3.4%]	22.2 [20%]	--
Hi/I_3	5	20.0 [5.3%]	5.08 [5.1%]	1.64 [4.1%]	15.3 [34%]	--

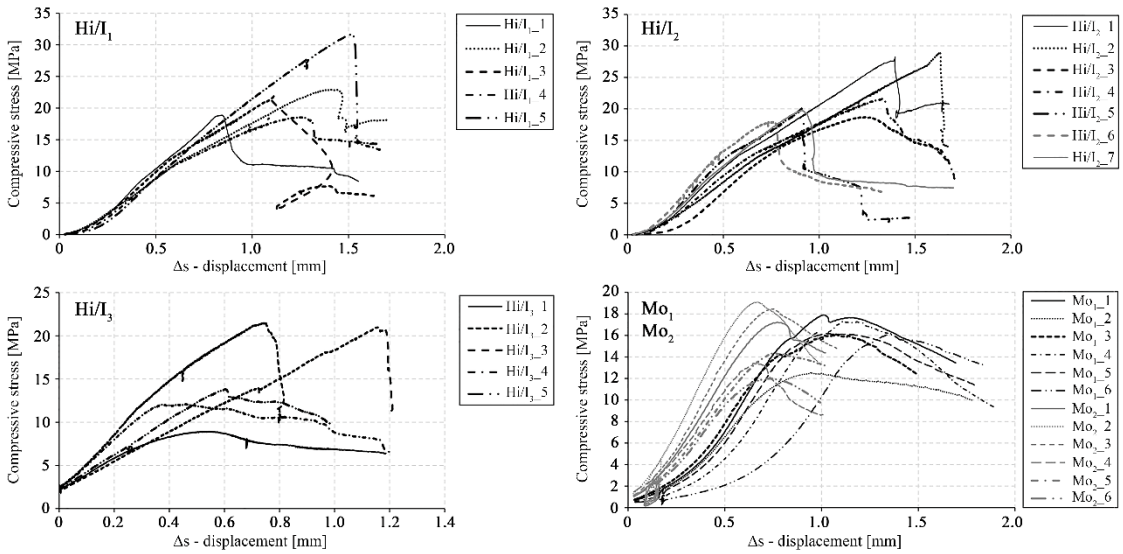

Fig. 6 The stress-displacement curves of the 29 assembled specimens under uniaxial compression

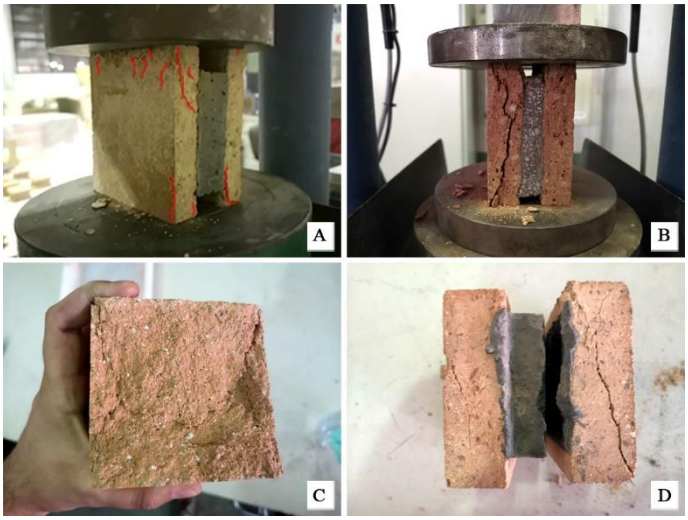

Fig. 7 The development of the failure mode during the test procedure. A) The surfaces of the specimen in contact with the platens develop small vertical cracks at the beginning of the loading. B) The arch-shaped crack developed through the width of each tile of the assembled specimen. C) Expulsion of the outer material after the crack has fully developed. D) Failure mechanism involving both a crack in the tile and a separation of the cement mortar and the tile

I.3. Numerical study

The proposed testing protocol was simulated using the Finite Element Method. The objective of the numerical analysis is to investigate the validity of the adopted experimental configuration for estimating the uniaxial compressive strength of thin clay tiles. Additionally, an insight is given on the influence of the thickness of the tiles and their mechanical properties, as well as the potential influence of the numerical parameters of the adopted modelling approach.

A continuum finite element approach was adopted with a distinct modelling of the tiles and the mortar. Fig. 8 presents the geometry and the used finite element mesh. The dimensions of the simulated clay tiles for the reference model were h_t = 100 mm (height), w_t = 100 mm (width), while different values for the thickness were considered (t_t = 20 mm; 30 mm; 45 mm). The dimensions of the binding mortar layer were h_m = 80 mm, w_m = 100 mm and t_m = 20 mm, as in the experimental campaign. Only a quarter of the specimen was modelled due to the symmetry along the two vertical middle planes (see Fig. 8). Isoparametric solid brick elements based on linear interpolation and 2 × 2 × 2 Gauss integration were used for the mesh. The experiment was simulated by applying a vertical displacement at the top of the tile, restraining the vertical displacement at its base. The symmetry of the specimen was considered by restraining the displacements normal to the two planes of symmetry (see Fig. 8). The system of nonlinear equilibrium equations was solved using a secant method along with a line-search procedure. Convergence was achieved for a ratio between the norm of the iterative residual forces and the norm of the total external forces is lower than 10^{-2} (1%). Numerical simulations were performed with the finite element software COMET [66], while pre- and post-processing with GiD [67] developed at CIMNE, Barcelona.

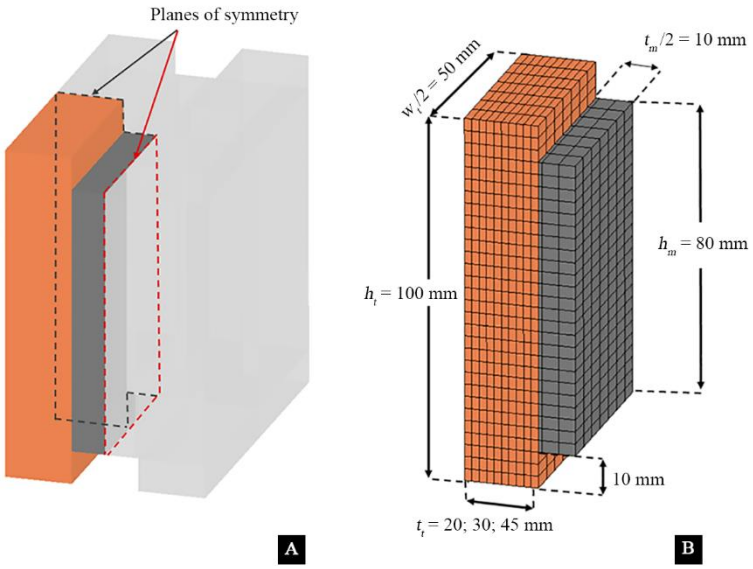

Fig. 8 A) Specimen with the planes of symmetry (non-simulated part in grey), B) Geometry of the reference model and finite element mesh

Cracking and crushing of the units and the mortar was simulated using a continuum damage mechanics formulation with damage induced orthotropic behaviour along the principal stress axes. The model uses two distinct damage indices corresponding to tensile damage (i.e., cracking) and compressive one (i.e., crushing) [68]. This choice permits the differentiation between the nonlinear tensile and compressive behaviour. In particular, the tensile response is characterised by a linear branch up to the maximum strength, followed

by an exponential softening branch. The compressive response is characterised by a parabolic hardening up to the maximum strength and a parabolic softening beyond it [69]. The failure criterion proposed by Lubliner et al. [70] was adopted in all simulations, with the modification introduced in [69] for controlling the shear behaviour. The above numerical strategy has been calibrated for the simulation of the compressive behaviour of masonry specimens in [71].

Table 5 presents the mechanical parameters for the tile and the mortar. The material properties for the tile correspond to those of the handmade solid clay tiles obtained in the experimental campaign presented in Section I.2. The tensile fracture energy is calculated as G_{f_t} [J/m²] = $0.04 \cdot f_t^{0.7}$ (f_t on MPa) and the compressive fracture energy as G_{f_c} [J/m²] = $1.6 \cdot f_{c,b}$ ($f_{c,b}$ on MPa) [72]. The selected failure criterion needs the definition of the parameter ρ, which controls the triaxial compression, the ratio between biaxial and uniaxial compressive strength $f_{b,c} / f_c$ and the parameter κ that controls the shear response [69]. The first two parameters were calibrated through the simulation of the standardized experimental tests under compression of the 'Mo' brick specimens with size 100 × 100 × 40 mm³ as described in Section I.2.1. The parameter κ was defined equal to 0.16 as in [69,71] and its effect on the numerical results is investigated through a sensitivity analysis presented in Section I.4. Linear elastic behaviour, with the Young's modulus corresponding to the experimentally obtained value, is adopted for the mortar as no damage was observed in it during the experimental campaign.

Table 5 Mechanical properties of tiles and the mortar used in the numerical simulations

Property	Tiles	Mortar
E (GPa)	5.55	34.20
ν (–)	0.11	0.25
f_t (MPa)	1.4	-
f_c (MPa)	17.4	-
G_{ft} (J/m²)	50	-
G_{fc} (J/m²)	27,840	-
f_{bc}/f_c	1.15	-
ρ (–)	0.65	-

Fig. 9 presents the tensile damage of the specimen at the end of each analyses for the three studied thickness of t_t = 20 mm, 30 mm and 45 mm. All cases are characterized by initial cracking at the interface between mortar and brick and at the middle of the tile in proximity with the cement mortar (Fig. 10a). This crack propagates slowly during the analysis, while cracks start appearing at the top and bottom ends of the tile (Fig. 10b). These two cracks progress symmetrically towards the interior of the tile, and finally one of the two dominates and separates the tile into two parts (Fig. 10c). This crack corresponds to the delamination of the external part of the tile as observed in the experimental tests. Moreover,

cracking exists as well in the mortar-tile interface, as was observed in some experimental tests.

Fig. 11 presents the vertical stress-strain graphs obtained from the numerical analyses. The curves resemble closely the experimental curves as obtained for the 'Hi/I' and 'Mo' specimens. The propagation of the crack that produces the separation of the tile into two parts results in the sudden drop of the capacity of the specimen for all cases and corresponds to the end of the analysis for the tile with a thickness of 30 mm. For the other two cases, the rest of the analysis is characterized by a plateau with crushing occurring at the bottom of the tile.

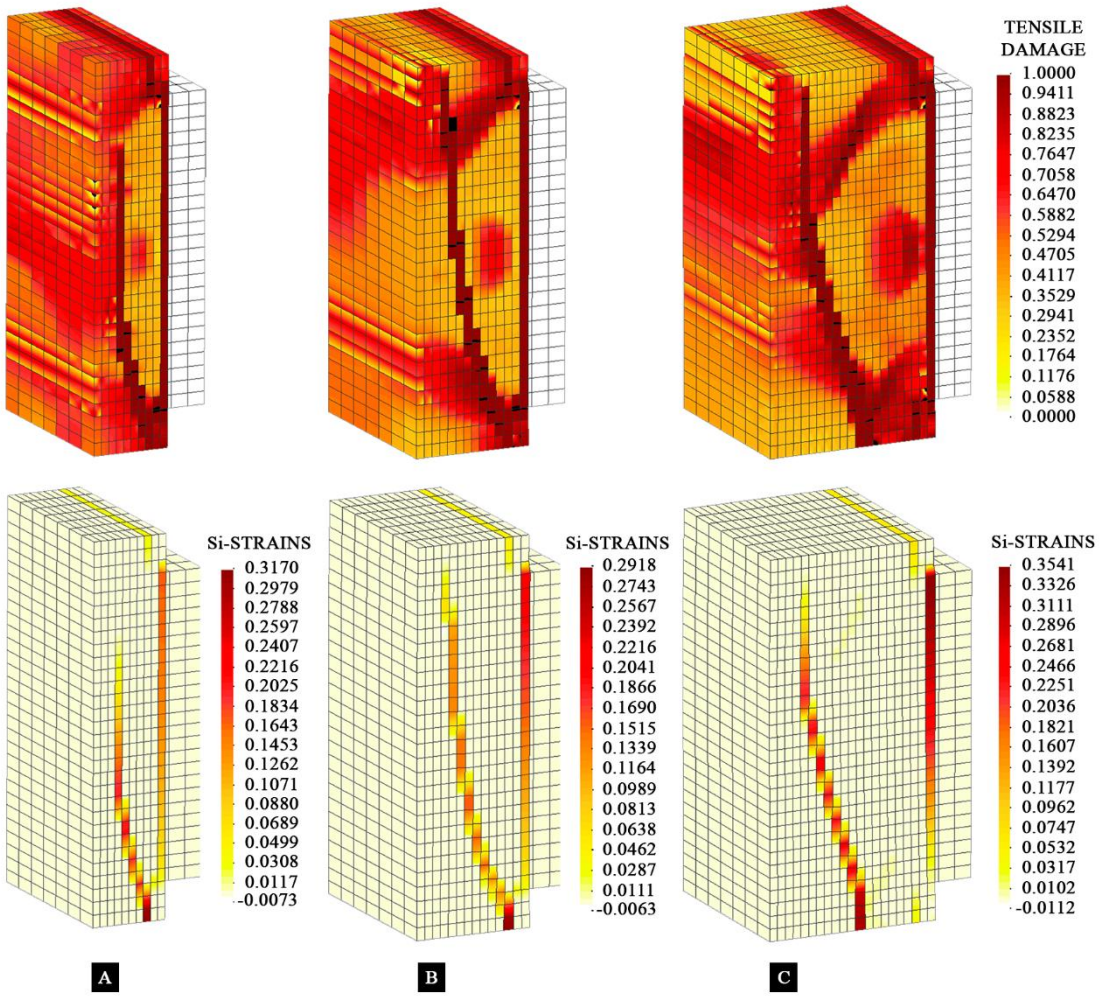

Fig. 9 Tensile damage (top) and maximum principal strains (bottom) contour for the analysis of a tile with thickness: A) 20 mm, B) 30 mm, and C) 45 mm

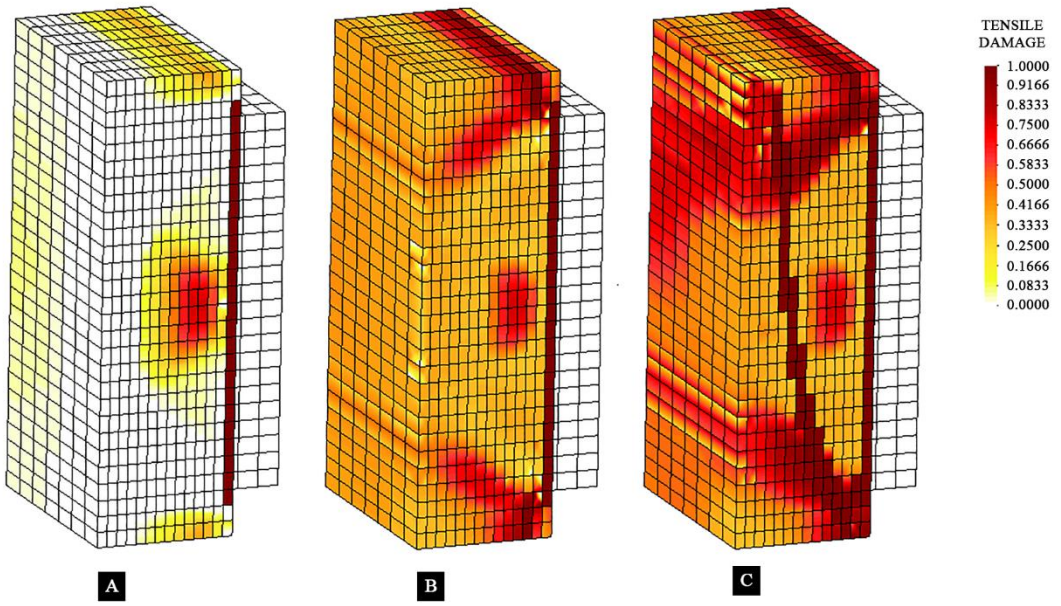

Fig. 10 Tensile damage of the simulated specimen with tile thickness 30 mm corresponding to a vertical displacement of: A) 0.30 mm, B) 0.45 mm and C) 0.60 mm

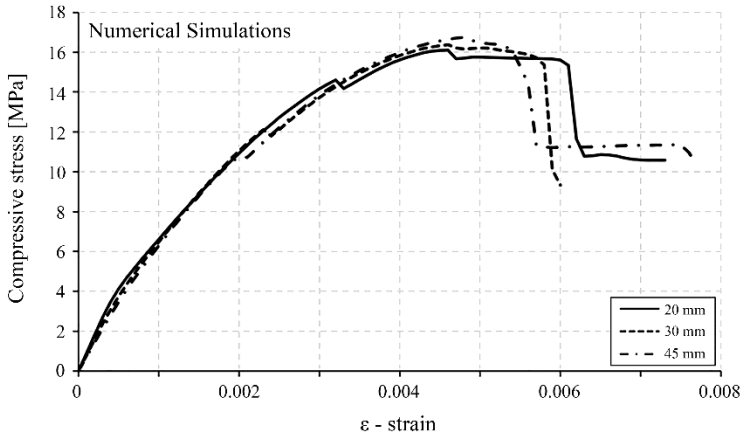

Fig. 11 Vertical strain against vertical stress for the three numerical simulations of the tiles with different thickness

I.4. Discussion

The experimental campaign using the modern handmade bricks ('Mo') allowed to obtain a correlation between the uniaxial compressive strength of a standardized single tile and that of the assembled specimen ($f_{c,b}/f_{c\,TILE}$). As presented in Table 4 (Section 2) and Table 6, this ratio was 1.08 and 1.10 for a slenderness ratio of 0.89 ('Mo_1' specimens with mean tile thickness of 46 mm) and 1.23 (Mo_2 specimens with mean tile thickness of 30 mm) respectively. The numerical analyses showed very similar results with $f_{c,b}/f_{c\,TILE,num}$ = 1.04 for a slenderness ratio of 0.90 (tile thickness of 45 mm) and 1.06 for a slenderness ratio of 1.25 (tile thickness of 30 mm) (Table 6). These results were complemented with the numerical simulation of a

specimen with a slenderness ratio 1.67 (tile thickness of 20 mm), resulting in $f_{c,b} / f_{c\ TILE,num}$ = 1.08. The experimental and numerical results show that tests with the proposed specimen allow estimates of the uniaxial compressive strength of thin tiles that are slightly lower than the values given by standardized tests (between 5% and 10% lower). A correlation between the slenderness ratio and the $f_{c,b} / f_{c\ TILE}$ seems to exist, with increasing slenderness resulting in lower values of the uniaxial compressive strength given by the proposed specimen.

The above results were further validated through a parametric numerical study. First, we investigated the influence of the parameter κ, controlling the shear response, which could not be calibrated through the experimental campaign. As described in [69], κ takes values between 0 and 1, with an increasing value resulting in a lower shear strength (for more information see [69] [73]). The variation of κ between 0.0 and 0.3 changes slightly the $f_{c,b} / f_{c\ TILE,num}$ without affecting the observed trend between slenderness and uniaxial strength prediction. As anticipated, a reduction in the value of κ for the same thickness results in a slight increase in the strength. The maximum change in the predicted compressive strength due to the variation of κ is approximately 7% for a tile with thickness of 45 mm. For the other two tile thickness, this variation drops to 5% and 3% for t_t = 30 mm and t_t = 20 mm, respectively. For all the cases, this parameter shows a marginal effect in the estimation of the compressive strength.

Table 6 Relationship between the compressive strength obtained from the numerical simulation of the proposed experiment ($f_{c\ TILE,num}$) with the uniaxial compressive strength of the tile ($f_{c,b}$).* Value for a tile thickness of 46 mm

	Numerical $f_{c,b} / f_{c\ TILE,num}$		
	t_t = 20 mm	t_t = 30 mm	t_t = 45 mm
κ = 0.0	1.05	1.04	1.02
κ = 0.16	**1.08**	**1.06**	**1.04**
κ = 0.3	1.12	1.09	1.09
ft = 1.0 MPa	1.13	1.09	1.08
ft = 1.4 MPa	**1.08**	**1.06**	**1.04**
ft = 1.8 MPa	1.06	1.05	1.04
Gft = 25 J/m²	1.09	1.07	1.05
Gft = 50 J/m²	**1.08**	**1.06**	**1.04**
Gft = 75 J/m²	1.07	1.06	1.08
Average Numerical	1.09	1.07	1.06
	$f_{c,b} / f_{c\ TILE}$		
Experimental	-	1.10	1.08*

Next, the variation of the tensile strength and the tensile fracture energy was investigated. Three values were used for each one: ft = 1.0 MPa; 1.4 MPa; 1.8 MPa and Gft = 25 J / m²; 50 J / m²; 75 J / m², with the middle values being the reference ones. The variation of these properties showed the same trend in the estimation of the compressive strength. For

any tile thickness, lower values of the tensile strength or the fracture energy result in lower compressive strength and vice versa. The effect of these properties is anticipated as both of them are related with the cracking that appears within the specimen and drives the collapse mechanism in both experimental and numerical results. Lower tensile strength results in earlier cracking, while lower fracture energy to a more rapid crack propagation.

In overall, the results of the sensitivity analysis, presented in Table 6, show that $f_{c,b} / f_{c\,TILE,num}$ lies for all the cases between 1.02 and 1.09. The results of the compressive fracture energy are omitted as this parameter does not influence the estimation of $f_{c,b} / f_{c\,TILE,num}$. It is noted that the same failure mechanism has been obtained for all the cases, independently on the change of the material and numerical properties.

I.5. Conclusions

This paper has presented a test setup for the uniaxial compressive testing of thin clay tiles used in the construction of timbrel masonry vaults. The new test setup was validated through the combination of an experimental campaign on modern and historical handmade clay tiles extracted from two 19th century industrial buildings in Barcelona (Spain) and from the early 20th extension of one of them, and finite element simulations. The following conclusions can be drawn from the analysis of the experimental and numerical results:

- A relatively easy and efficient procedure was applied to extract the historical tiles from existing vaults. Common electric tool were employed, such as a jackhammer to remove the pavement or the plaster, together with manual chisel, a trapezoidal trowel and a nylon hammer for the careful extraction of the tiles from the existing vaults.
- The tests on assembled specimens allowed a reliable testing in compression of the tiles. The test on the proposed assembled specimen avoided the possible influence of instability effects induced by the excessive slenderness of the individual tiles. No tile buckling failure was observed in the experimental investigation.
- The failure mode of the tiles in both, experimental and numerical results, was characterized by the splitting of the tile into two parts due to the propagation of a crack throughout the whole width of the tile. In some cases, a debonding between the tile and the cement mortar was also observed.
- The experimental and numerical results show that the proposed test setup can estimate the uniaxial compressive strength of the tile with a difference between 5% and 10% from the one given by tests on standardized brick specimens.
- The numerical investigation showed that the change in the thickness, as well as the variation of the tensile and shear strength and the tensile fracture energy, have a marginal influence on the estimation of the uniaxial compressive strength by using the proposed setup. The ratio between the uniaxial tensile strength of a single brick

(input data of the numerical model) and the uniaxial compressive strength computed using the proposed assembled specimen ranged between 1.02 and 1.09.

- Testing the thin tile using the proposed assembled specimen has proved to be an advantageous technique for the evaluation of the compressive strength of thin tile units. It is suggested to test at least a set of six units extracted from an existing vault to obtain a reliable estimation of the compressive strength.

Future works could address the extension of the experimental database by including the application to a wider sample of tiles extracted from existing timbrel vaults.

2.3. Paper II – Anisotropy and compressive strength evaluation of solid fired clay bricks by testing small specimens

A. Cabané, L. Pelà, P. Roca

Construction Building Materials 344 (2022) 128195

https://doi.org/10.1016/j.conbuildmat.2022.128195

Abstract. A study is presented on the use of a non-standard 40 × 40 × 40 mm^3 specimen for the experimental measurement of the compressive strength of solid fired clay bricks extracted from existing masonry buildings. The viability of such specimen has been assessed by comparison with experimental results obtained with the standard 100 × 100 × 40 mm^3 specimen. The use of the non-standard 40 × 40 × 40 mm^3 has two main advantages. First, it significantly reduces the volume of sampled material, which can be severely restrained in architectural heritage buildings. Second, it allows carrying out tests in the three brick dimensions (length, width and thickness), and therefore investigating the anisotropy that clay bricks can exhibit depending of their manufacturing process. The experimental campaign has focused on three different types of solid fired clay bricks, namely mechanically extruded, hydraulic press moulded, and handmade units, with a total amount of 461 specimens. Using the mentioned small cubic specimen, a detailed research on the compressive strength and the anisotropy of different solid clay brick types has been carried out by applying a statistical approach. The experimental results and the statistical processing have shown that the proposed specimen can be utilized for a reliable estimation of the compressive strengths along the three main directions of solid fired clay bricks.

II.1. Introduction

A large part of the built stock of many regions in the world consists of modern and historical masonry structures still in use and in need of maintenance and conservation interventions. Many of such structures are considered as architectural heritage due to their cultural value and to their contribution to the identity of historical towns and urban centres. The structural verification of masonry buildings, aimed to their maintenance or refurbishment, requires a detailed analysis of the performance against both gravity loads and horizontal actions. The analysis of existing masonry buildings, however, faces significant difficulties due to the complexity of masonry as both construction technology and structural material. One of the main difficulties lies in the realistic characterization of the mechanical properties and, more specifically, of the masonry compressive strength, which has often a critical influence on the structural performance of masonry members. The masonry

compressive strength depends largely on the compressive strength of components (units and mortar) [74]. In specific, knowledge on the compressive strength of bricks (along with that or mortar) may enable an estimation of that of masonry using available empirical or analytical equations [3,4].

The most common materials in historical masonry buildings are stone, solid clay bricks, adobe, and lime mortar. Solid fired clay brick masonry has been one of the most recurrent construction technologies for centuries. Generally, brick masonry has not deserved a research attention (including experimental research) comparable to that devoted to more modern structural materials such as concrete or steel. Despite encouraging advancements, significant additional research is still needed for an accurate and efficient characterization of the mechanical properties of masonry components in existing buildings.

The mechanical characterisation of solid fired clay bricks from samples extracted from existing buildings poses specific challenges due to the limited thickness of bricks, which in some geographical locations may be of the order of only 40 mm or less. In addition, sample extraction may be severely restricted in architectural heritage buildings. Testing in the laboratory small samples from solid clay bricks faces specific difficulties. First, the reduced height of the samples may induce excessive confinement when tested in a press machine, which may largely influence on the measured compressive strength. Second, the material heterogeneity and the possible material or geometrical imperfections also influence on the compressive strength and may compromise the representativeness of the measurements. Finally, the brick manufacture process can also influence on the strength by inducing anisotropy effects [55,75].

With regard to the confinement effect due to the specimen shape, recommendations for concrete can be found in the available scientific and technical literature. In specimens with height/diameter (or width) ratio greater than 2.0, the effect of confinement does not reach their central portion, which therefore experiences a uniaxial compression condition [58,59]. For specimens with slenderness under 1.5, the measured strength increases due to the restraining effect exerted by the testing machine. In particular, for concrete specimens with slenderness 1.0, the apparent strength is approximately 1.2 times larger than that obtained in specimens with slenderness 2.0, as indicated by Neville [59] and Schickert [58]. The only recommendations for bricks are offered by Page [76] who investigated the influence of the slenderness on calcium silicate units. Page [8] measured the brick unconfined compressive strength by testing the specimen with steel brush bearing platens. Page found that measuring the compressive strength with conventional bearing testing machine required tests on specimens with slenderness 3.0 in order to obtain values similar to those yielded by test carried out with the steel brush bearing platens. For specimens with slenderness 1.0 he found an apparent compressive strength 1.43 times higher than the one measured with specimens with slenderness 3.0. Reaching the slenderness that would be required to avoid confinement effects, however, is not possible in flat bricks characterized by a reduced

thickness, as it would require tests on extremely small specimens or stacked specimens. The small volume of the specimen largely increases the risk of sampling errors due to the unavoidable heterogeneities normally induced by the mixing and manufacturing procedure. The stacked specimens are allowed by the EN 772-1:2011+A1:2016 [9] standard, but require the use of a larger amount of material, which is often not possible in the case of heritage buildings. Nevertheless, tests on low-slenderness specimens become necessary in spite of their possible drawbacks. Both the ASTM C67/C67M-21 [47] and EN 772-1:2011+A1:2016 [9] standards concerning brick testing in compression propose specimens with reduced slenderness (1.0 to 0.33) for bricks with thickness below 50 mm. These standards foresee, in specific, the possibility of testing different specimen types in flatwise position.

Testing entire bricks or flat specimens does not allow a satisfactory characterization of the possible material anisotropy. The measure of the compressive strength along different brick orientations would be largely compromised by the very different slenderness shown by the unit along its different dimensions and would yield non-comparable measures. Previous research has focused on tests on whole bricks by applying the load perpendicular to the stretcher, header or bed dimensions [54,77] with the aim to measure the global brick strength as an entire unit. This type of tests, however, are oriented to measure global brick properties and are not useful to accurately characterize the material's anisotropy. Some other researches have more specifically focused on the measurement of the material anisotropy by testing comparable cubic or prismatic specimens along different brick dimensions. Aubert et al. [78] studied four types of extruded earth bricks by testing twelve 50 × 50 × 50 mm^3 specimens from each brick in two orientations (perpendicular and parallel to the extrusion plane), obtaining the highest strength in the direction perpendicular to the extrusion plane. Oliveira et al. [79] tested four 40 × 40 × 120 mm^3 specimens of mechanically produced solid clay bricks in flatwise and lengthwise brick positions. Fódi [54] measured the compressive strength of extruded solid clay bricks on eight 50 × 50 × 50 mm^3 specimens in each load direction. Krakowiak et al. [75] tested cylindrical specimens along the three brick directions, considering two types of extruded bricks with extrusion along the height and along the length respectively. Oliveira et al. [79], Fódi [54] and Krakowiak et al. [75] also obtained larger compressive strength along the extrusion plane. Finally, Salvatoni and Ugolini [80] carried tests on 40 × 40 × 40 mm^3 specimens of a modern handmade brick and found similar compressive strengths along the three directions.

This paper proposes the use of a small 40 × 40 × 40 mm^3 cubic specimen for the experimental measurement of the compressive strength of solid clay bricks along the three brick dimensions, enabling therefore the characterization of the material anisotropy. The interpretation of the experimental results is carried out according to a detailed statistical analysis. Among other advantages, by reducing the sample volume (compared to testing of entire bricks or larger specimens) this approach overcomes possible limitations arising from

the relatively small number of brick samples that can be extracted from existing buildings, especially when they belong to architectural heritage.

Sampling errors induced by the small specimen size (related to excessive heterogeneity, geometrical imperfection or inadequate failure) can be avoided by adapting well-known criteria, used in the case of concrete, for the selection and acceptance of appropriate specimens. The criteria adopted for concrete in the selection and testing of cubic brick specimens are described in the standards EN 12390-1:2022 [81] and EN 12390-3:2022 [82]. They concern the maximum acceptable aggregate diameter and satisfactory failure modes. In addition, the cubic specimen allows a slenderness (equal to 1.0) significantly larger than that of an entire unit and therefore is subjected to a lesser confinement effect during the test. Moreover, the cubic specimen enables an accurate characterization of the material anisotropy by using samples with the same slenderness through the three orientations (length, width and thickness). The interpretation of the experimental results has been carried out by means of a detailed statistical analysis, using well-known statistical tests, in order to detect possible outlier values and to decide about the comparability of experimental results corresponding to different samples.

The experimental campaign was carried out on three different solid clay bricks types characterized by different manufacturing procedures. The different brick types correspond to (1) mechanically extruded units, (2) hydraulic press moulded units, and (3) handmade units, including both modern and historical handmade bricks extracted from existing masonry buildings. The historical bricks were extracted from six 19th and early 20th century buildings in Barcelona (Spain), one of them with an extension built at the beginning of the 20th century. The case-studies include three residential buildings, two industrial facilities and one market. The case studies allowed a broader comparison of the experimental results obtained from the proposed cubic specimen with those derived from a standardized 100 × 100 × 40 mm^3 specimen defined in EN 772-1:2011+A1:2016 [9].

The research pays special attention to the use of the nonstandard 40 × 40 × 40 mm^3 specimen with the following specific objectives: (1) Analysing the consistency and reliability of the results obtained, as well as the acceptability of the experimental scattering; (2) Exploring the anisotropy in the compressive strength and comparing with previous experimental research results; (3) Characterizing the influence of the specimen shape on the estimation of the compressive strength by comparing the results obtained from the proposed cubic specimen with those yielded by the standard 100 × 100 × 40 mm^3 normalized specimen. The research has been based on the execution of a broad experimental campaign including tests on 323 40 × 40 × 40 mm^3 cubic specimens and additional 138 tests on standard 100 × 100 × 40 mm^3 specimens for the sake of comparison.

This paper is structured in four sections. After this introduction, Section II.2 presents the experimental campaign performed on brick units, including the description of the material, the specimen preparation and the test procedure. Section II.3 describes the

experimental results. Section II.4 analyses the influence of the anisotropy in the different manufactured units, the statistical analysis of the anomalous experimental results, and the shape-effect influence. The paper ends with Section II.5 presenting some conclusions and proposed future works.

II.2. Experimental study

This section presents the experimental campaign carried out on solid fired clay bricks manufactured according to three different procedures, corresponding to (1) mechanically extruded, (2) hydraulic press moulded and (3) handmade manufactured bricks. The handmade manufactured bricks include both modern and historical bricks, the latter collected from existing buildings. Details are provided on the description of the materials, the preparation of the proposed specimen, its geometry, and the testing setup. As mentioned above, the historical samples were collected from historical buildings, including three residential ones, two industrial ones and a market structure in Barcelona (Spain). Three of these buildings were built in the early 20th century and the other three were built in the 19th century. One of the industrial buildings from the 19th century includes a 20th century building extension. All experimental tests were carried out at the Laboratory of Technology of Structures and Materials of the Technical University of Catalonia (UPC-BarcelonaTech).

II.2.1. Materials

As mentioned, in this research, solid fired clay units manufactured according to three different procedures were studied (Fig. 12). The first type of bricks, corresponding to modern clay ones produced by mechanical extrusion, are identified herein with the acronym 'Ex'. The second type, corresponding to modern clay bricks produced by hydraulic press moulding, are identified with the acronym 'Hy'. The third type includes handmade modern and historical bricks. The modern handmade solid clay bricks include, in turn, three different subtypes, identified with the acronyms 'Mo$_1$' 'Mo$_2$' and 'Mo$_3$'. Although provided by the same manufacturer, the three types of modern handmade bricks correspond to different manufacturing series and show differing mechanical properties. The historical solid clay bricks were collected from seven different masonry walls from six buildings, following the RILEM recommendation LUMD1 for removal and testing specimens from existing buildings [83]. The historical bricks collected from the industrial buildings are identified with the acronyms 'Hi/I', while the ones taken from residential buildings are identified with the acronyms 'Hi/R', and those collected from the market building are identified with the acronym 'Hi/Ma'. The 'Mo', 'Hi/I', 'Hi/R' and 'Hi/Ma' were traditionally manufactured in a brickyard by moulding. According to the traditional procedure, the 'Mo' bricks were shaped in a wooden mould sprinkled with dry fine sand and, after being extracted from the mould, the bricks were fired into a coal-fired kiln. The modern mechanical type, 'Ex' and 'Hy' were

produced in an automated process. 'Ex' bricks were extruded along the thickness. They were cut and dried by mechanical automatized tools before being fired in a tunnel kiln with controlled heat conditions. The 'Hy' bricks were mechanical pressed on their beds into a mould. The mechanically extruded ('Ex'), hydraulic press moulded ('Hy') and modern handmade ('Mo') gave the possibility to test a larger number of specimens. However, the number of clay brick samples collected from historical buildings ('Hi/I', 'Hi/R' and 'Hi/Ma') was limited due to the restrictions imposed by their consideration as cultural heritage. Table 7 presents a description of the sampled materials in terms of origin, acronym, number of samples collected and average dimensions measured according to EN 772-16:2011 [60].

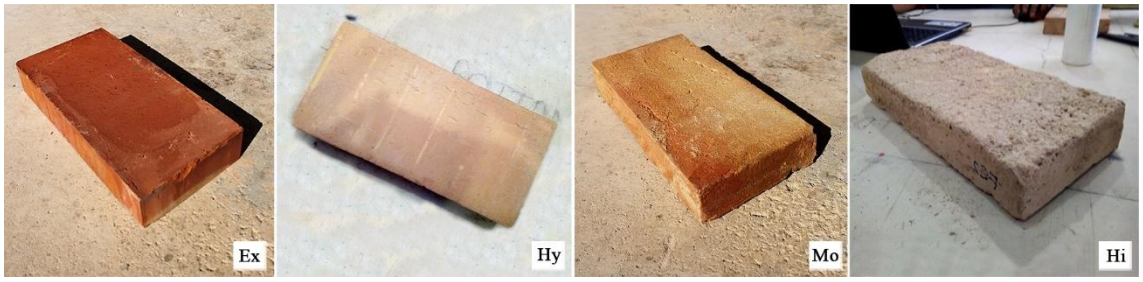

Fig. 12 Modern mechanically extruded solid clay brick ('Ex'), modern clay brick produced by hydraulic press moulding ('Hy'), modern handmade solid clay brick ('Mo'), and historical solid clay brick from existing building ('Hi')

Table 7 Sampled bricks in terms of origin, acronym (Acr.), number of samples collected and average dimensions. Values in brackets correspond to the coefficients of variation

Sampled materials			
Origin	Acr.	Num. bricks	Av. Dimensions (mm)
Mechanically Extruded	Ex	11	272 [0.4%] × 132 [0.9%] × 45 [0.7%]
Hydraulic Pressed	Hy	10	291 [0.0%] × 141 [0.0%] × 38 [0.1%]
Modern Handmade	Mo_1	13	306 [0.5%] × 147 [0.9%] × 46 [3.4%]
	Mo_2	6	311 [0.6%] × 149 [1.7%] × 46 [4.6%]
	Mo_3	6	306 [1.4%] × 146 [1.5%] × 46 [2.7%]
1878 Industrial	Hi/I_1	24	295 [1.3%] × 148 [2.8%] × 44 [4.3%]
Early 20th c. Industrial	Hi/I_2	6	293 [1.3%] × 140 [4.2%] × 49 [5.8%]
1927 Industrial	Hi/I_3	15	288 [0.7%] × 141 [1.5%] × 49 [5.8%]
1933 Market	Hi/Ma	6	285 [0.8%] × 139 [1.2%] × 47 [4.3%]
1840 Residential	Hi/R_1	8	294 [0.7%] × 145 [1.8%] × 45 [2.1%]
1880 Residential	Hi/R_2	6	294 [0.6%] × 145 [0.4%] × 56 [3.3%]
1930 Residential	Hi/R_3	6	394 [0.4%] × 145 [0.5%] × 49 [5.2%]

II.2.2. Preparation of specimens and testing procedure

The motivation behind the proposal of a new test specimen for the derivation of the compressive strength from solid clay bricks lies in the brick geometry (the limited brick

thickness) and the restrictions normally encountered in extracting samples from existing buildings.

Historical brick beds usually present irregularities caused by their manual manufacture. In particular, the bed surface may have material depressions that diminish its cross-sectional thickness irregularly. These geometric conditions make it difficult to test historical brick specimens flatwise without any surface preparation. To overcome this problem, standard EN 772-1:2011+A1:2016 [9] recommends to grind or cap with cement mortar the specimen bearing surfaces. Following the standard, in the present research the surfaces of the bricks were subjected to grind until the requirement of flatness and parallelism was achieved. After the grinding process, the remaining height of the samples was close to 40 mm due to the bed irregularities of the solid clay bricks collected from the existing buildings (with raw thickness ranging between 44 mm and 56 mm). The 40 mm height of test samples is referenced in the standard EN 772-1:2011+A1:2016 [9]. The 'Hy' had an original thickness less than 40 mm, but the industrialized production offered flatness and parallel beds. In this latter case, polishing of the surfaces was possible with a grinding below 1 mm.

To comply with the aims specified in Section II.1, it is proposed to test two specimen types. The first one, with dimensions 100 × 100 × 40 mm^3, is identified as '100'. The second one, measuring 40 × 40 × 40 mm^3, is identified as 'C40' and is characterized by a slenderness equal to 1. For a specimen with height of 40 mm, the standard EN 772-1:2011+A1:2016 [9] allows a width value ranging from 50 mm to 100 mm. Therefore, the '100' specimen satisfies the standard requirements. An alternative to the standard specimen is the 'C40' nonstandard specimen. The considered 40 mm cubic specimen this research is based on the proposal by Binda et al. [77] to measure the masonry material properties at a large scale. The 40 mm cubic specimen is sufficiently large to mitigate the possible effects due to the presence of inclusions and voids, as also suggested by Lourenço et al. [55]. Due to its limited volume, this cubic specimen requires only a small portion of the brick, leaving most of its material for other mechanical or physical characterisations. In addition, the proposed 'C40' specimen can be tested along the thickness (t), width (w) and length (l) dimensions with the same slenderness, allowing in this way the evaluation of the brick anisotropy. In the present research, at least three 'C40' specimens were obtained from each brick to test along each of the three directions.

Once the 'C40' specimens were obtained, a visual inspection of their surfaces was carried out. This examination was necessary to disregard specimens showing material imperfections (inclusions and voids) or an excessive aggregate diameter. To determine the acceptable aggregate diameter, the relationship between the diameter and the specimen edge indicated in the concrete standard EN 12390-1:2022 [81], was taken as a reference. The specimens with a ratio between the edge length and the diameter of the aggregate under 3.0 were discarded, leading to a maximum aggregate diameter of 11 mm. The standard EN

12390-1:2022 [81] was chosen because it is more restrictive than ASTM C42/C42M-20 [84], which allows a minimum edge equal to twice the nominal size of the aggregate. Fig. 13 presents the surfaces of some accepted and discarded 'C40' specimens based on the observed edge length to aggregate diameter ratio.

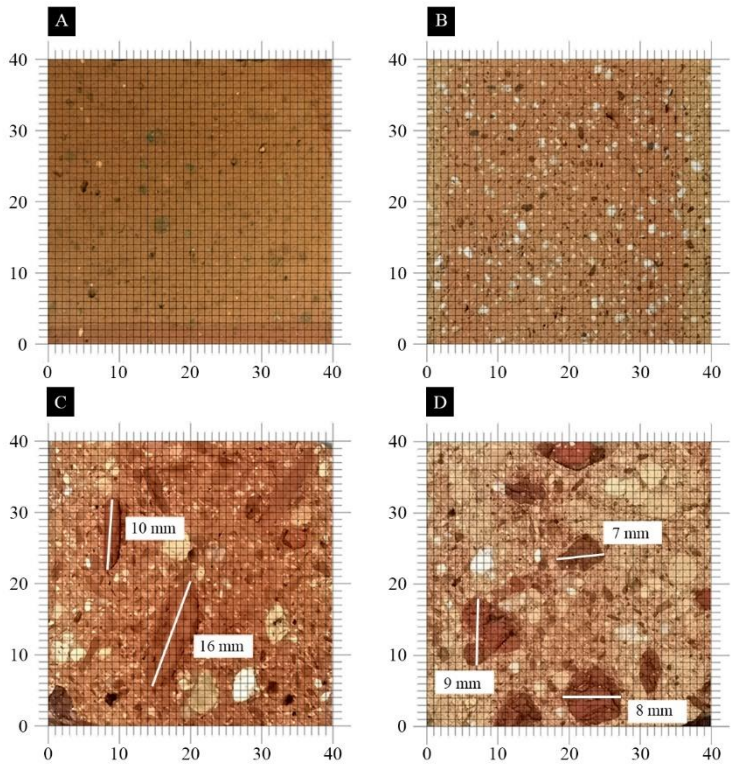

Fig. 13 Examples showing the edge length to aggregate diameter condition (grid values in mm) in 'C40' specimens: A) 'Ex' specimen with aggregate diameter under 2 mm; B) 'Mo' specimen example with aggregate diameter under 2 mm; C) 'Hi/R_3' discarded specimen with aggregate diameter over 11 mm; D) 'Hi/R_2' accepted specimen with aggregate diameter under 11 mm

The extraction of the historical bricks from the existing building was carefully carried out with a chisel and a mallet, as shown in Fig. 14. First, a jackhammer was used to remove the plaster and a neighbouring brick. Then, a thin chisel was used to remove the lime mortar joints around the brick to be extracted. Finally, a chisel was inserted under the brick bed with a metal mallet to separate and lever the brick. While levering the brick up, the chisel was inserted in different positions along the brick, trying to avoid any crack appearance in the clay unit. The bricks were extracted from inside the building to avoid masonry samples exposed to meteorological phenomena or ground moisture. The mortar remaining on the surface of the extracted bricks was removed manually using a wire brush with metal bristles without damaging the unit. Finally, the extracted bricks were packaged, labelled and transported to the laboratory.

Fig. 14 The extraction process of bricks from existing masonry walls: A) first, the plaster was removed using a jackhammer; B) then, the jackhammer was used to break and remove a neighbouring brick; C) next, a thin chisel was used to remove all the lime mortar joints around the brick; D) finally, a chisel was inserted under the bed of the brick to lever the brick

The proposed specimens described above were prepared in the laboratory according to the procedures specified in European Standards EN 772-1:2011+A1:2016 [9]. First, the brick beds were polished by a grinder equipped with a rotary disc until obtaining a constant thickness of 40 mm (Fig. 15a). This operation was aimed to guarantee the smoothness and flatness of the loading surfaces and any bearing surface imperfection. Next, two different specimen types (the '100' and 'C40' specimens) were extracted from each grinded brick using a table saw equipped with a water jet (Fig. 15b). The specimens were obtained from the central parts of the bricks, avoiding the extraction of these from the perimeter. Then, the specimens were dried in an oven at a constant temperature of 105 ± 5 ºC for 24 hours (Fig. 15c). Finally, the specimen dimensions were measured using a calliper with a precision of ±0.1 mm according to EN 772-16 [60]. A total amount of 138 standard '100' specimens and 323 nonstandard 'C40' specimens were obtained, including 39 'Ex' , 30 'Hy', 103 'Mo' and 289 'Hi' (130 'Hi/I_1', 24 'Hi/I_2', 47 'Hi/I_3', 18 'Hi/Ma', 26 'Hi/R_1', 22 'Hi/R_2' and 22 'Hi/R_3').

The specimens were tested making use of an Ibertest testing machine equipped with a load cell of 200 kN (AUTOTEST 200/10 SW) for the 'C40' specimens and 3000 kN (MEH-3000) for the '100' ones, and connected to a MD5 electronic module for data acquisition. The specimens were centred on the steel plates with the grinded surfaces orthogonal to the direction of the loading, and tested under force control at a rate of 0.15 MPa/s or 0.30 MPa/s (Fig. 15d). The rate was selected from EN 772-1:2011+A1:2016 [9] to guarantee a test duration of 60 s at least. The tests were stopped manually after registering the post-peak response.

Fig. 15 Manufacturing process of the specimens: A) the grinder equipped with a rotary disc to polish the bricks until obtaining a constant thickness; B) the table saw equipped with a water jet to cut the specimens; C) the specimens in the oven at a constant temperature of 105 ± 5 °C for 24 hours; D) 100 × 100 × 40 mm³ specimen tested in the hydraulic press

II.3. Experimental results

Table 8 presents the number of specimens and the average compressive strength of the tested standard '100' specimens with dimensions 100 × 100 × 40 mm³ ($f_{c,100}$), and of the 'C40' cubic specimens with dimensions 40 × 40 × 40 mm³ ($f_{c,C40}$), with their coefficients of variations (CV). The same table shows the compressive strengths of the latter in the different load orientations (t, w and l). The compressive strength of the samples was calculated by dividing the maximum compressive load by the cross-sectional area of the specimen. The displacement during the test was measured with the transducer installed in the actuator.

The coefficients of variation obtained in the measurement of the compressive strength range between 3.4% - 14% for mechanically extruded samples, 5.5% - 21% for hydraulic press moulded ones, 6.2% - 24% for modern handmade ones, and 11% - 29% for historical ones. The higher variation in historical bricks is due to the large inhomogeneity caused by their non-industrialised manufacturing. The lowest CV values are obtained for the 'Ex' and 'Hy' samples, with the exception of the 'Hy' 'C40' ones tested along the length, for which significant variation has been obtained. Mechanized extruded ('Ex') and hydraulic press moulded ('Hy') bricks exhibit higher average strength than both modern and historical handmade types. Among the historical bricks, 'Hi/I_2' and 'Hi/R_1' show the highest average strength, probably due to the higher quality of the material, while the historical bricks 'Hi/R_3' present the lowest average strength. The 'C40' specimens of the 'Hy', 'Mo$_1$' 'Mo$_2$' and 'Mo$_3$' bricks present similar strength averages among the tested unit directions (l, w and t). Conversely, different strengths $f_{c,C40}$ have been observed in the extruded ('Ex') and historical (Hi/Ma) bricks along the different directions. Both the 'Ex' and the 'Hi/Ma' bricks showed the lowest strength $f_{c,C40}$ along their width, and the largest strength $f_{c,C40}$ along their thickness.

The ratios between the compressive strength of the '100' and 'C40' specimens along the thickness ranges from 1.32 ('Hi/R_1' series) to 1.96 ('Hi/I_1' series). Section II.4 presents the in depth discussion about the effect of the specimen's shape and anisotropy on the compressive strength.

Table 8 Average compressive strength of the '100' samples ($f_{c,100}$) and 'C40' samples ($f_{c,C40}$), and ratio between the compressive strength measured on '100' and 'C40' samples $f_{c,100}$ / $f_{c,C40}$. Values in parentheses indicate the breakdown of 'C40' specimens tested along the three dimensions (t, w and l). Values in brackets indicate the coefficients of variation

Tested specimens							
Origin	'100'		'C40'				$f_{c,100}$ / $f_{c,C40}$
	Num. of specimens	$f_{c,100}$ (MPa)	Num. of specimens	$f_{c,C40}$ (MPa)			
				thickness (t)	width (w)	length (l)	
Ex	6	75.3 [3.4%]	33 (12/9/12)	51.1 [14.1%]	43.9 [8.8%]	50.1 [10.6%]	1.47
Hy	-	-	30 (10/10/10)	48.3 [5.5%]	49.8 [16.0%]	49.8 [21.0%]	-
Mo_1	13	24.9 [8.6%]	39 (13/13/13)	15.7 [6.2%]	14.0 [13.6%]	15.8 [11.1%]	1.59
Mo_2	6	34.9 [8.2%]	27 (14/6/7)	19.8 [15.0%]	19.4 [9.9%]	19.2 [20.9%]	1.76
Mo_3	-	-	18 (6/6/6)	10.5 [15.1%]	10.3 [24.2%]	9.7 [17.8%]	-
Hi/I_1	42	30.3 [25%]	88	15.4 [25.5%]	-	-	1.96
Hi/I_2	10	46.0 [21%]	14	26.5 [29.2%]	-	-	1.73
Hi/I_3	24	28.2 [15%]	23	15.8 [20.2%]	-	-	1.78
Hi/Ma	-	-	18 (6/6/6)	18.1 [22.8%]	13.3 [10.8%]	14.7 [15.2%]	-
Hi/R_1	13	46.1 [23%]	13	35.0 [25.6%]	-	-	1.32
Hi/R_2	12	24.0 [20%]	10	15.7 [21.5%]	-	-	1.53
Hi/R_3	12	15.1 [16%]	10	9.7 [18.5%]	-	-	1.56

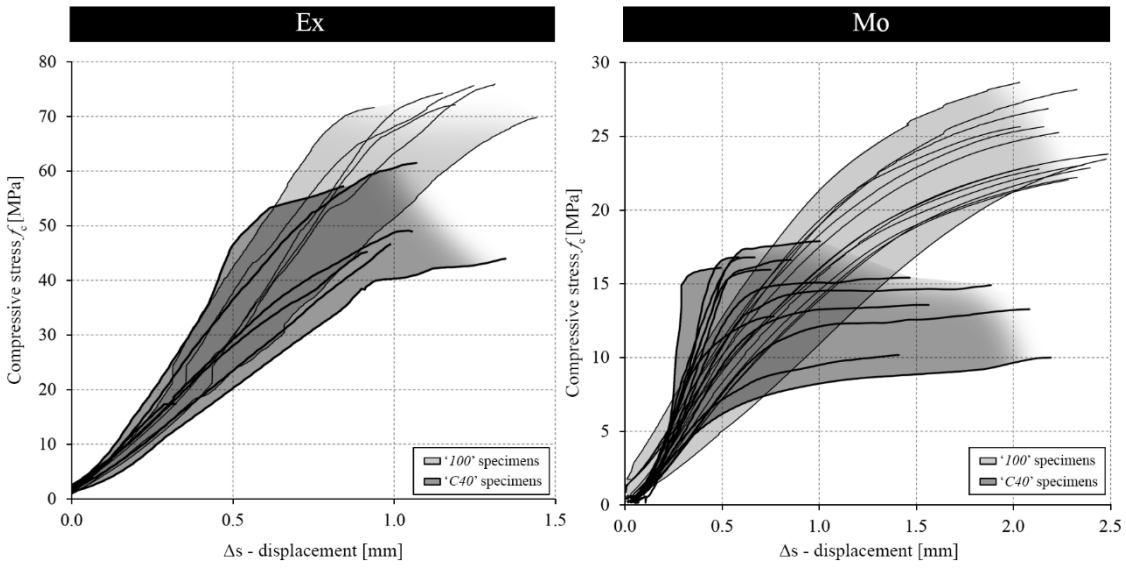

Fig. 16 Stress-displacement curves of the 18 mechanically extruded samples ('Ex'), and of the 26 modern handmade samples ('Mo_1') under uniaxial compression test along the brick thickness

Fig. 16 shows the stress-displacement curves of the '100' and 'C40' samples (along the thickness) of the extruded ('Ex') and modern handmade ('Mo1') brick types. The stresses acting on the specimens were computed as the ratio between the applied load and their cross-section area. The curves show an initial segment with increasing stiffness in all stress-displacement curves. This behaviour may be attributed to fact that the displacement was measured with the actuator and may be caused by the adjustment of the platens to the faces of the brick specimens. Beyond this initial segment, all curves present an approximately linear branch up to the maximum compressive strength. The 'Mo1' 'C40' specimens present an almost horizontal final branch before reaching the maximum. The linear branches of the 'Ex' 'C40' specimens are contained within the dispersion range exhibited by the '100' ones. This overlap shows that both specimens behave according to a similar elastic modulus, which suggest that their shape does not have a significant influence on the stiffness measured during the test. Conversely, in the case of the 'Mo1' specimens, the linear branches of the 'C40' and '100' specimens yield significantly different elastic moduli, suggesting that their stiffness may be influenced by the shape of the specimen.

The observed failure mode in both specimen types follows an hourglass shape, as shown in Fig. 17a, b, c, d, e and f, causing the complete separation of the outer parts. This failure mode is due to the confinement induced by the limited slenderness of the specimens. The acceptability of the failure modes in the 'C40' specimens was evaluated according to the recommendations of the concrete standard EN 12390-3:2020 [82] for cube specimens. Following this standard, satisfactory failures should show similar (approximately equal) cracking in the four exposed faces with little damage on the perimeter of the faces in contact with the platens. In turn, unsatisfactory failures present irregular cracked faces, tensile cracks or asymmetrical separation of the outer parts. Specimens showing this type of unsatisfactory failures should be disregarded. Following this approach, in the present research two specimens, respectively showing a tensile crack (Fig. 17g) and an asymmetrical separation of the outer parts (Fig. 17h), were discarded.

II.4. Discussion

This section presents two different studies based on the experimental results described in Section II.3. The first study focuses on the anisotropy of the material and the influence of the brick direction in the resulting compressive strength. In addition to the experimental campaign carried out within the present research, this study also considers experimental results from the available literature in the field. The second study is aimed to the derivation of an experimental correlation allowing the estimation of the compressive strength of the normalized standard '100' specimen from that obtained with the proposed 'C40' specimen. The section also includes a specific statistical analysis of outlier values potentially related with anomalous experimental results.

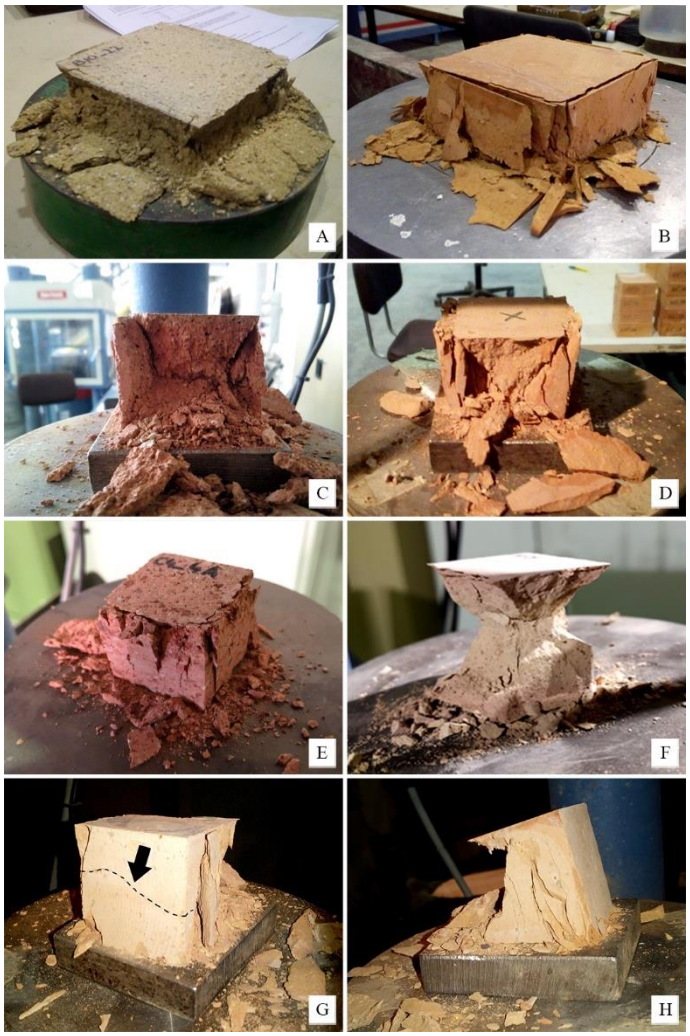

Fig. 17 Satisfactory and unsatisfactory failure modes: Satisfactory failures obtained for A) 'Mo' '100' specimen, B) 'Ex' '100' specimen, C) 'Mo' 'C40' specimen, D) 'Ex' 'C40' specimen, E) 'Hi' 'C40' specimen, and F) 'Hy' 'C40' specimen. Unsatisfactory failures obtained for G) 'Ex' 'C40' specimen having a tensile crack, and H) 'Ex' 'C40' specimen presenting an asymmetrical separation of the outer parts

II.4.1. Study on brick anisotropy

The experimental campaign on 'C40' specimens allowed the comparison of the compressive strength in the three brick orientations (t, w and l). This study has been performed on the mechanically extruded 'Ex', hydraulic press moulded 'Hy', modern handmade 'Mo' and historical 'Hi/Ma' specimens.

In fact, and as shown in Table 8 (Section II.3) and in Fig. 18, close values were found in each group for the three brick orientations. Fig. 18 presents in a boxplot the distribution of the data based on the quartiles (being the second and third quartiles coloured inside the boxes), and shows the median (depicted as a horizontal line inside the box), the average (depicted as a cross) and the possible outliers. The boxplot presents the distribution of the statistical data. Results in Fig. 18 shows that the statistical distribution of the compressive strength values has, in almost all cases, an asymmetrical shape with either positive or

negative skew. Asymmetrical distributions are identified by having neither the median nor the average in the centre of the box. Positive skewness occurs when the median falls below the average while negative skewness occurs in the opposite case. In addition, a larger spread in both value range and interquartile range is observed in industrialized bricks ('Ex' and 'Hy'), compared to the handmade ones. A light-tailed distribution can be seen in the handmade bricks ('Mo_1', 'Mo_2', 'Mo_3' and 'Hi/Ma') indicating a low kurtosis. It is recalled that kurtosis provides the measure of the sharpness of the peak in a data distribution in which the data values are concentrated around the average. Negative kurtosis means that the distribution has higher standard deviation than the normal distribution.

The boxplots present two potential outliers: (1) the minimum value within the 'Hy' specimens tested along the length, and (2) the maximum result within the 'Mo_2' specimens tested along the thickness. The analysis of these outliers is addressed in Section II.4.2.

The scientific literature discussed in Section II.1 includes only a limited number of references dealing with the experimental testing of brick specimens in compression under different orientations. Moreover, available references dealing with anisotropy in clay bricks focus mostly on mechanically extruded units. Fig. 19 shows experimental compressive strength values in different specimen orientations obtained by Aubert et al. [78], Salvatoni and Ugolini [80], Oliveira et al. [79], Fódi [54] and Krakowiak et al. [75]. The results from the references including all the experimental values are presented in a boxplot graph, while those corresponding to works that that only indicate the mean and standard deviation are presented as a point (mean) with a line calculated from the CV. Aubert et al. [78] obtained the largest strength in the direction perpendicular to the extrusion plane in extruded earth bricks. Oliveira et al. [79], Fódi [54] and Krakowiak et al. [75] also obtained the largest values through the extrusion plane in mechanically extruded solid clay bricks. In Krakowiak's research [75], bricks with two extrusion techniques showed maximum strength in relation to the extrusion plane as well. Finally, Salvatoni and Ugolini [80] obtained similar compressive strength values on modern handmade bricks regardless of the load direction. Thus, the literature reviewed indicates that an anisotropic response is normally observed in extruded bricks with the largest strength perpendicular to the extrusion plane. However, this anisotropic behaviour has not been found in handmade moulded bricks.

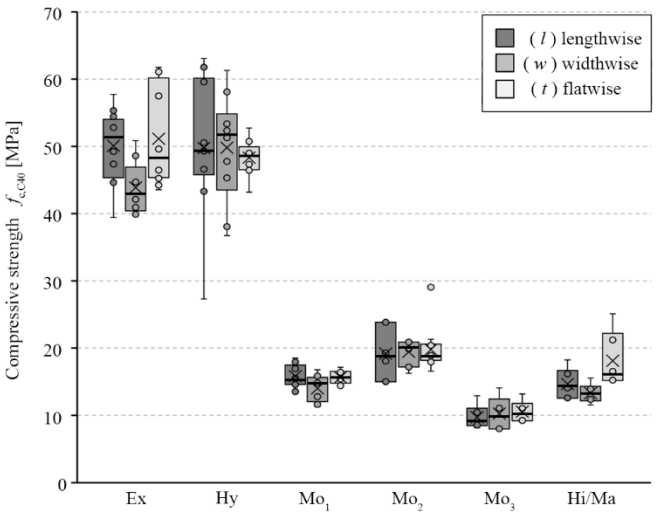

Fig. 18 Boxplot with lengthwise, widthwise and flatwise compressive strength values ($f_{c,C40}$) for the 'Ex', 'Hy', 'Mo1', 'Mo2', 'Mo3' and 'Hi/Ma' 'C40' specimens. Inside the boxes, the medians are represented with a horizontal line and the averages are represented with an X

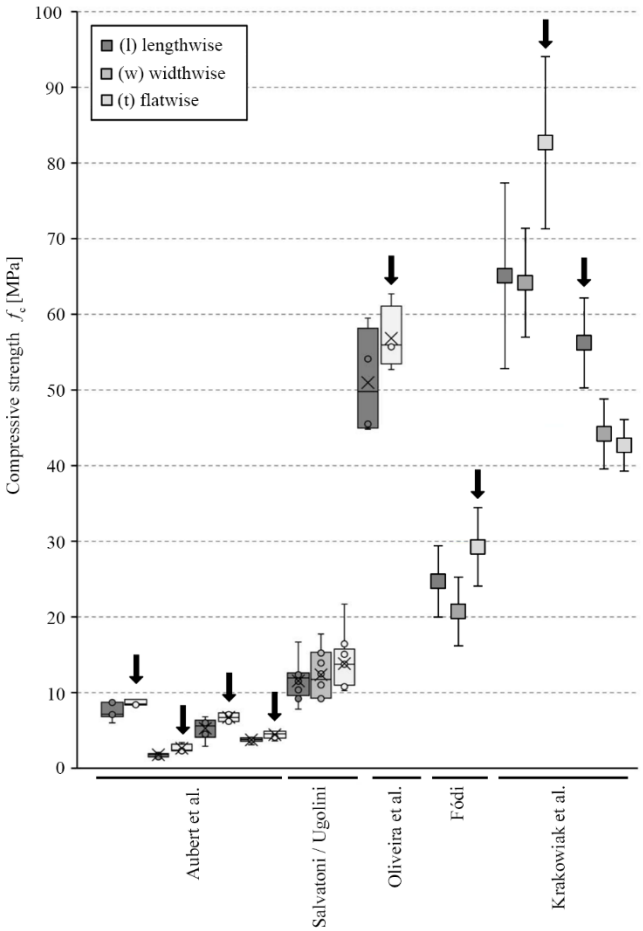

Fig. 19 Experimental compressive strengths along the different dimension of the brick as found in five available experimental programs in the literature Aubert et al. [78], Salvatoni and Ugolini [80], Oliveira et al. [79], Fódi [54] and Krakowiak et al. [75]. The arrows mark the cases of extruded units tested perpendicularly to the extrusion plane

The anisotropy of the brick types considered in the present study has been investigated through a statistical analysis. Fig. 20 shows the obtained histograms with the resulting probability distribution functions and Table 9 shows the skewness and kurtosis determined for the different group samples. The probability functions Fig. 20 are only a tentative adjustment as the samples of each group are limited in size. The histograms show symmetrical (with different kurtosis) and asymmetrical (with positive or negative skewness) distributions. More specifically, Table 9 indicates positive kurtosis for the 'Hi/Ma' (l) samples and close to zero or negative for the other cases. In addition, Table 9 indicates a general symmetry or minor skewness for all the cases. Skewness values under 0.5 (in absolute value) in the 'Hy' (t) (w), 'Mo$_1$' (t) (l) (w) and 'Mo$_2$' (t) (l) samples indicate a symmetric distribution. Absolute values between 0.5 and 1.0 indicate minor skewness, either positive or negative, in the 'Ex' (l) (t) (w), 'Hi/Ma' (l) (w), 'Ex' (l) and 'Hy' (l) samples. Finally, absolute values over 1.0 indicate a high degree of skewness, positive in the 'Mo$_3$' (l) and 'Hi/Ma' (t) samples and negative in the 'Mo$_2$' (w) ones.

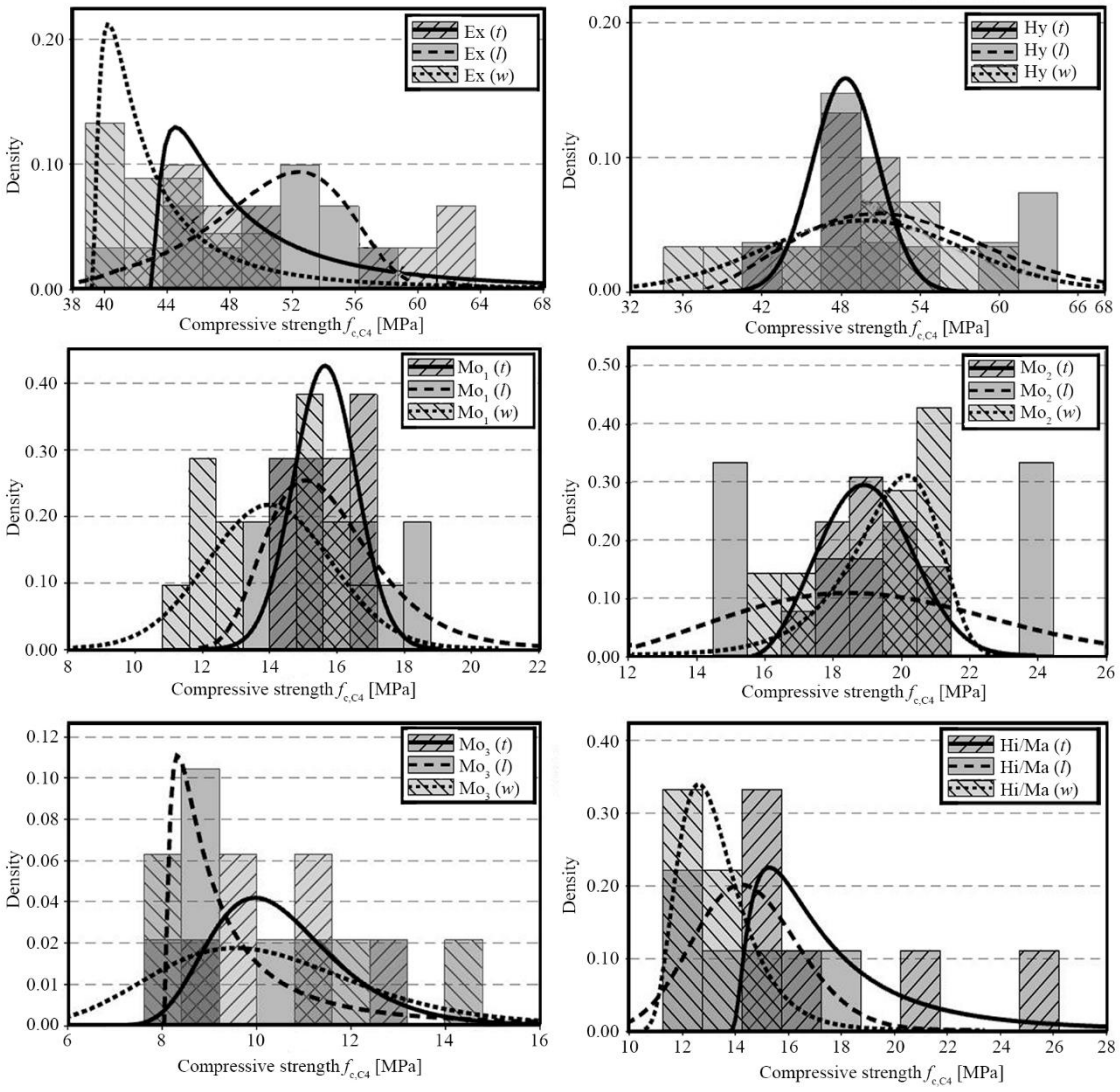

Fig. 20 Histograms and statistical distributions for the tested samples

Table 9 Skewness and kurtosis of the statistical distributions for the tested samples

	'Ex'			'Hy'			'Mo$_1$'		
	(l)	(w)	(t)	(l)	(w)	(t)	(l)	(w)	(t)
Skewness	-0.6	0.8	0.7	-0.8	-0.5	-0.3	0.3	-0.1	0.0
Kurtosis	-0.1	-0.4	-1.5	-1.4	-0.5	0.7	-1.2	-1.7	-1.2

	'Mo$_2$'			'Mo$_3$'			'Hi/Ma'		
	(l)	(w)	(t)	(l)	(w)	(t)	(l)	(w)	(t)
Skewness	0.3	-1.1	0.2	0.3	-1.1	0.2	0.3	-1.1	0.2
Kurtosis	-1.9	-0.5	-0.2	-1.9	-0.5	-0.2	-1.9	-0.5	-0.2

Schueremans [85] observed a positive skewness in a large campaign carried out with 50 handmade brick samples, whose results could be adjusted with a lognormal statistical distribution. However, the results obtained in the present research cannot be adjusted with lognormal distribution due to the large variability obtained in terms of kurtosis and skewness. Likewise, normality test and histogram analysis may have an insufficient capacity to detect whether the samples conform normal distribution due to the limited sample size.

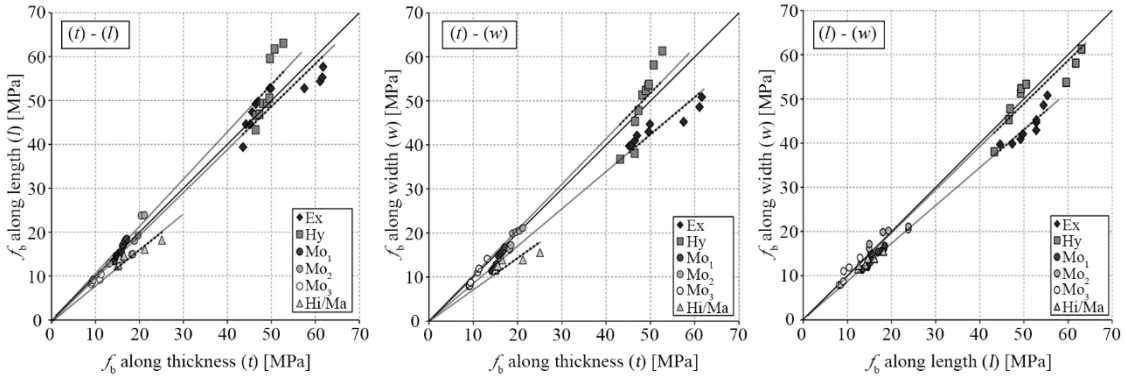

Fig. 21 The linear regression relating (t) – (l), (t) – (w) and (l) – (w) pairs of testing directions for 'Ex', 'Hy', 'Mo$_1$', 'Mo$_2$', 'Mo$_3$' and 'Hi/Ma' specimens

A graphic verification allows the detection of possible anisotropy in some of the sample series. As can be seen in Fig. 21, three linear regressions were performed pairing (t) – (l), (t) – (w) and (l) – (w) values for each type of brick. The trend line of each paired values was compared with the ideal line of 45 degrees denoting equal strengths along the two considered directions. Fig. 21 shows the similarity of compression strengths along thickness and length for the 'Ex' samples, while strength values along the width are meaningfully lower than those obtained along the other two directions. The 'Hy' series shows similar strength values in the three cases. The three 'Mo' series almost overlap the 45-degree regression line. The 'Hi/Ma' series also overlaps the 45-degree line for the paired strength values along length and width, while higher strength values are obtained along the thickness.

A new statistical evaluation was carried out to identify meaningful strength differences among the orientations, and to confirm the possible anisotropy of some brick types. A nonparametrical analysis was applied since the data could not be adjusted to a normal distribution and the number of samples in each population was small. Two nonparametric tests that can be used for this purpose, i.e., the Kruskal-Wallis test [86], and the Wilcoxon Sum Rank test [87]. The Kruskal-Wallis test [86] was used to compare the three data sets corresponding to the dimensions t, w and l, and determine whether they belong to the same data population. The Kruskal-Wallis test provides the probability of fulfilling the statistical hypothesis that the data sets belong to the same data population. Probabilities below 5% lead to reject the hypothesis while probabilities above 5% lead to accept it. The Wilcoxon Sum Rank test [87] compares two data sets and determines if the values of a reference data set are lesser, equal, or larger than the values of the other data set. The paired data sets tested were (t) – (l), (t) – (w) and (l) – (w).

The Kruskal-Wallis test indicated that the data sets along the three brick directions are coincident (i.e., correspond to a single population) for series 'Hy', 'Mo_1', 'Mo_2' and 'Mo_3', while series 'Ex' and 'Hi/Ma' are non-coincident data sets. The 'Ex' and 'Hi/Ma' series showed the lowest coincidence probability (2%), meaning that their compressive strengths along their three orientations can be assumed to be different. Coincidence probabilities above 5% were obtained for series 'Hy', 'Mo_1', 'Mo_2' and 'Mo_3' (50.5%, 7.2%, 79.9% and 56.7% probability respectively).

The Wilcoxon Sum Rank test was executed considering brick sample series for which the Kruskal-Wallis test indicated that the data sets were non-coincident, i.e., in series 'Ex' and 'Hi/Ma'. This complementary test indicated that the compressive strength along the thickness is larger than those along the length and width, and that the compressive strength along the length is larger than that measured along the width ($t > l > w$) in these series.

Using the previously presented statistical and graphical tests allows some conclusions on the anisotropy of the investigated brick types. Moderate anisotropy has been found in the extruded bricks 'Ex', in which the lowest compression strength is obtained along the width. In turn, the 'Hi/Ma' bricks show larger strength along the thickness than in the other two directions. In the rest of the brick series tested ('Hy', 'Mo_1', 'Mo_2' and 'Mo_3') no significant difference among the compressive strength is observed along the three orientations (t, w and l).

The anisotropy of extruded clay units has been investigated by other authors. Habelitz et al. [88] and Viani et al. [89] focused on the microstructure of extruded bricks. Krakowiak et al. [75] concluded that the micro-porosity exhibits a preferential orientation along the extrusion direction, directly affecting brick properties such as the water absorption, the modulus of elasticity and the strength. Kubiś et al. [90] and Bourret et al. [91] observed these microstructure irregularities and concluded that the anisotropy influences the thermal conductivity and the elastic properties. Makoond et al. [12,92] studied the dynamic elastic

properties in extruded bricks using ultrasonic pulse velocity testing, revealing different relative dispersions (indicating different elastic properties) among the different brick directions. Research on other materials produced by extruded techniques showed anisotropy in physical and mechanical properties, as in Maillard et al. [93] on earth bricks, Antal et al. [94] on Illite-Based ceramics, and Boussois et al. [95] on ceramics. The anisotropy of these materials was derived from the analysis of the manufacture process and the orientation of the clay mineral particles of the feeding material [96,97]. In general, the conclusions obtained by previous researchers are consistent with the anisotropy detected in the present study for extruded bricks.

II.4.2. Analysis of outliers to detect anomalous experimental results

The visual criteria considered in disregarding inadequate specimens have been indicated in Sections II.2.2 and II.3. These criteria have been actually applied in order to disregard specimens deemed inadequate because of the presence of material imperfections (inclusions and voids), excessive aggregate diameter or inadequate failure modes. In spite of this previous selective effort, additional statistical criteria have been also applied to disregard anomalous cases that might not have been visually recognized and may manifest as statistical outliers. Such outliers might be related to anomalies not easily detectable during the experiments, as for instance possible small load eccentricities causing an unexpected tensile failure mode, the lack of parallelism between the bearing surfaces, or excessive confinement exerted by the press platens.

As mentioned in the previous section, two possible outliers can be identified in this experimental campaign, as shown in Fig. 18, corresponding to (1) the minimum value within the 'Hy' specimens tested along the length and (2) the maximum value within the 'Mo_2' specimens tested along the thickness.

A careful evaluation of outliers requires an ad-hoc statistical analysis. Two tests are proposed to identify the potential outliers: the Grubbs test [98] and the Murphy test [99]. The Grubbs' test is used to determine whether a single outlying value within a set of measurements falls sufficiently apart from the average as to be statistically classified as not belonging to the same population (outlier). In this case, the value can be omitted in subsequent calculations. The Murphy's test determines whether the two largest observations within a set of measurements should be considered as outliers and omitted from the data set. The Murphy's test is applied to avoid the statistical masking and swamping effects [100,101] that may appear when two close outliers are present. Since the outlier tests are based on the assumption of normality, it is necessary to convert the obtained asymmetrical distribution into a normal one. Although, as mentioned, the brick samples investigated in this study do not comply, in general, with a lognormal distribution, this kind of distribution can in fact be utilized to model the 'Ex' (t) (w), 'Mo_3' (l), and 'Hi/Ma' (t) (l) (w) samples owing to its positive

skewness and adequate kurtosis. The corresponding lognormal distributions can be translated into a normal one using a logarithmic conversion, causing high data to compress and low ones to expand. In turn, the distributions of series 'Ex' (l), 'Hy' (l), 'Mo$_2$' (w), characterized by negative skewness, can be translated to a normal distribution using a square value conversion, which compresses the scale for low data and expands it for high ones.

The application of the Grubbs' test confirms the already identified potential two outliers with a critical value over 2.5%. This value indicates the threshold of statistical significance defining the upper and lower bounds of the confidence interval. Moreover, the Murphy's test did not identify any additional outlier. After extracting the outliers, the 'Hy' (l) series has a modified average of 52.3 MPa (CV of 13.9%), and the 'Mo$_2$' (t) series has a modified one of 19.1 MPa (CV of 7.1%). The extraction of the outliers reduces the CV almost by half, while the averages remain practically the same in both cases (with variations of +5% and +3.5% respectively).

II.4.3. Compressive strength correlation between standard and nonstandard specimens

Based on the experimental campaign presented, it has been possible to derive a correlation between the experimental compressive strength measured with the '100' specimen with that measured with the 'C40' (t) one ($f_{c,100}/f_{c,C40}$ ratio). This study has been performed on the 9 brick types indicated in Fig. 22. An average value of the $f_{c,100}/f_{c,C40}$ ratio equal of 1.65 has been obtained for the set of the different brick series, with an standard deviation of 0.20 (CV of 12%). The $f_{c,100}/f_{c,C40}$ ratio has been determined for different types of bricks produced with similar handmade manufacturing process, except the 'Ex' type. However, the 'Ex' samples show a ration (1.47) similar and within the range of the handmade ones. As shown in Table 8 (Section II.2) and Fig. 22, the ratio ranges between 1.32 and 1.96.

The box-plot graph in Fig. 22 shows two features already discussed apropos of Fig. 18, namely the generalized asymmetry of the distributions and the potential presence of outliers, the latter being apparently visible in the 'Hi/I$_1$' series. However, the application of the Grubbs and Murphy tests, as in Section II.4.2, indicated that such extreme values cannot be actually considered as outliers in this case.

A statistical analysis of the experimental $f_{c,100}/f_{c,C40}$ ratios was carried out in order to undertake a more detailed analysis of its variation, For this purpose, the histogram distribution of the $f_{c,100}/f_{c,C40}$ ratios was determined as shown in Fig. 23. The normality of the distribution was checked using the Shapiro-Wilk test [102], which confirmed that the experimental $f_{c,100}/f_{c,C40}$ ratios follow a normal distribution. However, the histogram of Fig. 23 shows an empty column in the range 1.60 – 1.70 where the average (1.65) is positioned. This peculiarity does not show any relationship with brick types (i.e., with their manufacture process) and is attributed to a purely random effect.

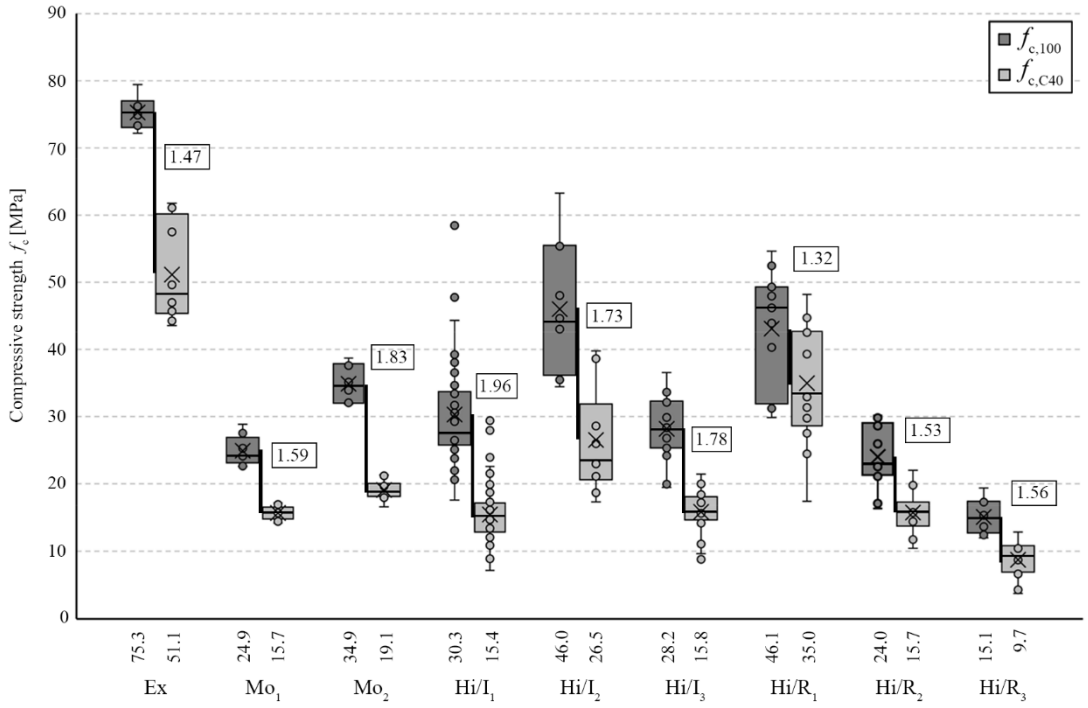

Fig. 22 Box-plot with $f_{c,100}$ and $f_{c,C40}$ values for the 'Ex', 'Mo', 'Hi/I' and 'Hi/R' samples. The numbers in the squares indicate the relation between the compressive strength averages of the '100' and 'C40' specimens ($f_{c,100}$ / $f_{c,C40}$) along the thickness. Inside the boxes, the medians are represented with a horizontal line and the averages are represented with an X. The numbers in the horizontal axis indicate the compressive strength averages for each sample

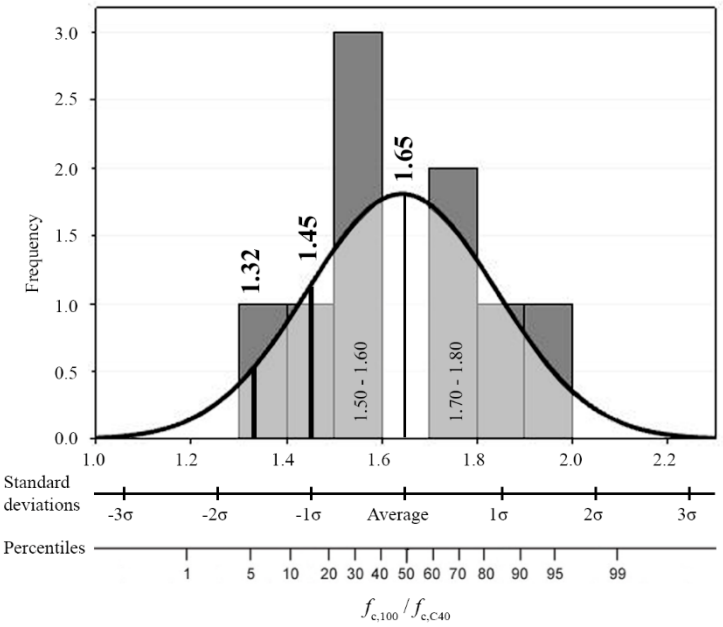

Fig. 23 Histogram and probability distribution function for $f_{c,100}$ / $f_{c,C40}$ ratios

A modified estimate of the $f_{c,100}/f_{c,C40}$ ratio, intended to be considered for an engineering estimation of the compressive strength of bricks from the 'C40' specimen, can be calculated based on the normal density distribution (Fig. 23). Specifically, the proposed engineering value is calculated as the value of the ratio for the -1σ standard score. The standard score (or z-score) is the number of standard deviations (σ) by which a value is above or below the average. Thus, the proposed engineering $f_{c,100}/f_{c,C40}$ ratio, located at the safe side with respect to the average, and corresponding to the score -1σ, is equal to 1.45. Fig. 23 shows its location in the normal distribution. As shown by the figure, the proposed value is a safe one in comparison with a large part of the values occurring according to the density distribution. Another possibility for an engineering estimation could consist in adopting the value corresponding to the 5% percentile. This second possibility is considered as too conservative in this case, as it yields a value equal to 1.32, which falls at the lower bound of the full set of experimental values.

II.5. Conclusions

A study has been presented on the viability of determining the compressive strength of solid clay bricks by testing non-standard small cubic specimens of dimensions 40 × 40 × 40 mm^3 (labelled as 'C40'). The use of this small specimen allows the measurement of the compressive strength along the three brick dimensions (length, width and thickness). Therefore, the 'C40' specimen has enabled the investigation of the anisotropic response that is observed in some brick types depending on their manufacturing process. Moreover, the use of this small specimen allows reducing the volume of material sampled from existing structures, which may be severely restricted in the case of architectural heritage. The viability in the use of the 'C40' sample has been investigated by comparing experimental results with those obtained with a standard 100 × 100 × 40 mm^3 specimen (labelled as '100').

The viability of the nonstandard 'C40' specimen was validated through an experimental campaign on mechanically extruded, hydraulic press moulded, modern handmade and historical handmade bricks, the latter extracted from six 19th century and early 20th century buildings in Barcelona (Spain). The following conclusions can be drawn from the experimental procedures and the analysis of the experimental results:

- A relatively easy and efficient procedure could be implemented to extract the historical bricks from existing walls. Common electric tools were employed, such as a jackhammer to remove the plaster, together with manual chisel and a nylon hammer for the careful extraction of the bricks.
- The failure mode of the 40 × 40 × 40 mm^3 specimen showed a characteristic hourglass shape. Successful failure modes were judged following standardized criteria for concrete cube specimens.

- A specific methodology has been proposed and applied for the post processing of the experimental results. The proposed methodology is based on a statistical analysis of the experimental data and includes the application of nonparametric statistical tests. This methodology could be similarly applied to extend the research to other brick types.
- The study shows that the extruded solid clay bricks investigated present a moderate anisotropy due to their manufacturing process. The smallest strength is obtained along the width and the largest one along the direction perpendicular to the extruded plane (which can be the thickness or the length depending on the manufacturing process). This observation has been corroborated from data found in the scientific literature. However, an almost isotropic behaviour has been obtained for the three handmade moulded bricks and the hydraulic press moulded ones herein investigated.
- The results of the experimental analysis show that the compressive strength measured on the two specimen types (the standard '100' and nonstandard 'C40') can be correlated by an average ratio $f_{c,100}/f_{c,C40}$ equal to 1.65 (CV of 12%) ranging between 1.32 and 1.96. This ratio allows the estimation of the compressive strength of the standard '100' specimen from that measured from the 'C40' one on solid fired clay brick. However, a more conservative and engineering ratio equal to 1.45 is proposed based on statistical considerations. The mechanically extruded specimens 'Ex' show a ratio (1.47) very similar to that of the handmade ones.
- The proposed 'C40' specimen has provided an advantageous technique for the evaluation of the compressive strength of solid clay bricks in existing masonry structures. In practical applications oriented to the characterization of existing brick masonries, it is suggested to test at least a set of twelve specimens from six different units to obtain a reliable estimation of the compressive strength.

Future works could address the extension of the experimental database to a largest sample of solid clay bricks, as well as a detailed study of the possible influence of the material's porosity on the compressive strength and anisotropy. This extension would allow a deeper confirmation of the results herein presented regarding the suitability of the proposed specimen and the anisotropy of different brick types.

2.4. Paper III – Effect of cross section aspect ratio and bearing surfaces treatment on the compressive strength of solid fired clay brick specimens

A. Cabané, L. Pelà, P. Roca

Construction Building Materials 383 (2023) 131397

https://doi.org/10.1016/j.conbuildmat.2023.131397

Abstract. This study addresses the evaluation of the confinement effect in the experimental determination of compressive strength in solid fired clay units. The experimental campaign has focused on two different types of solid fired clay bricks, namely mechanically extruded and handmade, with a total amount of 458 specimens. The research considers different standard specimens, such as whole or half brick, and 100 × 100 × 40 mm^3 specimen, and nonstandard 40 × 40 × 40 mm^3 specimen, subjected to different standard bearing surface treatments, i.e., grinding, capping with cement mortar or gypsum plaster, placing with birch plywood or fibreboard. Additionally, two novel bearing surface treatments are proposed, i.e., covering with gypsum powder, and placing two oiled PTFE leaves. The experimental campaign has focused on four main aspects. First, the evaluation of the compressive strength value in specimens with hardening response. Second, the influence of the cross section's aspect ratio, defined as the ratio between the specimen's length and width. Third, the influence of the bearing surface treatment on the determination of the compressive strength. Fourth, the evaluation of the standard compressive strength through the comparison amongst reference standards. The results highlight and quantify the different factors that influence the confinement, while detecting differences depending on the manufacturing process of the unit. In addition, the results reveal the use of oiled PTFE leaves as a promising and fast possibility of low boundary friction to obtain the strength regardless of the specimen shape.

III.1. Introduction

The load-bearing capacity of masonry structures depends on their components' strength, being the compressive strength of the units one of the main important parameters [7,74]. Regardless of the type and material of the unit tested, the experimental compressive strength depends on the specimen's dimensions and the confinement produced by the friction of the press steel platens on the specimen's bearing surfaces during the test [48]. The specimen's dimensions and the confinement effect can have a remarkable influence on the experimental evaluation of the compressive strength. The experimental assessment of the compressive strength on solid fired clay units has always been a subject of debate, and many

standards describe different specimen shapes, sizes and bearing surfaces treatments, showing an existing lack of consensus about a common procedure. In addition, available international standards and studies usually propose characterisation procedures and methodologies regardless the unit shape, form, material and manufacturing process.

Acquiring a full knowledge on the compressive strength of solid units is necessary to design adequate masonry structures as well as to evaluate existing ones. The experimental compressive strength characterisation of solid bricks is greatly affected by the stress developed on the specimen's bearing surface during the loading test, the reduced specimen slenderness due to its small height conditioned by the brick thickness, which can vary between 40 mm to 60 mm [103], and the cross section's aspect ratio between the length and width [5].

The analysis of the effect of the cross section's aspect ratio was addressed in few research studies available in the scientific literature. Page [76,104] studied three calcium silicate brick specimen types with the same length and height but different width, by testing them between 5 mm plywood sheets or between flexible brush platens. Khalaf et al. [5] studied four solid concrete unit specimen types by fixing the width and height and varying the length. Fódi [54] investigated three specimens of mechanically extruded solid fired clay bricks by changing their length by cutting off a part. A similar approach was followed by Salvatoni and Ugolini [80] for modern handmade solid fired clay bricks.

The stress developed on the specimen bearing surface was reported by Murray [105] in 1942, describing three possible stress conditions at the bearing surfaces of the specimens: the uniform uniaxial compressive stress, the vertical compressive stress and radial tensile stress when capping materials are used due to their deformation under load, and the vertical compressive stress with restraining radial stresses induced by friction between the bearing surface and the loading press platen.

Some authors investigated how to determine a uniform uniaxial ideal "unconfined" compressive strength by testing specimens with different capping or bearing surface treatments. The steel brush bearing platens proposed by Hilsdorf [106] for concrete specimens consisted of individual filaments with a cross section of 5 × 3 mm^2 spaced 0.2 mm and variable length from 90 to 140 mm depending on the concrete strength, soldered together in a solid platen with 35 mm of thickness. The brushes were originally used by Kupfer et al. [107] in 1969, and reported its use by Van Mier [48], Thomas et al. [108] and Binda et al. [77,109], among others. Page [76,110] reported the use of the brush platens in calcium silicate units but with different filament section and distribution, using filaments with circular cross section of Ø5.5 mm, 120 mm long, and spaced 0.8 mm. Hussein et al. [111] modified the brush platens to test high strength concrete and proposed the use of filaments with a cross section of 5 × 5 mm^2 and 75 mm long, soldered in a 40 mm thickness solid platen. Schickert [112], in 1973, used the Hilsdorf brushes with a filaments cross section of 4 × 4 mm^2 and 90 mm long,

and also proposed a piston system that divides the pressure platen into individual pistons with a cross section of 25 × 25 mm² connected to each other by elastomeric piece [113,114].

The scientific literature includes only a limited number of references about solid fired clay units, while more experimental studies can be found for concrete specimens. The first research was carried out by Gonnerman in 1924 [115], comparing the standard concrete specimens capped with cement mortar with strength ranging from 7 to 38 MPa, with alternative capping materials as gypsum or mixtures of cement and gypsum. Gonnerman [115] found that the concrete specimens had similar strength regardless of the capping material used. Purrinton et al. in 1926 [116] and McGuire in 1930 [117] proposed the use of fine sand placed in a confining container testing 14 MPa, 21 MPa, and 24 MPa concrete specimens. Purrinton et al. [116] reported that the strength of the concrete cylinders tested with sand cushion were similar to those capped with cement mortar, while McGuire [117] reported that the strength depends on the diameter of the restraining rings used to confine the sand. In 1928, Freeman [118,119] reported the use of sulphur mortar capping on 55 MPa strength concrete specimens. The research carried out in concrete specimens until the 70's focused on the comparison and validation of the specimens with strength up to 50 MPa capped with material such as cement mortar, sulphur mortar, plaster of Paris, high, medium and low strength gypsum, and mixtures of cement and gypsum (i.e., Troxel in 1941 [120], Vidal in 1942 [121], Masters et al. in 1952 [122], Werner in 1958 [123] and Saucier in 1972 [124]). Troxell [120] reported that concrete cylinders capped with high-strength gypsum or sulphur mortar had higher strength than those capped with plaster of Paris. Vidal [121] confirmed the Troxell results. Masters et al. [122] investigate the effects of the sulphur cap age and thickness on the strength, and found that higher experimental strengths were obtained in specimens with reduced thickness sulphur mortar caps. Werner [123] investigated aluminous cement mortar, plaster of Paris, mixtures of cement and plaster of Paris, high-strength gypsum, and sulphur, concluding that the use of different capping materials has greater effects on specimens made of high-strength concrete than on specimens of low-strength concrete. Saucier [124] used steel rings to confine the capping material because low-strength gypsum capping material provided lower experimental strength. In the 70's and 80's, sever studies investigated the use of an unbounded capping system composed of polychloroprene (commonly known as Neoprene ®) pads restrained by metal rings for testing of concrete specimens. Ozyildirim in 1985 [125], Carrasquillo et al. in 1987 [126] and Richardson in 1990 [127] compared the strength of the concrete specimens capped with sulphur mortar with unbonded specimens using Neoprene pads. Ozyildirim [125] and Richardson [127] tested concrete specimens up to 40 MPa and concluded that the strengths derived from the two capping methods showed no differences. Carrasquillo et al. tested specimens up to 114 MPa [126] concluding that the proposed Neoprene pad-cap system provided similar strength to those with sulphur caps. In the 90's the use of ground surfaces was incorporated to test high-strength concrete specimens and compared with the use of

Neoprene pads and sulphur caps (i.e., Chojnaki et al. in 1991 [128], Pistelli et al. [129], Lessard et al. [130], and French et al. in 1993 [131], and Carino et al. in 1994 [132]). Chojnaki et al. [128] reported that for 70 MPa and 90 MPa concrete specimens there are no significant differences between specimens capped with sulphur mortar and grinded ones. Pistelli et al. [129] reported that for concrete specimens between 20 MPa to 120 MPa the use of pad-cap Neoprene system provided slightly lower strengths than grinded ones. Lessard et al. [130] reported that, for concrete specimens between 115 MPa and 130 MPa, the strength of the specimens capped with sulphur are 85% of that of the grinded ones. French et al. [131] tested concrete cylinders with grinded surfaces, capped with sulphur mortar and unbounded Neoprene cap-pads, evidencing similar strengths. French et al. [131] reported violent failure due to the energy stored in the Neoprene pads affecting the post-ultimate behaviour of the specimens. RILEM TC 148-SSC [133] presented a research carried out by 10 universities in 1997 on 45 MPa and 75 MPa concrete specimens with high and low friction loading systems. The chosen low friction loading system was based on Polytetrafluoroethylene leaves (commonly known as PTFE or Teflon ®).

The research on the bearing surface treatment influencing masonry units were initially developed by Kelch et al. in 1958 [134], Dodd et al. in 1960 [135] and Morsy in 1968 [136]. Kelch et al. [134] studied the influence of the thickness of sulphur mortar and gypsum caps on clay masonry units, reporting similar small differences. Dodd et al. [135] studied different capped materials such as cardboard, plasterboard, insulating wallboard, cement mortar and dental gypsum plaster, reporting small strength difference too. Morsy [136] studied the influence of seven types of surface coating on ground and rough scaled solid clay units, i.e., steel plate, grind, plywood, hard-board, 6 layers of polythene, rubber with fibres, and pure rubber, reporting high strength differences depending on the bearing material. Page [76] studied in 1984 the influence of the birch plywood sheets in calcium silicate units, comparing with the unconfined units tested with brush platens. Khalaf et al. [137] studied different bearing surface treatments for masonry units in 1989, such as grinded, capped with cement mortar, plywood packing or using dental plaster in a polythene bag. Khalaf et al. [137] found that the grinded specimens were stronger than the other specimens, being the difference smaller for low or medium strength bricks. Khalaf et al. [137] recommended to test the solid brick specimens with grinded surfaces instead of considering capped ones, but packing was suggested to test the block specimens. Templeton et al. [138] studied the methods to prepare the bearing surfaces in 1990, as referred in the withdrawn of the ISO 9652-4 [139], i.e., grinding and capping with cement mortar, founding that the specimens capped with cement mortar offered lower compressive strength than the grinded ones. Page et al. [110], in 1991, studied the influence of the packing hollow concrete bricks using plywood or fibreboard, reporting a reduced experimental strength on specimens tested with fibreboard. Drysdale et al. [140] suggested in 1994 that masonry units can be tested using hard capping materials, such as sulphur mortar or gypsum plaster as indicated in the ASTM C67/C67M-21 [47], and

other capping materials, such as fibreboard, plywood or PTFE leaves, greased platens or brush platens. Drysdale et al. [140] evidenced that specimens tested with hard capped materials (gypsum plaster) produced higher experimental strengths, without establishing a relationship with those capped with soft materials like fibreboard. Crouch et al. [141] studied the use of the Neoprene pads in concrete masonry units in 1999, reporting a 20% reduction in strength for the specimens tested with Neoprene pads compared to those tested with gypsum cement caps, due to the excessive expansion of the Neoprene pads. In 2010, Lourenço et al. [55] recommended the use of oiled PTFE leaves to reduce the confinement while testing solid fired clay bricks. In 2016, Aubert et al. [78] compared grinding with placing oiled leaves of PTFE on 50 mm cubic specimens of earth bricks, finding similar compressive strengths.

Murray [105], Daniel et al. [142], Neville [59] and Morsy [136] prevented the use of flexible materials from being applied on bearing surfaces. Murray [105], Daniel et al. [142] and Neville [59] indicated the importance of limiting the differences of Poisson's ratios between the bound material and the specimen. Murray [105] suggested that the most desirable conditions results from using capping materials that are as strong as the tested material and have similar modulus of elasticity and Poisson's ratio. Daniel et al. [142] reported that soft capping materials, such as lead and rubber, can deform outwards when the specimen is loaded producing radial stresses. Thus, soft materials such as Neoprene reduce the apparent compressive strength of the specimen, as previously observed by Richardson in concrete specimens [127] and Crouch et al. in concrete units [141]. The capping Neoprene can produce higher confinement in the centre of the specimen than in the borders, as analysed by Braga et al. [143]. Kleeman et al. [144] studied the mechanical properties of four different materials commonly used as packing material in compression tests on masonry, i.e., plywood, hardboard, fibreboard and particle board, concluding that the packing material's tangent moduli increase with increasing stress, and so does the tangent shear moduli. Morsy [136] concluded that flexible materials such as polyethylene (PE), rubber, or rubber with fibres tend to deform under the load application because of their Poisson's ratio higher than that of the clay material [92,145]. Schickert [112] compared the lateral strains and experimental strengths of the specimens tested with grinded surface, lubricated aluminium sheets, and steel brush platens, reporting that the specimens tested with aluminium sheets has 94% the strength of the specimens tested with rigid steel platens , and 81% the strength of the specimens tested with steel brushes. In addition, the lateral strain measured close to the bearing surfaces was about 50% of that measured at half height on specimens tested with brush platens, 45% on specimens tested with aluminium sheets, and 20% to 30% on specimens tested with steel platens. Schickert [112] considered that lubricated aluminium sheets produced more unrestrained deformation than steel platens, being close to that produced using the brush platens. The research group of RILEM TC 148-SSC [133] tested concrete specimens using PTFE leaves (single or double) and concluded that the

strength and the pre-peak stress-strain behaviour became independent of the specimen slenderness.

International reference standards for masonry units recommend different surface treatments. The American ASTM C67/C67M-21 [47] for clay units recommends to cap the bearing surfaces with cement mortar, gypsum plaster or sulphur filler, while the ASTM C140/C140M-22b [146] for concrete and calcium silicate bricks specifies to cap the specimens with gypsum cement or sulphur filler following the ASTM C1552-16 [147]. The European EN 772-1:2011+A1:2016 [9] recommends to grind the surfaces or to cap them with cement mortar. The Australian AS/NZS 4456.4:2003 [11] recommends the use of two sheets of 4 to 6 mm plywood, hardboard or 12 mm thick fibreboard. The Canadian CAN/CSA A82:14 (R2018) [10] indicates the use of gypsum plaster or sulphur filler to cap the bearing surfaces, while the CAN/CSA A165-14 (R2019) [148] refers to the American ASTM C140/C140M-22b [146].

A review of the American and European standards for concrete testing shows that the American ASTM C39/C39M-21 [8] recommends grinding, capping with high-strength gypsum or sulphur mortar following the ASTM C617-10 [149], or capping with Neoprene pads following the ASTM C1231/C1231M-14 [150], while the European EN 12390-03:2022 [82] recommends grinding or capping with calcium aluminate cement, sulphur filler or iron sandbox.

This paper considers whole bricks, half bricks, 100 × 100 mm², and 40 × 40 mm² specimens for the experimental evaluation of the influence the cross section aspect ratio and the bearing surface treatment on the compressive strength of solid fired clay bricks. The analysed treatments considered are grinding, capping with cement mortar or gypsum plaster, placing birch plywood or medium density fibreboard (known as MDF). The interpretation of the experimental results is carried out according to a detailed analysis, quantifying the differences amongst the experimental strengths depending on the chosen approach. Additionally, this paper proposes the use of two novel bearing surface treatments to generate low boundary friction, i.e., covering with gypsum powder, and placing two oiled PTFE leaves. Few references have been found in the scientific literature about the use of gypsum powder related with the DIN 18555-9:2019-04 [2] for testing mortar joints, e.g. Pelà et al. [45], while other studies used talcum powder as covering material in concrete, e.g. Ghadami et al. [151] and RILEM TC 148-SSC [133]. Several references recommend to use oiled PTFE leaves, such as RILEM TC 148-SSC [133] and Hussein et al. [111] for concrete, Lourenço et al. [55] for solid clay bricks, and Aubert et al. [78] for earth bricks. This paper considers the use of two oiled PTFE leaves on each bearing surface to reduce the friction between the press platen and the specimen's surface, in order to ensure a more uniform distribution of stresses. The use of two leaves reduces the radial stresses caused by the deformations of the PTFE in contact with the press platen due to the very low coefficient of friction (around 0.04, as indicated by the manufacturers). In addition, the additional use of mineral oil between both PTFE leaves ensures minimising further the friction of the system.

This research offers the results of an experimental campaign on two different solid fired clay brick types characterised by different manufacturing process, i.e., mechanically extruded and handmade, including the execution of 458 laboratory tests. The research encompasses the following specific objectives: (1) evaluating a methodology to estimate an equivalent compressive strength value in specimens that exhibit a hardening response in the experimental stress-displacement curve; (2) exploring the influence of the specimen's cross section aspect ratio on the determination of the compressive strength; (3) determining the influence of the bearing surface treatment on the experimental compressive strength; and (4) comparing four available reference standards with different recommendations about specimens' geometry and surface treatments for the experimental determination of the compressive strength.

The paper is structured in five sections. After this introduction, Section III.2 presents the experimental campaign performed on solid fired clay bricks, including the description of the materials, the specimens' and bearing surfaces' preparation, and the testing procedure. Section III.3 shows the experimental results. Section III.4 analyses the experimental estimation of the equivalent compressive strength values for specimens with hardening response, the influence of the cross section's aspect ratio and of the different bearing surface treatments on the compressive strength, and the comparison of four different international standards for the determination of the compressive strength. The paper ends with Section III.5 presenting some conclusions and future works.

III.2. Materials and testing method

This section presents the experimental campaign executed on solid fired clay bricks, both mechanically extruded and modern handmade, to study the effect of the specimen's cross section aspect ratio and the use of different bearing surface treatments on the compressive strength. Details are provided about the materials, the preparation of specimens and their bearing surfaces, and the testing setup. All experimental tests were carried out at the Laboratory of Technology of Structures and Materials of the Technical University of Catalonia (UPC-BarcelonaTech).

III.2.1. Materials

Two types of solid fired clay units were considered in this research (Fig. 24). The first type of unit, identified with the acronym 'Ex', corresponds to modern solid fired clay bricks produced by mechanical extrusion in an automated process. The automated process consists in mixing the raw material in a pug mill, and when the clay is uniform in consistency is put into the hopper of the extruder. The hopper puts the clay into the barrel of the extruder. Inside the barrel, a rotating screw moves the clay through a die, which is shaped like the bed-plane of the brick. The 'Ex' units are extruded perpendicular to the bed surface. As the

extruded clay leaves the die, it is cut into the desired thickness by a wire cutter. The unit is then transported to a drying area, where it is dried before firing, loaded into a tunnel kiln, and fired with controlled heat conditions at 900 °C. The second type of unit, identified with the acronym 'Mo', corresponds to modern handmade solid fired clay bricks. 'Mo' units were traditionally manufactured in a brickyard by moulding. The raw material is mixed in a though and soaked in water for hours to soften it. The wet clay is shaped in a wooden mould sprinkled with dry fine sand. Then, the moulded clay brick is left to dry under the sun and, after extraction the mould, they are fired into a coal-fired kiln at 950 °C.

Fig. 24 Modern mechanically extruded solid fired clay brick ('Ex') (left), modern handmade solid fired clay brick ('Mo') (right)

The great availability of modern handmade ('Mo') and extruded ('Ex') units gave the possibility to test a larger number of specimens. Table 10 presents a description of the sampled materials in terms of origin, acronym and average dimensions measured according to EN 772-16:2011 [60], net (ρ_{nu}) and gross (ρ_{gu}) dry density, open porosity (P_0), water absorption capacity (W_s), initial rate of water absorption ($C_{w,i}$), elastic modulus (E_b), and Poisson's ratio (v_b). The net and gross dry density (ρ_{nu} and ρ_{gu}) were obtained according to EN 772-13:2001 [61] and EN 772-3:1999 [62], the open porosity (P_0) following the EN 772-4:1999 [152], the water absorption (W_s) following EN 772-21:2011 [63], and the initial rate of water absorption ($C_{w,i}$) following EN 772-11:2011 [153]. The values of elastic modulus (E_b) and Poisson's ratio (v_b) were determined following the testing procedures proposed in Makoond et al. [12].

Table 10 Classification of tested units in terms of origin, acronym, and average dimensions, net and gross dry density, open porosity, water absorption capacity, initial rate of water absorption, elastic modulus, and Poisson's ratio. Values in brackets correspond to the coefficients of variation

Sampled materials										
Origin	Acr.	Av. Dimensions (mm)	ρ_{nu} kg/m³	ρ_{gu} kg/m³	P_0 %	W_s %		$C_{w,i}$ kg/(m²×min)	E_b GPa	ν_b [-]
		EN 772-16	EN 772-13		EN 772-4	EN 772-21		EN 772-11	Makoond et al. [76]	
Mechanically extruded	Ex	272 [0.4%] × 132 [0.9%] × 45 [0.7%]	1529 [5.5%]	1677 [0.8%]	26.7 [5.7%]	17.5 [1.9%]	l	0.0405 [7.8%]	13.0 [15.1%]	0.20 [44%]
							w	0.0374 [9.4%]	11.5 [15.5%]	0.13 [43%]
Modern handmade	Mo	311 [0.6%] × 149 [1.7%] × 46 [4.6%]	1631 [5.6%]	1761 [1.2%]	25.5 [7.0%]	15.7 [7.0%]	l	0.0322 [20.1%]	6.3 [28.8%]	0.12 [49%]
							w	0.0316 [23.0%]	5.6 [24.0%]	0.10 [57%]

III.2.2. Shape of specimens

The shape of specimens was determined by analysing the available standards and the literature in the field. A total of four shapes for specimens was proposed, i.e., the whole brick identified as 'wh', the half brick identified as 'ha', the cut specimens with cross section measuring 100 × 100 mm² identified as '100' and 40 × 40 mm² identified as 'C40'. The proposed whole brick 'wh' is recommended by the AS/NZS 4456.4:2003 [11], CAN/CSA A82:14 (R2018) [10], IS 3495-1:2002 [154] and RILEM recommendation LUMA.1 [155]. The proposed half brick 'ha' is recommended by the ASTM C67/C67M-21 [47] by using a specimen with the full height and width of the original brick, and the length equal to one half of the full brick's length. The 'ha' is also allowed by AS/NZS 4456.4:2003 [11] and CAN/CSA A82:14 (R2018) [10] as long as the unit is symmetrical and the whole brick exceeds the capacity of the testing machine. The 100 × 100 mm² specimen '100' is included in the EN 772-1:2011+A1:2016 [9], and in the withdrawn of the ISO 9652-4:2000 [139]. The EN 772-1:2011+A1:2016 [9] does not specify the size of the specimen to be tested. However, it indicates the possibility of testing representative portions cut from the whole unit. The EN 772-1:2011+A1:2016 [9] does not indicate explicitly the need to test a square cross section sample, and its Table A.1 indicates only the width as reference parameter to evaluate the so-called "shape factors" accounting for the dimensions of the specimen. For a specimen with height below 50 mm, the standard EN 772-1+A1 only allows a width value ranging from 50 mm to 100 mm. Therefore, the proposed '100' specimen satisfies the European standard requirements. The 40 × 40 mm² specimen 'C40' was adopted by Cabané et al. [103] as a specimen of slenderness equal to one.

In addition, to analyse the effect of the cross section aspect ratio, stacked 'wh' and 'ha' specimens were made up, according with the EN 772-1:2011+A1:2016 [9] recommendation, placing one grinded specimen upon another grinded one, without any intermediate material.

Thus, two types of stacked specimens were proposed, i.e., the stacked whole brick identified as '2wh', and the stacked half brick identified as '2ha'.

A total amount of 458 specimens were prepared and tested, including 111 'wh', 97 'ha', 114 '100', 98 'C40', 20 '2wh', and 18 '2ha' specimens.

III.2.3. Treatments of the bearing surfaces of specimens

The specimens were prepared following a controlled procedure. First, the bricks were cut using a table saw equipped with a water jet to obtain 'ha', '100' and 'C40'. The '100' and 'C40' specimens were obtained from the central parts of the bricks. Then, the specimens were dried in an oven at a constant temperature of 105 ± 5 ºC for 24 hours. Finally, the specimens' dimensions were measured before preparing the bearing surfaces using a calliper with an accuracy of ±0.1 mm according to EN 772-16:2011 [60]. The specimens with grinded surfaces were also measured after the grinded process.

Different bearing surface treatments were considered, as explained in Section III.1, based on the available international standards for masonry clay units, the RILEM LUMA.1 recommendations, the ISO 9652-4:2000 withdrawn, and the scientific literature, i.e., grinding [9,139,155], capping with cement mortar [9,47,139,155], capping with rapid-setting industrial gypsum plaster [10,47,154], inserting a sheet of plywood [11], and inserting a sheet of fibreboard [11]. Capping with sulphur-filler [10,47,154] was not considered in this research for environmental and health issues as warned in the ASTM C1552-16 [147]. Another reason is that specimens capped with sulphur-filled exhibited similar compressive strength than those capped with cement mortar in previous research on concrete specimens [156,157]. The use of unbonded Neoprene pads [8] was also not considered in this research because its use has been highly questioned [59,105,136,141,142,158]. Instead, two other novel testing procedures were proposed in this research to reduce the friction effect, i.e., covering with gypsum powder, and inserting two oiled leaves of PTFE. The covering of the bearing surfaces with gypsum powder provided smoothing to the rough surfaces of the specimen, while the small diameter of the powder particles guaranteed reduced friction. The insertion of two oiled PTFE leaves was recommended by RILEM TC 148-SSC [133] to test concrete specimens, an also by Lourenço et al. [55] to test clay bricks.

To summarise, the considered treatments for the specimens' bearing surfaces were (1) grinding, (2) capping with cement mortar, (3) capping with gypsum plaster, (4) inserting a sheet of birch plywood, (5) inserting a fibreboard sheet, (6) covering with gypsum powder, and (7) inserting two oiled leaves of PTFE. Fig. 25 shows the specimens with the different bearing surface treatments considered in this research. Different materials and procedures were followed in the laboratory to prepare the bearing surfaces.

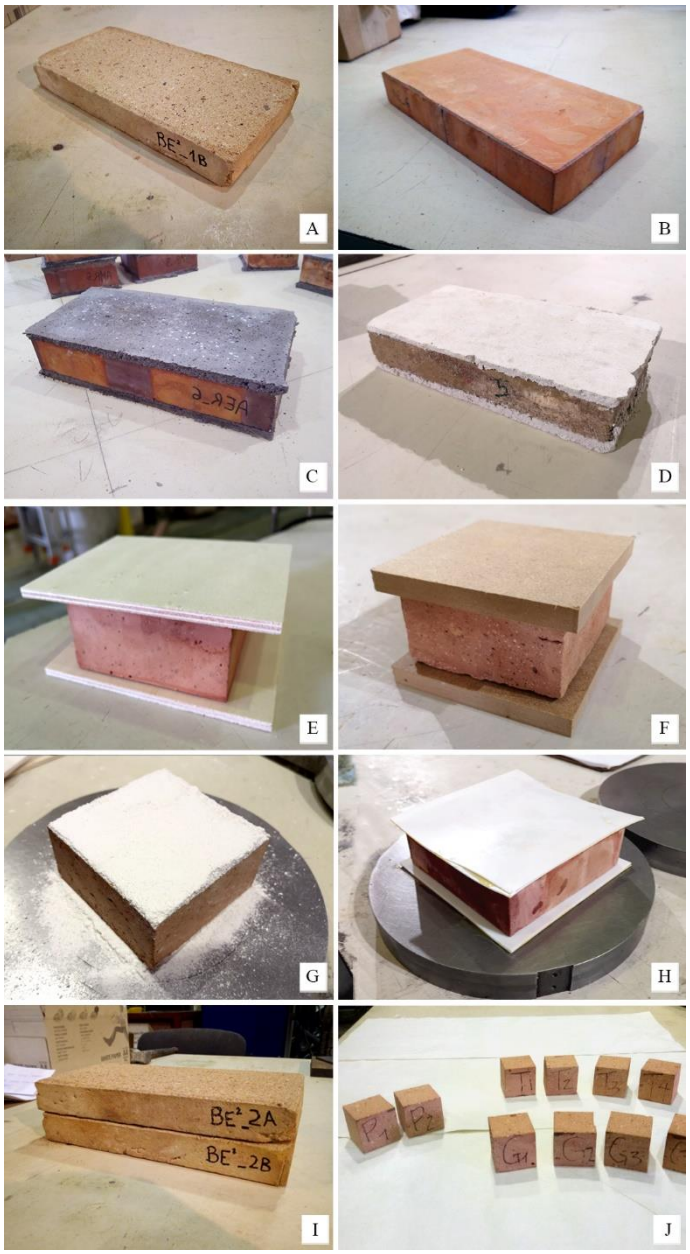

Fig. 25 The considered bearing surface treatments for compressive testing. A) Whole handmade brick with grinded surfaces. B) Whole mechanically extruded brick with grinded surfaces. C) Whole brick with cement mortar capped surfaces. D) Whole brick capped with gypsum plaster. E) '100' specimen with a sheet of 5 mm ply birch plywood. F) '100' specimen with a sheet of 12 mm fibreboard (MDF). G) '100' specimen covered with gypsum powder. H) Half brick with a leaf of PTFE. I) Stacked specimen composed of 2 grinded whole bricks. J) 'C40' specimens with grinded surfaces

(1) To grind the surfaces, a grinder fitted with a high speed rotating diamond disc was used until the requirements for flatness and parallelism were achieved. After the grinding process, the remaining height of the samples was 40 mm. The remaining height of the samples was conditioned by the original height of the bricks (with raw thickness ranging between 44 mm and 48 mm). Handmade ('Mo') bricks required a greater reduction of the

original thickness than the mechanically extruded ('Ex') units due to irregularities in the solid clay beds.

(2) To cap the surfaces with cement mortar, a composed mortar of 1 part of cement CEM II/A-L 42,5R and 3 parts of sand was used with a maximum grain size of 2 mm. Additionally, silica fume was used in 5% by weight of cement to increase the cap's compressive strength [159]. The mixture was made having a water-to-cement ratio of 0.50 and adding a water reducer [159]. The capping procedure was executed on a wooden plate coated with a film of oil, and a spirit level to ensure the specimen's horizontality. The time between capping one bearing surface and the other was 24 hours. After the second surface was capped, the specimens were aged 28 days before testing in laboratory conditions. The thickness of each cap was approximately 5 mm. The mortar's compressive strength (f_m) of 56.5 MPa (CV 16%) and the bending strength ($f_{flex,m}$) of 7.3 MPa (CV 16%) were evaluated according to EN 1015-11:2020 [6] by using 160 × 40 × 40 mm^3 prisms casted with the same material employed during the construction of the capped specimens.

(3) To cap the surfaces with gypsum plaster, a rapid-setting industrial gypsum was used. The mixture was made having a water-to-gypsum ratio of 0.5 l for each kg. The capping procedure was executed on a wooden plate coated with a film of oil, and a spirit level to ensure the specimen's horizontality. Before capping the specimens with gypsum, the surfaces were cleaned from dust, and coated with shellac to allow them to dry thoroughly. The shellac was applied with a conventional low-pressure spray gun. The time between capping one bearing surface and the other was 1 hour. After the second surface was capped, the specimens were aged 24 hours before testing in laboratory conditions. The thickness of each cap was approximately 5 mm. The gypsum's compressive strength (f_{gy}) of 5.7 MPa (CV 7.7%) and the bending strength ($f_{flex,gy}$) of 2.2 MPa (CV 7.8%) were evaluated according to EN 1015-11:2020 [6] by using 160 × 40 × 40 mm^3 prisms casted with the same material employed during the construction of the capped specimens.

(4) Two 5 mm thick plywood sheets were placed on top and bottom of the brick specimens. The 5 mm ply birch plywood had a longitudinal and transverse flexural strength of 82 MPa and 32 MPa, a longitudinal and transverse modulus of elasticity of 11 GPa and 6.6 GPa respectively, and a tensile strength along the fibres greater than 30 MPa, as indicated by the manufacturer. The length and width of the plywood sheets exceeded the specimens' dimensions by 10 mm to 30 mm.

(5) Two 12 mm thick fibreboard sheets were placed on top and bottom of the brick specimens. The 12 mm medium density fibreboard (MDF) had a flexural strength of 30 MPa, a tensile strength of 0.60 MPa, and a modulus of elasticity of 2.5 GPa, as indicated by the manufacturer. The length and width of the fibreboard exceeded each specimens' dimensions by 10 mm.

(6) To cover with gypsum powder, a thin uniform coat was used of dry powder gypsum with a grain size less than 1 mm. The lower powder coating was placed on a metal plate with

a gypsum thickness of approximately 5 mm. Then, the specimen was pressed firmly onto this layer, ensuring its horizontality with a spirit level. Finally, the upper powder coating with a thickness equal to the lower one was placed on the specimen and covered with a second metal plate.

(7) The treatment with two 1 mm thick oiled PTFE leaves placed on the top, and two other placed on the bottom of the brick specimens. The treatment previously includes the grinding of the specimen surfaces as specified in point (1). The mineral oil applied by brush had a viscosity index of 150. The length and width of the PTFE leaves exceeded the corresponding specimens' dimensions by 10 mm.

III.2.4. Testing procedures

The specimens were tested making use of two different testing machines with different loading capacity depending on the specimen's expected compressive strength. The Ibertest testing machine was equipped with three different load cell, 3000 kN (MEH-3000), 200 kN, and 10 kN (AUTOTEST 200/10 SW), and connected to a MD5 electronic module for data acquisition. The Ibertest AUTOTEST 200/10 SW was used for bending and compressive tests of the 160 × 40 × 40 mm^3 cement mortar and gypsum plaster capping material, and to test the specimens 'C40'. The Ibertest MEH-3000 was used to test all specimens except mechanically extruded ('Ex') whole brick 'wh'. The Suzpecar testing machine was equipped with a load cell of 5000 kN and connected to a FlexTest60 controller. All the 'Ex' whole bricks 'wh' were tested in the Suzpecar testing machine, regardless of the bearing surface treatment due to the need for loads greater than 3000 kN.

The specimens were centred on the steel plates with the bearing surfaces orthogonal to the direction of the loading. The specimens in the Ibertest machine were tested under force control, and the specimens in the Suzpecar machine were tested under force control until one-half of the expected maximum load and then under strain control. The application of the load was selected in order to meet the requirements of the reference standards. The AS/NZS 4456.4:2003 [11] allows a constant load application under force control between 0.15 MPa/s and 0.70 MPa/s, or under strain control between 1 to 5 mm/min without specifying a minimum test duration. The IS 3495-1:2002 [154] also indicates a constant load application of 0.23 MPa/s. The CAN/CSA A82:14 (R2018) [10] and ASTM C67/C67M-21 [47] recommends that the duration of the second half of the expected maximum load be between 60 and 120 seconds, without specifying a constant load application. The EN 772-1:2011+A1:2016 [9] recommends that the duration of the second half of the expected maximum load be over 60 seconds, offering an indicative table of load application between 0.05 MPa/s and 1.00 MPa/s. Thus, the specimens in the Ibertest machine were tested at 0.15 MPa/s, 0.30 MPa/s or 0.60 MPa/s rates depending on the specimen capacity to comply with all standards referenced in this research, and to guarantee that the second half of the expected maximum load be

between 60 seconds and 120 seconds. The specimens in the Suzpecar machine were tested at a rate of 0.30 MPa/s until reaching the half of the expected maximum load, and then under strain control at a rate of 1 mm/min.

The tests were stopped manually after registering the post-peak response of the force-displacement pattern. The specimens that showed a strain-hardening response, as explained in Section III.3.2, were stopped after 120 seconds ensuring all slope changes in the stress-displacement response.

III.3. Experimental results

This section presents the experimental results of compressive strength in solid fired clay brick specimens with different cross-section aspect ratio and different bearing surface treatments. First, details are given about the experimental average values of compressive strength and their coefficients of variation (CV), the number of specimens, the analysis of the stress-displacement graphs, and the description of the specimens' failure modes. Second, various methods are analysed for estimating an equivalent compressive strength in specimens that exhibit a hardening response.

III.3.1. Results derived from compression tests

Table 11 presents the number of specimens for each proposed treatment of the bearing surfaces, with their average compressive strength (f_c), and coefficients of variations (CV). The compressive strength of the samples was calculated by dividing the maximum compressive load by the cross-sectional area of the specimen. The displacement during the test was measured with the transducer from the actuator.

The 'Ex' 'wh' and 'ha' specimens showed similar compressive strengths for grinded, capped with cement mortar, capped with gypsum plaster, and placed with fibreboard sheets. The 'Mo' 'wh' and 'ha' grinded, capped with gypsum plaster, and covered with gypsum powder showed a hardening response without a maximum in the stress-displacement curve, and thus they required a careful post-processing analysis to propose an equivalent compressive strength value, see Section III.3.2. The 'Mo' '100' and 'C40' capped with gypsum plaster showed similar strengths. In both 'Ex' and 'Mo' types, the grinded specimens showed the highest average strength while those capped with gypsum plaster showed the lowest results. The 'C40' placed with plywood or fibreboard sheets showed the highest strength, while 'C40' covered with gypsum powder showed the lowest strength, even lower than the specimens tested with oiled PTFE leaves. The strengths obtained on the specimens tested with oiled PTFE leaves are similar for different specimens' cross sections within the respective 'Ex' and 'Mo' types of unit. The influence of specimen's length and bearing surface treatment on the compressive strength is presented in Section III.4.

The CV ranged between 1.6% - 26% for mechanically extruded ('Ex') units, and between 7% - 29% for modern handmade ('Mo') units. The 'Ex' bricks exhibited higher average compressive strength and a general lower CV than the 'Mo' bricks. The higher CV in 'Mo' units is due to the larger inhomogeneity of the bricks, as well as to their non-industrialised manufacturing. In addition, slightly lower CV values were obtained in 'Ex' grinded units, and the highest CV values were obtained in the 'Mo' specimens capped with gypsum plaster.

Fig. 26 shows the stress-displacement curves of the 'wh', 'ha', '100' and 'C40' samples of the mechanically extruded ('Ex') and modern handmade ('Mo') bricks with the different treatments of the bearing surfaces. The stress-displacement curves with different bearing surfaces yield significantly different experimental stiffness depending on the bearing surface treatment, being much more evident in the 'Mo' specimens.

The tested specimens exhibited two main different responses. On one hand, a strain-hardening response due to a confinement effect was observed in the 'Mo' 'wh' and 'ha' grinded, capped with gypsum plaster and covered with gypsum powder, producing a continuous increasing of stress and deformation. On the other hand, a softening post-peak response was observed in the other specimens. The determination of the compressive strength in the specimens exhibiting hardening may be hindered by the fact that a full failure may not be obtained. Specimens can maintain their load-bearing capacity due to triaxial confinement, and withstand very high levels of compression, despite undergoing a complete physical transformation involving a total loss of cohesion. Therefore, an estimation of an equivalent compressive strength could be associated with the level of compression for which the physical transformation occurs. To overcome this problem, a mathematical analysis is proposed in Section III.3.2 to determine a slope change in the stress-displacement response. Strain-hardening responses are also discussed in detail in Section III.4.1.

In addition, different responses are obtained depending on the specimen's bearing surface treatment. The curves of the specimens grinded, and capped with cement mortar are either overlapped or parallel, showing very similar stiffness that is the highest one amongst those derived from all the treatments. The curves of the specimens capped with gypsum plaster show a similar initial behaviour and stiffness than the grinded and capped with cement mortar, however the displacements during the test were strongly influenced by the size of the sample. The curves of the specimens 'Ex' with plywood sheets show a low initial stiffness. This behaviour may be related with the fact that the plywood is compressed and adapts to the specimen surface. After this initial behaviour, the curves exhibit increasing stiffness with approximately linear branch up to the strength. In addition, the 'Mo' specimens with plywood show lower stiffness in the final part of their stress-displacement response. The curves of the specimens tested with fibreboard show a rather constant stiffness up to the specimen strength. However, the curves of the 'Ex' 'wh' and 'ha' specimens show some irregularities in the stress-displacement response starting from 70 MPa. This change in behaviour can be influenced by the tensile failure of the fibreboard following the specimen

failure crack pattern. The curves of the specimens tested with gypsum powder show a similar behaviour to that of specimens with gypsum plaster. The curves of the specimens tested with two oiled PTFE leaves show a behaviour similar to that of the specimens grinded and capped with cement mortar, although they reach much lower values of strength and maximum displacement.

Table 11 Number of samples (N.) and average compressive strength (f_c) of the tested specimens with different bearing surfaces treatments and cross section aspect ratio. Values in brackets correspond to the coefficients of variation

Tested specimen															
Origin			Grinded		Cement Mortar Capped		Gypsum Plaster Capped		Birch Plywood Sheets		Fibreboard Sheets		Gypsum Powder Covered		Oiled PTFE leaves	
			N	f_c (MPa)	N	f_c (MPa)	N	f_c (MPa)	N	f_c (MPa)	N	f_c (MPa)	N	f_c (MPa)	N	f_c (MPa)
Ex	'wh'		10	90.0 [2%]	12	77.3 [7%]	8	63.8 [7%]	6	89.4 [2%]	6	76.7 [3%]	8	84.5 [8%]	6	29.9 [5%]
	'ha'		6	88.1 [4%]	6	81.9 [3%]	8	68.0 [7%]	6	77.0 [3%]	6	72.9 [5%]	6	73.8 [10%]	6	34.0 [7%]
	'100'		6	75.3 [3%]	6	59.3 [19%]	8	55.2 [7%]	6	75.2 [2%]	6	71.7 [2%]	6	66.4 [5%]	6	36.9 [6%]
	'C40'		12	51.1 [14%]	6	37.8 [26%]	6	29.7 [11%]	6	65.4 [11%]	6	68.2 [4%]	6	24.4 [10%]	6	36.4 [8%]
	'2wh'		8	57.7 [8%]	-	-	-	-	-	-	-	-	-	-	-	-
	'2ha'		6	59.6 [10%]	-	-	-	-	-	-	-	-	-	-	-	-
Mo	'wh'	P.2	9	29.6 [10%]	14	33.0 [15%]	8	24.8 [15%]	6	41.0 [16%]	6	36.7 [7%]	6	27.8 [10%]	6	10.3 [11%]
		P.3		35.3 [14%]				24.5 [25%]						27.2 [13%]		
		P.4		43.4 [9%]				27.1 [20%]						32.7 [19%]		
	'ha'	P.2	7	23.2 [20%]	16	25.1 [10%]	6	13.6 [9%]	6	27.2 [12%]	6	27.1 [7%]	6	20.7 [9%]	6	11.0 [20%]
		P.3		31.4 [14%]				16.1 [15%]						22.1 [10%]		
		P.4		33.0 [13%]				17.4 [12%]						25.0 [9%]		
	'100'		14	24.9 [8%]	10	20.2 [7%]	22	10.4 [14%]	6	23.8 [19%]	6	22.4 [8%]	6	15.9 [15%]	6	9.3 [19%]
	'C40'		6	11.5 [15%]	8	11.7 [23%]	8	10.7 [24%]	6	14.5 [29%]	6	17.8 [11%]	8	4.6 [22%]	8	8.0 [16%]
	'2wh'		12	22.7 [20%]	-	-	-	-	-	-	-	-	-	-	-	-
	'2ha'		12	17.8 [12%]	-	-	-	-	-	-	-	-	-	-	-	-

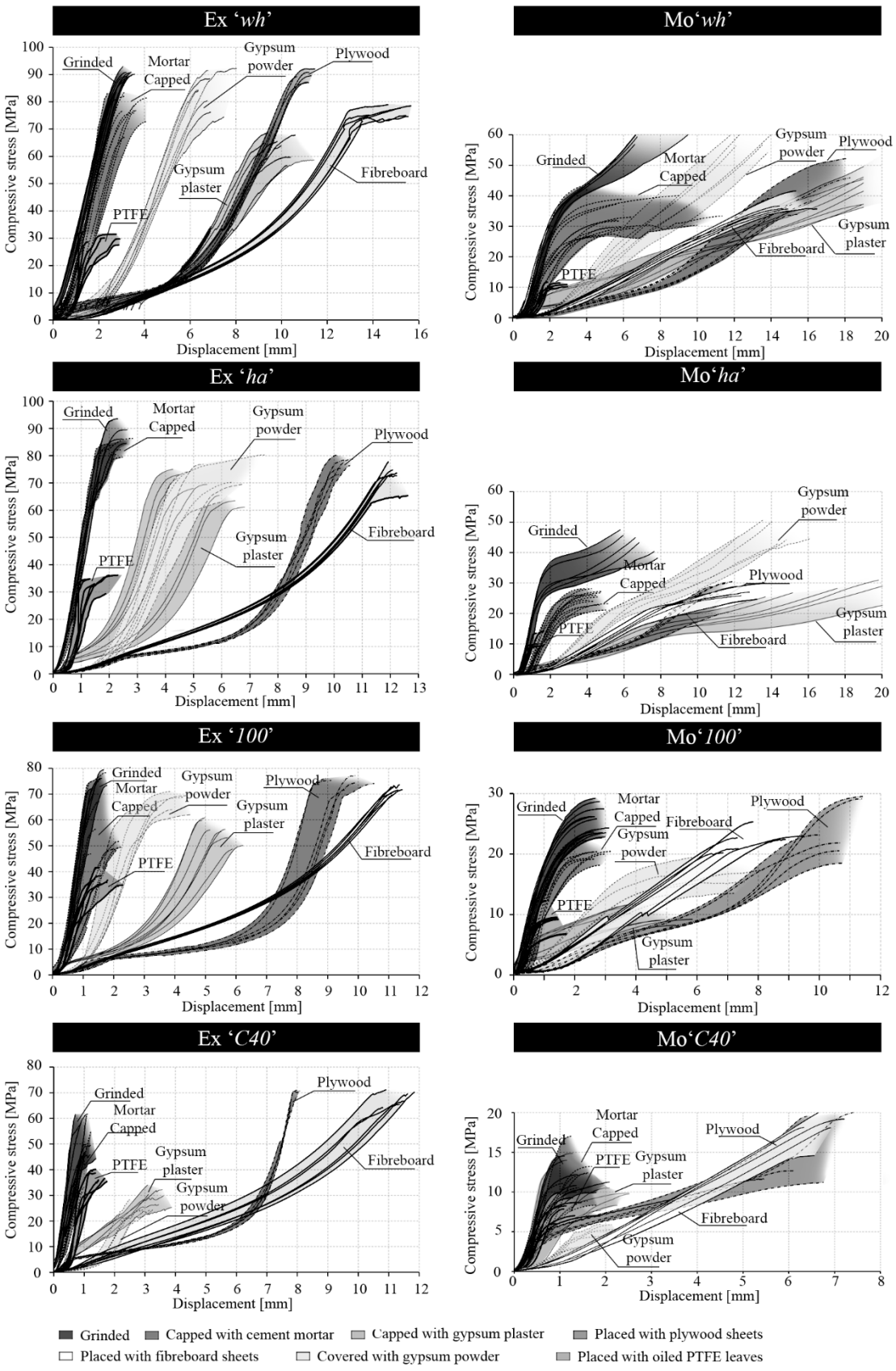

Fig. 26 Stress-displacement curves of the mechanically extruded ('Ex') and of the modern handmade ('Mo') of 'wh', 'ha', '100' and 'C40' specimens under compression with different treatments for the bearing surfaces

III.3.2. Experimental failure modes

Regarding the observed experimental failure modes, all non-stacked specimens exhibited splitting and separation of the outer parts (Fig. 27a to Fig. 27t), while stacked specimens showed the typical hourglass (Fig. 27s and t). Handmade ('Mo') '100' and 'C40' specimens, after removing the split outer parts, also showed the hourglass failure. The '100' capped with gypsum plaster (Fig. 27q), and '100' and 'C40' with plywood sheets (Fig. 27r) could be divided into two superimposed square frusta of pyramid at the end of the tests.

Fig. 27 Observed failure modes in the specimens with all bearing surface types. Handmade bricks 'Mo' from A) to E), K), L), O), Q), and R). Mechanically extruded bricks 'Ex' from F) to J), M), N), P), S), and T). A) and F) grinded, B) and G) capped with cement mortar, C) and H) capped with gypsum plaster, D) and I) placed with sheets of plywood, E) and J) placed with sheets of fibreboard, K) and M) covered with gypsum powder, L) and N) placed with two oiled PTFE leaves. O) 'Mo' 'C40' covered with gypsum powder, P) 'Ex' 'C40' placed with sheets of plywood, Q) 'Mo' '100' capped with gypsum plaster, R) 'Mo' '100' placed with plywood sheets, S) 'Ex' '2ha' grinded and stacked, T) 'Mo' '2wh' grinded and stacked

An in-depth evaluation of the experimental evidence allowed the detection of some differences in the failures modes, depending mainly on the surface treatment. The mechanically extruded units ('Ex') with grinded surfaces (Fig. 27f), with plywood sheets (Fig. 27i and p), and with fibreboard (Fig. 27j) presented a brittle response with multiple vertical cracks appearing on the edges. The 'Ex' 'wh' specimens with fibreboard sheets exhibited a sudden and noisy failure with detachment of material. The 'Ex' specimens capped with

mortar (Fig. 27g), with gypsum plaster (Fig. 27h) and covered with gypsum powder (Fig. 27m) presented a brittle response with spaced vertical cracks. The 'Ex' specimens with oiled PTFE leaves (Fig. 27n) showed fragmentation of the brick material evenly distributed throughout the specimen [75,89,97]. The 'Mo' 'wh' and 'ha' with grinded surfaces (Fig. 27a), capped with gypsum plaster (Fig. 27c) and covered with gypsum powder (Fig. 27k) showed the expulsion of the outer material while the specimen's core remained compact without material cohesion, as will be also highlighted in Section III.4.1. The 'Mo' specimens capped with cement mortar (Fig. 27b) or gypsum plaster (Fig. 27c) and covered with gypsum powder (Fig. 27k and o) presented also splitting of the outer parts with spaced vertical cracks. The 'Mo' specimens tested with plywood sheets (Fig. 27d), and with fibreboard (Fig. 27e) presented a total loss of cohesion of the perimeter as well as material expulsion. The 'Mo' specimens with oiled PTFE leaves (Fig. 27l) showed multiple vertical cracks evenly distributed throughout the edges of the specimen, with consequent loss of material cohesion.

A careful visual evaluation of the material interposed between the specimen and the press platens was executed after the tests. The cement mortar cap (Fig. 27b and g) showed a splitting failure according to an elliptical pattern close to the specimen's edges. The gypsum plaster (Fig. 27c and h) and the gypsum powder (Fig. 27k and m) appeared like a brittle thin sheet that could be easily separated from the 'Ex' specimens. The gypsum plaster and gypsum powder were stuck into the specimens' clay after the test, being impossible to peel off from the sample. The plywood sheets (Fig. 27d and i) were flattened over the specimen zone and presented the same crack patterns of the 'wh' and 'ha' specimen's beds, being either partially or completely embedded in '100' (Fig. 27r) and 'C40' specimens (Fig. 27p) respectively. The fibreboard sheets (Fig. 27e and j) presented the same pattern as that explained for plywood at the end of the tests. The PTFE leaves (Fig. 27l and n) did not show any deformation in 'Mo' specimens. However, the PTFE leaves showed the imprint of the 'Ex' specimens' fragmentation on their surfaces.

III.3.3. Specimens with hardening response

As explained in Section III.3.1, the 'Mo' 'wh' and 'ha' specimens with grinded surfaces, capped with gypsum plaster and covered with gypsum powder exhibited a hardening stress-displacement response. Since this peculiar behaviour does not allow one to identify unambiguously the compressive strength, this research proposes a novel method to estimate an equivalent compressive strength based on the identification of a representative point in the experimental stress-displacement response. Fig. 28a, b and c show the experimental stress-displacement curves of a representative specimen obtained from testing a 'wh' grinded specimen (Fig. 28a), and from testing a 'ha' capped specimen with gypsum plaster (Fig. 28b) or gypsum powder (Fig. 28c). The curves corresponding to specimens with grinded surfaces (Fig. 28a) and covered with gypsum powder (Fig. 28c) exhibit increasing stiffness at lower

stress levels, which are related with the adjustment of the platens to the bearing surfaces of the specimens. However, the curves of specimens capped with gypsum plaster (Fig. 28b) start with a high stiffness response, which progressively decreases probably due to the deformation of the gypsum plaster. After this common initial stage, all the curves present an inflexion point. After the first inflexion point, denoted as point 1, the stiffness decreases until reaching a second inflexion point, denoted as point 4, where the stiffness starts to increase until the loading is stopped at the end of the test. The inflexion points in the curves can be detected as the points with value zero in of the 2nd derivative (Fig. 28j, k and l).

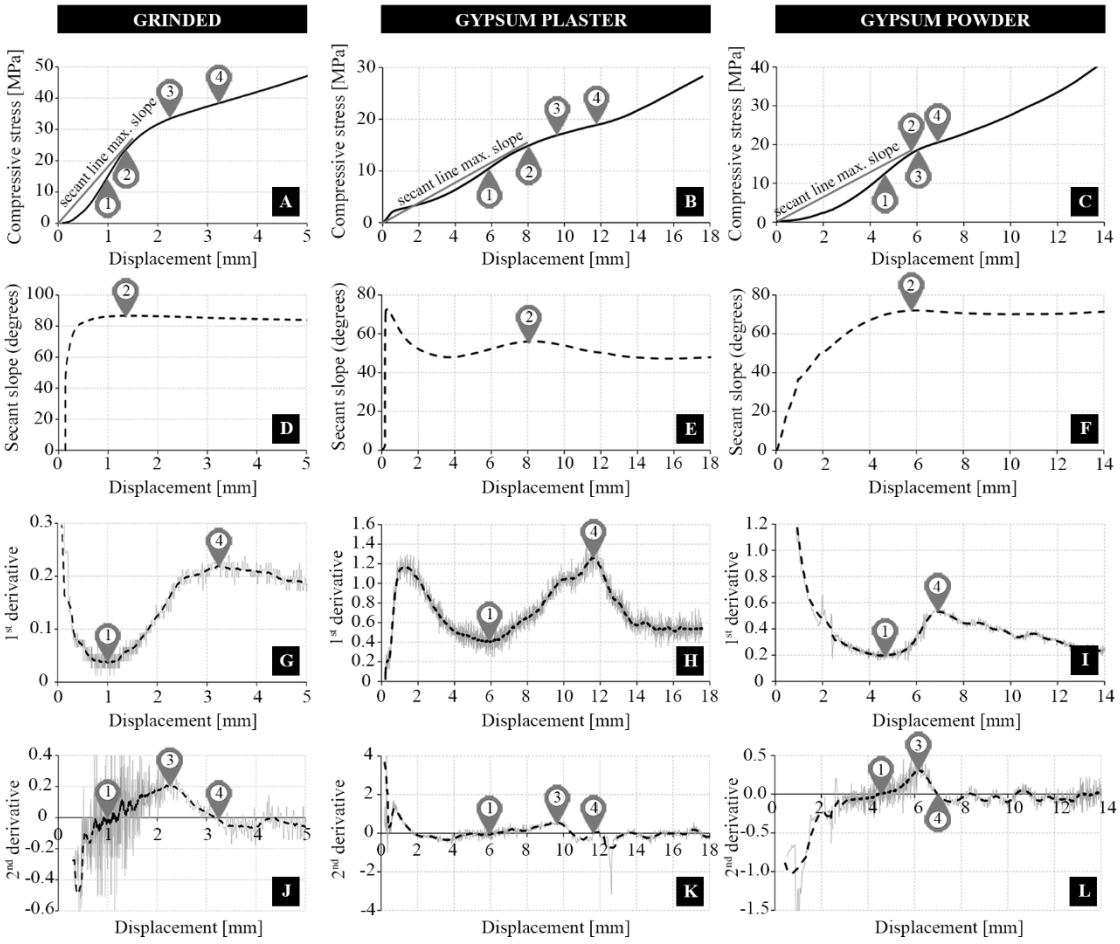

Fig. 28 A), B) and C) Experimental stress-displacement curves of representative specimens with hardening response obtained from handmade bricks ('Mo') with surfaces grinded, capped with gypsum plaster and covered with gypsum powder. The marked points correspond to the point of the maximum secant slope (point 2), the inflexion points of the stress-displacement curve (point 1 and 4), and the inflexion point of the 1st derivative function (point 3). D), E) and F) show the slope of the secant line that intersects the origin and the stress-displacement curve, evidencing the local maximum (point 2). G), H) and I) show the 1st derivative evidencing the local maximum (point 4) and the local minimum (point 1). J), K) and L) show the 2nd derivative evidencing the local maximum (point 3) and the considered points with zero value (points 1 and 4)

In order to approximate the estimation of the compressive strength in these specimens, four mathematical criteria are proposed to identify four significant points: the point of the maximum secant slope (point 2), the inflexion points of the stress-displacement curve (points 1 and 4), and the inflexion point of the 1st derivative function (point 3). The point of the maximum secant slope (point 2) is determined by the maximum slope of the line that intersects the origin of the function and the stress-displacement curve. Since the curve of the specimens capped with gypsum plaster (Fig. 28b) shows an initial stage with high stiffness, the considered point 2 was the second relative maximum of the secant slope-displacement curve (Fig. 28e). Fig. 28d, e and f show the graphs indicating the secant slope vs. displacement curve evidencing the points 2. The inflexion points of the stress-displacement curve are determined by the relative maximum (point 4) and the relative minimum (point 1) of the 1st derivative function, see Fig. 28g, h and i, as well as by the zero values of the 2nd derivative function, see Fig. 28j, k and l. The inflexion point of the 1st derivative is determined by the relative maximum of the 2nd derivative (point 3). Fig. 28j, k and l shows the 2nd derivative evidencing the relative maximum (point 3) in the graph.

The four options aforementioned indicate "representative points" in the experimental stress-displacement response that might be considered to evaluate the compressive strength in specimens exhibiting a hardening response. Section III.4.1 reports a comparative analysis amongst the different representative points.

III.4. Discussion

This section presents four analytical studies based on the experimental results described in Section III.3. The first study analysed the proposed method to estimate an equivalent compressive strength on specimens with hardening response. The second study focuses on the influence of the cross section's aspect ratio on the resulting experimental compressive strength. The third study is aimed to understand the relationship between the compressive strength of the specimens and the bearing surface treatment. The fourth study analyses the different approaches available for the evaluation of the compressive strength, according to different available reference standards. The second and third study considers additional experimental data from the available literature in the field to complement those derived from the present experimental campaign.

III.4.1. Evaluation of the compressive strength in specimens with hardening response

Section III.3.2 has highlighted the hardening response detected in 'Mo' 'wh' and 'ha' specimens with bearing surface grinded, capped with gypsum plaster and covered with gypsum powder, observing that it is possible to evaluate four "representative points" derived from a simple mathematical study of the stress-displacement experimental functions. This

Section presents a careful analysis of the levels of damage reached in the tested specimens at each proposed point, to identify the most adequate value of the compressive strength.

The approach for evaluating the geometric macroscopic damage on the specimens follows the descriptions for concrete of Stroeven [160] and Kotsovos [161,162]. Stroeven [160] described an initial damage stage as discontinuous and gradual, observing an increasing of crack length and number, and a second stage consisting mainly of the union of the previous cracks. Kotsovos [161,162] described four damage stages. First, initial isolated microcracks appear and remain stable. Second, the initial microcracks begin to branch out in the direction of maximum principal compressive stress. Third, branching cracks start to propagate by spreading relatively steadily. Fourth, the crack pattern becomes unstable and failure occurs, marked by a rapid increase within the total volume of the material. Fig. 29 shows the stress-displacement curves of the representative specimens, indicating the four representative points and the relevant specimens' levels of damage. In addition to the specimens with hardening already presented in Section III.3.2, the figure presents also two specimens with plywood sheets and with two oiled PTFE leaves as they also exhibited post-peak response with no clear compressive strength value. Fig. 29 shows the corner of the specimens to visualize two lateral edges. At point (1) the specimens began to show some diffuse and minor vertical cracking. At point (2) the specimens exhibited major vertical cracking. At point (3) the main cracks widened and new vertical cracks emerged. At point (4) all the cracks widened and the specimen exhibited important lateral expansion. , until the expansion stabilised causing a final increase of stiffness in stress-displacement curve until the test stopped. In the specimens with plywood sheets and with two oiled PTFE leaves, the considered points 1 and 2 can be obtained before reaching the peak or ultimate stress, when all the cracks connect and widen, and lateral expansion occurs in the post-peak.

The initial microstructure of the solid fired clay bricks depends of the firing temperature and the raw clay quality, where mineralogical and complex chemical reaction influence the brick material porosity, as explained by Fernandes et al. [163]. This porosity is related with the volume of void spaces in the material's microstructure. Fernandes et al. [164] reported that most common porosity in handmade solid fired clay bricks range between 25 and 35 vol.%. Krakowiak et al. [75] analysed the microstructure of the mechanically extruded solid fired clay bricks reporting that the size of the particles varies depending on mineralogy of raw material and processing conditions. During the linear range, the material microstructure presents resistance against the splitting of the bonded particles. The nonlinear behaviour begins once the particles start to unlink or split their bonds and crushed particles occupy the void spaces, as observed by Wang [165]. During the nonlinear behaviour, the brick material changes from cohesive to disjoint. In materials as clay, stone or concrete, the disjoined material cause a softening post-peak response with the expulsion of the outer parts. However, the 'Mo' 'wh' and 'ha' specimens showed a hardening nonlinear behaviour due to the confinement produced by the bearing surface treatment (grinded, capped with

gypsum plaster or covered with gypsum powder) together with the reduced slenderness of the specimen (less than 0.4 h/w [9]). The developed confinement, after the expulsion of the outer parts of the specimen, prevents the inner material subject to triaxial compression from further expulsion. Finally, once the material has lost its cohesion within a state of confinement, the crushed particles start the rearrangement of their microstructure again, recompacting the material. This behaviour can be compared with that observed in confined sand tested in compression, as analysed by Nakata [166] who observed that the yielding characteristics depend on the grading curve. This behaviour can be associated with the increase in stiffness obtained in the final branch of the test, before reaching the load limit of the loading machine.

The considered representative points (1), (2), (3) and (4) can be related with meaningful effects with different stages in the behaviour of the specimens under compression. Points (1) and (2) are also identifiable in the specimens with a post-peak response before achieving the peak ultimate stress. Point (3) can be related with the descriptions of the second stage by Stroeven [160] and the third stage by Kotsovos [161,162], where cracks start to propagate and join in a stable manner. Point (4) shows a lateral expansion with widening cracks, as identified by Kotsovos [161,162]. Point (4) also indicates an inflexion point in the stress-displacement curve, denoting the beginning of a hardening response. Table 11 in Section III.3.1 shows the equivalent compressive strength as derived from the reference values of the points 2, 3 and 4. In the following analysis reported in Section III.4, the equivalent compressive strength estimated by point 4 of the grinded, capped with gypsum plaster and covered with gypsum powder specimens will be used.

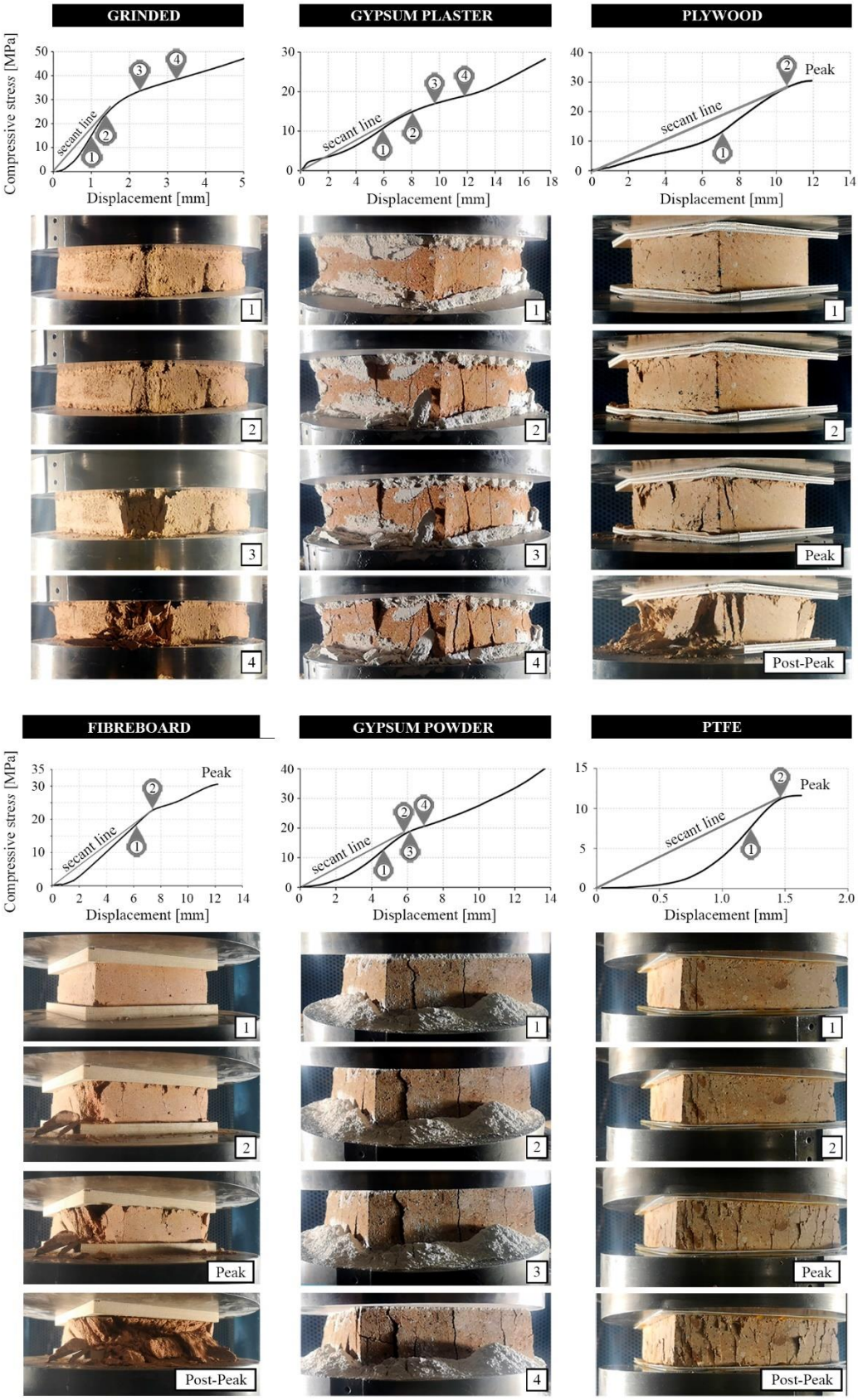

Fig. 29 Stress-displacement curves with hardening response for 'wh' and 'ha' specimens obtained from handmade bricks ('Mo') for different bearing surfaces treatments, with levels of damage corresponding to the proposed representative points

III.4.2. Study of the influence of cross section's aspect ratio on the compressive strength

The experimental campaign on 'wh' and 'ha' specimens of both the mechanically extruded ('Ex') and modern handmade units ('Mo') allowed the comparison of the compressive strength in specimens with different cross-section aspect ratio and bearing surface treatment. The ratio between the shorter edge, the width (w), and the longer edge, the length (l), has been considered as the cross section's aspect ratio w/l. The cross section's aspect ratios w/l in the experimental campaign were 0.49 and 0.97 for 'Ex' 'wh' and 'ha', and 0.48 and 0.96 for 'Mo' 'wh' and 'ha'. The specimens tested with oiled PTFE leaves has not been considered in the analysis, since the experimental results in Section III.3 show close values regardless of the specimen's shape.

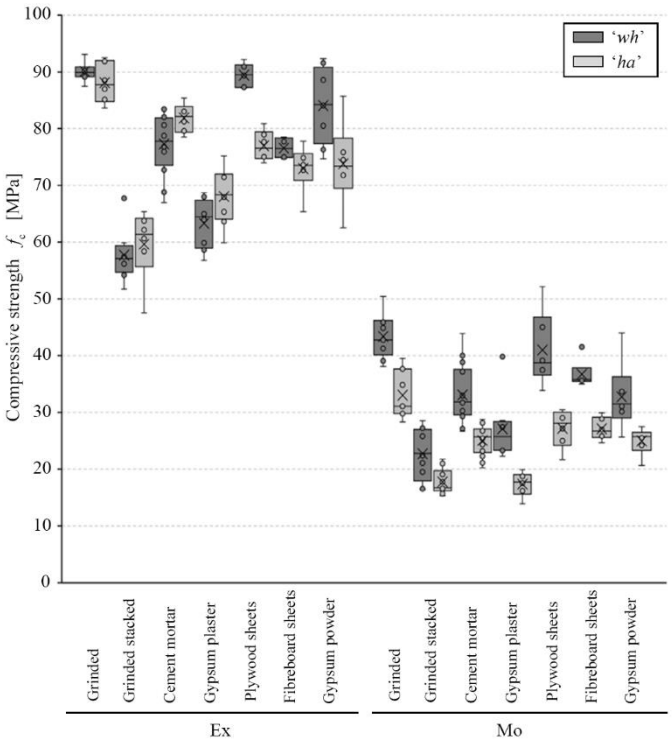

Fig. 30 Boxplot with 'wh' and 'ha' specimens' compressive strength values (f_c) for the 'Ex' and 'Mo' with different bearing surface treatment. Inside the boxes, the medians are presented with a horizontal line and the averages are presented with an X

Fig. 30 presents in a boxplot the distribution of the data based on the quartiles (being the second and third quartiles coloured inside the boxes), and shows the median (depicted as a horizontal line inside the box) and the average (depicted as a cross). As presented in Table 11 (Section III.2) and in Fig. 30, the mean and median strength values for 'ha' are higher than that for 'wh' in the 'Ex' for stacked, capped with cement mortar and capped with gypsum plaster, while 'wh' strength values are higher than that for 'ha' in the 'Ex' for grinded, placed with birch plywood sheets, placed with fibreboard sheets and covered with gypsum powder.

The 'Ex' specimens grinded and placed with fibreboard sheets, even if the 'wh' mean and median are higher than 'ha' ones, present the 'wh' distribution within the upper distribution of 'ha'. The mean and median strength values for 'wh' are higher than that for 'ha' in the 'Mo' specimens.

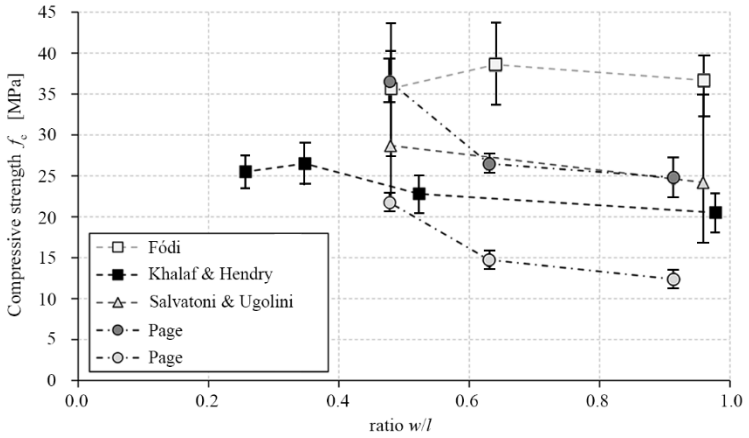

Fig. 31 Experimental compressive strength evaluated in specimens with different length/width ratio as found in five available experimental programs in the literature that tested solid units with different materials

The scientific literature discussed in Section III.1 reports only a limited number of references dealing with the experimental testing of brick specimens in compression studying the cross section's aspect ratio influence. Fig. 31 shows experimental compressive strength values in specimens with different cross section's aspect ratio (l/w) obtained by Page [76,104], Khalaf and Hendry [5], Fódi [54] and Salvatoni and Ugolini [80]. The results from the references, including all the experimental values, are presented in a graph presented as a point (mean) with a line indicating the CV. Page [76,104] testing calcium silicate samples with plywood sheets obtained the highest strength for the lowest cross section's aspect ratio (w/l). Khalaf and Hendry [5], testing solid concrete bricks, also obtained the highest strength for the lowest w/l, and concluded that the length of the unit affects as the width. Khalaf and Hendry [5] proposed the experimental equation $\delta_{100} = (h / \sqrt{A})^{0.37}$ to obtain the shape factor referring to a cubic specimen of 100 mm edge (δ_{100}), involving the specimen height (h) and the loading area (A). Fódi [54], after testing extruded solid fired clay bricks with grinded surfaces, obtained similar compressive strengths regardless of the w/l ratio, and concluded that the compressive strength depends on the width (smaller edge) and does not depend on the loaded area. Finally, Salvatoni and Ugolini [80], testing grinded modern handmade units, obtained, as Page [76,104] and Khalaf and Hendry [5], the highest compressive strength for the lowest w/l ratio. As explained in Section III.4.1, in the specimens tested by Salvatoni and Ugolini [80] the compressive strength was calculated as the point of maximum secant slope due their hardening response. Thus, the literature review indicates that a cross section's aspect ratio (w/l) influence is normally observed in calcium silicate bricks, solid concrete

bricks and handmade bricks. However, no apparent influence of the w/l ratio has been found in mechanically extruded bricks.

An in-depth analysis of the compressive strengths derived from the specimens with different cross section's aspect ratio (w/l) allows the detection of possible length influence in the mechanically extruded bricks ('Ex') and modern handmade bricks ('Mo'). A correlation can be made between the compressive strength average of the specimens with the w/l aspect ratio close to 1.0 ('ha'), denoted by f_{c_ha}, and the compressive strength average with the w/l aspect ratio close to 0.5 ('wh'), denoted by f_{c_wh}. Table 12 shows the f_{c_ha} / f_{c_wh} correlations obtained from the experimental data derived from this research using different bearing surface treatments and from the scientific literature. For the specimens with hardening response, the compressive strength was estimated as proposed in Section III.4.1. The mechanically extruded solid fired clay bricks ('Ex') show an experimental f_{c_ha} / f_{c_wh} ranging from 0.86 to 1.07, while Fódi [54] obtained 1.03. The concrete solid bricks tested by Khalaf and Hendry [5] showed f_{c_ha} / f_{c_wh} = 0.90. The modern handmade solid fired clay bricks ('Mo') show f_{c_ha} / f_{c_wh} ranging from 0.64 to 1.78, while Salvatoni and Ugolini [80] obtained 0.84. The calcium silicate bricks tested by Page [76,104] showed the lowest values of f_{c_ha} / f_{c_wh}, i.e., 0.57 and 0.68.

Table 12 f_{c_ha} / f_{c_wh} ratios of the experimental compressive strengths derived from specimens with aspect ratio close to 0.5 and 1.0, considering data from the current experimental program and from the literature. Values in brackets correspond to the coefficients of variation

f_{c_ha} / f_{c_wh} ratio		
	'Ex'	'Mo'
Grinded	0.98	0.76
Stacked	1.03	0.78
Cement mortar	1.06	0.76
Gypsum plaster	1.07	0.64
Plywood sheets	0.86	0.66
Fibreboard sheets	0.95	0.74
Gypsum powder	0.88	0.76
Average	0.97 [8.6%]	0.73 [7.6%]

References on scientific literature – ratio 'w/l ≈ 1.0' / ' w/l ≈ 0.5'				
Fódi [54]	Khalaf & Hendry [5]	Page [76,104]	Page [76,104]	Salvatoni & Ugolini [80]
Mechanically extruded solid fired clay brick	Moulded solid concrete brick	Calcium silicate solid brick	Calcium silicate solid brick	Moulded handmade solid fired clay brick
1.03	0.90	0.68	0.68	0.84

A significant influence of the cross section's aspect ratio (w/l) has been found in modern handmade bricks 'Mo', in which the highest compression strength is obtained in specimens with lower cross section's aspect ratio ('wh' specimen). This remarkable influence of the cross section's aspect ratio on the compressive strength of handmade bricks was also observed by

Salvatoni and Ugolini [80], as well as by Khalaf and Hendry in moulded solid concrete units [5] and by Page in calcium silicate bricks [76,104]. Slight influence of the cross section's aspect ratio has been found in mechanically extruded solid clay bricks 'Ex', as also observed by Fódi in mechanically extruded bricks [54].

III.4.3. Empirical correlation among compressive strengths derived from specimens with different bearing surface treatments

Based on the experimental campaign presented, this research has evaluated an empirical correlation between the compressive strengths derived from specimens with different bearing surface treatments ($f_{c,TR}$), making reference to the grinded surface treatment ($f_{c,GR}$) on 'wh', 'ha' and '100'. The grinded surface treatment is taken as reference since it produces the highest compressive strength value. Table 13 shows the following aspects: (1) the ratios between compressive strengths ($f_{c,TR}$ / $f_{c,GR}$) seem to be higher for mechanically extruded bricks ('Ex') than handmade bricks ('Mo'); (2) the ratios for specimens tested with two oiled PTFE have stepped values depending on the specimen's shape; (3) the ratios $f_{c,TR}$ / $f_{c,GR}$ for each treatment seem to be influenced by the slenderness of the specimen, since each treatment seems to produce different amount of confinement; (4) specimens capped with gypsum plaster has the lowest $f_{c,TR}$ / $f_{c,GR}$ ratio, except for 'C40' specimens that exhibited lowest $f_{c,TR}$ / $f_{c,GR}$ when covered with gypsum powder; (5) the ratios $f_{c,TR}$ / $f_{c,GR}$ for the specimens capped with gypsum plaster or covered with gypsum powder are different for 'Ex' and 'Mo' units due to the different response depending on the brick type; (6) the specimens with plywood and fibreboard show higher $f_{c,TR}$ / $f_{c,GR}$ ratios than 'C40' specimens.

Table 13 presents, together with the results derived from the experimental program of the current research, the compressive strength ratios on fired clay bricks obtained from the experimental results of RILEM recommendations [155], Khalaf et al. [137], Templeton et al. [138], Morsy [136], already mentioned in the literature review of Section III.1.

RILEM recommendations [155] specify that fired clay brick specimens grinded and capped with cement mortar bearing surface preparation exhibit different results, without quantifying such difference. Khalaf et al. [137] reported the compressive strength of whole hollow clay, frogged clay, and calcium silicate bricks, and concrete blocks with grinded surfaces, capped with mortar, with dental plaster, and placed with plywood sheets. The higher strength units (considered over 100 MPa) exhibited $f_{c,TR}$ / $f_{c,GR}$ = 0.80 for specimens grinded or capped with mortar, $f_{c,TR}$ / $f_{c,GR}$ between 0.52 and 0.62 for specimens capped with dental plaster, and 0.66 for specimens with plywood sheets. For medium strength bricks, the $f_{c,TR}$ / $f_{c,GR}$ ratios ranged between 0.94 and 1.07 for specimens capped with cement mortar, between 0.63 and 0.72 for specimens capped with dental plaster, and between 0.69 and 0.79 for specimens placed with plywood sheets. Templeton et al. [138] related the compressive strength of different types of modern clay bricks (mechanically extruded solid and perforated

units, solid handmade and hydraulic pressed solid units) with grinded surface and capped with cement mortar. Templeton et al. [138] proposed the experimental equation $f_{c,TR} = 0.707 f_{c,GR} + 8.534$ to relate the compressive strength between both treatments, obtaining $f_{c,TR} / f_{c,GR}$ ratios ranging between 0.78 and 0.80. Morsy [136] analysed ground and rough scaled clay units with seven types of bearing surface coating, i.e., steel, plywood, hardboard, 6 layers of polythene, rubber with fibres and pure rubber. The ratios between specimens tested with grinded surfaces and placed with plywood were 0.96 and 1.04, depending if the specimens tested with plywood had grinded or rough surfaces. The ratios with hardboard were between 0.87 and 0.94, depending on the direction of the fibres and if the specimen had grinded or rough surfaces.

Table 13 also considers available references dealing with bearing surface treatments in earth units (Aubert et al. [78]), and concrete specimens (RILEM TC 148-SSC [133]).

Table 13 Experimental ratios $f_{c,TR} / f_{c,GR}$ derived from the experimental program and from literature data. Values in brackets correspond to the coefficients of variation

Origin		Mortar capped	Gypsum plaster	Plywood sheets	Fibreboard sheets	Gypsum powder	Oiled PTFE leaves
Experimental $f_{c,TR} / f_{c,GR}$							
'Ex'	'wh'	0.86	0.70	0.99	0.85	0.93	0.33
	'ha'	0.93	0.77	0.87	0.83	0.87	0.39
	'100'	0.79	0.73	1.00	0.95	1.00	0.49
	'C40'	0.74	0.58	1.28	1.33	0.48	0.71
Average 'Ex'		0.83 [10%]	0.70 [12%]	1.04 [17%]	0.99 [23%]	0.82 [28%]	-
'Mo'	'wh'	0.76	0.63	0.94	1.04	0.76	0.24
	'ha'	0.76	0.53	0.82	0.86	0.76	0.33
	'100'	0.81	0.40	0.95	0.90	0.64	0.37
	'C40'	1.02	0.92	1.26	1.54	0.41	0.69
Average 'Mo'		0.89 [12%]	0.64 [35%]	1.06 [17%]	1.09 [29%]	0.63 [25%]	-
References on literature reviewed $f_{c,TR} / f_{c,GR}$							
LUMA.1 [155]		different					
Khalaf et al. [137] [a]		0.80 0.94 – 1.07	0.52 – 0.62 0.63 – 0.72	0.66 0.69 – 0.79			
Templeton et al. [138]		0.78 - 0.80					
Morsy [136]				0.96 - 1.04	0.87 – 0.94 [b]		
Aubert et al. [78] [c]							0.98 - 1.07
RILEM TC148-SSC [133] [d]							0.37 0.58 - 0.75 0.57 - 1.17

[a] Hard strength brick first row, Soft strength brick second row.

[b] Hardboard.

[c] Specimen slenderness 1.00.

[d] Specimen slenderness 0.25 first row, 0.50 second row and 1.00 third row.

Aubert et al. [78], after placing 2 mm PTFE leaves on 50 × 50 × 50 mm^3 extruded earth bricks, observed experimental compressive strength similar to that of grinded specimens. The ratios range between 0.98 and 1.07. RILEM TC 148-SSC [133] for concrete indicates that the compressive strength in grinded specimens increases when the slenderness decrease below 2, except when oiled PTFE leaves are used. The thickness of the used oiled PTFE leaves in RILEM TC 148-SSC [133] are 50 mm, 100 mm, and 500 mm. The RILEM recommendations allow to found different $f_{c,TR}/f_{c,GR}$ ratios depending on the specimen slenderness, 0.37 for h/w of 0.25, 0.58 to 0.75 for h/w of 0.50, and 0.57 to 1.18 for h/w of 1.00.

The analysis of the $f_{c,TR}/f_{c,GR}$ ratios presented in Table 13 show important conclusions about the influence of the bearing surface treatment on the compressive strength of the investigated brick types. Overall, the results show a clear correlation between the compressive strength of each bearing surface treatment ($f_{c,TR}$) and of the grinded surface ($f_{c,GR}$) for both mechanically extruded ('Ex') and modern handmade ('Mo') brick samples. The experimental campaign exhibited similar ratios of those derived from data available in the scientific literature, yet enlarging the experimental database. The specimens capped with cement mortar have similar ratios of those investigated by Khalaf et al. [137] (0.80 – 1.07) and Templeton et al. [138] (0.78 – 0.80). The specimens capped with gypsum plaster have similar ratios of those investigated by Khalaf et al. [137] (0.52 – 0.72). The specimens with birch plywood and fibreboard sheets also have a similar ratio of those investigated by Morsy [136] (0.95 -1.04 and 0.87 – 0.94), but differ from those studied by Khalaf et al. [137] for plywood sheets (0.69 – 0.79). The ratios close to 1.00 suggest that the lateral strains of the plywood and fibreboard were reduced as observed by Kleeman et al. [144]. It is noticed that the samples capped with gypsum plaster and covered with gypsum powder have different average $f_{c,TR}/f_{c,GR}$ depending on the brick type. There is no research available in the scientific literature comparing the compressive strength of grinded specimens with specimens covered with gypsum powder. The samples with oiled PTFE leaves have different ratios $f_{c,TR}/f_{c,GR}$ depending on the specimen's shape, since the influence of the specimen's slenderness seems to be attenuated as observed by RILEM TC 148-SSC [133]. RILEM TC 148-SSC [133] recommends the insertion of the oiled PTFE in concrete specimens to obtain similar strengths regardless of the specimen slenderness h/w. Although RILEM TC 148-SSC [133] remarks that the use of PTFE with a controlled application of oil can reduce the scattering, this research did not show any reduction in scattering with respect to the other proposed treatments (see Table 11).

Fig. 32 represents the results of the experimental program in a graphical manner, following the approach formulated by Morsy [52]. Different graphs refer different to types of unit ('Ex' or 'Mo') and specimens ('wh', 'ha', '100', and 'C40'). The relevant strength values for different surface treatments are reported on y-axis, while the x-axis can represent in a qualitative manner the amount of lateral restraint, as stated by Morsy. If we set the specimens with PTFE leaves as the reference ones, as PTFE leaves surface treatment showed

similar compressive strengths regardless of the specimen shape, one can detect in a visual manner which treatments present a relative increase or decrease of the lateral restraint during compression testing. The specimens capped with cement mortar or gypsum plaster, or covered with gypsum powder, are more susceptible to variations of lateral restraint, as the restraint can either decrease for 'C40' specimens or increase for the rest of specimens. The specimens with plywood or fibreboard sheets increase the lateral restraint regardless of the specimen type. The grinded specimens show the highest lateral restraint for 'wh', 'ha' and '100' specimens, except for 'C40' specimens.

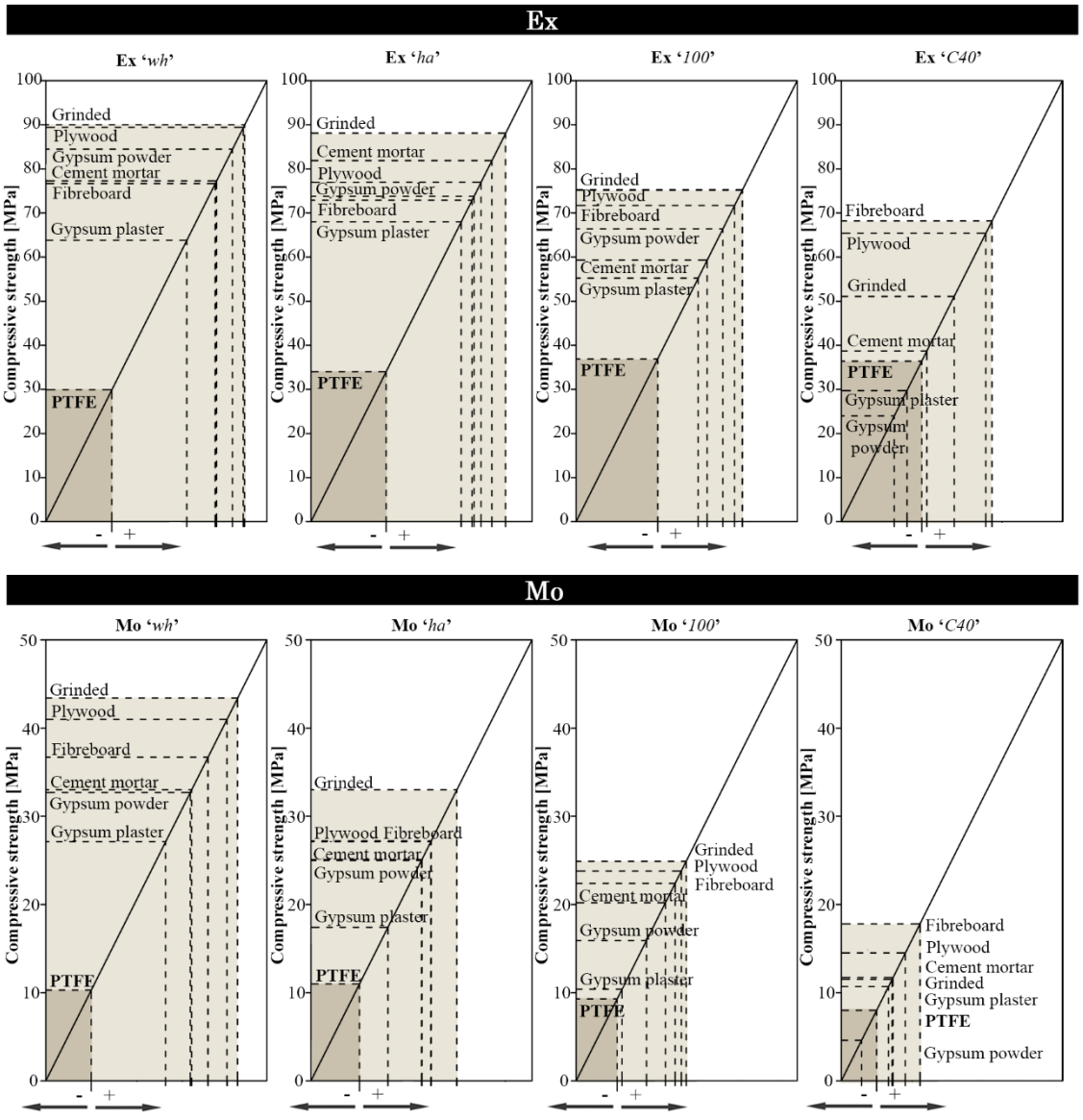

Fig. 32 Increase/decrease of the amount of lateral restraint according to different bearing surface treatments, making reference to specimens with oiled PTFE leaves

III.4.4. Evaluation of the compressive strength according to different international standards

Fig. 33 shows the standard compressive strengths derived from the experimental campaign following the different international standard recommendations. The experimental average compressive strength obtained by testing all types of specimens with oiled PTFE leaves have been used as a reference, i.e., 34.3 MPa (10.4% CV) of 'Ex' and 9.5 MPa (20.2% CV) of 'Mo'. The European standard EN 772-1:2011+A1:2016 [9] considers the use of the grinded specimens '100' and '2ha', and the specimen capped '100' with cement mortar. The experimental values have to be multiplied by a shape factor indicated in the Table A.1 of the standard, which is 0.7 for the '100' and 0.885 (interpolated value) for the '2ha'. Thus, the compressive strength according to the EN standard range between 41.5 MPa 52.7 MPa for 'Ex' and 14.1 to 17.4 MPa for 'Mo'. The American standard ASTM C67/C67M-21 [47] use the specimen 'ha' capped with cement mortar or capped with gypsum plaster. The ASTM standard does not specify the use of any shape factor. The CAN/CSA A82:14 (R2018) [10] use the specimen 'wh' and allow the specimen 'ha' to test capped with gypsum plaster. The CAN/CSA does not specify the use of any shape factor either. The ASTM and CAN/CSA standard compressive strengths are the highest values, ranging between 63.8 to 81.9 MPa for 'Ex' and 17.4 to 27.1 MPa for 'MPa'. The Australian standard AS/NZS 4456.4:2003 [11] use the specimen 'wh' and allow the specimen 'ha' to test placed with birch plywood sheets and fibreboard sheets. The experimental values require the use of an aspect ratio factor indicated in the standard, the interpolated 0.425 for 'Ex' and 0.375 for 'Mo' due to their different widths. The AS/NZS standard compressive strength are the lowest values, ranging between 31.0 to 38.0 MPa for 'Ex' and 10.2 to 15.4 MPa for 'Mo'. The AS/NZS values for 'ha' specimens tested with birch plywood or fibreboard sheets and 'Ex' 'wh' tested with fibreboard have close standard compressive strength values than specimens tested with oiled PTFE leaves in both brick types.

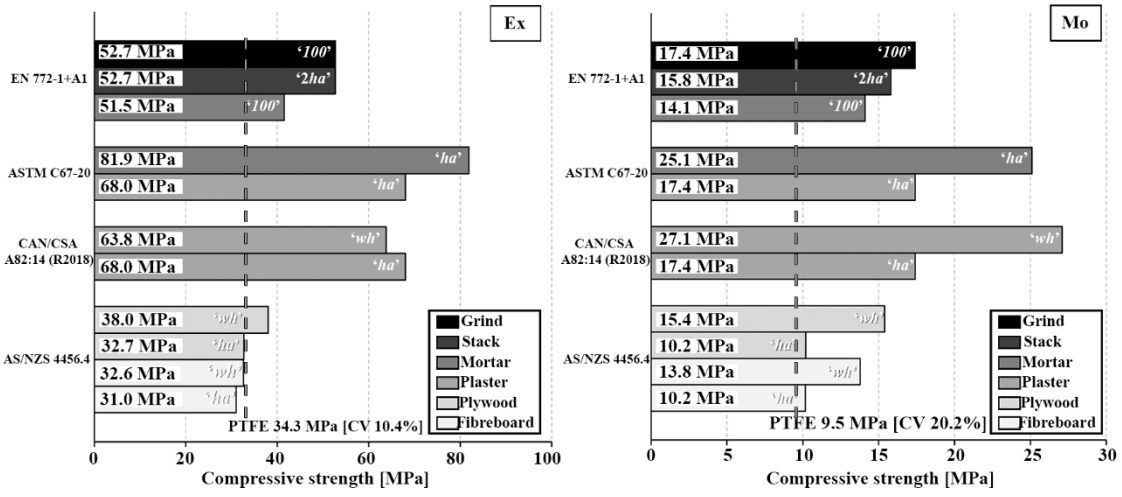

Fig. 33 Bar graph with the standard compressive strength of the references: EN 772-1:2011+A1:2016 [9], ASTM C67/C67M-21 [47], CAN/CSA A82:14 (R2018) [10], and the AS/NZS 4456.4:2003 [11]

III.5. Conclusions

This paper has presented novel experimental results about the compressive strength of fired clay brick solid samples with different shapes and surfaces treatments. A comprehensive experimental program considered a total amount of 458 specimens, derived from mechanically extruded ('Ex') and modern handmade ('Mo') bricks. The research has proposed first a novel method for the determination of the compressive strength in brick specimens with hardening response. Second, the paper has addressed the influence of the cross section's aspect ratio on the compressive strength. Third, the influence of bearing surface treatment has been analised indetail by investigating six different treatments, i.e., grinding, capping with cement mortar, capping with gypsum plaster, placement of plywood sheets, covering with gypsum powder, and covering with oiled PTFE leaves. Finally, the study has compared different methods of evaluating the compressive strength from the experimental measurements, according to different international standards for masonry testing. The following conclusions can be drawn from the analysis of the experimental results:

- The experimental tests on whole and half handmade brick specimens show a noticeable hardening response due to their low slenderness. allows simple method based on mathematical analysis of the stress-displacement experimental function is proposed to estimate the compressive strength.
- The experimental results and the scientific literature show that the cross section's aspect ratio is more influent in modern handmade solid fired clay bricks ('Mo') than in mechanically extruded ones ('Ex'). The ratios between the strengths of the whole brick and the half brick ('wh'/'ha') ranged between 0.88 and 1.06 for 'Ex' specimens, and between 0.64 and 0.78 for 'Mo'.
- The compressive strength measured on the specimens with different bearing surface can be characterized by the ratio $f_{c,TR}$ / $f_{c,GR}$ for slenderness under 0.4. The experimental ratio is 0.82 (CV of 8%) for specimens capped with cement mortar, and 0.93 (CV 7.5%) for specimens with birch plywood sheets, being similar to evidences available in the scientific literature. The experimental ratios $f_{c,TR}$ / $f_{c,GR}$ of the specimens tested with gypsum material seem to be influenced both by the manufacturing process and the unit's strength unit. The ratio for 'Ex' specimens is 0.74 (CV of 4.7%) for capping with gypsum plaster, and 0.94 (CV of 6.7%) for covered with gypsum powder. The 'Mo' specimens present a ratio of 0.52 (CV 21.8%) for capping with gypsum plaster, and 0.72 (CV of 9.3%) for capping with gypsum powder.
- The capped specimens has exhibited varying amount of lateral restraint, depending of the scross section aspect ratio. Specimens tested with plywood and fiberboard sheets show high values regardless of the specimen shape. The amount of lateral restraint in specimens with grinded surfaces seems to be influenced mainly by the slenderness of the specimen.

- Capping with gypsum powder has shown compressive strength values similar to those of the grinded specimens, and those with plywood sheets for 'Ex' bricks, and similar to the specimens capped with cement mortar for 'Mo' bricks. The use of gypsum powder can hardly be considered as a low friction surface treatment, since the compression loading compacts the powder during the execution of the test, inducing a mechanical behaviour similar to that of capping.
- Testing the specimen placed with two oiled PTFE leaves has proved to be an advantageous technique for the evaluation of the unconfined compressive strength of solid fired clay units. This technique has shown similar compressive strength values regardless of the specimen shape.
- The standards for the evaluation of the compressive strength in bricks present a great variety of approaches. The American ASTM and the Canadian CAN/CSA provide the highest values of compressive strength, while the Australian AS/NZS provide the lowest values.

As this research has focused on solid fired clay bricks, future works could address the extension of the experimental database by including the application to different materials, such as mudbricks, fly ash clay bricks, concrete units, and calcium silicate bricks, as well as to other manufacturing processes, such as dry pressed into a mould or mechanically extruded in different directions. Another topic of future research may be studying the possible influence of other parameters on the compressive strength and the failure mechanisms, such as the material's porosity and the mineralogical composition.

2.5 Paper IV – Influence of specimen slenderness and stacking on the experimental strength of solid fired clay bricks

A. Cabané, L. Pelà, P. Roca

Construction Building Materials (2023)

Under review

Abstract. This study evaluates the effect of the specimen's slenderness and stacking on the experimental compressive strength of solid fired clay units. The experimental campaign has focused on two different types of solid fired clay bricks, namely mechanically extruded and handmade, with a total amount of 382 specimens. The research considers different standard and non-standard specimens with varying width (40, 50, 60, 70, 80, 90, and 100 mm), and height (40, 80, and 120 mm). The experimental results evidence the influence of the stacking procedure on the compressive strength, with differences depending on the manufacturing process of the unit. The influence of specimen's slenderness on compressive strength exhibits a more regular trend in handmade brick specimens than in extruded brick specimens.

IV.1. Introduction

The determination of the mechanical properties of masonry structures faces significant challenges due to the intrinsic complexity of this composite material. The masonry compressive strength depends largely on the compressive strength of components, i.e., units and mortar [74]. Specifically, the compressive strength of the masonry is highly dependent on the compressive strength of units, allowing its estimation by using available empirical or analytical equations [3,4,7]. The experimental compressive strength depends on the specimen's dimensions, as the confinement is produced by the friction of the press' steel platens [167]. Acquiring a full knowledge on the compressive strength of solid units is necessary to design adequate masonry structures, as well as to evaluate existing ones.

The mechanical characterisation of solid fired clay bricks is highly conditioned by the limited thickness of bricks, which may be even of the order of 40 mm only. This geometrical condition affects the specimen's height adopted for laboratory testing, with direct consequences on the confinement effect. The European standard EN 772-1:2011+A1:2016 [9] does not specify the size of the specimen to be tested, and allows the possibility of testing representative portions cut from the whole unit. The standard includes the Table A.1 with "shape factors" depending on the specimen's height and width. The shape factor is the coefficient proposed by the EN standard [9] to convert the experimental compressive strength derived from generic units to a normalized value of compressive strength, equivalent to an

ideal 100 mm width × 100 mm height unit, as indicated in the Eurocode 6, EN 1996-1-1:2011+A1:2013 [3].

The scientific literature includes only a limited number of references about the slenderness' influence on compressive strength of solid fired clay units, while a higher number of experimental studies can be found for concrete specimens. One of the first researches was carried out by Hutchinson in 1923 [168] on concrete specimens with slenderness between 0.5 and 2.0, finding irregular values in specimens with slenderness below 0.5. An in-depth research was carried out by Gonnerman in 1925 [169] by testing specimens with slenderness between 0.5 and 4.0. Gonnerman observed that the experimental compressive strength decreases slightly in specimens with slenderness greater than 2.5, and it increases exponentially in specimens with slenderness below 1.5. Murdock et al. [170] described the research conducted in 1955 by Fry to determine the influence of the specimen's slenderness on different types of concretes with varying strength values. Fry observed that higher strength concretes are less affected by the specimen's slenderness. Murdock et al. [170] concluded in 1955 that there is a little change in the experimental compressive strength in specimens with slenderness between 1.5 and 2.5, that an increase in the strength occurs in specimens with slenderness below 1.3, and that specimens with slenderness below 1.0 should not be considered for testing. Murdock et al. also concluded that the correction factors related to the specimen slenderness need to vary according to the strength of the concrete. Kesler [171] published the results of a large experimental campaign carried out in 1959 by nine laboratories and planned by the ASTM Committee. Kesler concluded that greater corrections on the experimental strength must be made when slenderness decrease, and that the concrete specimens of lower strength required greater corrections than the higher strength ones. Hughes [172] showed that the ratio between the prism strength (with slenderness 2) and cube strength (with slenderness 1) can range from 0.59 to 0.99, detecting a possible influence of the type of aggregate and mix properties. Neville [173] described an empirical relationship for different shapes and sizes of specimens in terms of the their volumes. Neville [173] acknowledged that in the strength-slenderness curves, the evolution of the curvature depends, not only from the specimen slenderness, but also from the strength of the material itself and, in the case of concrete, from the fineness modulus of aggregate. Popovics [174] presented an analysis of published experimental data in 1966 by showing correlations between different specimen types, cubes (with slenderness 1), and prisms (with slenderness 2). Popovics presented the ratios between compressive strengths of cubes and prisms ranging from 0.56 to 1.0, and highlighted different factors that influence this relationship, such as the concrete strength, the aggregate, and the bearing surface treatment. Schickert [58,114] carried out an in-depth investigation in the 80's of the different shape coefficients present in the standards of the effect of confinement on the experimental results. Schickert detected three different relationships in the experimental strength vs. slenderness graphs derived from concrete specimens with slenderness between 0.25 and 4.0 [114]. For

slenderness values greater than 2.0-3.0, the strength tends to decrease slightly due to the appearance of buckling phenomena. For slenderness values lower than 2.0-3.0, the strength slightly increases up to slenderness values of 1.0-1.5, while it evidences a steeply increase for slenderness values lower than 1.0-1.5 due to the increasing confinement effect. Van Mier [167] presented the study of concrete specimens in his doctoral thesis in 1984, with slenderness values of 2.0, 1.0, and 0.5 by using brush-bearing platens to reduce the specimen confinement, and obtaining similar specimen's strengths regardless of their slenderness. Egermann [175] studied the influence of the specimen slenderness in 1990, by testing handmade bricks and mechanically extruded ones with slenderness between 0.5 and 3.0. Egermann showed that the experimental strength vs. slenderness graph of the handmade bricks specimens fits quite well the experimental soft concrete strength vs. slenderness graph published by Schickert [58], and the experimental strength vs. slenderness graph of the extruded bricks specimens fits well the experimental high strength concrete strength vs. slenderness graph published by Schickert [58]. Egermann produced a single strength vs. slenderness trend line regardless of the manufacturing process of the brick specimen, i.e., handmade or extruded. The trend line is nearly horizontal, i.e., it denotes constant compressive strength, for slenderness values greater than 1.5. However, between slenderness 1.5 and 1.0, the trend line shows a small increase in strength values as slenderness decrease, and for slenderness values less than 1.0, the trend shows an steeply increase of the strength values. The same phenomenon is also explained in RILEM TC 148-SSC [133] evidencing that higher strengths are obtained at lower slenderness because of the confinement exerted by the loading platens on the specimen.

The research on the influence of specimen's slenderness on compressive strength of masonry units is limited. Page [76,104] compared unconfined and confined compressive strength on calcium silicate bricks. The unconfined compressive strength was measured by testing the specimens with steel brush bearing platens, and the confined compressive strength was measured by testing the specimens with plywood sheets in contact with the bearing surfaces. Page found that the specimens with slenderness 3.0 presented the same strength value for confined and unconfined specimen. The results of Page research were also published by Hendry [74] and generated the actual aspect ratio factors of the Australian Standard AS/NZS 4456.4:2003 [11]. Khalaf et al. [5] studied the experimental shape factors by testing solid concrete bricks, and he compared the results with those reported in the European Standard EN 772-1:2011+A1:2016 [9]. Khalaf et al. observed highest compressive strength in lower slenderness specimens. Binda et al. [77,109] compared confined and unconfined cube specimens with 40 mm edge that were obtained from solid fired clay handmade bricks. The unconfined compressive strength was measured by testing the specimens with steel brush bearing platens, and the confined compressive strength was measured by testing two types of specimens, i.e., a single 40 mm edge cubic specimen, and a composite specimen obtained by stacking three 40 mm edge cubes. Binda observed that the

stacked specimens with slenderness 3.0 presented the same strength value as unconfined 40 mm edge cubes. Beer et al. [176,177] studied the European shape factors by testing calcium silicate units, autoclaved aerated concrete blocks, and lightweight aggregate concrete blocks. Beer et al. investigated specimens with slenderness ranging from 0.5 to 5.0, and concluded that there exists a deviation between experimental shape factors and those proposed by the EN 772-1:2011+A1:2016 [9]. Brameshuber et al. [178,179] also studied the influence of the specimen's slenderness on compressive strength, determining differences between experimental shape factors and EN standard ones. This difference is not constant and increases when the slenderness increases.

This paper proposes the use of specimens with slenderness between 0.4 and 3.0 to investigate the influence of slenderness and stacking on compressive strength, by testing mechanically extruded solid fired clay bricks and handmade units. The specimens' shape is proposed following the European Standard EN 772-1:2011+A1:2016 [9], given the geometric 40 mm thickness after the grinding process of the investigated units. In addition, the cubic specimen with 40 mm edge was considered by following the procedure developed by Cabané et al. [103]. Thus, the width of the resulting specimens are 40, 50, 60, 70, 80, 90, and 100 mm. Besides, the International Railway Union (UIC) recommends in the Leaflet 778-3R [1] the use of 40 × 40 × 80 mm^3 specimens. To reach the height of 80 mm, the European Standard allows stacking specimens without bonding material. Thus, this research includes 80 mm height specimens made by stacking two 40 mm height specimens, with widths ranging from 40 to 100 mm. Finally, the stacking of three 40 mm edge cubes was also considered to obtain specimens with a slenderness equal to 3.0.

This research offers the results of an extensive experimental campaign including the execution of 382 laboratory tests on 20 different specimens' configurations. The research encompasses the following specific objectives: (1) exploring the influence of the stacking procedure on the compressive strength obtained in the laboratory, and (2) determining the influence of the slenderness on the experimental compressive strength.

This paper is structured in five sections. After this introduction, Section IV.2 presents the experimental campaign performed on brick units, including the description of the materials, the specimens' preparation and the testing procedure. Section IV.3 presents the experimental results. Section IV.4 analyses the influence of the stacking procedure and the specimen slenderness on the compressive strength. The paper ends with Section IV.5 presenting some conclusions and future works.

IV.2. Experimental study

This section presents the experimental campaign executed on solid fires clay bricks, mechanically extruded and modern handmade, to study the effect of the specimen's shape based on the specimen's slenderness and the use of the stacked procedure to produce the specimens. Details are provided related with the materials, the preparation of specimens and the testing setup. All experimental tests were carried

out at the Laboratory of Technology of Structures and Materials of the Technical University of Catalonia (UPC-BarcelonaTech).

IV.2.1. Materials

Two types of solid fired clay units were considered in this research (Fig. 34). The first type of unit, identified with the acronym 'Ex', corresponds to modern solid fired clay bricks produced by mechanical extrusion in an automated process. The second type of unit, identified with the acronym 'Mo', corresponds to modern handmade solid fired clay bricks manufactured by traditionally handmade moulding process. The 'Ex' were extruded perpendicular to the bed surface, cut and dried by industrial automatized process, and fired in a tunnel kiln with controlled heat conditions at 900 °C. The 'Mo' were traditionally manufactured in a brickyard by moulding. The bricks were shaped in a wooden mould sprinkled with dry fine sand and, after extracted from the mould, the bricks were fired into a coal-fired kiln at 950 °C. Table 14 presents a description of the sampled materials in terms of origin, acronym and average dimensions measured according to EN 772-16:2011 [60].

Table 14 Classification of tested units in terms of origin, acronym (Acr.), and average dimensions. Values in brackets correspond to the coefficients of variation

Sampled materials		
Origin	Acr.	Av. dimensions (mm)
Mechanically extruded	Ex	272 [0.4%] × 132 [0.9%] × 45 [0.7%]
Modern handmade	Mo	311 [0.6%] × 149 [1.7%] × 46 [4.6%]

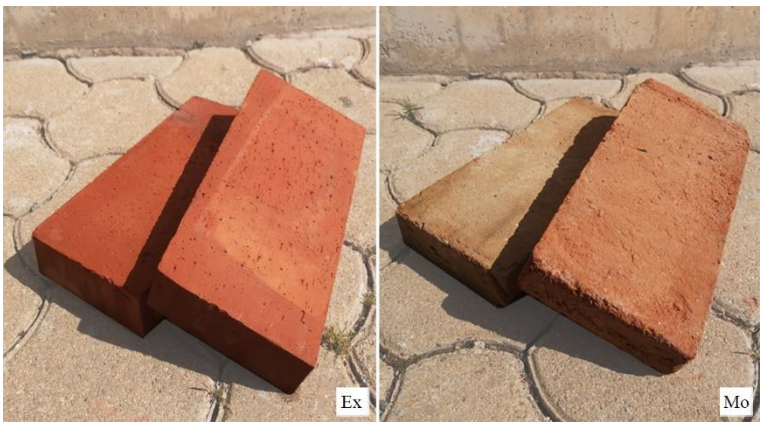

Fig. 34 Modern mechanically extruded solid fired clay brick ('Ex') (left), modern handmade solid fired clay brick ('Mo') (right)

IV.2.2. Preparation of specimens

The specimens were prepared following a controlled procedure in the laboratory, according to the European Standard EN 772-1:2011+A1:2016 [9]. Brick beds usually present irregularities, especially in case of manual manufacture. These geometric conditions make it difficult to test brick specimens flatly without any surface preparation. To overcome this problem, the EN 772-1:2011+A1:2016 [9] recommends grinding or cap with cement mortar

the specimen bearing surfaces. Following the European Standard, in the present research the bearing surfaces of the bricks were subjected to grind until the requirements of flatness and parallelism were achieved, avoiding the influence of the materials for bearing surface treatment, such as cement mortar, gypsum plaster, plywood or fibreboard [136–138,155]. Thus, the brick beds were polished by a grinder fitted with a rotary disc until reaching a constant thickness of 40 mm. After the grinding process, the remaining height of the samples was 40 mm due to the original thickness of the bricks (45 and 46 mm). Finally, the bricks were cut to obtain the desired specimens by using a table saw equipped with a water jet.

The shapes of the specimens were determined after analysing the available standards and the literature in the field. The specimens' geometry presented restrictions in height and width, due to the limited brick thickness. After the grinding process, the remaining height of the samples was close to 40 mm. The maximum width was determined by the European Standard EN 772-1:2011+A1:2016 [9], i.e., 100 mm for specimens with a height of 40 mm. Another type of specimen was selected, i.e., the 40 mm edge cubic specimen. The 40 mm edge cube is sufficiently large to mitigate the possible effects due to the presence of inclusions and voids, as indicated by Lourenço et al. [55]. The cubic specimen with 40 mm edge was the minimum size proposed by Binda et al. [77], and studied by Cabané et al. [103]. The available standards provide different specimens' shapes, e.g. the European Standard EN 772-1:2011+A1:2016 [9] allows a width value ranging from 50 mm to 100 mm for 40 mm height specimens. Although the American ASTM C67/C67M-21 [47], the Australian AS/NZS 4456.4:2003 [11] and the Canadian CAN/CSA A82-14 (R2018) [10] allow testing half brick and whole brick, these specimens were not considered in the present research to avoid non-squared specimens. In fact, Khalaf et al. [5] and Fódi [54] observed that the length of specimens with rectangular cross section has a remarkable influence on the compressive strength evaluation. Thus, this research proposes seven width sizes for specimens, i.e., 40, 50, 60, 70, 80, 90 and 100 mm width, and 40 mm height with slenderness (height/width) between 0.4 and 1.0.

Scientific literature and standard recommendations propose shape factors and specimen's slenderness up to 5. Page [76,104], Binda et al. [77,109], and Brameshuber et al. [178,179] studied specimens with slenderness up to 3. Beer et al. [176,177] and available standards such as EN 772-1:2011+A1:2016 [9] and AS/NZS 4456.4:2003 [11] propose shape factors for slenderness up to 5. However, to achieve a slenderness greater than 1.0 using the bricks proposed in this research, stacked specimens are necessary due to the 40 mm height of units. Thus, seven stacked specimens were proposed in addition, i.e., specimens with 40, 50, 60, 70, 80, 90 and 100 mm width and 80 mm height with slenderness (height/width) between 0.8 and 2.0. Additionally, to check the behaviour above slenderness 2.0, an extra 40 × 40 × 120 mm^3 specimen was considered, composed of three stacked cubic specimens with 40 mm edge. This same specimen configuration was also tested by Binda et al. [109].

To evaluate the influence of the stacking procedure, specimens with 40 mm width and 80 mm height can be tested along the width (w) and length (l) of the original unit, both stacked and unstacked, and compared between them and with the cubic specimen with 40 mm edge tested along the same orientations. Since it is not possible to manufacture an 80 mm height unstacked specimen to test through the thickness (t) of the unit, only the behaviours along the length (l) and width (w) directions can be compared. The comparison between the tests carried out on specimens tested along the same direction is important to avoid any influence due to the material anisotropy, as detected by Cabané et al. [103].

After obtaining the different shapes by saw cutting, the specimens were dried in an oven at a constant temperature of 105 ± 5 ºC. The drying process was monitored by consecutive weighing at 24-hour intervals, until the specimens were cooled in the laboratory environment for 4 hours before testing. Finally, the specimen dimensions were measured using a calliper with a precision of ±0.1 mm according to EN 772-16:2011 [60].

Table 15 Classification of tested specimens based on their height (h) and width (w) indicating the respectively proposed acronym (Acr.) and the specimen slenderness (λ). The specimens with 40 mm edge, the load orientation with respect to the brick is specified along the length (l) and width (w)

		Height (h) (mm)								
		40			80			120		
		Acr.	λ	Stacked/ Unstacked	Acr.	λ	Stacked/ Unstacked	Acr.	λ	Stacked/ Unstacked
Width (w) (mm)	40 (l)	-		-	(S)_40_{80}-l	2.00	Stacked	-		-
		40_{40}-l	1.00	Unstacked	(US)_40_{80}-l	2.00	Unstacked	-		-
	40 (w)	-		-	(S)_40_{80}-w	2.00	Stacked	-		-
		40_{40}-w	1.00	Unstacked	(US)_40_{80}-w	2.00	Unstacked	-		-
	40	40_{40}	1.00	Unstacked	40_{80}	2.00	Stacked	40_{120}	3.00	Stacked
	50	50_{40}	0.80	Unstacked	50_{80}	1.60	Stacked	-		-
	60	60_{40}	0.67	Unstacked	60_{80}	1.33	Stacked	-		-
	70	70_{40}	0.57	Unstacked	70_{80}	1.14	Stacked	-		-
	80	80_{40}	0.50	Unstacked	80_{80}	1.00	Stacked	-		-
	90	90_{40}	0.44	Unstacked	90_{80}	0.89	Stacked	-		-
	100	100_{40}	0.40	Unstacked	100_{80}	0.80	Stacked	-		-

A total amount of 382 specimens were prepared and tested, made up of 206 'Ex' and 176 'Mo'. The 382 specimens included 157 samples with 40 mm height, 211 samples with 80 mm height, and 14 samples with 120 mm height. Table 15 summarizes the twenty-one types of specimens tested for each brick type.

IV.2.3. Testing procedure

The specimens were tested making use of the Ibertest testing machine with different load capacities depending on the specimen compressive strength. The Ibertest testing machine was equipped with three different load cell, 3000 kN (MEH-3000), 200 kN, and 10

kN (AUTOTEST 200/10SW), and connected to a MD5 electronic module for data acquisition. The specimens were centred on the steel plates and tested under force control at a rate of 0.15, 0.30 or 0.60 MPa/s depending on the specimen capacity to guarantee at least a test duration of 60 s. The rates were selected according to the EN 772-1:2011+A1:2016 [9]. The tests were stopped manually after registering the post-peak response of the force-displacement pattern.

IV.3. Experimental results

Table 16 presents the number of specimens and the average compressive strength of the tested specimens along the thickness, together with their coefficients of variations. The unstacked specimens correspond to those of 40 mm height and the stacked specimens correspond to those of 80 mm height. The table also shows the compressive strengths of the 40 mm width and 80 mm height stacked and unstacked specimens, both tested along width (w) and length (l). The stacked and unstacked configurations of the specimens tested along (w) and (l) is indicated in Table 16. The compressive strength of the specimens was calculated by dividing the maximum compressive load by the cross-sectional area of the specimen. The displacement during the test was measured with the transducer from the actuator.

The coefficients of variation (CV) of the compressive strength range between 3.0% - 20% for mechanically extruded units, and between 5.3% - 27% for modern handmade units. Slightly higher variation in handmade bricks is due to the inhomogeneity caused by their non-industrialised manufacturing. Lowest CV values are obtained for the specimens with higher width. In both brick types, CV values are higher in stacked specimens than unstacked ones.

The 'Mo' specimens show a progressive compressive strength increase as the specimen's width increases. However, this is not observed in the extruded 'Ex' bricks.

Different compressive strengths have been observed in the extruded 'Ex' specimens stacked and unstacked with the same slenderness along the length and width, but similar compressive strengths have been observed in the handmade 'Mo' specimens. Section IV.4 presents the in-depth discussion of results about the effect of the stacked specimen and of the specimen's slenderness on the compressive strength.

Table 16 Number of samples (N.) and average compressive strength (f_c) of the 'Ex' and 'Mo' specimens. Values in brackets correspond to the coefficients of variation. The specimens with 40 mm edge, the load orientation with respect to the brick is specified along the length (l) and width (w), such as their stacked or unstacked configuration

'Ex'			Height (h) (mm)					
			40		80		120	
			N.	f_c (MPa)	N.	f_c (MPa)	N.	f_c (MPa)
Width (w) (mm)	40 (l)	(S) stacked		-	8	38.0 [15%]		-
		(US) unstacked	12	50.1 [11%]	36	52.0 [11%]		-
	40 (w)	(S) stacked		-	6	27.9 [19%]		-
		(US) unstacked	9	43.9 [8.8%]	36	46.6 [13%]		-
		40	12	51.1 [14%]	6	52.1 [7.7%]	7	44.6 [16%]
		50	6	64.3 [12%]	6	58.7 [20%]		-
		60	6	83.6 [5.3%]	7	66.9 [12%]		-
		70	6	77.2 [9.5%]	6	65.0 [20%]		-
		80	6	74.1 [3.0%]	6	59.8 [17%]		-
		90	6	75.3 [4.6%]	6	43.0 [13%]		-
		100	6	75.3 [3.3%]	7	54.9 [9.8%]		-

'Mo'			40		80		120	
			N.	f_c (MPa)	N.	f_c (MPa)	N.	f_c (MPa)
Width (w) (mm)	40 (l)	(S) stacked		-	8	12.5 [26%]		-
		(US) unstacked	13	15.8 [11%]	8	13.3 [18%]		-
	40 (w)	(S) stacked		-	8	11.9 [20%]		-
		(US) unstacked	13	14.0 [14%]	8	13.2 [26%]		-
		40	13	15.6 [6.2%]	9	10.0 [15%]	7	8.8 [27%]
		50	7	15.7 [10%]	6	11.7 [17%]		-
		60	10	18.0 [14%]	6	12.0 [14%]		-
		º70	6	18.7 [10%]	6	12.0 [11%]		-
		80	6	22.0 [8.4%]	6	12.7 [16%]		-
		90	6	22.8 [8.9%]	6	13.6 [5.3%]		-
		100	14	24.9 [8.6%]	10	16.5 [18%]		-

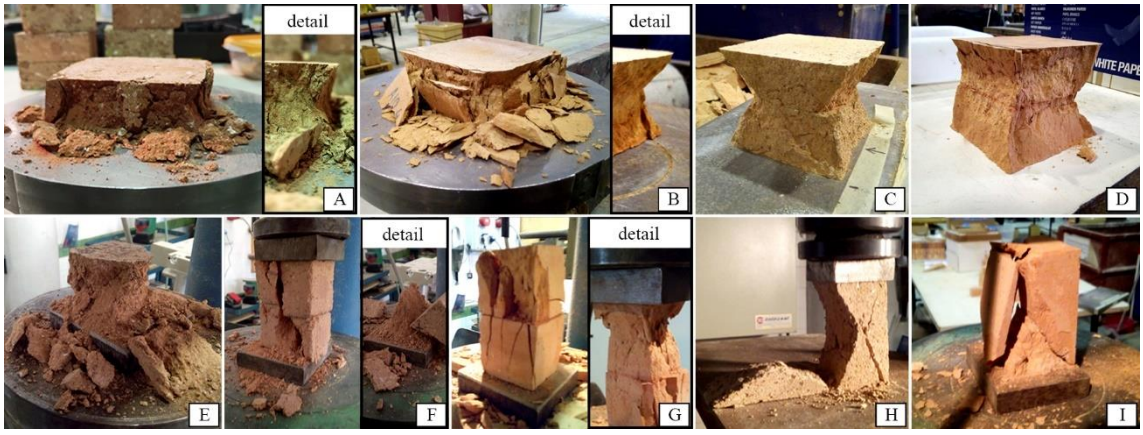

Fig. 35 The developed failure modes. A) Handmade 100 × 100 × 40 mm³ and hourglass shape detail. B) Extruded 100 × 100 × 40 mm³ and hourglass shape detail. C) Handmade 100 × 100 × 80 mm³ without outers parts. D) Extruded 100 × 100 × 80 mm³ without outers parts. E) Handmade 40 × 40 × 40 mm³. F) Stacked handmade 40 × 40 × 80 mm³ and detail of the bottom pyramid. G) Stacked Extruded 40 × 40 × 80 mm³ and detail of the upper pyramid. H) Handmade 40 × 40 × 80 mm³. I) Extruded 40 × 40 × 80 mm³

The observed failure mode exhibited by the specimens follows an hourglass shape, as shown in all samples in the Fig. 35, causing the complete separation of the outer parts. The overlapping cones of influence, which extended from the bearing surfaces, developed this spalling of the outer parts. As observed by RILEM TC 148-SSC [133] and van Vliet et al. [180], cracks growth usually in the unconfined regions and the hourglass failure mode is presented in the confined specimens. After evaluating one by one the different failure modes depending on the specimen's configuration, some differences could be noticed. The 40 mm height specimens (Fig. 35a and b) showed the expulsion of the outer material, while the remaining core remained compacted. Removing the expelled perimeter material, the hourglass shape was observed around the specimen's perimeter, see figures Fig. 35a and b. The stacked specimens with 80 mm height (Fig. 35c and d) presented a failure mode with a clear hourglass shape. Cubic specimens of 40 × 40 × 40 mm^3 (Fig. 35e) were evaluated, as explained by Cabané et al. [103], by using the indications of the concrete standard EN 12390-3:2022 [82]. The stacked specimens 40 × 40 × 80 mm^3 (Fig. 35f and g) presented continuous vertical cracks on the external faces, extending between bearing surfaces. Vertical cracks were uniformly distributed along all four faces of the sample. However, once the outer parts were removed, narrow pyramids of material were observed next to each one of the bearing surfaces, as shown in Fig. 35f. Finally, unstacked specimens of dimensions 40 × 40 × 80 mm^3 (Fig. 35h and i) presented an asymmetric failure mode with the spalling of two of the four external faces.

In the handmade bricks (Fig. 35h), influence cones were overlapping up to the central part of the specimen. The failures obtained were 'cone' and 'cone and shear', according to ASTM C39/C39M-21 [8]. In the extruded bricks (Fig. 35i) the influence cones rarely match on the centre. The failures obtained were 'cone and shear' and 'columnar' according to ASTM C39/C39M-21 [8]. The spalled faces coincided in all tested samples with the stretcher or header of the bricks according to the test direction.

IV.4. Discussion

This section presents two analytical studies based on the experimental results described in Section IV.3. The first study evaluates the influence of stacking on the compressive strength. The second study focuses on the evaluation of the specimen's slenderness and shape on the resulting compressive strength. This analytical study considers additional experimental data from the available literature in the field.

IV.4.1. Study on stacked and unstacked specimens

The experimental campaign on the 40 × 40 mm^2 cross-section specimens allowed the evaluation of the influence of the stacking procedure. Specimens with 80 mm height stacked and unstacked were compared for loading along the width and the length orientations. As

the possible anisotropy of the material may influence the comparisons [103], the compressive strengths of the 80 mm height stacked specimen ($f_{c,(S)\_40_{80}}$), 80 mm height unstacked specimen ($f_{c,(US)\_40_{80}}$), and 40 mm height cubic specimen ($f_{c,40_{40}}$) were measured along the same orientation.

Fig. 36 shows the compressive strength values of the 40 × 40 mm² cross-section specimens with 80 mm height, both stacked and unstacked, presenting in a boxplot the data distribution based on the quartiles (being the second and third quartiles coloured inside the boxes), the median (depicted as a horizontal line inside the box), and the average (depicted as a cross). As presented in Fig. 36, both boxes of the 'Ex' unstacked specimens have higher values than the boxes of the corresponding 'Ex' stacked specimens. However, the 'Mo' specimens exhibit boxes with very similar values, including maximum and minimum ones.

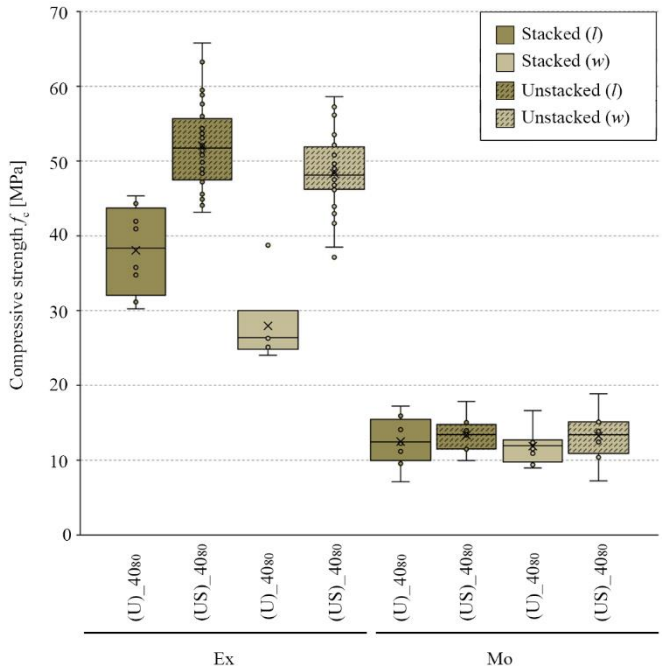

Fig. 36 Boxplot with Stacked ((S)_40_{80}) and Unstacked ((US)_40_{80}) 80 mm height specimens compressive strength values (f_c) for the 'Ex' and 'Mo' units tested along length (l) and width (w). Inside the boxes, the medians are presented with a horizontal line and the average are presented with an X

Table 17 presents the $f_{c,(S)\_40_{80}}$ / $f_{c,(US)\_40_{80}}$ ratio obtained along the length and the width, and the $f_{c,(S)\_40_{80}}$ / $f_{c,40_{40}}$ and $f_{c,(US)\_40_{80}}$ / $f_{c,40_{40}}$ ratios along the three orientations (l, w, and t). As presented in Fig. 36, Table 17 shows that the $f_{c,(S)\_40_{80}}$ / $f_{c,(US)\_40_{80}}$ ratios on mechanically extruded ('Ex') bricks are 0.73 and 0.60, and the $f_{c,(S)\_40_{80}}$ / $f_{c,(US)\_40_{80}}$ ratios on modern handmade ('Mo') bricks are 0.94 and 0.90. However, the ratios between the compressive strengths of a specimen with slenderness 2 and a specimen with slenderness 1 show higher values for the $f_{c,(US)\_40_{80}}$ / $f_{c,40_{40}}$ ratios (comparison between unstacked specimen of 80 mm height and 40 mm edge cube) than for the $f_{c,(S)\_40_{80}}$ / $f_{c,40_{40}}$ ratios (comparison between stacked

specimen with 80 mm height and 40 mm edge cube). The $f_{c,(S)\_40_{80}}$ / $f_{c,40_{40}}$ ratio along the thickness on 'Ex' is 1.02, higher than the 'Mo' one, 0.64.

The scientific literature discussed in Section IV.1 includes only a limited number of references dealing with the experimental testing of clay brick specimens under compression, comparing specimens' slenderness equal to 2 and 1. However, available references dealing with both slenderness can be found in concrete standards. Model Code [181] recommends a $f_{c,(US)\_40_{80}}$ / $f_{c,40_{40}}$ ratio of 0.80, American Standard ASTM C42/C42M-20 [84] recommends 0.87, European Standard EN 12390-3:2022 [82] does not specify any coefficient, Spanish concrete code EHE-08 [182] recommends a ratio between 0.70 and 0.90 depending on the concrete strength. However, some authors as Neville [59] or Hughes et al. [172] warn that the ratio between both slenderness is influenced by the mix proportions and the material strength.

Table 17 Ratios of the experimental compressive strength of 'Ex' and 'Mo' brick type. Ratio between stacked and unstacked 80 mm height specimens $f_{c,(S)\_40_{80}}$ / $f_{c,(US)\_40_{80}}$, ratio between stacked and 40 mm edge cubic specimen $f_{c,(S)\_40_{80}}$ / $f_{c,40_{40}}$, and ratio between unstacked and 40 mm edge cubic specimen $f_{c,(US)\_40_{80}}$ / $f_{c,40_{40}}$

	Ratios					
	'Ex'			'Mo'		
	(t)	(l)	(w)	(t)	(l)	(w)
$f_{c,(S)\_40_{80}}$ / $f_{c,(US)\_40_{80}}$	-	0.73	0.60	-	0.94	0.90
$f_{c,(S)\_40_{80}}$ / $f_{c,40_{40}}$	1.02	0.76	0.64	0.64	0.79	0.85
$f_{c,(US)\_40_{80}}$ / $f_{c,40_{40}}$	-	1.04	1.06	-	0.84	0.95

A statistical evaluation was carried out to identify meaningful strength differences among the stacking procedure, and to confirm the influence observe in Fig. 36 and Table 17. A nonparametrical analysis was applied since the data could not be adjusted to a normal distribution and the number of samples in each population was small as proposed by Cabané et al. [103]. The nonparametric test used for this purposed was the Wilcoxon Sum Rank test [87]. The Wilcoxon Sum Rank test [87] compares two data sets and determines if the values of a reference data set are lesser, equal or larger than values of the other data set. The paired data tested were Stacked-Unstacked both along the length and the width, for mechanically extruded ('Ex') and modern handmade ('Mo'). This test indicated that for compressive strength in 'Ex', both along the length and width, is larger for specimens unstacked than stacked with probability greater than 95%. This test also indicated that the compressive strength in 'Mo' is equal, regardless of the stacked or unstacked configuration.

Using the analysis previously presented, it is possible to draw some conclusions about the influence of the stacking procedure. A significant influence has been found in mechanically extruded bricks 'Ex', in which the highest compression strength is obtained in unstacked specimens. Such influence has not been found significant in modern handmade bricks 'Mo', in which similar compressive strength values are obtained.

IV.4.2. Influence of the slenderness (Shape effect)

This section presents the experimental comparisons among the compressive strengths derived from specimens with different slenderness. Fig. 37 shows the compressive strength value of each specimen with empty dots, and their average values with black dots. Square dots are related to specimens with 40 mm height, circular dots are related to specimens with 80 mm height, and rhomboidal dots are related to specimens with 120 mm height. The Fig. 37 also shows a representation of the statistical Z-score measured in terms of standard deviations from the mean to obtain the three levels of percentiles, i.e., 68.3%, 95.5% and 97.7% of the data probability. Three main aspects can be observed in Fig. 37. First, modern handmade brick specimens ('Mo') exhibit a clear gradual reduction of the compressive strength for increasing slenderness. Second, mechanically extruded brick specimens ('Ex') do not show such clear trend as the compressive strength vs. slenderness relationship exhibits fluctuations. Regardless of their height, the strength of specimens progressively increase when slenderness decreases up to 60 mm width, and then the strength starts to decrease. This reduction in strength occurs with the decrease in slenderness until reaching a 90 mm width, then strength increases with 100 mm width specimens. This occurs for both the 80 mm height specimens and the 40 mm height ones. (3) 'Mo' specimens with varying slenderness show rather equidistant 68.3%, 95.5%, and 97.7% percentiles from the mean. (4) 'Ex' specimens show irregular data probability depending on the specimen width.

The scientific literature discussed in Section IV.1 includes only a limited number of references dealing with the experimental effect of different slenderness on the compressive strength of solid clay units, but there is a larger number of references on concrete specimens. Three characteristic behaviours in the compressive strength vs. slenderness curves of Fig. 37 can be described, as also observed by Murdock et al. [170], Tucker [183], Schickert [58] or Egermann [175]. First, a steeply increase of the compressive strength is observed from approximately slenderness 1 to lower slenderness. Second, the compressive strength slightly decreases as the slenderness increases from 1 to 2. Third, a slightly decrease in the compressive strength of the specimen with slenderness greater than 2. Page et al. [76,104] considered the unconfined compressive strength for specimens with slenderness 5 while testing calcium silicate bricks. Hendry [184] and Khalaf et al. [5] considered it for specimens with slenderness 3 while testing solid concrete bricks.

A significant influence of the slenderness (h/l) has been found in specimens with slenderness below 1, in which the highest compression strength values are obtained. Mechanically extruded brick specimens show an erratic increase of compressive strength as slenderness decreases.

A statistical evaluation was carried out to identify the strength difference between specimens with different slenderness. The Kruskal-Wallis test [86] as a nonparametrical analysis was used for this purpose. The Kruskal-Wallis test was used to compare the three

data sets corresponding with slenderness 1, 2 and 3. The specimens used were 40_{40}, 40_{80} and 40_{120}. The specimens selected had the same width, avoiding the use of the 80_{80} specimen, to avoid influences produced by the size effect [185]. The Kruskal-Wallis test provides the probability of fulfilling the statistical hypothesis that the data sets belong to the same data population. The nonparametric test indicated that the data sets with slenderness 1, 2 and 3 are coincident (i.e., correspond to a single population) for 'Ex', while 'Mo' are non-coincident data sets. As Fig. 37 shows, 'Mo' specimens with slenderness 1 seems different than the specimens with slenderness 2 and 3. Thus, the Kruskal-Wallis tests was carried out again for 'Mo' specimens with slenderness 2 and 3. In this hypothesis, the nonparametric test indicated that the data sets with slenderness 2 and 3 are coincident for 'Mo'.

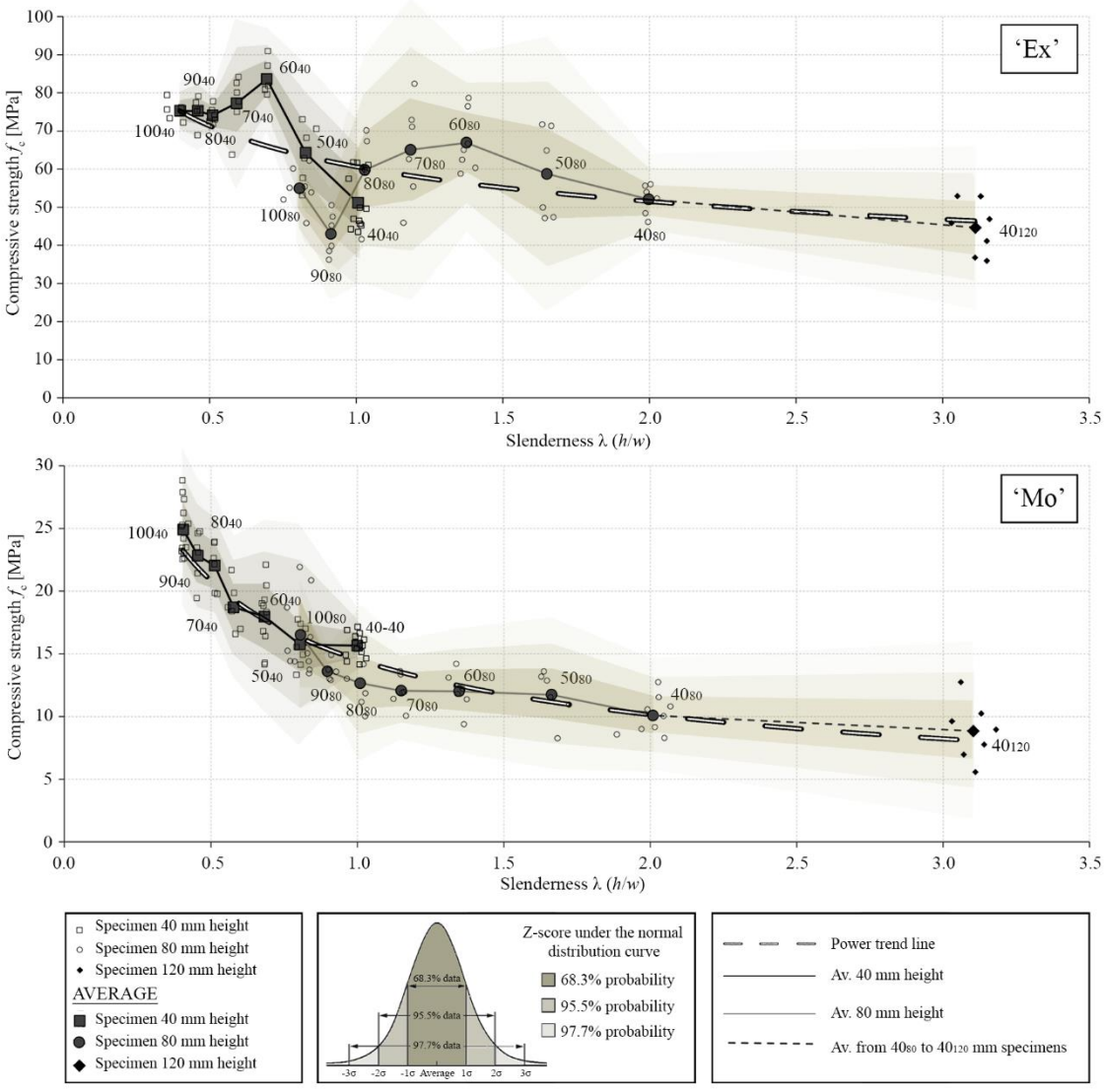

Fig. 37 Compressive strength vs. slenderness curve, showing with empty dots each experimental compressive strength and with black dots the compressive strength averages for each specimen type. The graph shows the probability values under a normalized distribution using the Z-scores of each average value as a reference. Coloured area represent the 97.7% data probability. The dashed line of white lines outlined in black represents the trend line for all the averages obtained

IV.5. Conclusions

This paper has presented novel results on the measurement of the compressive strength of clay brick solid samples. First, the influence of the stacking procedure on the strength has been investigated. Second, the influence of slenderness has been analized into detail by investigating twenty-one specimens shapes including slenderness between 3 and 0.4. The research has been performed through an extensive campaign on mechanically extruded ('Ex') and modern handmade ('Mo') bricks. The following conclusions can be drawn:

- The failure mode of the specimens showed a characteristic hourglass shape due to the confinement effect. This phenomena is even observe in specimens with slenderness 2 stacked and unstacked.
- The experimental results show that the influence of the stacked procedure on the experimental compressive strength is more evident in mechanically extruded flatwise solid fired clay bricks ('Ex') than in modern handmade solid fired clay bricks ('Mo'). The results of the experimental analyses show that the ratio between the compressive strengths of stacked and unstacked specimens tested along the width and length with slenderness 2 are 0.60 and 0.73 for 'Ex' specimens, respectively. However, the 'Mo' specimens show closed strengths for the same specimens types, 0.90 and 0.94 respectively. This influence has been corroborated based on a statistical analysis of the experimental data.
- The influence of specimen slenderness on the compressive strength is clear and regular in handmade solid fired clay bricks 'Mo' specimens. In particular, a steeply increase in experimental compressive strength is observed for slenderness below 1.0.
- Mechanically extruded flatwise solid fired clay bricks ('Ex') specimens exhibit an irregular strength vs. slenderness relationship for slenderness below 1.5.
- Testing stacked specimens with slenderness between 2 has proved to be an advantageous technique for the evaluation of the compressive strength of the modern handmade solid fired clay units ('Mo'). The stacked procedure does not influence the compressive strength and the same experimental set of compressive strength data is obtained for specimens with slenderness 2 and 3. The same experimental compressive strength for specimens with slenderness 2 and 3 indicate that the confinement effects is reduced.

Future research works may pursue the extension of the experimental database by including a much larger sample of different brick materials, e.g. derived from manufacture such as dry pressed into mould or mechanically extruded in different directions. Likewise, more in-depth research is necessary on the shape factors for slenderness above 3.0 in order to understand the influence of slenderness on the experimental strength of masonry units.

2.6. Paper V – Experimental evaluation of the elastic modulus of solid fired clay bricks and correlation with compressive strength

A. Cabané, L. Pelà, P. Roca

(2023) Under review

Abstract. This paper presents the experimental programme carried out to determine the elasticity modulus of solid fired clay bricks, and presents a novel testing setup for estimating the modulus of elasticity. The testing setup focuses on the design and development of a support for the clamp-on transducers, the specimen shape, i.e., cross-section and slenderness, and the testing procedures. The experimental campaign has focused on three different types of solid fired clay bricks, namely mechanically extruded, hydraulic press moulded, and handmade units, with a total amount of 419 specimens. Using the $40 \times 40 \times 80$ mm^3 specimen, a detailed research on the elastic modulus and the anisotropy of different solid clay brick types has been carried out. The experimental results have shown that the proposed specimen can be utilized for a reliable estimation of the elastic modulus.

V.1. Introduction

The elastic modulus is a crucial and fundamental material property that plays a critical role in the mechanical behaviour of structural elements. It characterizes the deformation behaviour of materials and is essential for the design of new structures as well as the assessment of the performance of existing ones. However, the measurement of the elastic modulus in brittle materials, such as bricks, presents significant challenges. Among such challenges are the need for measurement methods allowing the gradual loading of carefully prepared samples, the transducer-specimen surface interaction, the low deformation magnitudes, and the heterogeneity of the clay brick. Obtaining a complete understanding of the elastic modulus of solid clay units is crucial to designing adequate masonry structures and evaluating the mechanical behaviour of existing ones.

The scientific literature includes only a limited number of references about the elastic modulus influence on compressive strength on solid clay bricks. Hilsdrof [186] reported on Glanville and Barnett's empirical relationship, which was published in 1934 and expressed the elastic modulus of solid clay bricks as $E_b = 300 \cdot f_c$, in relation to their compressive strength. In a research conducted by Kaushik et al. [187], ten whole brick samples for each of four different types of bricks were analysed following the recommendations of ASTM C67 [47] and IS 3495 (IS 1992a) [154]. Kaushik et al. [187] proposed an experimental correlation between the elastic modulus and compressive strength equal to $E_b \approx 300 \cdot f_c$. However, the

observed data exhibits significant scattering beyond the correlation limits, which are estimated to be between 150 and 500 f_c.

At present, there is a lack of consensus within the scientific community regarding the appropriate methodology for measuring the elastic modulus of solid clay bricks. As a result, there is no universally recognized standard for conducting such test. A review of standards for concrete and stone materials indicates that establish procedures can be found in the American ASTM C469/C469M-22 [188],and ASTM D7012-14e1 [189] European EN 12390-13:2022 [190], and EN 14580:2006 [191], and Brazilian ABNT NBR 8522:2017 [192] standard. These standards also exhibit a lack of consensus among them. The ASTM propose the use of samples with circular cross-section, while European standards allow the use of prismatic samples. However, both standards specify that the samples must have a slenderness ratio of 2, where the slenderness is defined as the ratio between the length and the diameter or width. The ASTM standards do not propose any specific cycles of loading and unloading, while the European standard proposes three cycles and the Brazilian standard proposes four cycles. The European EN and Brazilian ABNT standards for testing concrete specify that the loads for each cycle should be held for 60 s. In contrast, the European standard for testing stone does not require any specific holding time for the loads.

This paper aims to establish a reliable protocol for testing the elastic modulus of solid fired clay brick specimens. The development process focuses on designing a support system for clamp-on transducers, determining the shape of the specimen (including cross-section and slenderness), and establishing a testing procedure. The proposed shapes for the specimens to calibrate the testing procedure include both circular and square cross-section, with slenderness ratio of 1 and 2. After calibrating the testing procedure using the proposed specimen shapes, the focus of the testing procedure shifts to investigating the compressive stress levels during the loading and unloading cycles.

This research offers the results of an extensive experimental campaign including the execution of 419 laboratory test. The research encompasses the following specific objectives: (1) recommend a testing procedure for the experimental measurement of the elastic modulus of the bricks, (2) exploring the anisotropy in the elastic modulus, and (3) calibrate an empirical correlation between the compressive strength and the elastic modulus.

This paper is divided into five sections. Following the introduction, Section V.2 details the experimental campaign performed on brick units, including the description of the materials, clamp-on transducers support, specimen preparation, and testing procedure. Section V.3 presents the experimental results. Section V.4 analyses the influence of the stacking procedure and the specimen slenderness on the compressive strength. Finally, Section V.5 concludes the paper by summarizing the conclusions and suggesting future works.

V.2. Experimental programme

This section presents the methodology and the experimental tests carried out on solid fired clay bricks to characterize their elasticity modulus, E_b. The experimental programme was performed in solid fired clay bricks manufactured according to three different procedures, corresponding to (1) mechanically extruded, (2) hydraulic press moulded, and (3) handmade bricks. The handmade manufacture bricks include both modern and historical bricks. The historical handmade samples were collected from historical buildings, including three residential ones and two industrial structures in Barcelona (Spain). Four of these buildings were built in the early 20th century and the other one was built in the 19th century. The information in this section includes the material description, the support development for clamp-on strain transducers, the specimen shape and preparation, and the testing setups. These experimental tests were carried out at the Laboratory of Technology of Structures and Materials of the Technical University of Catalonia (UPC-BarcelonaTech).

V.2.1. Materials

This research examines solid fired clay bricks manufactured through three distinct procedures. The first type, identified as 'Ex', are modern clay bricks produced through mechanical extrusion. The second type, identified as 'Hy', are modern clay bricks produced through hydraulic press moulding. The third type encompasses both modern and historical handmade clay bricks. The modern handmade bricks are divided into three subtypes: 'Mo_1', 'Mo_2', and 'Mo_3'. Despite being manufactured by the same producer, the three modern handmade brick types correspond to different manufacturing series and display varying mechanical properties. The historical solid clay bricks were obtained from five different masonry buildings using RILEM recommendation LUMD1 [83] for specimen removal and testing. The industrial building's historical handmade bricks are labelled as 'Hi/I', while the residential building's historical handmade bricks are labelled as 'Hi/R'.

The 'Mo', 'Hi/I', and 'Hi/R' were traditionally manufactured in a brickyard by moulding. In this traditional process, the 'Mo' were shaped using a wooden mould that was sprinkled with dry, fine sand. After being removed from the mould, the bricks were fired into a coal-fired kiln. The modern mechanical type, 'Ex' and 'Hy' were produced using an automated process. 'Ex' bricks were extruded along the thickness and then cut and dried using mechanical, automated tools before being fired in a tunnel kiln with controlled heat conditions. Meanwhile, 'Hy' bricks were mechanically pressed onto their beds using a mould. Table 18 reports a brief summary of the sampled materials in terms of manufacturing and origin, construction year, acronym, number of specimens and average dimensions.

Table 18 Sampled bricks in terms of origin, acronym (Acr.), and average dimensions in mm. Values in brackets correspond to the coefficients of variations

Sampled materials		
Origin	Acr.	Av. dimension (mm)
Mechanically Extruded	Ex	272 [0.4%] × 132 [0.9%] × 45 [0.7%]
Hydraulic Pressed	Hy	291 [0.0%] × 141 [0.0%] × 38 [0.1%]
Modern Handmade	Mo_1	306 [0.5%] × 147 [0.9%] × 46 [3.4%]
	Mo_2	311 [0.6%] × 149 [1.7%] × 46 [4.6%]
	Mo_3	306 [1.4%] × 146 [1.5%] × 46 [2.7%]
1910-20 Industrial	Hi/I_1	295 [1.2%] × 145 [2.4%] × 54 [4.3%]
1927 Industrial	Hi/I_2	288 [0.7%] × 141 [1.5%] × 49 [5.8%]
1880 Residential	Hi/R_1	294 [0.6%] × 145 [0.4%] × 56 [3.3%]
1930 Residential	Hi/R_2	294 [0.4%] × 145 [0.5%] × 49 [5.2%]
1930 Residential	Hi/R_3	290 [1.4%] × 140 [1.3%] × 45 [4.7%]

V.2.2. Development of a support device for clamp-on transducers

The compressive stress tests were carried out using external clamp-on transducers to control the specimen deformation. The specimens were composed of a basic unit fitted with a 50 mm extension piece for vertical strains and 20 mm for horizontal strain. The strain gauges used convert the movement of a probe tip into an electrical signal. This probe tip can accept displacements of ±2.5 mm, with a deviation from the characteristic curve of less than 0.05% of the full-scale value, and with a resolution of 10^{-17} mm and an accuracy class of 0.1 (DD1 strain transducer, with DD1/ZV and DD1/ZA).

To enhance data acquisition, a metallic bracing mechanism to hold the clamp-on transducers was developed. The bracing mechanism allows precise adjustment of the clamping force of the measuring instrument on the sample. This prototype was proposed as an auxiliary tool to measure Young's modulus (E_b) and Poisson's ratio (v) holding three vertical clamp-on transducers and one horizontal. In this research, only Young modulus is calibrated. Each transducer is held in a threaded steel bar with a nut. The horizontal transducer nut is not fully tightened, allowing a 3D movement to adjust to the specimen surface. The vertical transducers are fully tightened on a piece that can be moved in 2D by pushing a screw from their back through. The main structure is supported by a four-legged lower fastening system with a height-adjustable system that ensure the horizontality of the setup. Fig. 38a shows the brace prototype that facilitates clamping the transducers in a prismatic specimen with a square size ranging from 30 to 50 mm, and Fig. 38b illustrates a schematic diagram indicating the position where the vertical and horizontal strains were measured on the specimen.

The phases of placement and adjustment of the specimen and transducers were designed to speed up and minimize the time spent performing the test. First, the brace mechanism was placed in the centre of the press platens, and if necessary, the sensors were levelled by adjusting the four-legged lower fastening system. Secondly, the specimen was

introduced to the centre of the developed apparatus (Fig. 38c). Next, the specimen was placed in contact with the horizontal sensor, ensuring its horizontality. Then, the vertical transducers were attached to the sample surface by means of a screw that pushes the back where the transducers had been fixed (Fig. 38d). Strong pressure from the transducers on the sample surface should be avoided to prevent lateral confinement. Finally, the lower fastening system was withdrawn upwards to avoid contact with the press plate (Fig. 38e), keeping the transducers in contact with the specimen in a self-supporting way. Fig. 38f shows the specimen ready to be tested.

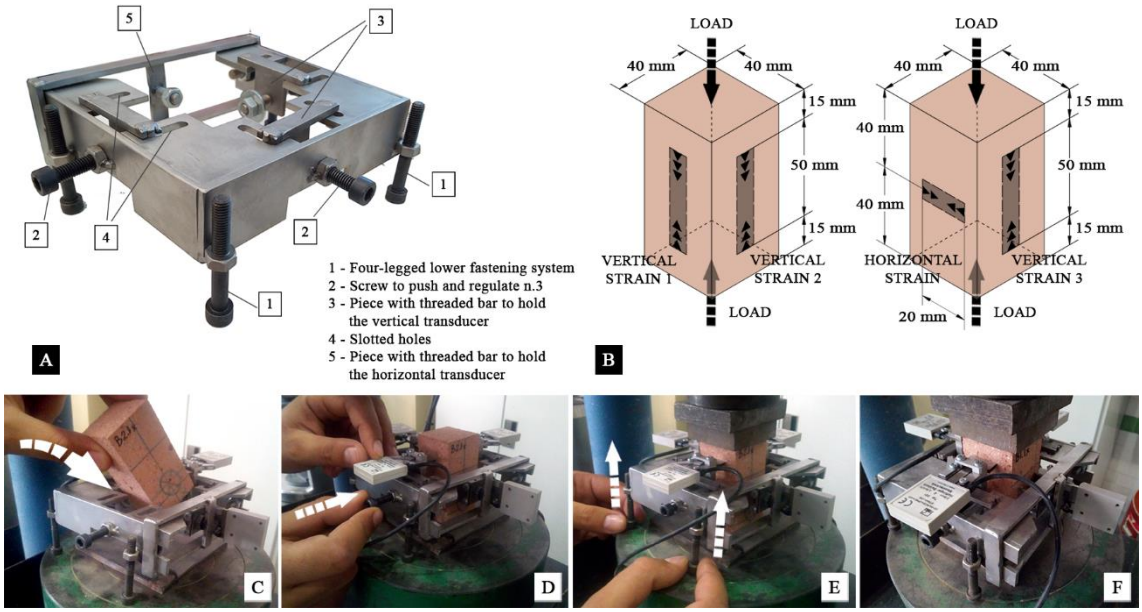

Fig. 38 A) Metallic bracing device to hold the clamp-on transducers. B) Schematic diagram with the position where the vertical and horizontal strains were measured on the specimen. C) The prismatic specimen positioned in the device where the clamping transducer have been placed. D) Attachment of the transducers to the sample surface by means of a screw that pushes the back where the transducers have been fixed. E) Withdrawal of the four-legged lower fastening system to avoid contact with the press plate. F) The specimen ready to be tested

V.2.3. Specimen type and preparation

The proposal of a new experimental setup is motivated by the absence of a reference standard for the measurement of the elastic modulus of clay units. Previous research available in the scientific literature has considered different specimens shapes and sizes, resulting in diverse load cross-sections and slenderness ratios. To define an appropriate specimen, prior research is needed focussing on the effect of the specimen cross-section shape and slenderness.

First, to analyse the influence of the load cross-section shape, a circular cross-section with a Ø37 mm is considered, as proposed by Pelà et al. [193], Winnicki et al. [194], Drougkas et al. [195], and Oliveira et al. [79]. In addition, specimens with square cross-section with side of 40 mm, are considered, as proposed by Makoond et al. [12], and Binda et al. [109]. Fig. 39a shows two cross-sectional specimens, intended to be tested along the same direction,

which were obtained from a single brick sample. In both cases, the specimen height was fixed at 40 and 80 mm, while preserving a height-to-diameter/width ratio of 1 and 2.

Second, to analyse the influence of the specimen slenderness on the test configuration, a research was conducted using square cross-section specimens with a side of 40 mm. Two slenderness, 1 and 2, were assessed by testing unstacked specimens with height of 40 and 80 mm, respectively. The use of the specimen 40 × 40 × 40 mm^3 was validated by Cabané et al. [103], and the use of the specimen 40 × 40 × 80 mm^3 was validated in previous Section IV. Fig. 39b shows the two specimen types obtained from a single brick sample. The 40 × 40 × 40 mm^3 (slenderness 1) was tested along the length, width and thickness of the brick. The 40 × 40 × 80 mm^3 (slenderness 2) was tested only along the length and width due to the reduced thickness of the proposed bricks.

To correlate the elastic modulus and the compressive strength, squared cross-sectional specimens with slenderness 2 (40 × 40 × 80 mm^3) were tested along the specimen length and width. Fig. 39c shows the large scale campaign using the 40 × 40 × 80 mm^3 specimens.

Table 19 Classification of tested specimens based on their shape, indicating the specimen acronym (Acr.), the number of tested samples (N.), the brick type sampled, the specimen dimensions, the specimen slenderness (λ), the load orientation with respect to the brick: (l) length, (w) width, and (t) thickness, and the setup calibration objective

Specimen specifications						
Acr.	N.	Brick type	Load	Specimen dimension (mm)	λ	Setup calibration objective
$Ø37_{80}$-l	4	'Mo$_3$'	length	Ø37 × 80 mm^3	2.16	(1) Cross-section, circular vs square
$Ø37_{80}$-w	2		width			
$Ø37_{40}$-t	4		thickness	Ø37 × 40 mm^3	1.08	
40_{80}-l	184	'Ex', 'Hy', 'Mo$_2$', 'Mo$_3$', 'Hi/I', 'Hi/R'	length	40 × 40 × 80 mm^3	2.00	(1) Cross-section, circular vs square (2) Slenderness 1 vs 2 (3) Load/Unload cycles (max. and min stresses) (4) Strength – Elastic modulus relationship
40_{80}-w	185		width			
40_{40}-l	12	'Ex', 'Mo$_1$', 'Mo$_2$', 'Mo$_3$'	length	40 × 40 × 40 mm^3	1.00	(1) Cross-section, circular vs square (2) Slenderness 1 vs 2
40_{40}-w	12		width			
40_{40}-t	16		thickness			

The specimens considered in the experimental program were prepared according to the procedures described in the EN 772-1:2011+A1:2016 [9]. First, the brick beds were ground using a rotary diamond disc grinder to achieve a uniform thickness of 40 mm. This step was perform to ensure the smoothness and flatness of the loading surfaces and to eliminate any imperfections on the bearing surfaces. Next, the specimens were extracted from the brick. The square cross-sectional specimens were cut using a table saw equipped with a water jet, and the circular cross-section specimens were cored by drilling. Then, the specimens were dried in an oven at a constant temperature of 105 ± 5 ºC for 24 hours. Finally, the loading surfaces were lightly dry-polished on a 3-axis vertical milling machine fitted with a rotary

diamond disc to guarantee a great flatten precision. Before testing, the specimens were measured using a calliper with a precision of ±0.1 mm according to EN 772-16:2011 [60]

A total amount of 419 specimens were obtained, including 142 specimens for the first proposal, i.e., focussing on the effect of cross-section shape and slenderness, and 277 specimens for the second proposal, i.e., 40 × 40 × 80 mm^3 specimens tested along the length and width. Table 19 summarizes the seven types of specimens tested.

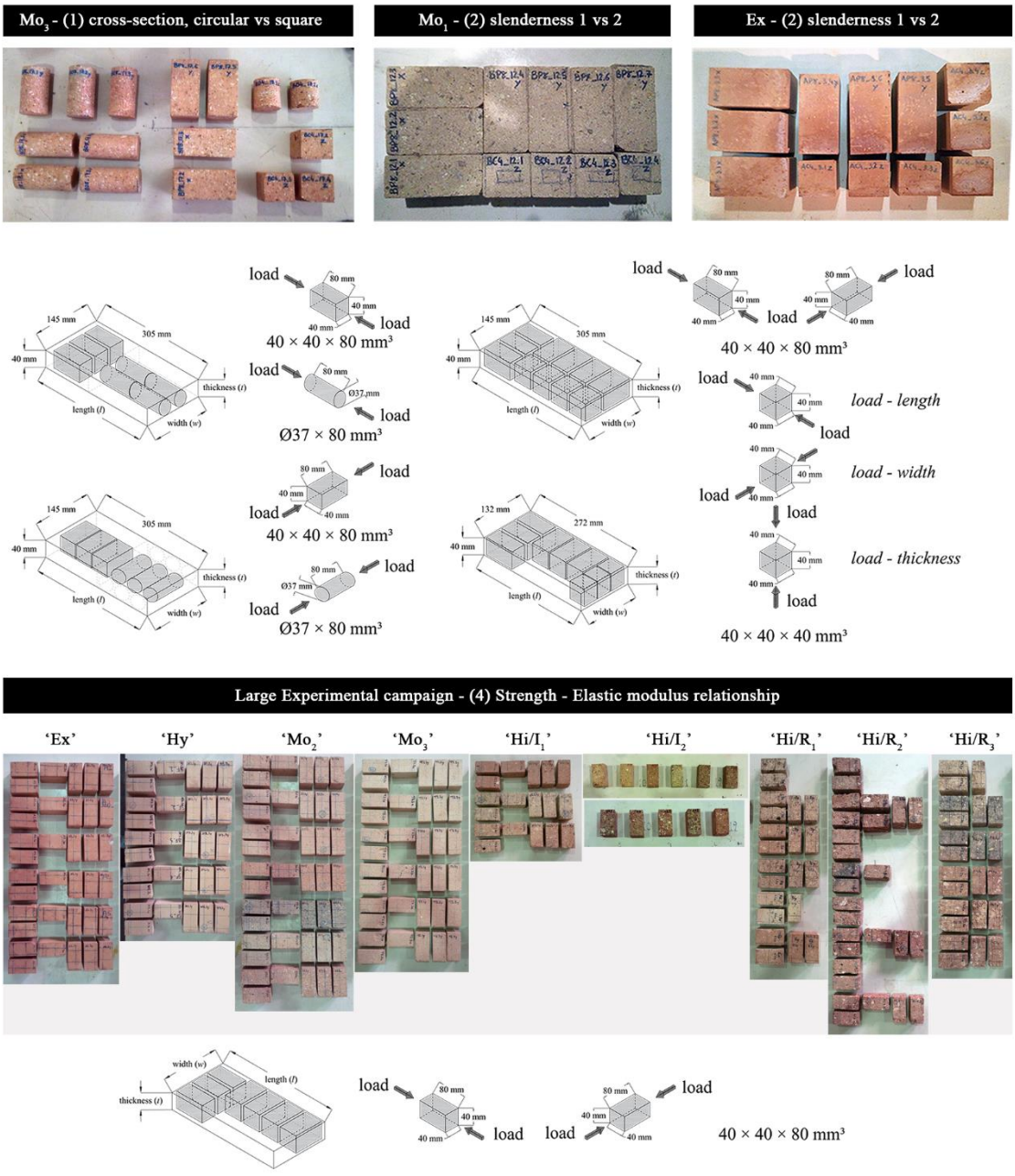

Fig. 39 View of the prepared specimens A) 'Mo$_3$' circular and square cross-section specimens to be tested along the same direction, which were obtained from a single brick sample. B) 'Ex' and 'Mo$_1$' square cross-section specimens tested with slenderness 1 and 2 along the length, width and thickness. C) Large scale campaign testing 40 × 40 × 80 mm^3 specimens along length and thickness for different types of specimens

V.2.4. Experimental setup

The specimens were tested making use of the Ibertest testing machine equipped with a 200 kN load cell capacity (AUTOTEST 200/10 SW). The load cell was connected to an MD5 electronic module for data acquisition, and external clamp-on transducers (DD1 strain transducer, with DD1/ZV and DD1/ZA) were used to measure strain, with a sampling rate of 5 Hz. The mechanical characterisation of the brick samples was carried out in two consecutive test procedure. First procedure, the compressive strength, f_c, was tested on one specimen from each brick sample. Second procedure, the elastic modulus, E_b, was tested on the remaining specimens.

In the first procedure, the specimens were centred on the steel platens with ground surfaces orthogonal to the direction of loading, and tested under force control at a rate of 0.15 MPa/s or 0.30 MPa/s. The testing rate was selected from EN 772-1:2011+A1:2016 [9] to ensure a minimum test duration of 60 s. The tests were manually stopped after recording the post-peak response.

In the second procedure, the external strain-measuring equipment (DD1 with ZV and ZA) were clamped to the specimen using the support system described in Section V.2.2. The test was conducted in two consecutive stages. In the first stage, during the compression test, load/unload cycles were applied under displacement control to analysed the elastic behaviour of the sample. The load/unload procedure consists in increasing the load gradually until the specimen begins to deform, or "yield", then, the load is held constant for a period to allow the specimen to stabilize under the load. Once the specimen has stabilized, the force is gradually release, or "unloaded". This load and unload process is repeated multiple times. Fig. 40 shows the diagrammatic representation of the stress-time relationship of the load/unload procedure. To eliminate the influence of creep, and also to achieve the seating of the transducers, at least three cycles of load/unload are recommended by ASTM E111-17 [196] by EN 12390-13:2022 [190], ASTM C469/C469M-22 [188], and ABNT NBR 8522:2017 [192] for concrete, and by EN 14580:2006 [191], and ASTM D7012-14e1 [189] for stone. Neville [59] observed for concrete that the stress-strain curve on the third and fourth load cycle exhibits with similar slopes. The maximum and minimum stresses of the cycles were chosen as a fixed portion of the strength determined in the first procedure. Each maximum and minimum stress was held constant for 60 s to avoid residual stresses. The calibration of the minimum and maximum stresses is presented in Section V.2.4.1. The second stage is aimed to measure its compressive strength. After the last loading cycle, the load was increased under force control at a constant rate of load application until the maximum load is reached.

The elastic modulus E_b was calculated between the minimum and maximum stress-strain point of the last loading cycle by dividing the stress increment by the corresponding vertical strain. The vertical strain was calculated as the total deformation divided by the

effective extensometer length. The minimum and maximum strains and stresses points were considered as the average values of the cycle interval.

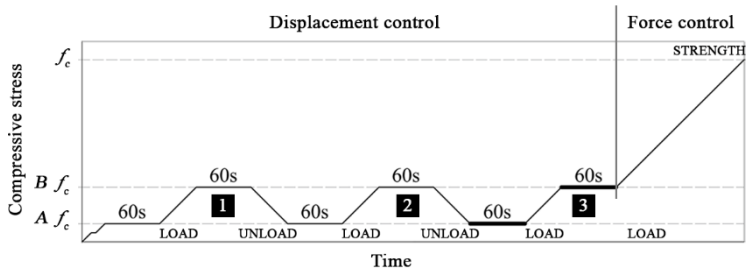

Fig. 40 Diagrammatic representation of the stress-time relationship of the load/unload procedure with three load/unload cycles denoting the minimum and maximum stress averages considered for the calculation of the elastic modulus.

V.2.4.1. Experimental testing setup calibration

The elastic modulus was determined ascertaining the slope of the line that connects two specific points on the stress-strain curve, referred to as the secant modulus (or chord modulus according to ASTM). There are currently no established standards or recommendations for determining the elastic modulus of the masonry units, except the in the Leaflet 778-3R [1] of the International Union of Railways (UIC). The Leaflet 778-3R [1] proposes to derive the elastic modulus from the secant modulus in the range 25% f_c to 75% f_c. To identify suitable nominal maximum and minimum stress levels for the elastic modulus test, the guidelines outlined in the American ASTM, the European EN, and the Basilian ABNT standards for concrete and stone were taken as a reference. For concrete specimens, the ASTM C469/C469M-22 [188] fixed the lower stress at 50 millionths the strain at compressive strength, f_c, while the upper stress is set at 40% f_c. The EN 12390-13:2022 [190] proposes two methodologies, with Method A recommending a lower stress level on 0.5 MPa, and Method B recommending a lower stress level between 10% f_c and 15% f_c. In both methodologies, the upper stress level is recommended to be set at 30% f_c. The ABNT NBR 8522:2017 [192] recommends the same stress levels than EN 12390-13:2022 [190] Method A, from 0.5 MPa to 30% f_c. For stone specimens, ASTM D7012-14e1 [189] provides several methods for calculating the elastic modulus. These include utilizing the tangent modulus at 50% f_c, and the secant modulus between undetermined stress levels, but with illustrative proposals with the ranges of 25% f_c to 50% f_c, and 40% f_c to 60% f_c. The EN 14580:2006 [191] recommends stress levels from 2% f_c to 30% f_c. All the stress levels recommended by the reference standards are summarized in Table 20.

Different approaches have been proposed for the stress ranges used in the characterization of the secant modulus in solid clay bricks. Among the proposed ranges are: 5% - 30% f_c by Kaushik et al. [197], 10% - 30% f_c by Pelà et al. [193], 15% - 85% f_c by Totoev

et al. [198], 30% - 60% f_c by Pelà et al. [193] and Binda et al. [109], 30% - 50% f_c by Winnicki et al. [194], 30% - 70% f_c by Oliveira et al. [79], and 40% - 60% f_c by Drougkas et al. [195]. Therefore, no single criterion is available for determining the upper and lower percentages of stress. Table 20 includes the referenced scientific literature.

Due to the lack of consensus in the determination of the range of stress levels, four maximum and minimum loading setups were analysed. The considered setups in this research were 2% - 30%, f_c, 5% - 30%, f_c, 10% - 30% f_c, and 30% - 60% f_c. Table 20 also shows the proposed loading setups.

Table 20 Lower and Upper stress levels on the load/unload setup recommended by concrete and stone standards, proposed in the scientific literature and considered in this research

Load and Unload stress level references		
Reference	Stress level	
	Lower	Upper
Standards		
UIC Leaflet 778-3R [1]	25% f_c	75% f_c
ASTM C469/C469M-22 [188]	At 50 millionths the strain at f_c	40% f_c
EN 12390-13:2022 [190], Method A	0.5 MPa	30% f_c
EN 12390-13:2022 [190], Method B	10% f_c to 15% f_c	30% f_c
ABNT NBR 8522:2017 [192]	0.5 MPa	30% f_c
ASTM D7012-14e1 [189]	25% f_c 40% f_c	40% f_c 60% f_c
EN 14580:2006 [191]	2% f_c	30% f_c
Reference on scientific literature		
Kaushik et al. [197]	5% f_c	30% f_c
Pelà et al. [193]	10% f_c 30% f_c	30% f_c 60% f_c
Totoev et al. [198]	15% f_c	85% f_c
Binda et al. [109]	30% f_c	60% f_c
Winnicki et al. [194]	30% f_c	50% f_c
Oliveira et al. [79]	30% f_c	70% f_c
Drougkas et al. [195]	40% f_c	60% f_c
Considered by researcher		
Stress levels loading setup	2% f_c 5% f_c 10% f_c 30% f_c	30% f_c 30% f_c 30% f_c 60% f_c

V.3. Experimental results

This section presents the experimental results on the compressive strength and elastic modulus of solid fired clay brick specimens. The elastic modulus was obtained with the analysis of the strain raw data acquired by the three vertical transducers using the developed checks set out in Makoond et al. [12].

Table 21 presents the compressive strength and elastic modulus values obtained for specimens with different shape, i.e., cross-section and slenderness. Table 22 presents the elastic modulus measured by testing under the four stress levels proposed, while Table 23 reports the large-scale experimental campaign carried out on 'Ex', 'Hy', 'Mo', 'Hi/I' and 'Hi/R' bricks.

Table 21 Number of samples (N.) and average compressive strength (f_c) and elastic modulus ($E_{b\ 10\text{-}30}$) of the tested specimens with different shapes, i.e., cross-section and slenderness. Values in brackets correspond to the coefficient of variation

Specimens for shape influence					
	Specimen		N.	f_c (MPa)	$E_{b\ 10\text{-}30}$ (MPa)
'Mo$_3$'	40 × 40 × 80 mm^3	length	3	10.9 [16.1%]	6872 [28.9%]
		width	3	22.2 [16.6%]	7749 [30.7%]
	Ø37 × 80 mm^3	length	4	17.0 [29.9%]	7087 [29.7%]
		width	2	9.0 [14.6%]	5974 [35.4%]
	Ø37 × 40 mm^3	thickness	4	10.4 [4.6%]	3926 [55.9%]
	40 × 40 × 40 mm^3	thickness	4	13.6 [3.3%]	4677 [18.2%]
'Mo$_1$'	40 × 40 × 80 mm^3	length	18	11.6 [29.5%]	3566 [33.4%]
		width	23	11.5 [21.6%]	3774 [42.8%]
	40 × 40 × 40 mm^3	length	6	10.5 [15.1%]	3566 [32.8%]
		width	6	10.1 [18.4%]	3784 [66.7%]
		thickness	6	11.9 [19.6%]	1501 [61.8%]
'Ex'	40 × 40 × 80 mm^3	length	18	53.2 [7.9%]	12740 [18.8%]
		width	18	47.1 [13.3%]	10260 [13.3%]
	40 × 40 × 40 mm^3	length	6	51.0 [13.9%]	23494 [45.2%]
		width	6	50.6 [7.0%]	20953 [37.0%]
		thickness	6	45.7 [7.3%]	23921 [30.9%]

Table 21 presents for 'Mo$_3$' the values for two cross-sections, circular and square, along length, width, and thickness. Table 21 also presents for 'Mo$_1$', 'Ex' specimens the values for two slenderness, 1 and 2, and also along length, width, and thickness. The elastic modulus of the 'Mo$_1$' specimens exhibited limited variability with slenderness ratios of 1 and 2, ranging from 3566 MPa to 3784 MPa. In contrast, the 'Ex' specimens exhibited higher elastic modulus values, ranging from 23494 MPa to 10260 MPa. The elastic modulus of the 'Ex' specimens presented difference between slenderness ratios of 1 and 2. The elastic modulus for the slenderness ratio of 1 was almost double that of the respective slenderness ratio of 2 specimens. The lowest coefficients of variation (CV) were obtained testing the 40 × 40 × 80

mm³ and Ø37 × 80 mm³ specimens, i.e., slenderness 2. The significant CV observed in the elastic modulus of specimens with slenderness 1 can be attributed to the influence of the external factors, i.e., the confinement. This effect, as observed by Binda [199], is due to the confinement against lateral expansion caused by the friction between the specimen and the press platens. The confinement effects can be detected by the proximity of the vertical clamped transducer to the limits of the specimen.

Table 22 presents the influence on the elastic modulus, E_b, of the stress levels considered in the load/unload compressive stress cycles. The load ranges up to 30% f_c were obtained from a single 'Mo$_3$' brick, while high load range, i.e., 30% f_c to 60% f_c was carried out by testing 'Ex' and 'Mo$_1$' specimens. While all three proposed ranges (2% f_b to 30% f_b, 5% f_b to 30% f_b, and 10% f_b to 30% f_b) for measuring the compressive strength of handmade brick samples are considered valid, the range of 10% to 30% f_b will be adopted for the following research. The use of lower ranges, such as 2% f_b or 5% f_b, may require the application of low loads during testing, which can increase the output errors of the hydraulic press data acquisition or strain clamp-on transducers. The experimental findings suggest that the range of 30% to 60% f_c results in higher mean values of elastic modulus (E_b) when compared to the range of 10% to 30% f_c for modern handmade brick samples 'Mo$_1$'. However, the elastic modulus of mechanically extruded samples 'Ex' remains relatively unchanged across both ranges. It is worth noting that subjecting the specimens to a load exceeding 60% f_c can cause deformation, thereby affecting the integrity of the results.

Table 22 Number of samples (N.) and average compressive strength (f_c) and elastic modulus (E_b) of the tested specimens with different testing stress level proposed. Values in brackets correspond to the coefficient of variation

Specimens for stress levels proposed						
Specimens		f_c (MPa)	E_b (MPa)			
			2% - 30% f_c	5% - 30% f_c	10% - 30% f_c	30% - 60% f_c
'Mo$_3$'	length	15.1 [8.9%]	5197 [2.7%]	5348 [6.1%]	5172 [9.3%]	-
'Mo$_1$'	length	11.6 [29.5%]	-	-	3566 [33.4%]	4209 [29.6%]
	width	11.5 [21.6%]	-	-	3773 [42.8%]	4298 [36.2%]
'Ex'	length	53.2 [7.9%]	-	-	12740 [18.8%]	12971 [16.5%]
	width	47.1 [13.3%]	-	-	10260 [13.3%]	10486 [13.7%]

Table 23 presents the results of the large-scale experimental campaign on the measurement of the compressive strength and elastic modulus carried out on mechanically extruded 'Ex', hydraulic press mould 'Hy', modern 'Mo' and historical 'Hi' handmade bricks. The experiments involved the use of specimens with square cross-section and slenderness 2, and a testing setup that applied stress levels ranging from 10%% to 30% f_c. The compressive strength and elastic modulus were tested along the brick length and width. The CV obtained in the measurement of the elastic modulus were both 15% for 'Ex', 7.3% and 8.5% for 'Hy', between 20% and 29% for 'Mo', and between 9.9% and 35.6% for 'Hi'. The higher variations

in historical bricks is due to the large inhomogeneity caused by their non-industrialised manufacturing. Mechanically extruded and Hydraulic press moulded bricks exhibit higher average elastic modulus than both modern and historical handmade types. Section V.4 presents an empirical correlation between the compressive strength and elastic modulus and also analyses the effect of the specimen's anisotropy on the elastic modulus.

Table 23 Number of samples (N.) and average compressive strength (f_c) and elastic modulus ($E_{b\,10\text{-}30}$) of the tested specimens along the length and width in a large experimental campaign. Values in brackets correspond to the coefficient of variation

Specimens from large experimental scale				
Specimen		N.	f_c (MPa)	$E_{b\,10\text{-}30}$ (MPa)
'Ex' Mechanically extruded	length	18	50.3 [10.6%]	13072 [15.1%]
	width	18	50.1 [6.8%]	11499 [15.5%]
'Hy' Hydraulic press mould	length	15	53.9 [7.1%]	15962 [7.3%]
	width	20	55.3 [11.9%]	16669 [8.5%]
'Mo_2' Modern handmade	length	18	19.4 [19.1%]	8148 [20.4%]
	width	24	19.5 [19.6%]	7643 [21.7%]
'Mo_3' Modern handmade	length	21	18.1 [18.7%]	6343 [28.8%]
	width	28	17.2 [22.0%]	5608 [24.0%]
'Hi/I_1' 1910-20 Industrial	length	10	10.2 [23.8%]	5668 [27.7%]
	width	11	11.2 [20.8%]	5692 [18.5%]
'Hi/I_2' 1927 Industrial	length	6	16.3 [21.3%]	7851 [34.2%]
	width	5	14.8 [36.8%]	6437 [20.5%]
'Hi/R_1' 1880 Residential	length	12	12.1 [24.1%]	5999 [33.9%]
	width	9	13.6 [14.5%]	6730 [14.8%]
'Hi/R_2' 1930 Residential	length	27	9.2 [27.9%]	5158 [35.6%]
	width	6	8.7 [14.9%]	4876 [25.8%]
'Hi/R_3' 1930 Residential	length	18	9.2 [27.0%]	5730 [9.9%]
	width	11	9.3 [22.4%]	6213 [21.5%]

The failure modes observed in the different specimen types exhibit an hourglass shape, as evidenced by the samples shown in Fig. 41, resulting in complete separation of the outer regions. This spalling of the outer regions was initiated by the overlapping cones of influence that extended from the bearing surface As observed by RILEM TC 148-SSC [133] and Vliet et al. [180], cracks propagation typically occurs in the confined regions, and the hourglass failure mode is commonly observed in the confined specimen. The acceptability of the failure modes was assessed using established concrete standards, specifically EN 12390-3:2020 [82] for specimens with circular cross-section and with square cross-section with slenderness 1, and ASTM C39/C39M-21 [8] for specimens with square cross-section and slenderness 2. EN 12390-3:2020 [82] provides a series of schematic drawings indicating satisfactory and unsatisfactory failure modes. ASTM C39/C39M-21 [8] failures into five types, namely cone, cone and split, cone and shear, shear and columnar. Fig. 41 presents the failure modes obtained in mechanically extruded ('Ex'), hydraulic press moulded ('Hy'), modern handmade

('Mo'), and historical handmade ('Hi/I_1'). The failure modes of the 'Ex' specimens show the fractures of the failure predominantly in corresponding bed brick faces. The types of failure identified in 'Ex' specimens are mainly cone and split, cone and shear, and columnar failures being less frequently observed (Fig. 41a). The failure modes observed in the 'Hy' specimens only occurs in faces that do not correspond with the bed brick faces. The failures identified in 'Hy' correspond only to columnar failures (Fig. 41b). The failure modes observed in the 'Mo' specimens predominantly involve fractures in faces that do not correspond to the bed brick faces and rarely occur in bed brick faces. The identified failures in 'Mo' specimens mainly consist of cone, cone and split, and cone and shear (Fig. 41c). The failure modes observed in the 'Hi' specimens involve the four faces. The failures in 'Hi' specimens mainly consist of cone, cone and split, and cone and shear (Fig. 41d).

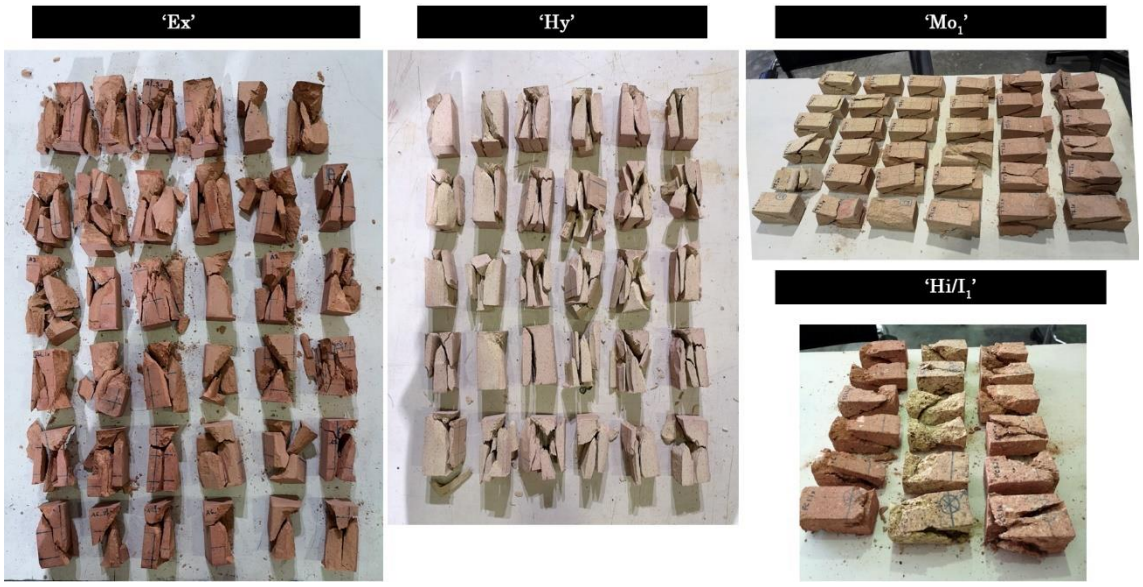

Fig. 41 Failure modes in 40 × 40 × 80 mm³ specimens form mechanically extruded bricks 'Ex', hydraulic press moulded 'Hy', modern handmade 'Mo', and historical handmade form 1910-20 industrial building 'Hi/I_1'. The 'Ex', 'Mo$_1$' and 'Hi/I_1' specimens are displayed with their corresponding bed brick faces facing upwards, while 'Hy' specimens are displayed with their corresponding bed brick faces turned over.

V.4. Discussion

This section presents two different studies based on the experimental results described in Section V.3. The first study focuses on the anisotropy of the material and the influence of the brick direction on the resulting elastic modulus. The second study focuses on the experimental correlation among compressive strength and elastic modulus.

The calibration of the test procedure, as outlined in Section V.2 and Section V.3, consisted in tests on unstacked 40 × 40 × 80 mm³ specimens with grinded bearing surfaces along the length or width in a hydraulic press. The strain was controlled and measured by positioning vertical clamp-on transducers that were mounted on an external support

specifically designed for this test. The test was carried out in two phases. Firstly, the test was executed under displacement control and three load/unload cycles were performed. The minimum and maximum stress level were determined based on 10% and 30% of the compressive strength of the sample type. Each stress level was maintained for a duration of 60 seconds prior to loading or unloading. Secondly, the test was executed under force control until the maximum stress was reached.

V.4.1. Study on anisotropy

The experimental campaign on 40 × 40 × 80 mm³ specimens allowed the comparison of the elastic modulus in the two brick orientations, i.e., length and width. This study has been performed on the mechanically extruded 'Ex', hydraulic press moulded 'Hy', modern handmade 'Mo', and historical 'Hi' specimens.

In fact, and as shown in Table 23 (Section V.3) and in Fig. 42, close values were found in each group for the two brick orientations. Fig. 42 depicts a boxplot that displays the distribution of data based on quartiles. The second and third quartiles are represented by boxes, which are shaded. The median is indicated by a horizontal line inside the box, while the average is represented by a cross. As shown in Fig. 42, the boxes of 'Ex' indicate distinct populations, with values measured along the length being higher than those measured along the width. However, handmade ones, whether modern or historically manufactured, display boxes with similar values, including in most instances close maximum and minimum values.

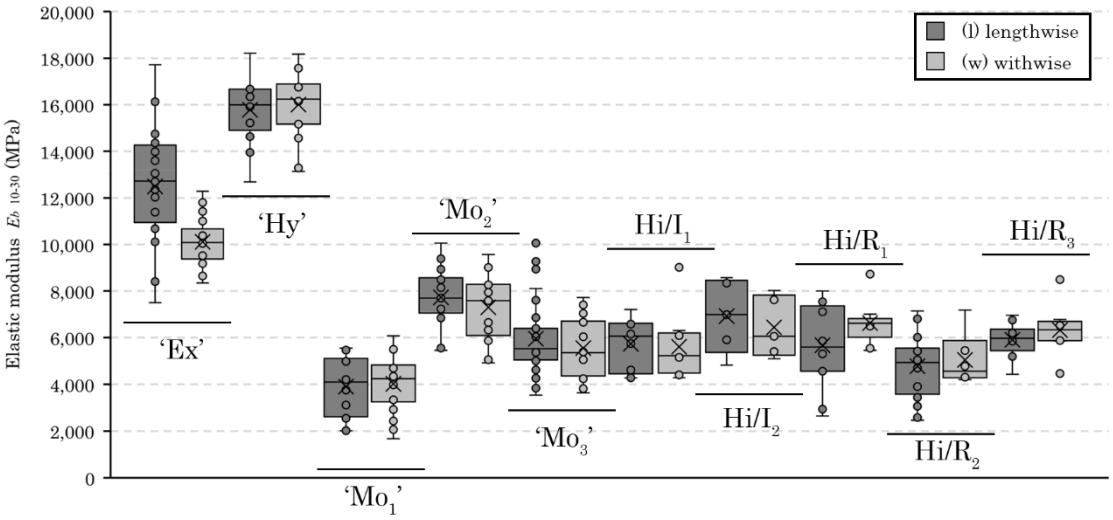

Fig. 42 Boxplot with lengthwise and widthwise elastic modulus (E_b) for the 'Ex', 'Hy', 'Mo', 'Hi/I', and 'Hi/R' specimens. Inside the boxes, the medians are represented with a horizontal line and the average are reproduced with an X

As proposed by Cabané et al. [103], the anisotropy of the 'Ex' and 'Mo' brick types was investigated through a statistical analysis. Fig. 43 displays the resulting histograms and probability distribution functions obtained for the 'Ex', 'Mo$_1$', 'Mo$_2$', and 'Mo$_3$' groups. The

histograms generally exhibit symmetrical distributions with no apparent skewness, but with an evident difference in kurtosis for 'Ex' specimens tested along the width.

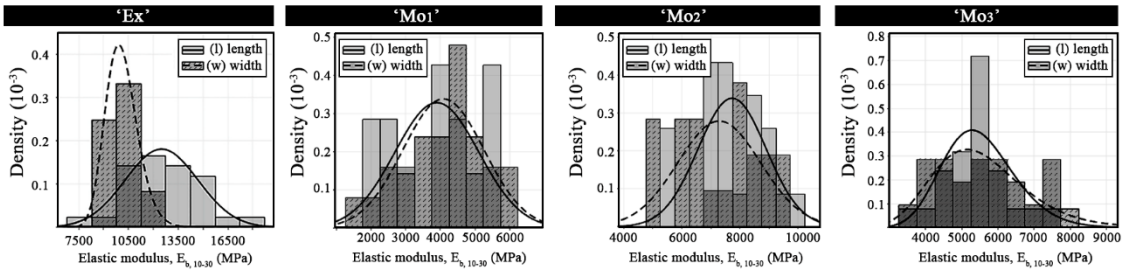

Fig. 43 Histograms and statistical distributions for the tested specimens

To identify significant differences in strength among loading orientations and confirm the observed influence in Fig. 42 and Fig. 43, a statistical evaluation was performed. A non-parametric analysis was employed as suggested by Cabané et al. [103], since the data could not be fitted to a normal distribution. The non parametric Mann-Whitney test [200] was used for this purposed. The Mann-Whitney test [200] is a statistical method that compares two data sets to determine whether the values of one data set are significantly greater than, lesser than, or equal to the values of the other data set. This test identifies that the elastic modulus of the 'Ex' specimens along the width was lesser than the elastic modulus along the length. In contrast, the 'Hy', 'Mo', 'Hi/I', and 'Hi/R' specimens did not exhibit any significant difference in elastic modulus for the two orientations, i.e., along the length and width. This phenomena was also observe by Makoond et al. [92] testing the dynamic the dynamic elastic properties of the bricks, and by Cabané et al. [103] studying the anisotropy on 40 mm edge specimens from solid clay bricks.

V.4.2. Empirical correlation among compressive strength and elastic modulus

An experimental correlation has been established between the elastic modulus and the compressive strength of the tested samples. Fig. 44 shows the experimental relationship between the compressive strength values and the elastic modulus. Each specimen tested, differentiated by tested along the length and along the width, is represented as a data point on the graph. The proposed trend line does not incorporate the 'Ex' specimens, due to their anisotropic behaviour identified in Section V.4.1. Additionally, Fig. 44 shows the relationships depending on the loading orientations. These figures also do not include the 'Ex' specimens in the trend lines.

Two trend lines were found to better fit the experimental data, linear and power trend line. The correlation coefficient was 0.94 and 0.87 respectively. The linear trend line is represented by equation (1), while the power trend line is represented by equation (2). Upon analysing the trend lines individually based on the orientation of the load, i.e., tested along

the length and width, it was observed that the resulting equations exhibited a high degree of similarity. Equations (1.1) and (1.2) depict the trend lines while equations (2.1) and (2.2) represent the power trend lines, both obtained from individual analyses based on the load test orientation.

General lineal trend line:

$$E_b = 324 \cdot f_c \quad (1)$$

Lineal trend line along length and along width:

$$E_{b\ length} = 332 \cdot f_c \quad (1.1)$$

$$E_{b\ width} = 320 \cdot f_c \quad (1.2)$$

General power trend line:

$$E_b = 927 \cdot f_c^{0.69} \quad (2)$$

Power trend line along length and along width:

$$E_{b\ length} = 1046 \cdot f_c^{0.66} \quad (2.1)$$

$$E_{b\ width} = 986 \cdot f_c^{0.67} \quad (2.2)$$

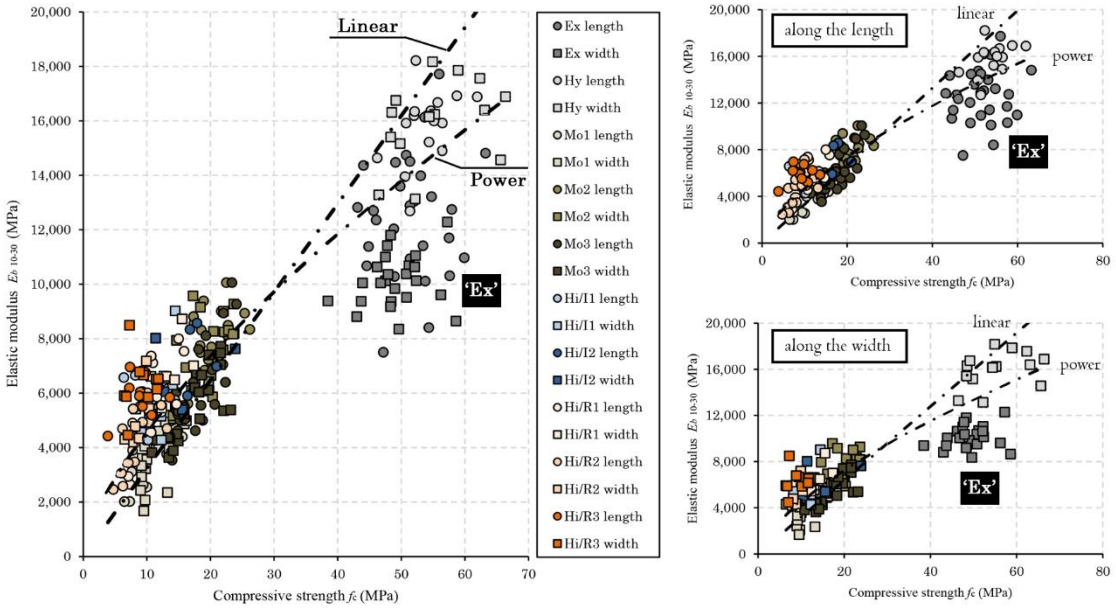

Fig. 44 Empirical correlation among compressive strength and elastic modulus in brick specimens: 'Ex', 'Hy', 'Mo_2', 'Mo_3', 'Hi/I', and 'Hi/R' tested along the length and width. Linear trend line excluding 'Ex' specimens (left). Empirical correlation of specimens along the length excluding 'Ex' from the trend line (right up). Empirical correlation of specimens along the width excluding 'Ex' from the trend line (right down)

Neville [59] evidenced that, for concrete, the modulus of elasticity increases as the compressive strength of concrete increases. However, there is no consensus on the exact nature of this relationship. The scientific literature proposes different empirical relationships between the compressive strength and the elastic modulus. The UIC Leaflet 778-3R [1] suggests the elastic modulus of brick specimens as 50% greater than the average tensile value

obtained via bending procedures. The ACI 318-19 [201] for concrete suggest the equation $E_b = 4700 \cdot \sqrt{f_c}$. Other empirical relationships for brick masonry are provided by ACI 530/530.1-13 [202] and EN 1052-1:1999 [203]. The ACI 530/530.1-13 [202] suggests equation $E_{k\_ACI} = 700 \cdot f_{k\_ACI}$, while EN 1052-1:1999 [203] suggests $E_{k\_EN} = 1000 \cdot f_{k\_EN}$. Only two references were found in the scientific literature concerning the relationship between the compressive strength and elastic modulus of clay bricks. Hilsdrof [186] reported that Glanville and Barnett published an empirical relationship in 1934, which expressed the elastic modulus of clay bricks as $E_b = 300 \cdot f_c$ in terms of their compressive strength. Kaushik et al. [187] conducted a study on four different types of bricks by analysing ten whole brick samples for each type following the ASTM C67-00 [47] and IS 3495 (IS 1992a) [154] recommendations. Kaushik et al. proposed the experimental correlation $E_b \approx 300 \cdot f_c$. However, the observed data exhibit a significant scattering beyond the correlation limits, with the limits estimated to be between $150 \cdot f_c$ and $500 \cdot f_c$. Fig. 45 includes the experimental results published by Drougkas et al [195], Oliveira et al. [79], Binda et al. [109],and Pelà et al. [193] testing handmade bricks using different specimens configuration and test procedure. Remarkably, the values reported by these authors are situated below the trend line, both for the linear and power models.

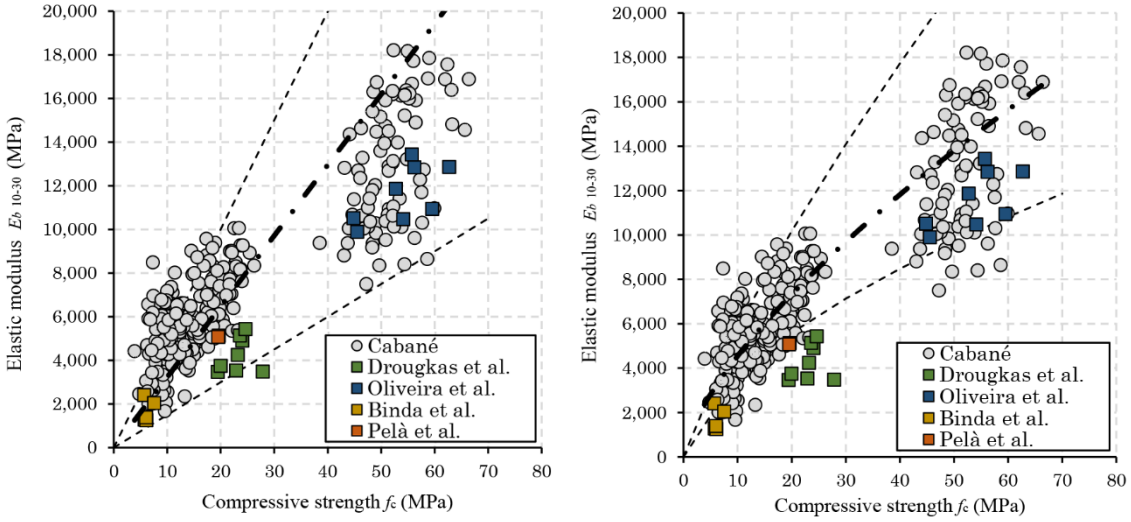

Fig. 45 Empirical linear (left) and power (right) correlation among compressive strengths and elastic modulus in solid clay bricks, including trend lines and estimated trend limits. The graph includes additional experimental data from available scientific literature

Fig. 45 also features secondary lines that encompass the limits of the experimental values. The linear trend line exhibits elastic modulus values for handmade bricks slightly above the trend line, whereas values for industrially manufactured bricks, both 'Ex' and 'Hy', are located below it. The proposed by Kaushik et al. [187], which suggest that the relationship limits between the elastic modulus and compressive strength fall within the range of 150 to 500 times the compressive strength, has been chosen for the limits. The power trend line

considering the secondary lines yields a more robust alignment to the general trend of the individual experimental values obtained. The adoption of the power trend line reduces the range of uncertainty for the higher values of compressive strength and elasticity. The lines that establish the limits, as previously mentioned, have resulted in a variation of the exponent from 0.69 to 0.8 and 0.7.

A correlation has been determined between the compressive strength and the elastic modulus for 40 × 40 × 80 mm^3 specimens. As expected, the specimens with the highest compressive strength values exhibit the highest elastic modulus values. The relationship among elastic modulus and compressive strength can be modelled with either a linear or power form correlation, both of which fit well for the lower values. The range of experimental elastic modulus values obtained was from 1600 to 18300 MPa.

V.5. Conclusions

This paper has presented a test setup for the elastic modulus testing of solid fired clay bricks commonly used in the construction of masonry walls. The new test setup was validated through the experimental campaign on mechanically extruded, hydraulic press moulded, modern and historical handmade bricks, the latter extracted from five 19th and early 20th century buildings in Barcelona (Spain). The following conclusions can be drawn from the experimental procedures and the analysis of the experimental results:

- An effective and straightforward procedure can be implemented to extract historical bricks from existing walls. Common electric tools can be employed, such as a jackhammer to remove the plaster, together with manual chisel and a nylon hammer for the careful extraction of the bricks.
- Testing 40 × 40 × 80 mm^3 specimens, i.e., square cross-section specimens with slenderness 2, using an on-purpose developed support for clamp-on transducers has proved to be an advantageous technique for the evaluation of the elastic modulus of solid fired clay bricks. A detailed testing procedure has been formalized for this purpose. It is suggested to test at least a set of six specimens extracted from different bricks to obtain a reliable estimation of the elastic modulus.
- It has been observed that the failure modes of the 40 × 40 × 80 mm^3 specimens depend on the brick manufacture. Different brick types show fracture in different faces with respect to the bed one
- The study shows that the mechanically extruded solid fired clay bricks investigated present anisotropy in terms of their elastic properties due to their manufacturing process. The smallest elastic modulus is obtained along the width. This observation is consistent with the already mentioned anisotropy observed on the compressive strength and the observations from previous scientific publications. However, an

almost isotropic behaviour has been obtained for the hydraulic press moulded, modern handmade, and historical handmade bricks herein investigated.

- The experimental results indicate that the most effective approach for assessing the elastic modulus of solid fired clay bricks involves the use of specimens with grinded bearing surfaces and with slenderness equal to 2. Such specimens minimize the influence of the confinement, leading to more precise strain measurements.
- The experimental results show a clear relationship between the compressive strength value and elastic modulus. The scientific reference and the experimental research provide the $E_B = 300 \cdot f_c$ correlation, where E_b is the elastic modulus of the brick, and f_c is the compressive strength of the tested specimen. However, the experimental trend line $E_b = 927 \cdot f_c^{0.69}$ with the estimated trend limits shows a better relationship. The experimental correlation does not include the mechanically extruded bricks.

Future research could expand upon the experimental database to include a larger sample of solid clay bricks. Additionally, a more detailed study of the potential impact of porosity on the elastic modulus and anisotropy could be conducted. Furthermore, to investigate the elastic modulus across the thickness, stacked specimens could be employed. The values of stacked and unstacked specimens could be compared in specimens tested along three orientations, i.e., length, width, and thickness.

Chapter 3

Calibration of MDT

3.1. Introduction

The procedures to characterize structures can be classified in Destructive Tests (DT), Minor Destructive Tests (MDT), and Non-Destructive Tests (NDT).

Destructive Tests (DT) consists of testing structural elements until bringing them to failure to define their mechanical behaviour. This method includes the destruction of the specimens to determine chemical and mechanical properties. Mechanical properties can be tested using different types of loads or tests setups such as tension, compression, shearing, torsion, bending or buckling. Compressive test determines the material stress-strain behaviour under compressive strength loads. The compressive stress-strain behaviour allows to determine elastic modulus, yield point, compressive strength, and fracture energy, among others. Tensile test determines the yield strength and the tensile strength. Tensile strength can also be determined by indirect methods tests as bending and shearing.

Minor Destructive test Test (MDT) are defined as: "*Tests in which there is sufficient mechanical interaction between the test device and the building or building element to both cause change which is visible to the naked eye and to produce useful structural data but which do not pose any threat to the structural stability of the building or element nor cause any irreparable aesthetic damage.*" [204]. Different test methodologies and procedures exist to test in-situ the material properties. The most common MDT are the flat jack, both single and double; the extraction of small samples such as cylinders core drilling masonry, mortar joints, bricks; pull-off; pull-out; sclerometers; and penetrometers.

Non-destructive tests (NDT) can be defined as an examination or test carried out in a structural element without changing or altering the element with the objective to determine or estimate the geometry, the configuration of the structural elements, the presence of structural damage, discontinuities, among others. The most common methods are based in

the propagation of sonic and electromagnetic waves such as radars, ultrasonics, impact-echo, ultrasonics and sonic thermography, among others.

The proper calibration of NDT and MDT is crucial in reducing the amount and size of samples collected from existing masonry building. This is especially important when characterizing masonry structures with historical significance or cultural value. By minimizing the amount of destructive testing, the heritage can be preserved while still obtaining accurate data on their properties. Proper calibration ensures that we can achieve a balance between preservation and scientific research.

3.2. Paper VI – Laboratory and in-situ mechanical characterisation of masonry components by comparing destructive and minor destructive tests techniques

A. Cabané, L. Pelà, P. Roca

Journal of Building Engineering (2023)

Under review

Abstract. This paper is a review of some potential techniques for in-situ evaluation of the properties of masonry components by using minor destructive testing (MDT) techniques. The results derived from MDT were empirically correlated with the compressive strength obtained by using well-known destructive testing (DT) techniques executed in the laboratory. The experimental campaign focused on two different MDT techniques, the Pin Penetration Test (PPT) and the Helix screw Pull-out Test (HPT). The PPT is based on the measurement of the depth of penetration of a steel pin to assess the compressive strength. The HPT is based on the measurement of the pull-out load necessary to extract a steel tie inserted into a hole drilled in a brick or mortar joint. The experimental campaign also includes the validation of the Double Punch Test (DPT), comparing the results with the strength obtained from specimens following EN 1015-11/A1. The experimental results highlight the relation between the MDT measurements and the compressive strength obtained by DT. Although both the PPT and HPT are useful for the evaluation of the compressive strength of masonry components, the former exhibits a lower dispersion than the latter in the experimental results.

VI.1. Introduction

The cultural architectural heritage plays a vital role in defining the identity of a society, reflecting its history, traditions, and values. It encompasses a wide range of structures, from grand palaces and monuments to humble dwellings and vernacular buildings, which have been passed down from generation to generation. However, the preservation of this heritage is not always straightforward, as buildings and sites are often subject to environmental actions and human factors that cause degradation or alteration. In response to this challenge, the International Scientific Committee on the Analysis and Restoration of Structures of Architectural Heritage (ISCARSAH) published a set of intervention recommendations in 2003 [205,206]. These recommendations provide guidance on the appropriate methods and techniques for the conservation, restoration, and rehabilitation of cultural architectural heritage. They emphasize the need to balance the

preservation of original material and techniques with the practical demands of contemporary use and safety requirement. One crucial aspect of the conservation process is the characterisation and analysis of historical masonry, which involves the evaluation of the materials properties, construction techniques, and structural behaviour of the buildings. Some different techniques exists to evaluate the properties, i.e., Destructive Testing (DT), Minor Destructive Testing (MDT), and Non-Destructive Testing (NDT). Less invasive techniques, such as MDT and NDT, are recommended to preserve the building heritage, since DT involves the extraction of masonry components or large samples of masonry to be tested destructively that can result in significant damage to the building.

MDT techniques are increasingly recognized as a valuable tool for the characterisation and analysis of masonries. There is a wide range of testing equipment available to evaluate the condition of a building [207] causing little damage to the existing structure. Brick and mortar, as individual components, can be assessed by means of penetration methods, pull-out tests, break-off tests, surface hardness test, and ultrasonic and impact-echo test [207,208]. Calibrating MDT with DT is essential for obtaining accurate and reliable results in the characterisation of existing masonry. This calibration involves selecting representative samples for MDT that can be compared with the results obtained by DT. The comparison of MDT and DT results can reveal any discrepancies or limitations in the MDT techniques, allowing the adjustment of the methods accordingly. The calibration is also important for ensuring the reproducibility and reliability of the results. It allows the establishment of a standardized methodology that can be applied consistently across different buildings and contexts.

This research focuses on the use of the Pin Penetration Test (PPT) and the Helix screw Pull-out Test (HPT) as MDT methods. The principles of the PPT, developed in USA, are that the depth of penetration of a steel pin gives an indication of compressive strength. Vekey [209] explained that the Windsor probe was tried by Albrecht and Engelke in 1964 and followed by the BRE Group. According to Vekey [209], BRE Group abandoned the research since the four lime and aerated mortars types tested had a poor relationship with the PPT. However, the average values presented by the BRE Group show the influence of the moisture present in the samples to characterize the compressive strength by the experimental DT test and the PPT. Other research on penetration tests, such as Felicetti et al. [210], are related to the number of impacts required to drive the pin, usually 5 mm. The principles of the HPT, developed in UK, is that the pull-out load of a self-tapping stainless steel tie inserted in a hole drilled into masonry brick or mortar joint, gives indications of the compressive strength. Vekey [209] presented the PPT in 1991 as a simple and promising test, although the results showed a high variability. Later, Ferguson et al. [211] and Ferguson [212] suggested that the method was viable for strengths in the range between 2 and 10 MPa and improved the test methodology. Vekey [213] offered the calibrated reference curve relating the compressive strength of the mortar to the pull-out force of the helix in 1997.

Finally, in BRE Group [214] and RILEM 127 MS D.9 [215] published the methodology of the test, indicating a non-linear relationship between the compressive strength and the pull-out force. The MDT results were compared with the compressive strength derived from DT on bricks and mortar joints by testing brick specimens following the European standard EN 772-1:2011+A1:2016 [9] and mortar joint specimens following the Double Punch Test (DPT) described in the DIN 18555-9:2019-04 [2] and in International Union of Railways (UIC) Leaflet 778-3R [1]. Pelà et al. [45,193] also calibrated PPT and HPT by comparison with DPT results on lime mortar joints extracted from walls built in the laboratory to replicate historical masonry.

This research offers the results of an extensive experimental campaign including bricks and mortar joints of 8 different masonry walls of 7 existing historical buildings in the city of Barcelona (Spain), and two types of masonry walls built in the laboratory. The campaign includes the execution of DT of 125 brick and 398 mortar joint specimens in the laboratory, and 398 PPT and 343 HPT in-situ MDT tests. The research encompasses the following specific objectives: (1) exploring the capability of the DPT test to determine the compressive strength of mortars, (2) calibrating an empirical correlation among compressive strength and penetration depth using PPT, and pull-out strength using HPT.

This paper is structured in five sections. After this introduction, Section VI.2 presents the experimental campaign performed on brick units and mortar joints, including the description of the material, the specimen preparation, and the test procedure. Section VI.3 presents the experimental results. Section VI.4 analyses the influence of the DPT test on the determination of the compressive strength of mortars, and the calibration of an empirical correlation among compressive strength and MDT methodologies proposed, i.e., PPT and HPT. The paper ends with Section VI.5 presenting some conclusions and future works.

VI.2. Experimental study

This section presents the experimental campaign executed on masonry components, corresponding to (1) solid fired clay bricks, both mechanically extruded and modern handmade, and (2) lime and cement mortar joints. The handmade manufactured bricks include both modern and historical bricks, the latter collected from existing buildings. The mortar includes joints from wall specimens produced in the laboratory, and joints from existing buildings. Details are provided on the description of the materials, the preparation and geometry of the proposed laboratory specimens, and the laboratory and in-situ testing setup. As mentioned, the historical samples (bricks and mortar joints) were tested and collected from historical buildings, including four residential ones and three industrial structures in Barcelona, Spain. Four of these building were built in the early 20th century and the other three were built in the 19th century. One of the industrial building from the 19th century includes a 20th century building extension. All experimental MDTs were carried

out in-situ in the historical building, and the DTs were carried out at the Laboratory of Technology of Structures and Materials of the Technical University of Catalonia (UPC-BarcelonaTech).

VI.2.1. Materials

This research studies solid fired clay bricks and mortar joints from masonry structures. First, solid fired clay units manufactured according to two different procedures were considered. The first type of bricks, corresponding to modern clay ones produced by mechanical extrusion, are identified herein with the acronym B_'Ex'. The second type of bricks includes handmade modern and historical solid fired clay units. The modern handmade ones are identify with the acronym B_'Mo', and the historical ones collected from existing masonry walls are identified with the acronym B_'Hi'. Second, mortar joints were considered as manufactured with two different binders either produced in laboratory or collected from historical buildings. The first type corresponding with lime mortar joints are identified with the acronym MJ_'L', and the second ones, manufactured with cement are identified with the acronym MJ_'C'. The specimens from historical buildings include the 'Hi' in the acronym such as MJ_'L'_'Hi' and MJ_'C'_'Hi'.

The mechanically extruded and modern handmade solid clay bricks were used to manufacture masonry walls in the laboratory. Two types of walls were produced. First type of walls was built using handmade bricks (B_'Mo') and lime mortar (MJ_'L') to replicate a historic masonry. For more information on these specimens, the reader is referred to the research by García-Ramonda et al. [216]. Second type of wall was built using mechanically extruded bricks (B_'Ex') and cement mortar (MJ_'C') to replicate 20th century masonry structures. To obtain further details about these specimens, readers are directed to the study conducted by Huang et al. [217]. The historical solid clay bricks and mortar joints were collected from seven different masonry walls from six buildings, following the RILEM recommendations LUMD1 for removal and testing of specimens extracted from existing buildings [83]. The historical bricks and mortar joints collected from the industrial building are identified with the acronyms 'Hi/I', while the ones taken from residential buildings are identified with the acronyms 'Hi/R'. Fig. 46 shows three different types of wall: (1) solid fired clay mechanically extruded bricks with cement mortar joints (B_'Ex' & MJ_'C'), (2) solid fired clay handmade bricks with lime mortar joints (B_'Mo' & MJ_'L'), both manufactured in the laboratory, and (3) solid fired clay handmade bricks with lime or cement mortar joints (B_'Hi' & MJ_'L'_'Hi') from existing historical buildings.

The solid fired clay bricks types considered in this research were produced by using two different procedures. The B_'Ex' was extruded perpendicular to the bed surface, cut and dried by mechanical automatized tools, and fired in a tunnel kiln with controlled heat conditions at 900 °C. The second type of unit, the B_'Mo' and B_'Hi', were traditionally

manufactured in a brickyard by shaping in a wooden mould sprinkled with dry fine sand and, after being extracted from the mould, the bricks were fired into a kiln.

The mortars produced in the laboratory were manufactured by using two different binders. The MJ_'L' was based on a commercial premixed hydraulic lime mortar classified as M5 according to EN 998-2:2018 [65], adding limestone filler to the premixed mortar to reduce its compressive strength as proposed by Segura et al. [218] to replicate a lower strength historical mortar. The MJ_'C' was based on a commercial premixed cement mortar classified as M7.5 according to EN 998-2:2018 [65]. The mortar's compressive strength (f_m) was evaluated according to EN 1015-11:2020 [6] by using 40 × 40 × 40 mm^3 cubes casted with the same material employed during the construction of the wall specimens. The campaign executed in the laboratory allowed the possibility of manufacturing two walls for each type of lime mortar proposed. The two walls built with MJ_'L' mortar had a compressive strength f_m equal to 3.54 MPa and 3.47 MPa with a coefficient of variation of 19.4% and 20.1% respectively, and the two walls built with MJ_'C' mortar had a f_m equal to 7.64 MPa and 5.59 MPa, with a coefficient of variation of 32.7% and 8.6% respectively.

Table 24 presents a description of the sampled materials in terms of origin, acronym, number of samples or building zones tested, average dimensions of bricks measured according to EN 772-16:2011 [60], and the thickness for mortar joints. The characterisation campaigns carried out in large existing buildings allowed the possibility of extracting and testing samples from more than one wall. The number of zones tested in each historical building have been indicated. In the historical buildings 'Hi/I$_3$' and 'Hi/R$_2$' only the mortar joins were characterised by MDT, and in the 'Hi/I$_2$' and 'Hi/I$_4$' an extra zone with cement mortar joints were tested. The characterisation campaign in the laboratory allowed the manufacturing of two walls for each type of mortar, i.e., they were considered as two different testing zones.

Fig. 46 Masonry walls manufactured with modern mechanically extruded solid fired clay brick and cement mortar (B_'Ex' & MJ_'C') (left), with modern handmade solid fired clay brick and lime mortar (B_'Mo' & MJ_'L') (centre), with historical handmade solid fired clay brick and lime mortar (B_'Hi/I$_4$' & MJ_'L'_'Hi/I$_4$') (right)

Table 24 Classification of solid fired clay units and mortar joints in terms of origin, acronym, number of zones or samples, and average dimensions. Values in brackets correspond to the coefficients of variation

Sampled materials			
Solid fired clay bricks (B)			
Origin	Acronym	N. of samples	Av. dimensions (mm)
Mechanically Extruded	B_'Ex'	1	272 [0.4%] × 132 [0.9%] × 45 [0.7%]
Modern Handmade	B_'Mo'	1	311 [0.6%] × 14 [1.7%] × 46 [4.6%]
Mortar Joint (MJ)			
Origin	Acronym	N. of samples	Av. dimensions (mm)
Lime M5 + limestone filler	MJ_'L'	2	15 [18.2%]
Cement M7.5	MJ_'C'	2	12 [14.7%]
Historical existing buildings (B & MJ)			
Origin	Acronym	N. of zones	Av. dimensions (mm)
1878 Industrial	B_'Hi/I_1'	5	295 [1.3%] × 148 [2.8%] × 44 [4.3%]
	MJ_'L'_'Hi/I_1'	5	16.6 [17.1%]
Early 20th c. Industrial	B_'Hi/I_2'	1	293 [1.3%] × 140 [4.2%] × 49 [5.8%]
	MJ_'L'_'Hi/I_2'	1	14.8 [18.3%]
	MJ_'C'_'Hi/I_2'	1	13.7 [26.4%]
1910-20 Industrial	MJ_'L'_'Hi/I_3'	1	16.8 [20.4%]
1927 Industrial	B_'Hi/I_4'	3	288 [0.7%] × 141 [1.5%] × 49 [5.8%]
	MJ_'L'_'Hi/I_4'	4	17.6 [11.5%]
	MJ_'C'_'Hi/I_4'	1	18.7 [26.8%]
1840 Residential	B_'Hi/R_1'	2	294 [0.7%] × 145 [1.8%] × 45 [2.1%]
	MJ_'L'_'Hi/R_1'	2	12.1 [20.6%]
1880 Residential	MJ_'L'_'Hi/R_2'	2	14.7 [19.4%]
1905 Residential	B_'Hi/R_3'	1	295 [0.7%] × 145 [4.2%] × 44 [5.8%]
	MJ_'L'_'Hi/R_3'	1	13.6 [12.3%]
1930 Residential	B_'Hi/R_4'	1	394 [0.4%] × 145 [0.5%] × 49 [5.2%]
	MJ_'L'_'Hi/R_4'	1	16.5 [18.1%]

VI.2.2. Destructive testing (DT) specimens and procedures

DT techniques carried out in this research involve two compressive strength testing procedures. The tests were carried out at the Laboratory of Technology of Structures and Materials of the Technical University of Catalonia (UPC-BarcelonaTech), but first the samples had to be collected from the existing buildings and transported to the laboratory. Fig. 47a shows the extraction of the historical bricks from the existing buildings carried out with a mallet and a chisel. First, a jackhammer was used to remove the plaster and the neighbouring bricks. Then, a thin chisel was used to remove the lime mortar joints around the brick to be extracted. Finally, a chisel was inserted under the brick bed with a metal mallet to separate and lever the brick. During this procedure, some mortar joints could be collected while the masonry wall was gradually dismantled. Fig. 47b shows how some joints remained unstacked after losing adherence from the brick. Others joints remained exposed

and could be removed using a very sharp thin chisel. Finally, the samples collected were packaged, labelled, and transported to the laboratory.

VI.2.2.1. Preparation of specimens

The proposed brick specimens were prepared according to the procedures specified in the European Standard EN 772-1:2011+A1:2016 [9]. First, the brick beds were polished by a grinder fitted with a high speed rotating diamond disc until requirement for smoothness and flatness were achieved. Next, the specimen measuring 100 × 100 × 40 mm^3 was extracted using a table saw equipped with a water jet. Then, the specimens were dried in an oven at a constant temperature of 105 ± 5 °C for 24 hours. Finally, the specimen dimensions were measured using a calliper with a precision of ±0.1 mm according to EN 772-16:2011 [60]. Fig. 47c shows a sample of brick specimens. A total amount of 125 brick specimens were prepared and tested, made up of 6 B_'Ex', 13 B_'Mo', and 106 B_'Hi'. The 106 B_'Hi' specimens include 77 from B_'Hi/I' and 29 from B_'Hi/R'. The proposed mortar joint specimen were prepared according to the procedures specified in the German standard DIN 18555-9:2019-04 [2]. The mortar bed joints extracted between the bed bricks had low consistency and cohesion that made the preparation of regular specimens difficult. It was not possible to test mortar slabs with exact dimensions of 50 × 50 mm^2 as recommended by the German standard. The thickness of the specimens, corresponding with the joint thickness, were measured with a calliper. The specimens were tested the same day of the extraction without having been dried to ensure that the sample collected maintained a degree of humidity similar to that of the conditions in the existing wall. Fig. 47d shows a sample of mortar joint specimens collected from an existing building. A total amount of 416 mortar joint specimens were prepared and tested, made up of 35 MJ_'C', 31 MJ_'L', and 350 MJ_'Hi'. The 350 MJ_'Hi' specimens include 19 MJ_'C'_'Hi' and 331 MJ_'L'_'Hi'.

VI.2.2.2. Testing procedure

The specimens were tested making use of the Ibertest testing machine with different load capacities depending on the specimens' compressive strength. The Ibertest testing machine was equipped with three different load cells, 3000 kN (MEH-3000), 200 kN and 10 kN (AUTOTEST 200/10SW), and connected to a MD5 electronic module for data acquisition. The brick specimens were tested using the MEH-3000, centring on the steel plates, and testing under force control at a rate of 0.15, 0.30 or 0.60 MPa/s depending on the specimen's capacity to guarantee at least a test duration of 60 s. The rates were selected according to the EN 772-1:2011+A1:2016 [9]. The tests were stopped manually after registering the initial post-peak response of the force-displacement pattern. Fig. 47e shows a brick specimen sample in the testing machine. The mortar joints were subjected to the Double Punch Test (DPT) according to DIN 18555-9:2019-04 [2] and the International Union of Railways (UIC)

Leaflet 778-3R [1], and tested using the load cell capacity of 10 kN with loading punches, which had a diameter of 20 mm. The mortar joint specimens needed a gypsum powder layer with a thickness of 1 mm interposed between the specimen and the loading punches to regularize the bearing surfaces and ensure a homogeneous loading, following the indications of Pelà et al. [45,219], and Matysek et al. [220]. The specimens were tested under force control and ensuring that the test would last between 30 and 90 s. Fig. 47f shows the DPT configuration.

Fig. 47 Sample collection procedure in historical existing building, preparation of the specimens, and testing procedures. A) Extraction of the brick sample from existing wall, B) extraction of the mortar joint from existing wall, C) 100 x 100 x 40 mm^3 brick specimens prepared to be tested, D) mortar joint specimens prepared to be tested, E) brick specimen testing configuration, F) mortar joint testing configuration

To verify the results of the DPT, it is proposed to carry out standardized specimens recommended according to EN 1015-11:2020 [6] by using 40 × 40 × 40 mm^3 cubes. As explained above, the laboratory specimens were casted with the same material employed during the construction of the wall specimens. The historical buildings do not allow the collection of 40 × 40 × 40 mm^3 cubes from existing joints. However, the industrial building 'Hi/I_4' allowed larger mortar samples to be collected, since the brick masonry walls were combined with irregular natural stone walls. The amorphous mortar samples were taken to the laboratory and carved into cubes with edges greater than 40 mm using with the multitool Dremel ® (Fig. 48a). Lastly, the edges of the specimens were dry-polished by a 3-axis vertical milling machine fitted with a rotary diamond disc to reduce with high precision the lengths

to 40 mm (Fig. 48b). This aimed to guarantee that the loading surfaces were smooth and on the same plane, avoiding any possible source of imperfection on the loading planes. Finally, 10 'Hi/I_4' 40 × 40 × 40 mm^3 cubic specimens were obtained, 1 from the zone 1, 2 from the zone 3, and 7 from the zone 4 (Fig. 48c). The compressive strength tests were carried out following the EN 1015-11:2020 [6] recommendations, but a gypsum powder layer with a thickness of 1 mm was placed to regularize the bearing surfaces and ensure a homogeneous loading as in DPT (Fig. 48d).

Fig. 48 Mortar specimen manufacturing process from the existing historical building 'Hi/I_4'. A) Carving mortar cubes from amorphous collected samples. B) Dry polishing with a 3-axis vertical milling machine fitted with a rotary diamond disc. C) 40 x 40 x 40 mm^3 cubes specimens obtained. D) Cube specimen tested in a hydraulic press

VI.2.3. Minor destructive testing (MDT) procedures

MDT techniques considered in this research involves two in-situ test, the Pin Penetration Test (PPT) [208] and the Helix screw Pull-out Test (HPT) [215]. In-situ testing requires first removal of the plaster with a jackhammer, uncovering an approximate surface area of 1 m^2 with more than 10 horizontal mortar joints exposed. Fig. 49 shows the tests layout, as well as the sequence of the operations during the PPT and HPT.

PPT is a MDT method developed to evaluate in-situ the compressive strength of the concrete, mortars and bricks by using a commercial tool that follows the ASTM C803/C803M [221] and the BSI 1881-207:1992 [222] recommendations. The used tool is produced by the James Instruments Inc., under the copyrighted name Windsor Pin Test System ®. The procedure for PPT is executed on the stretcher brick faces and 10 mm thickness mortar joints as follows. A 3 mm diameter steel pin, with a conical end, is inserted into the device. The retraction nut is tightened until the trigger mechanism closes to hold the spring in place and then it is completely loosened. The stored potential energy of the tool is 108 N·m with the loaded spring compressed to 20 mm. The device is positioned perpendicularly to the surface to be tested (Fig. 49a). The trigger is pulled while holding the device against the surface. The

manufacturer of the commercial tool indicates that the device has enough force to test concrete cubic specimens up to a maximum of 46.1 MPa and mortars in a range between 0.8 and 50.7 MPa. After the driven pin is taken out carefully by hand, a bulb air blower is used to remove the residual material inside the hole. Then, a micrometre is inserted to the bottom of the hole using the knurled thimble on the head of the micrometre (Fig. 49b) with a reading accuracy of 0.001 inch (0.0254 mm). The micrometre reading is noted. The penetration is obtained by subtracting the reading from one inch (25.4 mm).

The Helix screw Pull-out Test (HPT) is a MDT method developed to characterize in-situ the low strength mortar joints by using a commercial tool that follows the RILEM TC 127-MS D.9 [215] recommendations. The used helices are produced by the Helifix Company UK, under the copyrighted name ResiTie ®. In this research, the HPT was used to test the bricks on their stretcher faces, and the mortar joints with thickness up to 10 mm. According to a previous research focusing on HPT in low strength mortars [223,224], a 3 mm diameter pilot hole was executed and preferred to the 4 or 4.5 mm diameter pilot one suggested by Vekey and Ferguson [212,213,215]. However, a 4 mm diameter pilot hole was preferred over the 5 mm specified by Ferguson et al. [211] for bricks. The procedure for HPT is executed as follows. A pilot hole of 3 mm diameter is made in the mortar joints with a drill working at the minimum speed and with the tightening power adjusted at the weakest position. A pilot hole of 4 mm diameter is made in the bricks using a rotary-hammer drill with a masonry bit (Fig. 49c). In both cases, the drilled hole has a depth of 35 mm. Then, an austenitic stainless-steel Grade 304 (1.4301) helical tie with a diameter of 1/4 in. (6.3 mm) is mounted into a supplementary tool. While holding it horizontally, the tool is hammered carefully until the helical tie is introduced into the pilot hole to a depth of 30 mm and results embedded in the masonry component (Fig. 49d). This process allows the helical tie to rotate and cut a thread in the mortar or the unit during insertion. After insertion, a Load Test Key (LTK) is screwed onto the remaining outer part of the tie. The LTK restrains from rotating the helical tie during the test, assuring a shear failure in the tested material. The Load Test Unit (LTU) is connected to the LTK and the mechanism is rotated to screw down the tie and take up any slack. The LTU provides the contact with the material's surface by means of a steel annulus. The load is applied by turning a grip lever to increase progressively the load until failure (Fig. 49e). The maximum load reached during the test is recorded as the pull-out force (Fig. 49f). The manometer of the commercial tool allows a pull-out load up to 3000 N, with a reading accuracy of 100 N. At least 10 HPT tests executed as suggested by Ferguson [212] who specified that 10 HPT data are sufficient to distinguish between different mortars, and later recommended by BRE Group [214] and RILEM TC 127-MS D.9 [215].

A total amount of 398 PPT and 343 HPT were carried out in-situ and in laboratory. The 398 PPT are made up of 151 PPT in bricks and 347 PPT in mortar joints, and the 343 HPT are made up of 114 HPT in bricks and 229 HPT in mortar joints.

Fig. 49 Minor Destructive Technique (MDT) steps executed in existing masonry buildings. A) The PPT device positioned perpendicularly to the surface into be tested, B) the micrometre inserted to the hole to read the penetration produced by the PPT device, C) the rotary-hammer drill used to make the HPT pilot holes, D) the helical tie of the HPT hammered into the pilot hole, E) the HPT grip lever applying the load by turning it manually until failure, F) the failure mechanism in brick specimens testing the HPT

VI.3. Experimental results

The DT included compressive strength evaluation of clay units following the EN 772-1:2011+A1:2016 [9], of mortar with 40 mm edge cubes according to EN 1015-11:2020 [6], and of mortar joints through DPT following the DIN 18555-9:2019-04 [2] and the International Union of Railways Leaflet 778-3R [1]. The compressive strength of the brick specimens was calculated by dividing the maximum compressive load by the cross-sectional area of the specimen. The experimental values obtained by testing the 100 × 100 × 40 mm^3 brick specimens have to be multiplied by a shape factor indicated in the Table A.1 of the EN standard, which is 0.7. The experimental values obtained by DPT of the mortar joint samples have two possibilities depending on the considered reference standard. The DIN 18555-9:2019-04 [2] considers the compressive strength as the maximum load by the cross-sectional area of the punch. However, the UIC Leaflet 778-3R [1] further considers the application of a correction factor of 0.7. The compressive strength derived from DPT can thus by derived from the following equation (1).

$$f_c^{\,m} = \alpha \cdot \frac{4 \cdot F_{ult}}{\pi \cdot \emptyset^2} \qquad (1)$$

Where F_{ult} is the maximum loas, Ø is the punch diameter, α = 1 according to the DIN 18555-9:2019-04 [2] and α = 0.7 according to the UIC Leaflet 778-3R [1].

The MDT techniques considered in this research are the PPT and de HPT. As mentioned before, the PPT measures the depth of penetration of the steel pin, which can be empirically correlated to the material strength. This relationship is significantly influenced by the properties and proportions of the aggregates [222]. Although there are no specific studies about the factors affecting the geometry of the fracture zone, this research provided recurrent observations of a cone-shaped fractured region in the surroundings of the pin driven into the material. Since the spring of the tool can loose potential energy, it is important to check the calibration of the equipment at the beginning of each campaign.

As already mentioned before, the HPT measures the pull-out force, which can be empirically correlated to the material strength thorough a calibrated curve, such as the one provided by Vekey et al. [213]. The RILEM TC 127-MS D.9 [215] evidences that the relationship between pull-out force and strength is not linear, as also observed by Vekey et al. [209]. Benedetti et al. [224], made a mechanical interpretation by supposing that the tool does not produce a significant radial compression state, thus the tangential stress (τ_H) due to the pulling out force (F) produced during the helix extraction is derived from the embedment length (L) and external diameter (D_e) of the helix, as the equation (2) describes.

$$\tau_H = \frac{F}{\pi \cdot D_e \cdot L} \qquad (2)$$

Table 25 presents the MDT results in bricks and mortar joints, including the number of specimens, the average value of the physical tested (strength, depth, and tangential stress) with their coefficients of variations in brackets.

Table 26 presents the comparison between DPT and EN 1015-11/A1:2020 [6] compressive strength derived from building and laboratory samples, including the number of specimens, the average compressive strength values, and their coefficients of variation. The compressive strength values presented in Table 26 shows higher coefficient of variation in DPT than in tests executed following the EN 1015-11/A1:2020 [6]. The table also shows the relationship between the compressive strength by using DPT (f_{m_DPT}) and the strength by following the EN 1015-11/A1:2020 [6] (f_{m_EN}).

Table 25 Number of samples (N.) and average value of the brick and mortar joint specimens. Values represent the brick compressive strength (f_c) in MPa, the mortar joint compressive strength (f_m) by the DPT and the DIN [2] and

International Union of Railway (UIC) Leaflet 778-3R [1] interpretation, the PPT penetration in mm, and de HPT indicating the tangential strength (τ_H) in MPa. Values in brackets correspond to the coefficient of variation

	Brick					
	f_c [9]		PPT (depth)		HPT (τ_H)	
	N.	Av [MPa]	N.	Av [mm]	N.	Av [MPa]
B_'Ex' & MJ_'C'	6	52.7 [3.4%]	10	4.3 [8.0%]	-	-
B_'Mo' & MJ_'L'	13	17.4 [8.6%]	22	5.9 [17%]	11	2.55 [35%]
B_'Hi/I_1' & MJ_'L'_'Hi/I_1'	12	18.4 [21%]	10	6.9 [24%]	10	2.86 [14%]
	10	32.2 [21%]	10	6.4 [13%]	10	2.80 [9.2%]
	6	22.9 [13%]	10	6.1 [11%]	10	2.74 [16%]
	6	17.5 [17%]	10	6.1 [12%]	10	3.02 [20%]
	9	21.3 [23%]	10	6.2 [15%]	10	2.81 [10%]
B_'Hi/I_2' & MJ_'L'_'Hi/I_2'	10	32.2 [21%]	10	6.2 [17%]	10	3.38 [14%]
B_'Hi/I_4' & MJ_'L'_'Hi/I_4'	11	19.0 [18%]	12	5.6 [10%]	10	2.39 [23%]
	10	20.0 [12%]	11	6.3 [39%]	10	2.50 [37%]
	3	19.1 [4.6%]	10	5.8 [30%]	10	2.62 [14%]
B_'Hi/R_1' & MJ_'L'_'Hi/ R_1'	10	35.4 [18%]	9	5.1 [10%]	-	-
			9	5.0 [20%]	-	-
B_'Hi/R_3' & MJ_'L'_'Hi/ R_3'	7	15.2 [18%]	8	6.3 [4.7%]	10	1.63 [18%]
B_'Hi/R_4' & MJ_'L'_'Hi/ R_4'	12	16.8 [20%]	-	-	3	2.07 [8.4%]

	Mortar joint							
	f_m DPT [1,2]				PPT (depth)		HPT (τ_H)	
	N.	DIN Av [MPa]	UIC Av [MPa]	CV	N.	Av [mm]	N.	Av [mm]
B_'Ex' & MJ_'C'	20	8.32	4.08	[36%]	11	8.2 [10%]	5	2.22 [37%]
	15	4.07	1.99	[33%]	12	8.8 [20%]	8	0.41 [49 %]
B_'Mo' & MJ_'L'	20	3.00	1.47	[28%]	13	9.2 [16%]	10	1.13 [38%]
	11	7.65	3.75	[25%]	8	11.8 [16%]	7	0.97 [28%]
B_'Hi/I_1' & MJ_'L'_'Hi/I_1'	33	1.09	0.53	[31%]	20	10.8 [4.3%]	16	0.68 [35%]
	22	0.39	0.19	[34%]	13	10.9 [4.8%]	10	0.77 [24%]
	23	0.44	0.22	[25%]	20	18.7 [38%]	17	0.92 [66%]
	31	1.38	0.68	[33%]	10	10.6 [8.3%]	10	0.73 [18%]
	18	1.84	0.90	[33%]	10	10.1 [5.9%]	11	1.29 [20%]
B_'Hi/I_2' & MJ_'L'_'Hi/I_2'	16	0.47	0.23	[32%]	10	10.5 [10%]	10	0.68 [24%]
B_'Hi/I_2' & MJ_'C'_'Hi/I_2'	9	15.1	7.40	[31%]	10	6.3 [8.3%]	6	3.24 [12%]
B_'Hi/I_3' & MJ_'L'_'Hi/I_3'	12	0.62	0.30	[16%]	10	9.0 [15%]	10	1.24 [35%]
B_'Hi/I_4' & MJ_'L'_'Hi/I_4'	26	3.46	1.70	[37%]	11	8.7 [15%]	15	1.71 [35%]
	25	2.06	1.01	[34%]	10	9.6 [21%]	10	0.77 [27%]
	13	1.79	0.88	[39%]	6	9.2 [15%]	6	0.58 [41%]
	10	3.82	1.87	[20%]	10	7.9 [25%]	10	1.31 [64%]
B_'Hi/I_4' & MJ_'C'_'Hi/I_4'	10	13.3	6.52	[45%]	5	6.2 [9.8%]	5	3.18 [13%]
B_'Hi/R_1' & MJ_'L'_'Hi/ R_1'	16	4.23	2.07	[38%]	9	8.1 [10%]	6	1.64 [9.6%]
	16	2.06	1.01	[50%]	9	8.4 [17%]	5	1.75 [15%]
B_'Hi/R_2' & MJ_'L'_'Hi/ R_2'	10	0.37	0.18	[17%]	15	10.8 [9.0%]	15	0.79 [29%]
	22	0.61	0.30	[36%]	15	11.0 [9.8%]	15	0.47 [32%]

B_'Hi/R_3' & MJ_'L'_'Hi/ R_3'	10	2.68	1.31	[19%]	10	11.7 [7.7%]	10	1.48 [20%]
B_'Hi/R_4' & MJ_'L'_'Hi/ R_4'	28	1.51	0.74	[35%]	-	-	12	0.87 [36%]

Table 26 Number of samples (N.) and average compressive strength of the mortar samples, and ratio between the compressive strength measured on mortar joints by DPT and on 40 mm edge cubs following the EN 1015-11:2020 (f_{m_DPT}/ f_{m_EN}). DPT values are presented using DIN and UIC equation. Values in brackets indicate the coefficient of variation

Experimental Results								
	DPT (f_{m_DPT})				N.	EN 1015-11 (f_{m_EN})	f_{m_DPT}/ f_{m_EN}	
	N.	DIN	UIC	CV			DIN	UIC
MJ_'C'	20	8.32	4.08	[36%]	6	5.6 [8.6%]	1.49	0.73
	15	4.07	1.99	[33%]	6	7.6 [33%]	0.54	0.26
MJ_'L'	20	3.00	1.47	[28%]	6	3.5 [19%]	0.86	0.42
	11	7.65	3.75	[25%]	6	3.5 [20%]	2.19	1.07
MJ_'L' Hi/I_4	26	3.46	1.70	[37%]	1	2.0 [-]	1.73	0.85
	13	1.79	0.88	[39%]	2	1.7 [10%]	1.05	0.84
	10	3.82	1.87	[20%]	7	3.3 [21%]	1.15	1.62

VI.4. Discussion

This section presents two analytical studies based on the experimental results described in Section VI.3. The first study analyses the correlation between the DPT and the standard compression test on mortars and studies the approaches available for the evaluation of the compressive strength according to different available reference. The second study focusses on the correlation between the MDT (PPT and HPT) and the compressive strength determined using DT. This second study considers additional experimental data from the available literature in the field to enlarge the experimental database.

VI.4.1. Evaluation of the compressive strength by DPT according to different standards

The experimental campaign on mortars allowed the comparison between the strengths obtained by DPT and by EN 1015-11:2020 [6], as presented in Table 26. Such comparison is plotted in Fig. 50. As explained in Section VI.3, the DIN 18555-9:2019-04 [2] and the UIC Leaflet 778-3R [1] provide different evaluation of the DPT compressive strength. For this reason, Fig. 50 reports the trend lines corresponding to the two different criteria established by the two standards for the calculation of the DPT compressive strength. The figure also reports the ideal 45-degrees line denoting equal strengths from the DPT and the standard compressive test according to EN 1015-11:2020 [6]. Fig. 50 shows a greater dispersion in the strength values obtained following the DIN standard. However, the trend line of the UIC Leaflet strength values has an inclination meaningfully lower that obtained by the DIN standard, which is almost parallel to the 45-degree line. In the following sections, the DPT

strength values obtained following DIN 18555-9:2019-04 [2] will be considered as the reference to be correlated to PPT and HPT measurements.

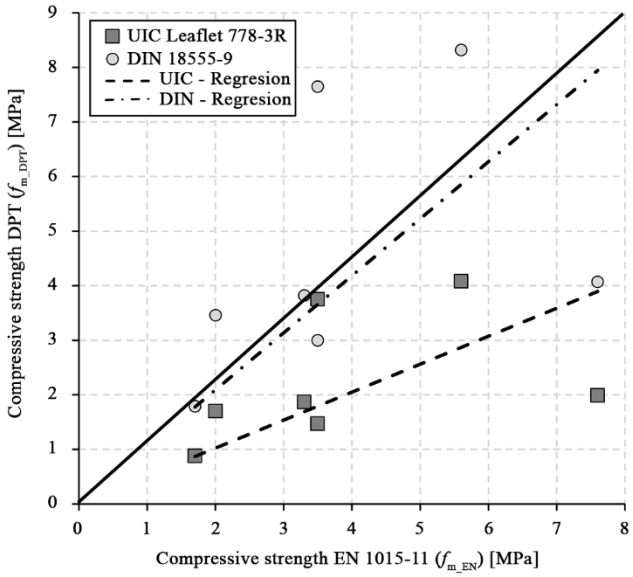

Fig. 50 The linear regression relating DPT and EN 1015-11:2020 [6] compressive strengths on mortars specimens. Standards DIN 18555-9:2019-04 [2] and UIC Leaflet 778-3R [1] are used for the evaluation of the DPT strengths

VI.4.2. Empirical correlation between compressive strength and penetration depth derived from PPT

Based on the experimental campaign presented, an experimental correlation between the penetration depth from PPT and the compressive strength of the samples tested has been determined, see Fig. 51a. The points represent the relationship between the average compressive strength and penetration depth for samples tested in the same characterisation zone or in the laboratory. The values are presented in the graph as a point (mean) with a line indicating the standard deviation. The graph includes the B_'Ex' experimental values (52.7 MPa), even if the manufacturing company does not recommend to test specimens up to 46.1 MPa. In addition, the National Research Council Canada [207] indicates this method for use with concrete strength less than 30 to 40 MPa, and ACI 228.1R-03 [208] do not recommend to test specimens up to 28 MPa. The area exceeding the thresholds recommended by the manufacturer and publications has been indicated on the graph with a hatch. The graph also shows an outlier, the 7.6 MPa compressive strength value of MJ_'L'. Table 26 shows that, the DPT strength is much higher than that obtained in the laboratory using the standardized process according to EN 1015-11:2020 [6]. Thus, one of the MJ_'L' strength was eliminated to obtain the trend line. Fig. 51a shows the power trend function, which has a correlation coefficient of 0.82 and follows the equation (3).

$$f_{m\_DPT} = \sqrt[0.17]{\frac{10.2}{depth}} \quad (3)$$

The scientific literature discussed in Section VI.1 reports only two references dealing with the experimental testing of mortars by using the PPT, since previous research did not specify or provided information about the steel pin diameter or the potential energy of the tool. Pelà et al. [45,223] analysed wallettes manufactured in the laboratory using natural hydraulic lime mortar (NHL), while Tohidi [225] evaluated wallettes produced in the laboratory using NHL and Calcium lime (CL). Both campaigns were executed at the Universitat Politècnica de Catalunya (UPC). Fig. 51b shows the experimental data obtained in this research, together with those from the two aforementioned studies at UPC. This figure shows that the penetration depth tends to infinity when the compressive strength is 0 MPa. This trend makes it difficult to identify specimens with low strength, since a minimal variation in the penetration depth reading causes the correlated strength to vary greatly.

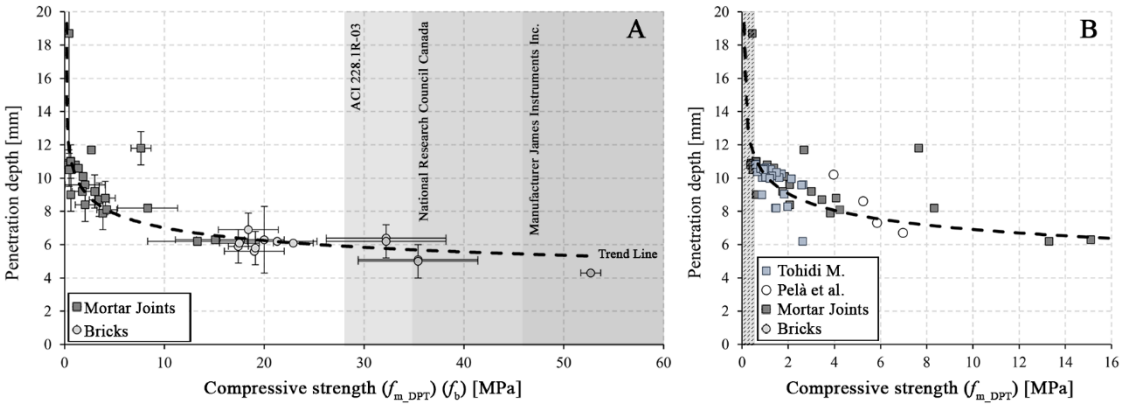

Fig. 51 Empirical correlation among compressive strength and penetration depth in bricks and mortars using PPT. A) Experimental average strength including deviation bars and trend line, with the different maximum strengths referenced by hatching. B) Integration of additional experimental data from available scientific literature

VI.4.3. Empirical correlation between compressive strengths and tangential strengths derived from HPT

Based on the experimental campaign presented above, the study has determined an experimental correlation between the tangential strength obtained using HPT and the compressive strength of the samples. Fig. 52a shows the relation of the experimental compressive strength values in specimens and the tangential strength calculated from the pull-out force in HPT. The points represent the relationship between the average compressive strength and tangential strength for samples tested in the same characterisation zone or laboratory specimen. The values are presented in the graph as a point (mean) with a line indicating the standard deviation. Some previous research [214,215] indicate that the

method is limited by the yield strength of the helical steel screw used. The manufacturing company specifies that the ties has a tensile strength capacity of 10 MPa. Considering yield stress to one third of the tensile strength, the representative pull-out force is 3 kN, coinciding with the maximum reading capacity of the manometer. The 3 kN pull-out force means a tangential strength of 5.3 MP, according to Benedetti et al. [224]. However, Ferguson et al. [211,212] indicated that the optimum compressive strength range for the test is between 2 and 10 MPa, while Vekey et al. [213] specified a range between 3 and 10 MPa, BRE Group [214] specified 7 MPa as the maximum strength, and RILEM TC 127-MS D.9 [215] recommends values up to 8 MPa. The areas exceeding the thresholds recommended by the manufacturer and publications have been indicated on the graph with a hatch. The Fig. 52a shows the strength - penetration depth power trend line with a correlation coefficient of 0.78 according to the equation (4). Fig. 52b is a zoom from Fig. 52a showing the compressive strength of mortars up to 10 MPa.

$$f_{m\_DPT} = \sqrt[0.37]{\frac{\tau_H}{0.83}} \qquad (4)$$

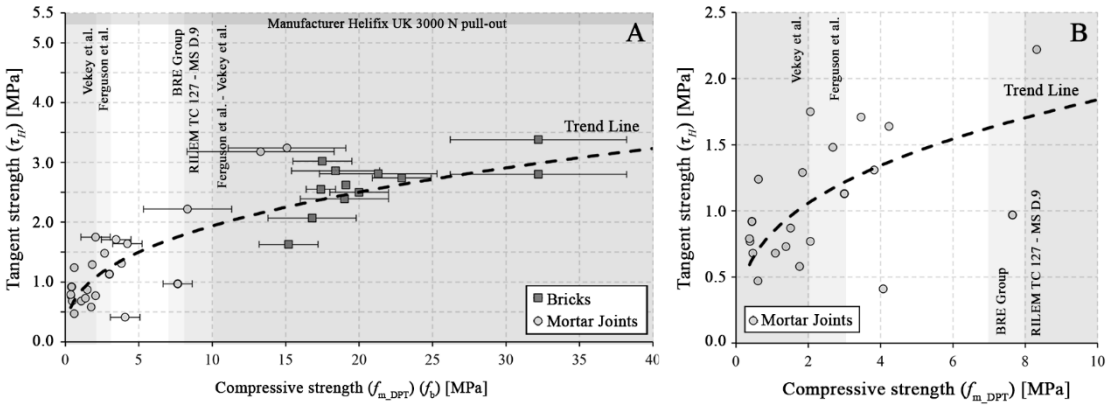

Fig. 52 Empirical correlation between compressive strength and HPT tangent strength in bricks and mortars. A) Experimental average strengths including deviation bars and trend line, with the different indicated maximum strength referenced by hatching. B) Experimental average strengths in mortars up to 10 MPa

The scientific literature discussed in Section VI.1 reports only a limited number of references dealing with the HPT of bricks and mortars samples. Fig. 53 shows an power trend line based the experimental data derived from HPT in the present research, together with those published by Vekey [209], Ferguson et al. [211], Ferguson [212], Vekey et al. [213], and Pelà et al. [45,223]. Values above 10 MPa seems to follow the proposed trend. A significant correlation has been found between compressive strength and HPT, except for the data related to the AAC blocks of Ferguson et al. [211], and to the mortar values of Ferguson [212] and Vekey et al. [213], so other factors can be influencing the experimental pull-out loads, such as the granulometry or the dilatancy of the tested material.

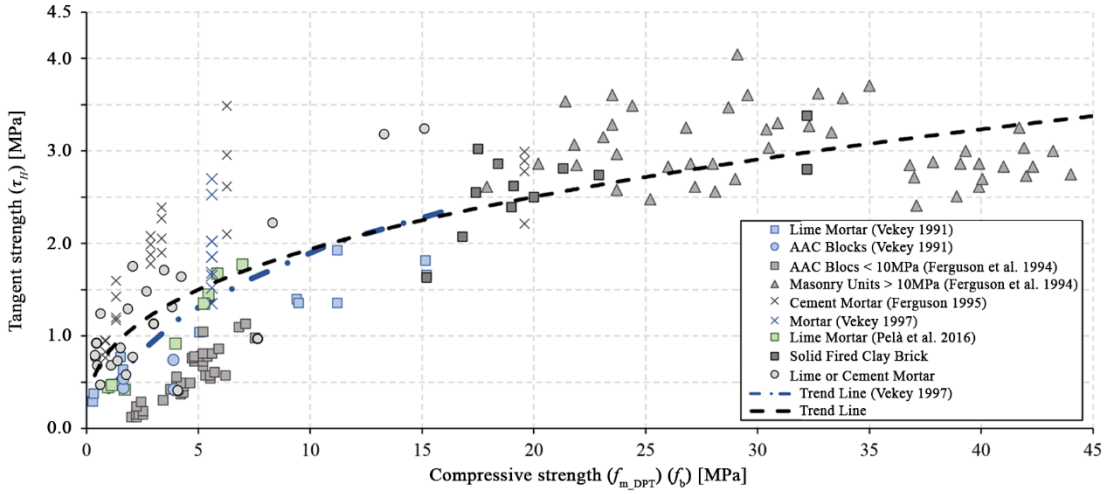

Fig. 53 Empirical correlation among compressive strengths and tangent strengths in bricks and mortars derived from HPT of this experimental program. The graph includes additional experimental data from available scientific literature

VI.5. Conclusions

This paper has presented accurate results on the measurement of the compressive strength on clay brick solid samples and mortar joints by using MDT. First, the validation of the DPT procedure has been analysed by comparing DPT strength experimental values with compressive strengths following the EN 1015-11:2020 [6] recommendations. Second, the empirical correlation between compressive strength and penetration depth using PPT has been analized by investigating 14 brick types and 22 mortar joint types. Third, the empirical correlation between compressive strength and tangential strengths using HPT has been analized into detail by investigating 12 brick types and 23 mortar joint ones. The research has been performed through an extensive campaign on mechanically extruded ('Ex') and handmade bricks, including modern ('Mo') and historical ('Hi') units extracted form existing buildings. The following conclusions can be drawn from the analysis of the experimental results:

- The MDT considered in this research need a precise execution process. This accuracy makes it quite dependent on the person running and interpreting the tests results. However, correct training and practive is easy to achieve.
- The current stage of the research can guarantee a range of approximation between the MDT and the compressive strength that is more clear in PPT than in HPT.
- The PPT is difficult to adjust for compressive strength values lower than 0.5 MPa, and the standard deviation may depend on the material aggregates. This technique can only test the material surface, so it requires other complementary MDT techniques.

- A general trent relating the HPT measurement with the compressive strength has been also determined. However, the experimental values do not adjust satisfactorily to the trend line. Different factors such as the granulometry or dilatancy can affect the test results, among other.

Future works could address the extension of the experimental database by including the application to a large sample of different brick and mortar materials. Likewise, further in-depth research of the HPT technique is needed.

Chapter 4

Conclusions

4.1 Summary

The experimental validation of masonry's main mechanical properties is a highly valuable methodology for ensuring their reliable assessment. The present work has focused on the investigation of two main experimental parts available to assess the mechanical characterisation of masonry in existing structures by means of laboratory and in-situ experimental techniques. The primary aim of these campaigns was to employ minor destructive testing (MDT) techniques even development and calibrating novel testing procedures in laboratory. This research involves the use of a significant number of specimens to evaluate the factors that influence compression tests of various types of bricks. The bricks considered include mechanically extruded, hydraulic press moulded, modern handmade, and historical handmade bricks collected from existing buildings in Barcelona, Spain. The historical handmade bricks used in this study were collected from eight different buildings form 19th and early 20th centuries. These buildings included structures used for industrial, residential, and market purposes. The present research comprises six experimental research campaigns aimed at characterizing masonry. These campaigns constituted the base of six publications, identified in this document as Paper I to VI. Two of these have already been published. The analysis of the experimental campaigns provides valuable insights into the compressive strength test and the resulting confinement effect in the specimens.

Chapter 2 has described five research, four on the compressive strength, and one on the elastic modulus of solid fired clay bricks. The mechanical characterisation of compressive strength involves the research of several factors, including the study of tiles with reduced thickness, the proposal of a novel cubic specimen with a 40 mm edge, brick anisotropy, the influence of specimen length and bearing surface on compressive strength and the development of new testing methodologies, the influence of the stacking procedure, and the

confinement produced by the specimen slenderness. The elastic modulus characterisation involves the research on proposal a testing protocol, developing an external support for the clamp-on transducers, analysing the specimen shape, i.e., the cross-section and the slenderness, and the testing setup.

Chapter 3 include the calibration of two MDT technique, i.e., the Pin Penetration Test (PPT) and Helix screw Pull-out Test (HPT). Both research includes the use of commercial tools. The MDT techniques were carried out in-situ in existing buildings, on bricks and mortar joints. A comparison was made between the results obtained from in-situ testing and laboratory testing. The purpose of this comparison was to assess the degree of correlation between the two sets of results and to validate the accuracy of in-situ testing methodologies for predicting the behaviour of masonry structures.

4.2 Conclusions

This section summarises the main specific conclusions obtained for the experimental programme, the correlation study and the analytical approach.

I. Experimental setup and numerical evaluation of the compression test on thin tiles for masonry timbrel vaults

- It has been possible to propose a relatively easy and efficient procedure to extract historical tiles from existing vaults. Common electric tools could be employed for this purpose, such as a jackhammer to remove the pavement or the plaster, together with manual chisel, a trapezoidal trowel and a nylon hammer for the careful extraction of the tiles.
- The tests on assembled specimens allowed a reliable testing in compression of the tiles. The test on the proposed assembled specimen avoided the possible influence of instability effects induced by the excessive slenderness of the individual tiles. No tile buckling failure was observed in the experimental investigation.
- The failure mode of the tiles was characterized by the splitting of the tile into two parts due to the propagation of a crack throughout the whole width of the tile. The numerical simulation predicted also the type of failure. In some cases, debonding between the tile and the cement mortar was also observed.
- It has been verified that that the proposed test setup can estimate the uniaxial compressive strength of the tile in a satisfactory way with only a difference between 5% and 10% from the one given by tests on standardized brick specimens. This limited difference has been also verified through numerical simulation.
- The parametric studies carried out by numerical investigation have showed that the change in the thickness, as well as the variation of the tensile and shear strength and the tensile fracture energy, have only a marginal influence on the estimation of the

uniaxial compressive strength by using the proposed setup. Using the numerical simulation, it was possible to conclude that ratio between the uniaxial tensile strength of a single brick (input data of the numerical model) and the uniaxial compressive strength computed using the proposed assembled specimen ranged between 1.02 and 1.09.

- Testing the thin tile using the proposed assembled specimen has proved to be an advantageous technique for the evaluation of the compressive strength of thin tile units. It is suggested to test at least a set of six units extracted from an existing vault to obtain a reliable estimation of the compressive strength.

II. Anisotropy and compressive strength evaluation of solid fired clay bricks by testing small specimens

- It was possible to develop a relatively easy and efficient procedure to extract the historical bricks from existing walls. Common electric tools were employed, such as a jackhammer to remove the plaster, together with manual chisel and a nylon hammer for the careful extraction of the bricks.
- The failure mode of the $40 \times 40 \times 40$ mm^3 specimen showed a characteristic hourglass shape. In the testing of cubic brick specimens, successful failure modes were judged and, in some cases, rejected as non-meaningful for the estimation of the compressive strength following standardized criteria for concrete cube specimens.
- A specific methodology has been proposed and applied for the post processing of the experimental results on brick compressive strength and anisotropy. The proposed methodology is based on a statistical analysis of the experimental data and includes the application of nonparametric statistical tests. This methodology could be similarly applied to extend the research to other brick types.
- The study shows that the extruded solid clay bricks investigated present a moderate anisotropy due to their manufacturing process. This observation has been corroborated from data found in the scientific literature. However, an almost isotropic behaviour has been obtained for the three handmade moulded bricks and the hydraulic press moulded ones herein investigated.
- The compressive strength measured on the standard '100' and the nonstandard cubic 'C40' specimens can be correlated through an average ratio $f_{c,100} / f_{c,C40}$ equal to 1.65 (CV of 12%) ranging between 1.32 and 1.96. This ratio allows the estimation of the compressive strength of the standard '100' specimen from that measured from the 'C40' one on solid fired clay brick. However, a more conservative and engineering ratio equal to 1.45 is also proposed based on statistical considerations.
- The proposed 'C40' specimen has provided an advantageous technique for the evaluation of the compressive strength of solid clay bricks in existing masonry

structures. In practical applications oriented to the characterization of existing brick masonries, it is suggested to test at least a set of twelve specimens from six different units to obtain a reliable estimation of the compressive strength.

III. Effect of cross section aspect ratio and bearing surfaces treatment on the compressive strength of solid fired clay brick specimens

- The experimental tests on whole and half handmade brick specimens show a noticeable hardening response due to their low slenderness. Although this response makes it difficult to objectively measure a meaningful uniaxial compressive strength value, a criterion has been proposed allowing to determine a representative value. The criterion proposed is based on a simple method derived from a mathematical analysis of the stress-displacement experimental curve.
- The experimental results and the scientific literature show that the cross section's aspect ratio is more influent in modern handmade solid fired clay bricks ('Mo') than in mechanically extruded ones ('Ex'). According to the research carried out, the ratio between the strengths of the whole brick and the half brick ('wh'/'ha') range between 0.88 and 1.06 for 'Ex' specimens, and between 0.64 and 0.78 for 'Mo'.
- It is proposed to characterise the compressive strength measured on the specimens with different bearing surface using the ratio $f_{c,TR} / f_{c,GR}$ where $f_{c,TR}$ is the strength of the treated specimen and $f_{c,GR}$ is the strength of grinded specimen, taken as reference value. The ratio is intended for specimen slenderness under 0.4. The experimental ratio $f_{c,TR} / f_{c,GR}$ is equal to 0.82 (CV of 8%) for specimens capped with cement mortar, and 0.93 (CV 7.5%) for specimens with birch plywood sheets, being both similar to the evidence available in the scientific literature. The experimental ratios $f_{c,TR} / f_{c,GR}$ of the specimens tested with gypsum material seem to be influenced by both the manufacturing process and the unit's strength unit. The ratio for 'Ex' specimens is 0.74 (CV of 4.7%) for capping with gypsum plaster, and 0.94 (CV of 6.7%) for covered with gypsum powder. The 'Mo' specimens present a ratio of 0.52 (CV 21.8%) for capping with gypsum plaster, and 0.72 (CV of 9.3%) for capping with gypsum powder.
- The capped specimens have exhibited a varying amount of lateral restraint, which is dependend upon the cross section aspect ratio. Specimens tested with plywood and fiberboard sheets show high compressive strength values regardless of the specimen shape. The amount of lateral restraint in specimens with grinded surfaces seems to be influenced mainly by the slenderness of the specimen.
- Capping with gypsum powder has produced compressive strength values similar to those of the grinded specimens. Such values are also similar to those obtained with plywood sheets for 'Ex' bricks, or those obtained for specimens capped with cement mortar in the case of 'Mo' bricks. The use of gypsum powder can hardly be considered

as a low friction surface treatment since the compression loading compacts the powder during the execution of the test, inducing a mechanical behaviour similar to that of capping.

- Testing the specimen placed with two oiled PTFE leaves has proved to be an advantageous technique for the evaluation of the unconfined compressive strength of solid fired clay units. This technique has yielded similar compressive strength values regardless of the specimen shape.
- The standards for the evaluation of the compressive strength in bricks present a wide variety of approaches. The American ASTM and the Canadian CAN/CSA lead to the estimation of the highest values of compressive strength, while the Australian AS/NZS provide the lowest values.

IV. Influence of specimen slenderness and stacking on the experimental strength of solid fired clay bricks

- The failure mode of the solid clay specimens tested in compresion has been in general characterised by a hourglass shape induced by the the confinement induced by both the geometriy of the specment and the frictional contact with the press plattens. This phenomenon is observe even in both staked and unstacked specimens with slenderness equal to 2.
- The experimental results show that the influence of the stacked procedure on the compressive strength is more evident in mechanically extruded solid fired clay bricks ('Ex'), tested flatwsie, than in modern handmade solid fired clay bricks ('Mo'). the compressive strengths of stacked and unstacked In the case of specimens with slenderness equal to 2 a compressive strength ratio has been obtained between stacked and unstacked 'Ex' specimens of 0.60 along the width and 0.73 aong the length respectively. However, the 'Mo' specimens show a closer relationship between both specimen types, with rations equa l to 0.90 along the width and 0.94 along the length respectively. This influence has been corroborated by means of a a detailed statistical analysis of the experimental data.
- The influence of the specimen slenderness on the compressive strength is clear and regular in handmade solid fired clay bricks ('Mo' specimens). In particular, a steeply increase in experimental compressive strength is observed for slenderness below 1.0.
- Mechanically extruded flatwise solid fired clay bricks ('Ex') specimens exhibit an irregular relationship between strength and . slenderness for slenderness below 1.5.
- Testing stacked specimens with slenderness between 2 has proved to be an advantageous technique for the evaluation of the compressive strength of the modern handmade solid fired clay units ('Mo'). The stacked procedure does not influence on the compressive strength.

- It has been observed that similar compressive strength values are obtained for specimens with slenderness 2 and 3, showing that for this slenderness range the confinement only has a limited.influcence.

V. Experimental evaluation of the elastic modulus of solid fired clay bricks and correlation with compressive strength

- An effective and straightforward procedure can be implemented to extract historical bricks from existing walls. Common electric tools can be employed, such as a jackhammer to remove the plaster, together with manual chisel and a nylon hammer for the careful extraction of the bricks.
- Testing 40 × 40 × 80 mm^3 specimens, i.e., square cross-section specimens with slenderness 2, using an on-purpose developed support for clamp-on transducers has proved to be an advantageous technique for the evaluation of the elastic modulus of solid fired clay bricks. A detailed testing procedure has been formalized for this purpose. It is suggested to test at least a set of six specimens extracted from different bricks to obtain a reliable estimation of the elastic modulus.
- It has been observed that the failure modes of the 40 × 40 × 80 mm^3 specimens depend on the brick manufacture. Different brick types show fracture in different faces with respect to the bed one
- The study shows that the mechanically extruded solid fired clay bricks investigated present anisotropy in terms of their elastic properties due to their manufacturing process. The smallest elastic modulus is obtained along the width. This observation is consistent with the already mentioned anisotropy observed on the compressive strength and the observations from previous scientific publications. However, an almost isotropic behaviour has been obtained for the hydraulic press moulded, modern handmade, and historical handmade bricks herein investigated.
- The experimental results indicate that the most effective approach for assessing the elastic modulus of solid fired clay bricks involves the use of specimens with grinded bearing surfaces and with slenderness equal to 2. Such specimens minimize the influence of the confinement, leading to more precise strain measurements.
- The experimental results show a clear relationship between the compressive strength value and elastic modulus. The scientific reference and the experimental research provide the $E_B = 300 \cdot f_c$ correlation, where E_b is the elastic modulus of the brick, and f_c is the compressive strength of the tested specimen. However, the experimental trend line $E_b = 927 \cdot f_c^{0.69}$ with the estimated trend limits shows a better relationship. The experimental correlation does not include the mechanically extruded bricks.

VI. Laboratory an in-situ characterisation of masonry components by comparing destructive and minor destructive techniques

- The MDT considered in this research need a precise execution process. This accuracy required by the test procedure make them quite dependent on the person running and interpreting the tests results. However, correct training and practice is easy to achieve and can strongly contribute to a more stable evaluation and interpretation.
- The research carried out has allowed the derivation of an experimental relationship to estimate the compressive strength of solid clay bricks based on MDT measurements. The relationship derived are more reliable for the PPT that for the HPT techniques.
- The PPT method does not allow a reliable estimation of the compressive strength for strength values lower than 0.5 MPa. Moreover the standard deviation of the measurements may depend on the material aggregates. It must also be taken into account that this technique can only test the material located at the surface and therefore may require other inspection techniques to control the in-depth material homogeneity.
- A general trent relating the HPT measurement with the compressive strength has been also determined. However, the experimental values do not adjust satisfactorily to the trend line. Different factors such as the granulometry or dilatancy can affect the test results, among other.

4.3 Suggestions for future works

The challenges met in the present research, and the requirements for further study identified through it, suggest a set of suggestions for future works. The proposal future works are intended to extend the applicability of the methods proposed and the enlarge the experimental evidence attained.

I. Experimental setup and numerical evaluation of the compression test on thin tiles for masonry timbrel vaults

Future works could address the extension of the experimental database by including the application to a wider sample of tiles extracted from existing timbrel vaults.

II. Anisotropy and compressive strength evaluation of solid fired clay bricks by testing small specimens

Future works could address the extension of the experimental database to a largest sample of solid clay bricks, as well as a detailed study of the possible influence of the material's porosity on the compressive strength and anisotropy. This extension would allow

a deeper confirmation of the results herein presented regarding the suitability of the proposed small cubic specimen and the anisotropy of different brick types.

III. Effect of cross section aspect ratio and bearing surfaces treatment on the compressive strength of solid fired clay brick specimens

As this research has focused on solid fired clay bricks, future works could address the extension of the experimental database by including the application to different materials, such as mudbricks, fly ash clay bricks, concrete units, and calcium silicate bricks. The results could be also extended to bricks obtained through different manufacturing processes, such as dry pressed into a mould or mechanically extruded in different directions.

IV. Influence of specimen slenderness and stacking on the experimental strength of solid fired clay bricks

Future research may pursue the extension of the experimental database by including a much larger sample of different brick materials, e.g. derived from manufacture processes such as bricks dry pressed into mould or mechanically extruded in different directions. Likewise, more in-depth research is necessary on the shape factors for slenderness above 3.0 in order to better understand the influence of slenderness on the compressive strength of masonry units.

V. Experimental evaluation of the elastic modulus of solid fired clay bricks and correlation with compressive strength

Future research could expand the experimental database to include a larger sample of solid clay bricks. Additionally, a more detailed study of the potential impact of porosity on the elastic modulus and anisotropy could be conducted. Furthermore, to investigate the elastic modulus across the thickness, stacked specimens could be employed. The values of stacked and unstacked specimens could be compared in specimens tested along three orientations, i.e., length, width, and thickness.

VI. Laboratory an in-situ characterisation of masonry components by comparing destructive and minor destructive techniques

Future works could address the extension of the experimental database by including the application to a large sample of different brick and mortar materials. Likewise, further in-depth research of the HPT technique is needed.

Bibliography

[1] Railway Technical Publications (UIC), Leaflet 778-3R: Recommendations for the inspection, assessment and maintenance of masonry arch bridges, (1995).

[2] Deutsche Norm, DIN 18555-9:2019-04 Testing of mortar containing mineral binders - Part 9: Determining the compressive strength of hardened mortar, (2019).

[3] European Committee for Standardization (CEN), EN 1996-1-1:2011+A1:2013 Eurocode 6 - Design of masonry structures - Part 1-1: General rules for reinforced and unreinforced masonry structures, (2013).

[4] Masonry Standard Joint Committe (MSJC), ACI 503.1-05/ASCE 6-05 / TMS 602-05) Specification for masonry structures, (2005).

[5] F.M. Khalaf, A.W. Hendry, Masonry unit shape factors from test results, in: Proc. Br. Mason. Soc., Stoke on Trent, 1994: pp. 136–139. https://www.masonry.org.uk/downloads/masonry-unit-shape-factors-from-test-results/.

[6] European Committee for Standardization (CEN), EN 1015-11:2020 Methods of test for mortar for masonry - Part 11: Determination of flexural and compressive strength of hardened mortar, (2020).

[7] J. Segura, L. Pelà, P. Roca, Monotonic and cyclic testing of clay brick and lime mortar masonry in compression, Constr. Build. Mater. 193 (2018) 453–466. https://doi.org/10.1016/j.conbuildmat.2018.10.198.

[8] American Society for Testing and Materials (ASTM), C39/C39M-21 Standard Test Method for Compressive Strength of Cylindrical Concrete Specimens, (2021). http://www.astm.org/cgi-bin/resolver.cgi?C39C39M.

[9] European Committee for Standardization (CEN), EN 772-1:2011+A1:2016 Methods of test for Masonry Units - Part 1: Determination of Compressive Strength, (2016).

[10] Standards Council of Canada, CAN/CSA A82:14 (R2018) Fired masonry brick made from clay or shale, (2018). https://www.csagroup.org/store/product/CAN%25100CSA-A82-14/.

[11] Australian Standards, AS/NZS 4456.4 Masonry units and segmental pavers and flags - Methods of test Determining compressive strength of masonry units, (2003).

[12] N. Makoond, A. Cabané, L. Pelà, C. Molins, Relationship between the static and dynamic elastic modulus of brick masonry constituents, Constr. Build. Mater. 259 (2020) 120386. https://doi.org/10.1016/j.conbuildmat.2020.120386.

[13] Á. Truñó, Construcción de bóvedas tabicadas, Instituto Juan de Herrera, 2004.

[14] L. Moya, Bóvedas tabicadas, Ministerio de la Gobernación Dirección General de Arquitectura Servicio de Publicaciones, 1947. http://dgha.gob.do/.

[15] R. Gulli, Arte y técnica de la construcción tabicada, in: S. Huerta (Ed.), Las Bóvedas Guastavino En América, Instituto Juan de Herrera, 2001: pp. 59–72. https://bovedastabicadas.files.wordpress.com/2014/02/gulli-2001_arte-y-tc3a9cnica-de-la-construccic3b3n-tabicada.pdf.

[16] S. Huerta, The Mechanics of Timbrel Vaults: A Historical Outline, in: A. Becchi, M. Corradi, F. Foce, O. Pedemonte (Eds.), Essays Hist. Mech. Mem. Clifford Ambrose Truesdell Edoardo Benvenuto, Birkhäuser Basel, Basel, 2003: pp. 89–134. https://doi.org/10.1007/978-3-0348-8091-6_5.

[17] N. Zawisny, C. Fivet, J. Ochsendorf, Guastavino design of the 1909 thin brick dome of the Cathedral of St John the Divine, Constr. Hist. 32 (2017) 39–66. https://doi.org/10.2307/26476167.

[18] F.L. de San Nicolás, Arte y uso de la arquitectura: con el primer libro de Euclides traducido en castellano: primera parte, 1796. http://bibliotecadigital.jcyl.es/i18n/consulta/registro.cmd?id=13394.

[19] F.-F. d'Espié, Manière de rendre toutes sortes d'édifices incombustibles; ou Traité sur la construction des voûtes, faites avec des briques et du plâtre, dites voûtes plates, et d'un toit de brique, sans charpente, appelé comble briqueté., 1754.

[20] M.-A. Laugier, Essai sur l'architecture, 1753.

[21] E. Martínez, El proyecto de bóvedas tabicadas siguiendo reglas de proporción, in: Actas Del Décimo Congr. Nac. y Segundo Congr. Int. Hispanoam. Hist. La Construcción, Instituto Juan de Herrera, Donostia-San Sebastián, 2017: pp. 1367–1380. https://doi.org/http://oa.upm.es/22064/.

[22] J.L. González, Configuración constructiva de las bóvedas «convexas» de la iglesia de la Colonia Güell, obra de Antonio Gaudí, in: A. Graciani, S. Huerta, E. Rabasa, M. Tabales (Eds.), Actas Del Terc. Congr. Nac. Hist. La Construcción, Sevilla, I. Juan de Herrera, SEdHC, U. Sevilla, Junta Andalucía, COAAT Granada, CEHOPU, 2000: pp. 431–436.

[23] J.M. Adell, A. García Santos, Gaudí y las bovedas de las escuelas de la Sagrada Familia, Inf. La Construcción. 56 (2005) 31–45. https://doi.org/10.3989/ic.2005.v57.i496.461.

[24] R. Guastavino, Essay on the theory and history of cohesive construction, applied especially to the timbrel vault, Boston, 1893. http://www.antichefornaci.it/files/biblioteca/Guastavino_Essay_on_the_theory_and_history_of_cohesive_construction_applied_especially_to_the_timbrel_ vault.pdf.

[25] E.F. Stevens, Rafael Guastavino stands on recently laid tile arch along Boylston Street, construction of the McKim Building, (1889).

https://www.digitalcommonwealth.org/search/commonwealth:ms35tx59m.

[26] C. Comas, Sala de tissatges, (1907).

[27] W. Dunn, Notes on the stresses in framed spires and domes, J. R. Inst. Br. Archit. 11 (1904) 401–412. https://archive.org/details/in.ernet.dli.2015.56181/page/n471/mode/2up.

[28] S. Huerta, Mechanics of masonry vaults: The equilibrium approach, in: P. Lourenço, P. Roca (Eds.), Hist. Constr. 2001, Possibilities Numer. Exp. Tech. Proc. 3rd Int. Semin., Guimarães, 2001: pp. 47–70. https://www.researchgate.net/publication/39424866_Mechanics_of_masonry_vaults_The_equilibrium_approach.

[29] J. Heyman, The stone skeleton, Int. J. Solids Struct. 2 (1966) 249–279. https://doi.org/10.1016/0020-7683(66)90018-7.

[30] P. Roca, M. Cervera, G. Gariup, L. Pela', Structural analysis of masonry historical constructions. Classical and advanced approaches, 2010. https://doi.org/10.1007/s11831-010-9046-1.

[31] A. Paricio, Secrets d'un sistema constructiu: l'Eixample, Edicions UPC, 2001. http://library1.nida.ac.th/termpaper6/sd/2554/19755.pdf.

[32] J.G. de Churtichaga, Aspectos constructivos de la reconstruccion de Villanueva de la Cañada. El uso de los sistemas de bóvedas tabicadas y su perspectiva histórica, Conarquitectura. 8 (2003) 81–93. http://www.chqs.net/archivos/informes/archivo_13_articulo_villanueva.pdf.

[33] R. Lacuesta, Catalan industrial architecture in the last quarter of the 19th century and first quarter of the 20th century, Catalan Hist. Rev. 75 (2017) 59–75. https://doi.org/10.2436/20.1000.01.132.

[34] A. Feu i Jordana, Les voltes de rajola doblada: Construcció i seguretat estructural de les esglésies barroques catalanes, Universitat Politècnica de Catalunya, 2017. http://upcommons.upc.edu/tesis.

[35] R. Gulli, La memoria delle tecniche: Le Corbusier e la volta catalana, Clua edizioni, 1994.

[36] J.M. Adell, A. Rolando, Luis Moya y las bóvedas tabicadas en la posguerra española, Inf. La Construcción. 56 (2005) 25–29. https://doi.org/10.3989/ic.2005.v57.i496.460.

[37] A.J. Mas, J.M. Adell, Eladio Dieste y la cerámica estructural en Uruguay, Inf. La Construcción. 56 (2005) 13–23. https://doi.org/10.3989/ic.2005.v57.i496.459.

[38] ICOMOS, ICOMOS (2003) - ICOMOS Charter, Princ. Anal. Conserv. Struct. Restor. Archit. Herit. (2003) 3–6. https://www.icomos.org/charters/structures_e.pdf.

[39] D. López, T. Van Mele, P. Block, La bóveda tabicada en el siglo XXI, Inf. La Construcción. 68 (2016) 162. https://doi.org/10.3989/ic.15.169.m15.

[40] P. Block, M. Rippmann, Das katalanische Gewölbe – Ein Konstruktionsprinzip mit Geschichte und Zukunft / The Catalan Vault – A Historical Structural Principle with

a Bright Future, DETAIL. 5 (2013) 528–536.

[41] P. Block, J. Ochsendorf, Thrust network analysis: A new methodology for three-dimensional equilibrium, J. Int. Assoc. Shell Spat. Struct. 48 (2007) 167–173.

[42] M. Rippmann, L. Lachauer, P. Block, Interactive vault design, Int. J. Sp. Struct. 27 (2012) 219–230. https://doi.org/10.1260/0266-3511.27.4.219.

[43] D. López, M. Domènech, M. Palumbo, "Brick-topia", the thin-tile vaulted pavilion, Case Stud. Struct. Eng. 2 (2014) 33–40. https://doi.org/10.1016/j.csse.2014.09.001.

[44] D. López, M. Domènech, J. Brazo, P. Block, Thin-tile vault for the Seventh World Urban Forum in Medellín, IASS-SLTE 2014 Symp. (2014). http://www.block.arch.ethz.ch/brg/files/lopezlopez-2014-iass-thin-tile-vault-seventh-world-urban-forum-medellin-2014_1410359059.pdf.

[45] L. Pelà, P. Roca, A. Aprile, Combined In-Situ and Laboratory Minor Destructive Testing of Historical Mortars, Int. J. Archit. Herit. 12 (2018) 334–349. https://doi.org/10.1080/15583058.2017.1323247.

[46] D. Marastoni, L. Pelà, A. Benedetti, P. Roca, Combining Brazilian tests on masonry cores and double punch tests for the mechanical characterization of historical mortars, Constr. Build. Mater. 112 (2016) 112–127. https://doi.org/10.1016/j.conbuildmat.2016.02.168.

[47] American Society for Testing and Materials (ASTM), C67/C67M-21 Standard Test Methods for Sampling and Testing Brick and Structural Clay Tile, (2021). https://doi.org/10.1520/C0067_C0067M-21.

[48] M. Van J.G.M., Strain-Softening of Concrete under Multiaxial Loading Conditions., Tech. Hogesch. Eindhoven. (1984). https://doi.org/10.6100/IR145193.

[49] D.L. López, M.D. Rodríguez, Tile vaults. Structural analysis and experimentation / Voltes de maó de pla. Anàlisi estructural i experimentació / Bóvedas tabicadas. Análisis estructural y experimentación, 2015.

[50] D. López, M. Doménech, M. Palumbo, Using a construction technique to understand it: thin-tile vaulting, in: Universidade do Minho (Ed.), SAHC2014 – 9th Int. Conf. Struct. Anal. Hist. Constr., 2014. http://www.hms.civil.uminho.pt/sahc/2014/topic13-fullpaper037.pdf.

[51] J. Llorens, M. Llorens, M.A. Chamorro, J. Gómez, C. Barris, Experimental study on the vertical interface of thin-tile masonry, Constr. Build. Mater. 261 (2020) 119976. https://doi.org/10.1016/j.conbuildmat.2020.119976.

[52] J. Llorens, M. Llorens, M.A. Chamorro, J. Soler, Experimental Behavior of Brick Masonry under Uniaxial Compression on Parallel-to-Face Brick. Single-Leaf Case Study, Int. J. Archit. Herit. 14 (2020) 23–37. https://doi.org/10.1080/15583058.2018.1503361.

[53] J. Llorens, M.À. Chamorro, J. Fontàs, M. Alcalà, M. Delgado-Aguilar, F. Julián, M. Llorens, Experimental Behavior of Thin-Tile Masonry under Uniaxial Compression.

Multi-Leaf Case Study, Materials (Basel). 14 (2021) 2785. https://doi.org/10.3390/ma14112785.

[54] A. Fódi, Effects influencing the compressive strength of a solid, fired clay brick, Period. Polytech. Civ. Eng. 55 (2011) 117. https://doi.org/10.3311/pp.ci.2011-2.04.

[55] P.B. Lourenço, F.M. Fernandes, F. Castro, Handmade Clay Bricks: Chemical, Physical and Mechanical Properties, Int. J. Archit. Herit. 4 (2010) 38–58. https://doi.org/10.1080/15583050902871092.

[56] P. Matysek, M. Witkowski, A Comparative Study on the Compressive Strength of Bricks from Different Historical Periods, Int. J. Archit. Herit. 10 (2016) 396–405. https://doi.org/10.1080/15583058.2013.855838.

[57] J. Morton, M.D. Kotsovos, M.N. Pavlovvic, S.M. Seraj, An initial investigation of the shape factor platen effects when testing masonry units to determine the material compressive strength, in: Proc. 9th Int. Brick Block Mason. Conf., 1991: pp. 653–661. http://www.hms.civil.uminho.pt/ibmac/1991/653.pdf.

[58] G. Schickert, Formfaktoren der Betondruckfestigkeit, Die Bautechnik. Ausgabe B. 58 (1981) 52–57.

[59] A.M. Neville, Properties of concrete, Pearson Education Limited, 2011. http://www.crcnetbase.com/doi/10.1201/b10546-17.

[60] European Committee for Standardization (CEN), EN 772-16:2011 Methods of test for masonry units - Part 16: Determination of dimensions, (2011).

[61] European Committee for Standardization (CEN), EN 772-13:2001 Methods of test for masonry units. Part 13: Determination of net and gross dry density of masonry units (except for natural stone), (2001).

[62] European Committee for Standardization (CEN), EN 772-3:1999 Methods of test for masonry units. Part 3: Determination of net volume and percentage of voids of clay masonry units by hydrostatic weighing, (1999).

[63] European Committee for Standardization (CEN), EN 772-21:2011 Methods of test for masonry units. Part 21: Determination of water absorption of clay and calcium silicate masonry units by cold water absortion, (2011).

[64] P.B. Lourenço, J.C. Almeida, J.A. Barros, Experimental Investigation of Bricks Under Uniaxial Tensile Testing, J. Br. Mason. Soc. Mason. Int. 18 (2005).

[65] European Committee for Standardization (CEN), EN 998-2:2018 Specification for mortar for masonry. Part 2: Masonry mortar, (2018).

[66] COMET, Coupled Mechanical and Thermal analysis, http://www.cimne.com/comet/, (2016).

[67] GiD v.14.0.4, The personal pre and post-processor, http://www.gidhome.com/, (2020).

[68] R. Faria, J. Oliver, M. Cervera, A strain-based plastic viscous-damage model for massive concrete structures, Int. J. Solids Struct. 35 (1998) 1533–1558. https://doi.org/10.1016/S0020-7683(97)00119-4.

[69] M. Petracca, L. Pelà, R. Rossi, S. Oller, G. Camata, E. Spacone, Regularization of first order computational homogenization for multiscale analysis of masonry structures, Comput. Mech. 57 (2016) 257–276. https://doi.org/10.1007/s00466-015-1230-6.

[70] J. Lubliner, J. Oliver, S. Oller, E. Oñate, A plastic-damage model for concrete, Int. J. Solids Struct. 25 (1989) 299–326. https://doi.org/10.1016/0020-7683(89)90050-4.

[71] L. Pelà, S. Saloustros, P. Roca, Cylindrical samples of brick masonry with aerial lime mortar under compression: Experimental and numerical study, Constr. Build. Mater. 227 (2019) 116782. https://doi.org/10.1016/j.conbuildmat.2019.116782.

[72] M. Angelillo, P.B. Lourenço, G. Milani, Masonry behaviour and modelling, in: Mech. Mason. Struct., 2014. https://doi.org/10.1007/978-3-7091-1774-3.

[73] S. Saloustros, M. Cervera, L. Pelà, Tracking multi-directional intersecting cracks in numerical modelling of masonry shear walls under cyclic loading, Meccanica. 53 (2018) 1757–1776. https://doi.org/10.1007/s11012-017-0712-3.

[74] A.W. Hendry, Structural Masonry, Iowa State Univ. Bull. 59 (1998). https://doi.org/10.1007/978-1-349-14827-1.

[75] K.J. Krakowiak, P.B. Lourenço, F.J. Ulm, Multitechnique Investigation of Extruded Clay Brick Microstructure, J. Am. Ceram. Soc. 94 (2011) 3012–3022. https://doi.org/10.1111/j.1551-2916.2011.04484.x.

[76] A.W. Page, A study of the influence of brick size on the compressive strength of calcium silicate masonry, University of Newcastle Faculty of Engineering, 1984.

[77] L. Binda, G. Mirabella Roberti, C. Tiraboschi, S. Abbaneo, Measuring masonry material properties, in: Proc. U.S.-Italy Work. Guidel. Seism. Eval. Rehabil. Unreinforced Mason. Build., National Center for Earthquake Engineering Research, Pavia, Italy, 1994: pp. 326–347.

[78] J.E. Aubert, P. Maillard, J.C. Morel, M. Al Rafii, Towards a simple compressive strength test for earth bricks?, Mater. Struct. 49 (2016) 1641–1654. https://doi.org/10.1617/s11527-015-0601-y.

[79] D. V. Oliveira, P.B. Lourenço, P. Roca, Cyclic behaviour of stone and brick masonry under uniaxial compressive loading, Mater. Struct. 39 (2007) 247–257. https://doi.org/10.1617/s11527-005-9050-3.

[80] P. Salvatoni, M. Ugolini, Comportamento di elementi in muratura fino a collasso: prove sperimentali e modellazione numerica, Politecnico di Milano, 2016. https://www.politesi.polimi.it/bitstream/10589/133545/3/2017_04_Ugolini_Salvatoni.pdf.

[81] European Committee for Standardization (CEN), EN 12390-1:2022 Testing hardened concrete - Part 1: Shape, dimensions and other requirements for specimens and moulds, (2001).

[82] European Committee for Standardization (CEN), EN 12390-3:2020 Testing

hardened concrete. Part 3: Compressive strength of test specimens, (2020).

[83] TC 76-LUM, LUMD1 - Removal and testing of specimens from existing masonry, in: RILEM (Ed.), Tech. Recomm. Test. Use Constr. Mater., 1st Editio, London, 1991: pp. 501–502. https://doi.org/https://doi.org/10.1201/9781482271362.

[84] American Society for Testing and Materials (ASTM), C42/C42M-20 Standard Test Method for Obtaining and Testing Drilled Cores and Sawed Beams of Concrete, (2018). https://doi.org/10.1520/C0042_C0042M-18.

[85] L. Schueremans, Probabilistic evaluation of structural unreinforced masonry, Katholieke Universiteit Leuven, 2001. https://lirias.kuleuven.be/handle/123456789/160474.

[86] W.H. Kruskal, W.A. Wallis, Use of Ranks in One-Criterion Variance Analysis, J. Am. Stat. Assoc. 47 (1952) 583–621. https://doi.org/10.1080/01621459.1952.10483441.

[87] F. Wilcoxon, Individual Comparisons by Ranking Methods, Biometrics Bull. 1 (1945) 80. https://doi.org/10.2307/3001968.

[88] S. Habelitz, G. Carl, C. Rüssel, Processing, microstructure and mechanical properties of extruded mica glass-ceramics, Mater. Sci. Eng. A. 307 (2001) 1–14. https://doi.org/10.1016/S0921-5093(00)01968-7.

[89] A. Viani, R. Ševčík, M.-S. Appavou, A. Radulescu, Evolution of fine microstructure during firing of extruded clays: A small angle neutron scattering study, Appl. Clay Sci. 166 (2018) 1–8. https://doi.org/10.1016/j.clay.2018.09.002.

[90] M. Kubiś, K. Pietrak, Ł. Cieślikiewicz, P. Furmański, M. Wasik, M. Seredyński, T.S. Wiśniewski, P. Łapka, On the anisotropy of thermal conductivity in ceramic bricks, J. Build. Eng. 31 (2020). https://doi.org/10.1016/j.jobe.2020.101418.

[91] J. Bourret, N. Tessier-Doyen, R. Guinebretiere, E. Joussein, D.S. Smith, Anisotropy of thermal conductivity and elastic properties of extruded clay-based materials: Evolution with thermal treatment, Appl. Clay Sci. 116–117 (2015) 150–157. https://doi.org/10.1016/j.clay.2015.08.006.

[92] N. Makoond, L. Pelà, C. Molins, Dynamic elastic properties of brick masonry constituents, Constr. Build. Mater. 199 (2019) 756–770. https://doi.org/10.1016/j.conbuildmat.2018.12.071.

[93] P. Maillard, J.E. Aubert, Effects of the anisotropy of extruded earth bricks on their hygrothermal properties, Constr. Build. Mater. 63 (2014) 56–61. https://doi.org/10.1016/j.conbuildmat.2014.04.001.

[94] D. Antal, T. Húlan, A. Trník, I. Štubňa, J. Ondruška, The Influence of Texture and Firing on Thermal and Elastic Properties of Illite-Based Ceramics, Adv. Mater. Res. 1126 (2015) 53–58. https://doi.org/10.4028/www.scientific.net/AMR.1126.53.

[95] K. Boussois, S. Deniel, N. Tessier-Doyen, D. Chateigner, C. Dublanche-Tixier, P. Blanchart, Characterization of textured ceramics containing mullite from phyllosilicates, Ceram. Int. 39 (2013) 5327–5333.

https://doi.org/10.1016/j.ceramint.2012.12.038.

[96] F. Händle, The Art of Ceramic Extrusion, Springer International Publishing, Cham, 2019. https://doi.org/10.1007/978-3-030-05255-3.

[97] R. Bartusch, F. Händle, Laminations in Extrusion, in: F. Händle (Ed.), Extrus. Ceram. Eng. Mater. Process., Springer, Berlin, Heidelberg, 2009: pp. 187–210. https://doi.org/10.1007/978-3-540-27102-4_10.

[98] F.E. Grubbs, Sample Criteria for Testing Outlying Observations, Ann. Math. Stat. 21 (1950) 27–58. https://doi.org/10.1214/aoms/1177729885.

[99] R.B. Murphy, On test for outlying observations, Princeton University, 1951.

[100] R.G. McMillan, Tests for one or two outliers in normal samples with unknown variance, Technometrics. 13 (1971) 87–100. https://doi.org/10.1080/00401706.1971.10488756.

[101] S.M. Bendre, Masking and Swamping Effects on Tests for Multiple Outliers in Normal Sample, Commun. Stat. - Theory Methods. 18 (1989) 697–710. https://doi.org/10.1080/03610928908829928.

[102] S. Shapiro, M.B. Wilk, An Analysis of Variance Test for Normality (Complete Samples), Biometrika. 52 (1965) 591–611. http://www.jstor.org/stable/2333709.

[103] A. Cabané, L. Pelà, P. Roca, Anisotropy and compressive strength evaluation of solid fired clay bricks by testing small specimens, Constr. Build. Mater. 344 (2022) 128195. https://doi.org/10.1016/j.conbuildmat.2022.128195.

[104] A.W. Page, R. Marshall, The influence of brick and brickwork prism aspect ratio on the evaluation of compressive strength, in: Proc. 7th Int. Brick Block Mason. Conf., Melbourne, Australia, 1985: pp. 653–664.

[105] W.M. Murray, Discussion, in: ASTM Proc., American Society for Testing and Materials (ASTM), 1942: pp. 1047–1048.

[106] H.K. Hilsdorf, Die Bestimmung der zweiachsigen Festigkeit des Betons, Schriftenr. Des DAfStb. 173 (1965) 68.

[107] H. Kupfer, H.K. Hilsdorf, H. Rusch, Behavior of Concrete Under Biaxial Stresses, ACI J. Proc. 66 (1969) 656–666. https://doi.org/10.14359/7388.

[108] K. Thomas, D.C. O'Leary, Tensile Strength Tests on Two Types of Brick, in: 2nd Int. Brick Block Mason. Conf., Stoke-on-Trent, England, 1970: pp. 69–74. http://www.hms.civil.uminho.pt/ibmac/1970/69.pdf.

[109] L. Binda, C. Tiraboschi, S. Abbaneo, Experimental Research to Characterise Masonry Materials, Mason. Int. 10 (1997) 92–101.

[110] A.W. Page, P.W. Kleeman, The influence of capping material and platen restraint on the failure of hollow masonry units and prisms, in: Proc. Ninth Int. Brick/Block Mason. Conf., Berlin, 1991: pp. 662–670.

[111] A. Hussein, H. Marzouk, Finite element evaluation of the boundary conditions for biaxial testing of high strength concrete, Mater. Stuctures. 33 (2000) 299–308.

https://doi.org/https://doi.org/10.1007/BF02479700.

[112] G. Schickert, On the influence of different load application techniques on the lateral strain and fracture of concrete specimens, Cem. Concr. Res. 3 (1973) 487–494. https://doi.org/10.1016/0008-8846(73)90087-2.

[113] G. Schickert, H. Winkler, Versuchsergebnisse Zur Festigkeit Und Verformung Von Beton Bei Mehraxialer Druckbeanspruchung, Dtsch Ausschuss Stahlbet. (1977). https://opus4.kobv.de/opus4-bam/frontdoor/index/index/year/2015/docId/404.

[114] G. Schickert, Schwellenwerte beim Betondruckversuch, Dtsch. Ausschuss Fuer Stahlbet. (1980). https://opus4.kobv.de/opus4-bam/frontdoor/index/index/year/2015/docId/380.

[115] H.F. Gonnerman, Effect of End Condition of Cylinder on Compressive Strength of Concrete, ASTM Proc. 24. Part I (1924) 1036–1065. https://catalog.hathitrust.org/Record/102103985.

[116] W.F. Purrington, J. McCornick, A Simple Device to obviate Capping of Concrete Specimens, in: ASTM Proc., American Society for Testing and Materials (ASTM), 1926: pp. 488–492.

[117] D.D. McGuire, Testing Concrete Cylinders Using Confined Sand Cushion, in: ASTM Proc., American Society for Testing and Materials (ASTM), 1930: pp. 515–517.

[118] P.J. Freeman, Capping Device for Concrete Cylinders, in: Eng. News-Record, 1928: p. 111.

[119] P.J. Freeman, Method of Capping Concrete Cylinders Using Sulfur Compound, in: ASTM Proc., American Society for Testing and Materials (ASTM), 1930: pp. 518–520.

[120] G.E. Troxell, The Effect of Capping Methods and End Conditions Before Capping Upon Compressive Strength of Concrete Test Cylinders, in: ASTM Proc., American Society for Testing and Materials (ASTM), 1941: pp. 1039–1052.

[121] E.N. Vidal, R.F. Blanks, Absorbtive Form Lining, in: Int. Concr. Abstr. Portal - J. Proc., 1942: pp. 253–268. https://www.concrete.org/publications/internationalconcreteabstractsportal/m/details/id/8600.

[122] F.M. Masters, A.C. Loewer, The Effects of Capping Materials on the Apparent Strength of Concrete Specimens, in: AS, American Society for Testing and Materials (ASTM), 1952: pp. 30–36.

[123] G. Werner, The Effect of Capping Material on the Compressive Strength of Concrete Cylinders, in: ASTM Proc., American Society for Testing and Materials (ASTM), 1958: pp. 1166–1186.

[124] K.L. Saucier, Effect of Method of Preparation of Ends of Concrete Cylinders for Testing., U S Army Eng Waterw Exp Stn, Misc Pap C-72-12. (1972).

[125] C. Ozyildirim, Neoprene Pads for Capping Concrete Cylinders, Cem. Concr.

Aggregates. 7 (1985) 25. https://doi.org/10.1520/CCA10040J.

[126] P.M. Carrasquillo, R.L. Carrasquillo, Effect of Using Unbonded Capping Systems on the Compressive Strength of Concrete cylinders, Mater. J. 85 (1987) 141–147. https://www.concrete.org/publications/internationalconcreteabstractsportal/m/details/id/1799.

[127] D. Richardson, Effects of testing variables' effects on the comparison of neoprene pad and sulfur mortar-capped concrete test cylinders, ACI Mater. J. 87 (1990) 489–495. https://www.concrete.org/publications/internationalconcreteabstractsportal.aspx?m=details&i=1890.

[128] B. Chojnacki, P. Read, Compressive Strength Test Procedures for Testing High Strength Concrete: Final Report, (1991).

[129] M.F. Pistilli, T. Willems, Evaluation of Cylinder Size and Capping Method in Compression Strength Testing of Concrete, Cem. Concr. Aggregates. 15 (1993). https://doi.org/10.1520/CCA10588J.

[130] M. Lessard, O. Challal, P.-C. Aticin, Testing High-Strength Concrete Compressive Strength, Mater. J. 90 (1993) 303–307. https://www.concrete.org/publications/internationalconcreteabstractsportal/m/details/id/3876.

[131] C.W. French, A. Mokhtarzadeh, High Strength Concrete: Effects of Materials, Curing and Test Procedures on Short-Term Compressive Strength, PCI J. 38 (1993) 76–87. https://doi.org/10.15554/pcij.05011993.76.87.

[132] N.J. Carino, G. William F., Effects of Testing Variables on the Measured Compressive Strength of High-Strength (90 MPa) Concrete, National Bureau of Standards, Gaithersburg, Maryland, 1994. https://nvlpubs.nist.gov/nistpubs/Legacy/IR/nistir5405.pdf.

[133] J.G.M. van Mier, S.P. Shah, M. Arnaud, J.P. Balayssac, A. Bascoul, S. Choi, D. Dasenbrock, G. Ferrara, C. French, M.E. Gobbi, B.L. Karihaloo, G. König, M.D. Kotsovos, J. Labuz, D. Lange-Kornbak, G. Markeset, M.N. Pavlovic, G. Simsch, K.-C. Thienel, A. Turatsinze, M. Ulmer, H.J.G.M. van Geel, M.R.A. van Vliet, D. Zissopoulos, Strain-softening of concrete in uniaxial compression, Mater. Struct. 30 (1997) 195–209. https://doi.org/10.1007/BF02486177.

[134] N.W. Kelch, F.E. Emme, Effect of Type, Thickness, and Age of Capping Compounds on the Apparent Compressive Strength of Brick, ASTM Bull. 230. (1958) 38–41.

[135] C.M. Dodd, T.D. McGee, A comparison of various methods of capping brick, structural tile, and concrete block for compressive strength tests, Iowa State Univ. Bull. 59 (1960) 1–11. https://iucat.iu.edu/catalog/6584165.

[136] E.H. Morsy, Mortar properties influencing brickwork strength - Chapter 6: The influence of end and joint conditions of different rigidities on the failure characteristics of bricks and brick masonry, University of Edimburg, 1968.

http://hdl.handle.net/1842/12695.

[137] F.M. Khalaf, A.W. Hendry, Effect of bed-face preparation in compressive testing of masonry units, in: Proc. 2nd Int. Mason. Conf., London, 1989: pp. 129–130. https://www.masonry.org.uk/downloads/effect-of-bed-face-preparation-in-compressive-testing-of-masonry-units/.

[138] W. Templeton, G.J. Edgell, The Compressive Strength of Clay Bricks Ground or Mortar Capped, Mason. Int. 4 (1990) 66–67. https://www.masonry.org.uk/downloads/the-compressive-strength-of-clay-bricks-ground-or-mortar-capped/.

[139] International Standard, ISO 9652 Masonry - Part 4: Test methods (Withdrawn), (2000).

[140] R.G. Drysdale, A.A. Hamid, L.R. Baker, Masonry Materials, in: Prentice-Hall Inc. (Ed.), Mason. Struct. Behav. Des., Englewood Cliffs, New Jersey, 1994: pp. 112–181.

[141] L. Crouch, M. Knight, R. Henderson, W. Sneed, Unbonded Capping for Concrete Masonry Units, Mason. Mater. Testing, Appl. (1999) 62–74. https://doi.org/10.1520/STP14201S.

[142] I.M. Daniel, A.J. Durelli, Photothermoelastic analysis of bonded propellant grains, Exp. Mech. 1 (1961) 97–104. https://doi.org/10.1007/BF02324072.

[143] G.C. Braga, L.C. Mendes, Analysis of Neoprene Bearings on Requests and Strains, Int. J. Appl. Eng. Res. 15 (2020) 40–47. https://www.ripublication.com/ijaer20/ijaerv15n1_06.pdf.

[144] P.W. Kleeman, A.W. Page, The in-situ properties of packing materials used in compression tests, Mason. Int. 4 (1990) 68–74.

[145] J. Nichols, Y. Totoev, Experimental determination of the dynamic Modulus of Elasticity of masonry units, 15th Aust. Conf. Mech. Struct. Mater. (2013) 1–7.

[146] American Society for Testing and Materials (ASTM), C140/C140M-22b Standard test methods for Sampling and Testing Concrete Masonry Units and Related Units, (2022). https://doi.org/10.1520/C0140-13.

[147] American Society for Testing and Materials (ASTM), C1552-16 Standard Practice for Capping Concrete Masonry Units, Related Units and Masonry Prisms for Compression Testing, (2016). https://doi.org/10.1520/C1552-16.

[148] Standards Council of Canada, CAN/CSA A165 SERIES-14 (R2019) Standards on concrete masonry units, (2019). https://www.csagroup.org/store/product/2702048/.

[149] American Society for Testing and Materials (ASTM), C617-10 Standard Practice for Capping Cylindrical Concrete Specimens, (2010). https://doi.org/10.1520/C0617-10.

[150] American Society for Testing and Materials (ASTM), C1231/C1231M-14: Standard Practice for Use of Unbonded Caps in Determination of Compressive Strength of Hardened Concrete Cylinders, (2014). https://doi.org/10.1520/C1231_C1231M-14.

[151] J. Ghadami, M. Nematzadeh, Effect of bond shear stress on compressive behaviour

of steel tube-confined concrete with active and passive confinement, Eur. J. Environ. Civ. Eng. 22 (2018) 783–810. https://doi.org/10.1080/19648189.2016.1219878.

[152] European Committee for Standardization (CEN), EN 772-4 Methods of test for masonry units. Part 4: Determination of real and bulk density and of total and open porosity for natural stone masonry units, (1999).

[153] European Committee for Standardization (CEN), EN 772-11 Methods of test for masonry units. Part 11: Determination of water absorption of aggregate concrete, autoclaved aerated concrete, manufactured stone and natural stone masonry units due to capillary action and the initial rate of water absorption, (2011).

[154] Bureau of Indian Standards, IS 3495 Methods of Tests of Burnt Clay building brick - Part 1: Determination of compressive strength, (2002).

[155] T. 76-LUM, LUMA.1 - Compressive strength of masonry units, in: RILEM (Ed.), Tech. Recomm. Test. Use Constr. Mater., 1st Editio, London, 1991: pp. 456–458. https://doi.org/https://doi.org/10.1201/9781482271362.

[156] A. Delibes, G. Gonzalez, Estudio de la influencia que los distintos tipos de refrentado ejercen en el ensayo a compresión de probetas de hormigón, Inf. La Construcción. 29 (1976) 67–73. https://informesdelaconstruccion.revistas.csic.es/index.php/informesdelaconstruccion/article/view/2745/3055.

[157] R. Hooton, C. Lobo, G. Mullings, R. Gaynor, Effect of capping materials and procedures on the measured compressive strength of high-strength concrete, Cem. Concr. Aggregates. 16 (1994) 173. https://doi.org/10.1520/CCA10296J.

[158] D.N. Richardson, Effects of testing variables on the comparison of neoprene pad and sulfur mortar-capped concrete test cylinders, ACI Mater. J. 87 (1990) 489–495. https://doi.org/10.14359/1890.

[159] ACICommittee 234, ACI 234R-96 Guide for the Use of Silica Fume in Concrete, (2000).

[160] P. Stroeven, Geometric probability approach to the examination of microcracking in plain concrete, J. Mater. Sci. 14 (1979) 1141–1151. https://doi.org/https://doi.org/10.1007/BF00561298.

[161] M.D. Kotsovos, Fracture processes of concrete under generalised stress states Fracture processes of concrete under generalised stress states, Matériaux Constr. 12 (1979) 431. https://doi.org/https://doi.org/10.1007/BF02476287.

[162] M.D. Kotsovos, Failure criteria for concrete under generalised stress states, Imperial College of Science and Technology of London, 1974. https://spiral.imperial.ac.uk/bitstream/10044/1/21060/2/Kotsovos-M-1975-PhD-Thesis.pdf.

[163] F.M. Fernandes, P.B. Lourenço, F. Castro, Ancient Clay Bricks: Manufacture and Properties, in: Mater. Technol. Pract. Hist. Herit. Struct., Springer Netherlands,

Dordrecht, 2010: pp. 29–48. https://doi.org/10.1007/978-90-481-2684-2_3.

[164] F.M.C.P. Fernandes, Evaluation of two novel NDT techniques: Microdrilling of clay bricks and Ground Penetrating Radar in masonry, Universidade do Minho, 2006. https://doi.org/10.29327/549675.

[165] G. Wang, X. Zhang, X. Liu, Y. Xu, J. Lu, Microscopic Evolution of Pore Characteristics and Particle Orientation of Granite Residual Soil in One-Dimensional Compression, Geofluids. 2022 (2022) 1–13. https://doi.org/10.1155/2022/8380656.

[166] Y. Nakata, M. Hyodo, A.F.L. Hyde, Y. Kato, H. Murata, Microscopic Particle Crushing of Sand Subjected to High Pressure One-Dimensional Compression, Soils Found. 41 (2001) 69–82. https://doi.org/10.3208/sandf.41.69.

[167] J.G.M. Van Mier, Strain-softening of concrete under multiaxial loading conditions, Technische Hogeschool Eindhoven, 1984. https://doi.org/https://doi.org/10.6100/IR145193.

[168] G.W. Hutchinson, Correction Data for Comparative Test Results From Field Data, in: Am. Concr. Inst., 1923: p. 191.

[169] H.F. Gonnerman, Effect of Size and Shape of Test Specimen on Compressive Strength of Concrete, Struct. Mater. Res. Lab. Lewis Inst. Bulletin 1 (1925).

[170] J.W. Murdock, C.E. Kesler, Effect of Length of Specimen on the Apparent Compressive Strength of Concrete, ASTM Comm. C9 Concr. Concr. Aggregates. (1955).

[171] C.E. Kesler, Effect of length to diameter ratio on compressive strength - an ASTM cooperative investigation, (1959).

[172] B.P. Hughes, B. Bahramian, R.M. Zimmerman, Cube tests and the uniaxial compressive strength of concrete, Mag. Concr. Res. 18 (1966) 161–164. https://doi.org/10.1680/macr.1966.18.56.161.

[173] A. Neville, A General Relation for Strengths of Concrete Specimens of Different Shapes and Sizes, J. Proc. 63 (1996) 1095–1110. https://doi.org/10.14359/7664.

[174] S. Popovics, Relations between various strengths of concrete, in: 46th Symp. Concr. Strength, Highway Research Board, 1966: pp. 67–94. http://onlinepubs.trb.org/Onlinepubs/hrr/1967/210/210-003.pdf.

[175] R. Egermann, Zur nachträglichen Bestimmung der mechanischen Eigenschaften von Mauerziegeln, Erhalt. Hist. Bedeut. Bauwerke. (1990) 159–182.

[176] I. Beer, P. Schubert, Determination of shape factors for masonry units, in: Proc. 13th Int. Brick Block Mason. Conf., Amsterdam, 2004. http://www.hms.civil.uminho.pt/ibmac/2004/218.pdf.

[177] I. Beer, P. Schubert, Sum Einfluss der Steinformate auf die Mauerwerkdruckfestigkeit - Formfaktoren für Mauersteine, Mauerwerk-Kalender 2005. (2005) 89–126.

[178] W. Brameshuber, M. Graubohm, Formfaktoren für Mauersteine, Mauerwerk. 18 (2014) 15–26. https://doi.org/10.1002/dama.201400606.

[179] W. Brameshuber, U. Schmidt, I. Beer, German investigations on shape factors for masonry units and high precision elements, Mason. Int. 20 (2007) 61–68.

[180] M.R.A. van Vliet, J.G.M. van Mier, Experimental investigation of concrete fracture under uniaxial compression, Mech. Cohesive-Frictional Mater. 1 (1996) 115–127. https://doi.org/10.1002/(SICI)1099-1484(199601)1:1<115::AID-CFM6>3.0.CO;2-U.

[181] Comité Euro-International du Béton EPF Lausane, [CEB-FIP] Model Code 1990: Design Code, Thomas Telford Services Ltd, 1993.

[182] Comisión Permanente del Hormigón, EHE-08 Instrucción de Hormigón Estructural, 2010th ed., Ministerio de Fomento, 2008.

[183] J. Tucker, Effect of length on the strength of compressive test specimens, in: Proceedings, ASTM, 1945: p. 976.

[184] A.W. Hendry, B.P. Sinha, S.R. Davies, eds., Design of Masonry Structures, CRC Press, 2017. https://doi.org/10.4324/9780203362402.

[185] Z.P. Bažant, Size effect on structural strength: a review, Arch. Appl. Mech. (Ingenieur Arch. 69 (1999) 703–725. https://doi.org/10.1007/s004190050252.

[186] H.K. Hilsdorf, Masonry Materials and their physical properties, in: Proc. Int. Conf. Struct. Des. Tall Concr. Mason. Build. ASCE, New York, NW, USA, 1972: pp. 981–999.

[187] H.B. Kaushik, D.C. Rai, S.K. Jain, Stress-Strain Characteristics of Clay Brick Masonry under Uniaxial Compression, J. Mater. Civ. Eng. 19 (2007) 728–739. https://doi.org/10.1061/(ASCE)0899-1561(2007)19:9(728).

[188] American Society for Testing and Materials (ASTM), C469/C469-22 Standard Test Method for Static Modulus of Elasticity and Poisson's Ratio of Concrete in Compression, (2022). https://doi.org/10.1520/C0469_C0469M-22.

[189] American Society for Testing and Materials (ASTM), D7012-14 Standard test method for compressive strength and elastic moduli of intact rock core specimens under varying states of stress and temperatures, (2014).

[190] European Committee for Standardization (CEN), EN 12390-13:2022 Testing hardened concrete - Part 13: Determination of secant modulus of elasticity in compression, (2022).

[191] European Committee for Standardization (CEN), EN 14580 Natural stone test methods. Determination of static elastic modulus, (2005).

[192] Associação Brasileira de Normas Técnicas (ABNT), NBR 8522:2017 Concreto – Determinação dos módulos estáticos de elasticidade e de deformação e da curva tensão-deformação, (2017).

[193] L. Pelà, E. Canella, A. Aprile, P. Roca, Compression test of masonry core samples extracted from existing brickwork, Constr. Build. Mater. 119 (2016) 230–240.

https://doi.org/10.1016/j.conbuildmat.2016.05.057.

[194] A. Winnicki, T. Stryszewska, S. Kańka, S. Seręga, Influence of porosity and moisture on mechanical properties of ceramic brick - analytical homogenisation approach, in: Proc. 11th Int. Symp. Brittle Matrix Compos. BMC 2015, 2015: pp. 53–62.

[195] A. Drougkas, P. Roca, C. Molins, Compressive strength and elasticity of pure lime mortar masonry, Mater. Struct. 49 (2016) 983–999. https://doi.org/10.1617/s11527-015-0553-2.

[196] American Society for Testing and Materials (ASTM), E111-17 Standard Test Method for Young's Modulus, Tangent Modulus, and Chord Modulus, (2017). https://doi.org/10.1520/E0111-04R10.

[197] H.B. Kaushik, D.C. Rai, S.K. Jain, Stress-Strain Characteristics of Clay Brick Masonry under Uniaxial Compression, J. Mater. Civ. Eng. 19 (2007) 728–739. https://doi.org/10.1061/(ASCE)0899-1561(2007)19:9(728).

[198] Y.Z. Totoev, J.M. Nichols, A Comparative Experimental Study of the Modulus of Elasticity of Bricks and Masonry, in: Proc. 11th Int. Brick Block Mason. Conf., Shanghai, China, 1997: pp. 30–39.

[199] L. Binda, M. Facchini, G. Mirabella Roberti, C. Tiraboschi, Electronic speckle interferometry for the deformation measurement in masonry testing, Constr. Build. Mater. 12 (1998) 269–281. https://doi.org/10.1016/S0950-0618(98)00009-9.

[200] H.B. Mann, D.R. Whitney, On a Test of Whether one of Two Random Variables is Stochastically Larger than the Other, Ann. Math. Stat. 18 (1947) 50–60. https://doi.org/10.1214/aoms/1177730491.

[201] American Concrete Institute, ACI 318-19 Building Code Requirements for Structural Concrete, 2019.

[202] Masonry Standards Joint Committee (MSJC), Specification for Masonry Structures (ACI 530.1-05/ASCE 6-05/TMS 602-05), (2004).

[203] European Committee for Standardization (CEN), EN 1052-1 Methods of test for masonry - Part 1 : Determination of compressive strength, (1999).

[204] B. de Vekey, In-Situ evaluation of the physical and chemical state of masonry structures, in: L. Binda, R.C. de Vekey (Eds.), RILEM TC 177-MDT Work. On-Site Control Non-Destructive Eval. Mason. Struct., 2003: pp. 159–166. https://www.rilem.net/publication/publication/31.

[205] ISCARSAH, Recommendations for the analysis, conservation and structural restoration of architectural heritage, (2003).

[206] P. Roca, The Iscarsah Guidelines on the Analysis, Conservation and Structural Restoration of Architectural Heritage, in: 12th Int. Conf. Struct. Anal. Hist. Constr., CIMNE, 2021: pp. 1629–1640. https://doi.org/10.23967/sahc.2021.290.

[207] National Research Council Canada, Review of Non-Destructuve Test Methods for Assessing Strength, Serviceability and Deterioration in Buildings, (1993).

[208] ACI 228.1R-03, In-Place Methods to Estimate Concrete Strength Reported, ACI Comm. Reports. (2003) 44.

[209] R.C. de Vekey, In-Situ Tests for Masonry, in: Proc. 9 Th Int. Brick Block Mason. Conf., Berlin, Germany, 1991: pp. 620–627.

[210] R. Felicetti, N. Gattesco, A penetration test to study the mechanical response of mortar in ancient masonry buildings, Mater. Struct. 31 (1998) 350–356. https://doi.org/10.1007/BF02480678.

[211] W.A. Ferguson, J. Skandamoorthy, The screw pull-out test for the in-situ measurement of the strength of masonry materials, in: Proc. 10th Int. Brick Block Mason. Conf., Calgary, Canada: Masonry Council of Canada, 1994: pp. 1257–66.

[212] W.A. Ferguson, Further Data on the Screw Pull-out Test for the In-situ Measurement of the Strength of Some Masonry Materials, Mason. Int. 9 (1995) 25–30. https://www.masonry.org.uk/downloads/further-data-on-the-screw-pull-out-test-for-the-in-situ-measurement-of-the-strength-of-some-masonry-materials/.

[213] R.C. de Vekey, M. Sassu, Comparison of non-destructive in-situ mechanical test on masonry mortars: The PNT-G method and the helix method, in: Proc. 11th Int. Brick Block Mason. Conf., Tongji University, Shanghai, China, 1997: pp. 376–384. http://www.hms.civil.uminho.pt/ibmac/1997/376.pdf.

[214] BRE Group, Digest421 Measuring the compressive strength of masonry materials: the screw pull-out test, 1997. https://www.brebookshop.com/details.jsp?id=325216.

[215] R.C. de Vekey, RILEM TC 127-MS: Test for masonry materials and structures. MS-D.9 determination of mortar strength by the screw (helix) pull-out method, Mater. Struct. 30 (1997) 325–327. https://doi.org/10.1007/BF02480682.

[216] L. Garcia-Ramonda, L. Pelà, P. Roca, G. Camata, Experimental cyclic behaviour of shear masonry walls reinforced with single and double layered Steel Reinforced Grout, Constr. Build. Mater. 320 (2022) 1–36. https://doi.org/10.1016/j.conbuildmat.2021.126053.

[217] D. Huang, A. Albareda, O. Pons, Experimental and Numerical Study on Unreinforced Brick Masonry Walls Retrofitted with Sprayed Mortar under Uniaxial Compression, Buildings. 13 (2023). https://doi.org/10.3390/buildings13010122.

[218] J. Segura, D. Aponte, L. Pelà, P. Roca, Influence of recycled limestone filler additions on the mechanical behaviour of commercial premixed hydraulic lime based mortars, Constr. Build. Mater. 238 (2020). https://doi.org/10.1016/j.conbuildmat.2019.117722.

[219] L. Pelà, A. Benedetti, D. Marastoni, Interpretation of experimental test on small specimens of historical mortars, in: Jerzy Jasieńko (ed) (Ed.), Struct. Anal. Hist. Constr., Wroclaw, Poland, 2012.

[220] P. Matysek, S. Seręga, S. Kańka, Determination of the Mortar Strength Using Double Punch Testing, Procedia Eng. 193 (2017) 104–111. https://doi.org/10.1016/j.proeng.2017.06.192.

[221] American Society for Testing and Materials (ASTM), ASTM C803/C803M-18 Standard Test Method for Penetration Resistance of Hardened Concrete, (2018). https://doi.org/10.1520/C0803_C0803M-18.

[222] Standard British (BSI), BS 1881-207:1992 Testing concrete. Recommendations for the assessment of concrete strength by near-to-surface tests, (1992).

[223] L. Pelà, P. Roca, A. Aprile, Comparison of MDT techniques for mechanical characterization of historical masonry, Struct. Anal. Hist. Constr. Anamn. Diagnosis, Ther. Control. - Proc. 10th Int. Conf. Struct. Anal. Hist. Constr. SAHC 2016. (2016) 769–775. https://doi.org/10.1201/9781315616995-104.

[224] A. Benedetti, M. Tarozzi, Interpretation formulas for in situ characterization of mortar strength, Constr. Build. Mater. 242 (2020) 118093. https://doi.org/10.1016/j.conbuildmat.2020.118093.

[225] M. Tohidi, Experimental Mechanical Characterization of Historical Mortars by Windsor Pin Penetrometer, Universitat Politècnica de Catalunya, BarcelonaTech, 2012.

Masonry structures are among the most abundant construction typologies in the world, having been commonly built until the second half of the 20th century. The determination of the mechanical properties of these structures entails significant difficulties given the intrinsic complexity of masonry as a composite material. For this reason, the accurate evaluation of masonry buildings against vertical and horizontal actions requires the development and improvement of techniques for the characterisation of the mechanical properties of existing masonry and their components.

This thesis presents an extensive experimental program on the characterisation of solid fired clay bricks, including the case of both handmade bricks and mechanically extruded ones. The research has also comprised extensive campaigns on the mechanical characterisation of bricks and mortar in existing historic buildings in Barcelona (Spain), using minor destructive tests (MDT). The main objective of the in-situ experimental campaigns was the calibration and validation of the MDT techniques by comparison with results obtained through destructive tests (DT) applied in the laboratory.

The laboratory experimental campaigns involved the study and improvement of existing techniques and the development of new ones for the mechanical characterisation of masonry components. The research has focused on the measurement of mechanical parameters of solid clay bricks, such as the compressive strength and the modulus of elasticity. Currently, there is a lack of unanimity in the scientific literature and also among the standards on how to evaluate the compressive strength, which in any case requires of a large number of specimens and the use of various tools and techniques. Also, there are no reference standards on the determination of the modulus of elasticity and, therefore, new proposals on standardizable methodologies are needed. In spite of the challenges encountered in the experimental characterization of bricks, different methodod have been proposed in this research in order to allow their mechanical characterization. The proposed approaches and method have shown their suitability and practical applicability.

Finally, a test methodology is recommended for each of the parameters studied in the research, whose final objective is the correlation between the MDT values and the DT values.